TRANSACTIONS OF THE AMERICAN SOCIETY FOR METALS

JUNE, 1942

lume XXX Number 2

The TRANSACTIONS *of the*

AMERICAN SOCIETY FOR METALS

Published quarterly and Copyrighted, 1942, by the AMERICAN SOCIETY FOR METALS
7301 Euclid Avenue, Cleveland, Ohio

SUBSCRIPTIONS: (members) $2.50 per year
(non-members) $5.00 per year, $2.00 per copy
Foreign (non-members) $6.50 per year, $2.50 per copy

Entered as second class matter, November 9, 1931, at the Post Office at Cleveland, Ohio, under the Act of March 3, 1879

RAY T. BAYLESS, *Editor*

Vol. XXX June 1942 No 2

The object of the Society shall be to promote the arts and sciences connected with either the manufacture or treatment of metals, or both.

Table of Contents

THERMALLOY

X-RAY INSPECTED HEAT and CORROSION RESISTANT CASTINGS

- ★ RETORTS
- ★ MUFFLES
- ★ TRAYS
- ★ BOXES
- ★ LEAD POTS
- ★ SALT POTS
- ★ CYANIDE POTS

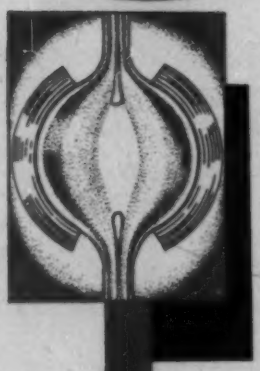

Progress Impels X-Ray Inspection

THERMALLOY *the "EYE" of QUALITY*

THE ELECTRO ALLOYS COMPANY

CASTINGS FOR HEAT CORROSION

ELYRIA, OHIO

QUALITY CASTINGS SINCE 1919

WEAR TESTS ON FERROUS ALLOYS

By O. W. Ellis

Abstract

After summarizing the results of previous work done at the Ontario Research Foundation on the resistance to abrasion of ferrous alloys in small ball mills of various types, the author shows how important can be the effects of oxygen on the wear of iron-carbon and of 15 per cent chromium-iron-carbon alloys of carbon contents varying from 1 per cent to 3 per cent; the value of chromium in conferring resistance to abrasion is shown to be lost in the absence of the corroding agent, oxygen.

That chemical combination of iron and oxygen probably accounts for much of the "iron loss" in mills, whether the "iron" is in the form of balls or liners, is suggested by the results of tests in a small steel lined mill, the pressure within which increased when nitrogen was the atmosphere and decreased when oxygen was the atmosphere within the mill.

The conditions under which the abrasive effects of a certain grinding medium (Lake Shore primary bowl sands) on a series of iron-carbon alloys could be reversed are discussed, though no clue is given as to why this reversal occurs. The profound influence of oxygen upon the resistance to abrasion of ferrous alloys is further emphasized by these tests.

A comparison is made between two ferrous alloys of rather similar microstructure, essentially austenitic, and of practically the same indentation hardness, one of which, a nickel-chromium steel, lost only about one-third of the weight of the other, a manganese steel, when tested in an atmosphere of oxygen.

The tests were designed to give some idea of—

(a) The effect of varying the ratio of liquid to solid in the charge upon the loss of weight of balls and their efficiency in grinding.

(b) The effect of varying the atmosphere in the mill upon the efficiency of grinding.

(c) The effect of varying the pH of the charge upon the efficiency of grinding.

A paper presented before the Twenty-third Annual Convention of the Society held in Philadelphia, October 20 to 24, 1941. The author, O. W. Ellis, is director, department of engineering and metallurgy, Ontario Research Foundation, Toronto, Canada. Manuscript received June 10, 1941.

These tests were conducted in hermetically sealed porcelain jars, using Ottawa sand as the medium of abrasion.

A description is given of a laboratory ball mill in which (1) the partial pressure of oxygen or other gas can be maintained constant throughout a test, or (2) the pressure within the mill can be measured at any time during a test.

THE resistance to abrasion of ferrous alloys has been the subject of considerable investigation at the Ontario Research Foundation during the past five or six years. At the Toronto meeting of the American Foundrymen's Association in 1935, the author, together with his colleagues J. R. Gordon, now assistant to the vice-president, The International Nickel Company of Canada, Limited, Copper Cliff, and Dr. G. S. Farnham, now with the Department of Mines, Ottawa, presented a paper on "The Wear Resistance of White Cast Iron," which described in some detail the results of abrasion tests made on various iron-carbon alloys.

The method of test employed porcelain jars of standard dimensions, having a capacity of one U. S. gallon; the charge in each jar consisted either of 1-inch diameter balls or of ¾-inch normal cylinders weighing in all about 1¼ pounds, 4 pounds of ¼-inch silicon carbide grain, and 1¼ pounds of water. The jars were sealed, placed in a motor driven six-jar mill and rotated 160,000 times at 60 revolutions per minute. They were then emptied, the cylinders or balls were dried and weighed, and later returned to the jars with fresh silicon carbide and water and subjected to further abrasion (160,000 revolutions of the mill). The tests were continued until the cylinders or balls had lost about 10 per cent of their original weight. The results of the tests were presented graphically in the earlier series, in which the cylinders, machined from cast rods, were used, and in terms of so-called "wear numbers" in the later series, in which cast balls were used. These wear numbers represented the sums of the losses of weight in milligrams per square centimeter of original surface of sample which occurred during 5 or 10 runs, respectively, of 160,000 revolutions.

In Fig. 1 is reproduced a series of curves which shows the percentage losses of weight with time of ¾-inch normal cylinders. The curves show that, under the above conditions of test, (a) white iron containing 2 per cent of carbon is more resistant to abrasion than

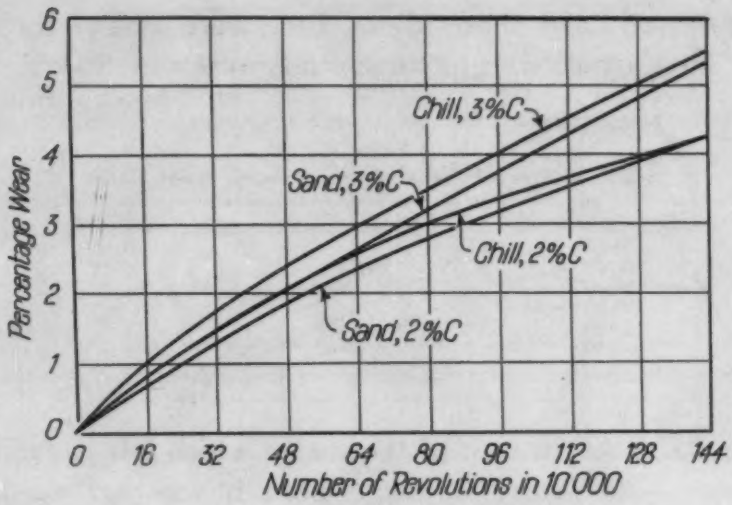

Fig. 1—Wear Tests of Chill and Sand Cast Irons.

white iron containing 3 per cent of carbon, and (b) sand-cast white iron is more resistant to abrasion than chill-cast white iron.

The conclusions resulting from the tests on the balls were as follows:

(I) Given a suitable abrading medium, the ball mill may be used to measure the wear resistance of white cast iron.

(II) The higher the carbon content of white iron, the less consistent are the results of wear tests on cast balls made from this material.

(III) The higher the carbon content of the straight iron-carbon alloys, the lower is their wear resistance under the conditions of test described, other things being equal.

(IV) Variations in manganese up to about 1 per cent are practically without effect upon the wear resistance of white iron. No benefits accrue from adding up to 6 per cent of manganese to white iron containing ledeburite.

(V) Increase of silicon from about ¾ per cent to about 1½ per cent has little or no effect on the wear resistance of white cast iron, but results in a remarkable increase in that of mottled irons.

(VI) Sulphur is deleterious in its effect on the wear resistance of white cast iron under the above conditions of test.

A later contribution to the literature was the American Exchange Paper "Wear Tests on Ferrous Alloys" which was presented by the author at the Derby meeting of The Institute of British Foundrymen in 1937. Most of this paper dealt with the results of experiments in a continuous mill. In one series of tests, primary

bowl sands from Lake Shore Mines, Ltd., were used as the abrading medium. The particle sizes of these sands were as follows:

Table I
Particle Size of Lake Shore Primary Bowl Sands

Particle Sizes	Per Cent
+60	45–60
60–80	10–15
80–100	9½–10½
100–150	up to 10
150–200	1½–9½
−200	11½–17½

From 83 to 89 per cent of the sludge which left the mill during the tests was −200 mesh; less than 3 per cent was +60 mesh.

The groups of balls which underwent test in the continuous mill were weighed before and after each week's run. However, the same weight of sands did not pass through the mill each week, though, on the average, 500 pounds of sand was fed, without interruption, to the mill during each run. The ratio of water to sands was kept at 30 per cent throughout the tests. The mill was rotated at 30 revolutions per minute during the first ten runs and at 60 revolutions per minutes during the last two.

The balls were tested in groups of ten, the number tested per run varying between 290 and 320. The number was held at 310 during the last nine runs. The number of alloys undergoing test during any run varied from twenty-nine to thirty-two and was thirty-one in the last nine runs. Altogether 4780 pounds of sands were passed through the mill during the twelve runs which constituted this series of experiments.

The results of some of the tests in the continuous mill are shown graphically in Fig. 2.

The most surprising fact that developed from these tests was that the resistance to abrasion in Lake Shore sands of the straight iron-carbon alloys increased with increasing carbon content. As this was contrary to the result obtained in the tests (1935) with silicon carbide, it was decided to determine the order of wear of the straight iron-carbon alloys when tested in porcelain jars (a) with Lake Shore sands, (b) with granite, and (c) with silicon carbide. The results of these tests are shown in Table II.

These tests brought out the point that the order of wear of these alloys, when tested in sands in the porcelain jars, was the same as

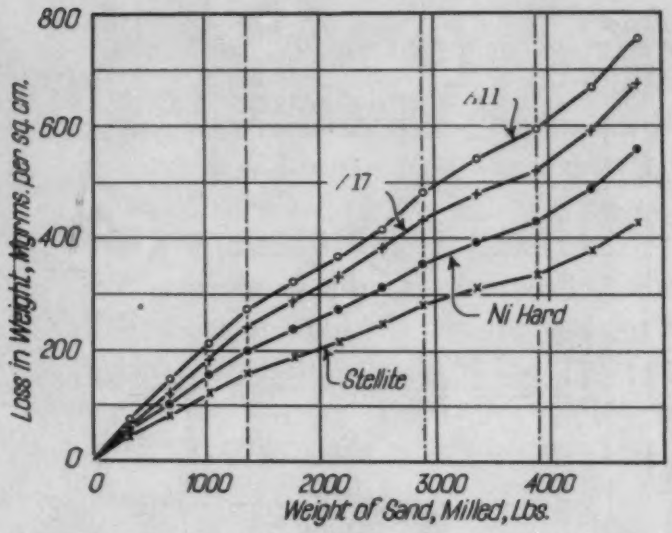

Fig. 2—Loss in Weight of Various Materials Related to the Weight of Sand Milled.

	C	Si	Mn	Cr	Ni
A17	1.02	1.32	1.08	3.08	5.95
A11	1.58	1.36	5.85	....	....

Table II
Order of Wear of Straight Iron-Carbon Alloys When Tested in Porcelain Jars

Carbon Per Cent	Silicon Per Cent	Manganese Per Cent	Relative Loss of Weight		
			Sands	Granite	Silicon Carbide
0.95	0.72	1.05	114.4	100.0	100.0
1.43	0.79	1.07	109.2	107.8	106.4
2.02	0.75	1.15	104.6	120.6	118.2
2.41	0.72	1.20	104.3	138.6	133.6
2.95	0.80	1.05	100.0	167.2	155.0

The alloy showing the least wear has been taken as the standard—100—in each case.

that when tested in sands in the continuous mill. They showed also that the chances were good that tests in porcelain jars would serve as a guide to the behavior of alloys in larger mills.

An attempt was made to check this last point by making a run with 310 balls (thirty-one alloys) in the continuous mill, using silica instead of sands as the abrading medium. The orders of wear of the iron-carbon alloys when tested (a) in a porcelain jar and (b) in the continuous mill are given in Table III.

Table III
Comparison of Order of Wear of Iron-Carbon Alloys in Silica Sand

Carbon Per Cent	Silicon Per Cent	Manganese Per Cent	Relative Loss of Weight	
			Porcelain Jar	Continuous Mill
0.95	0.72	1.05	100.0	102.4
1.43	0.79	1.07	106.4	100.0
2.02	0.75	1.15	118.2	107.9
2.41	0.72	1.20	133.6	111.4
2.95	0.80	1.05	155.0	116.5

The alloy showing the least wear has been taken as the standard—100—in each case.

Table IV

Approximate Relative Abrasive Effects of Different Minerals

Alloy Number	Chemical Analysis					Order of Wear In			
	Carbon Per Cent	Silicon Per Cent	Manganese Per Cent	Nickel Per Cent	Chromium Per Cent	Silica	Feldspar	Marble	Talc
B-1	0.93	0.62	1.10	....	....	100 (302)	100 (309)	100 (65)	100 (100)
B-2	1.48	0.60	1.14	....	....	96	105	111	101
B-3	1.89	0.80	0.88	....	....	111	115	142	145
B-4	2.48	0.81	0.95	....	....	121	131	152	158
B-5	3.10	0.81	1.06	....	....	130	122	188	177
B-11	0.97	0.80	0.98	2.50	....	118	100	106	136
B-12	1.43	0.77	1.00	2.60	....	108	85	98	99
B-13	1.95	0.77	0.91	2.55	....	108	93	117	118
B-14	2.45	0.79	1.01	2.52	....	119	99	122	132
B-15	2.77	0.75	1.06	2.58	....	123	104	182	145
B-16	1.01	1.29	0.92	....	2.42	99	84	83	67
B-17	1.47	1.50	0.94	....	2.59	103	89	105	84
B-18	1.97	1.47	0.92	....	2.54	108	83	115	99
B-19	2.47	1.49	0.99	....	2.46	116	98	129	114
B-20	3.02	1.32	0.76	....	2.54	124	107	155	160
B-21	1.00	1.22	0.90	....	7.67	104	52	88	63
B-22	1.43	1.26	0.91	....	8.05	95	66	92	68
B-23	2.17	1.17	1.03	....	7.41	102	73	102	71
B-24	2.63	1.32	0.92	....	7.56	111	89	114	83
B-25	2.98	1.33	0.98	....	7.52	118	98	129	104
B-26	1.07	1.29	1.00	....	15.2	107	44	32	45
B-27	1.56	1.30	1.08	....	14.8	111	48	40	58
B-28	2.05	1.32	0.95	....	15.1	116	55	74	54
B-29	2.58	1.30	0.94	....	14.9	112	64	102	62
B-30	2.98	1.50	0.95	....	15.2	115	90	115	73

These experiments in the continuous mill led to a consideration of the abrasive effects of different minerals on five groups of ferrous alloys varying in carbon content from about 1 to about 3 per cent. The results of the tests on these alloys are given in Table IV.

The numbers in Table IV are the relative losses of weight of the twenty-five alloys which occurred during the grinding of 10,000 pounds of each of the four minerals, silica, feldspar, marble and talc. The ratio of water to mineral in the feed was approximately 3 to 10 throughout the tests. The speed of the mill was 60 revolutions per minute.

The values in parentheses adjacent to the first numbers in the four columns to the right of Table IV are the total weights in milligrams per square centimeter of surface of the 0.93 per cent carbon steel balls which were lost during these tests. Using these values, the losses of weight of the other balls which occurred under the same conditions of test can be estimated.

These tests confirm the conclusion that the higher the carbon content of the iron-carbon alloys (the first group of alloys in Table IV), other things being equal, the lower is their resistance to abrasion. They also support the opinion that the higher the carbon content of other ferrous alloys, other things being equal, the lower is their resistance to abrasion. However, they offer no explanation of the anomalous behavior of the iron-carbon alloys in Lake Shore primary bowl sands.

It would seem that mineralogical hardness *per se* is not the only property of minerals which can affect the wear of alloys in the ball mill. Otherwise, for example, the orders of wear of alloy B-26 in silica (107) and in feldspar (44) would not have differed so substantially. As the author pointed out in the 1937 paper, "It is probable that in its influence upon the wear of metals and alloys in mills, the arrangement of the atoms on the crystal lattices is as significant as the mineralogical hardness of abrasive materials. The energy absorbed in grinding a substance of high mineralogical hardness, but with gliding planes along which slip can readily proceed, may quite well be less than that absorbed in the grinding of a substance of low mineralogical hardness, but with a crystal structure more resistant to fracture by cleavage."

Other factors which are likely to affect the wear of alloys in the ball mill are the acidity or alkalinity of the charge. Yet another is the ball mill atmosphere. In this connection a series of experiments has been conducted in a rubber lined porcelain jar, for which a rubber lined aluminum alloy lid of special design was made. This lid was provided with two stopcocks which, on the one hand, could be closed so as to hermetically seal the jar and through which, on the

other hand, gas could be introduced into or withdrawn from the jar.

In preparation for each test in this modified jar a large glass beaker was partly filled with 4 pounds of ¼-inch grain silicon carbide. A day or so before the test was started, the silicon carbide was covered with cold tap water, which previously had been boiled, and allowed to soak for some time, after which the gas, oxygen, air or cracked ammonia, with which the jar was to be filled during the abrasion test, was bubbled through the water until it had become saturated. Water was then decanted off until 1.71 pounds (30 per cent of the total charge used in the test) remained. pH tests were made on the decanted water.

The silicon carbide and water remaining in the beaker were now poured into the rubber lined jar, wherein ten balls had already been placed. The lid of the jar was applied and the jar tightly sealed.

Table V

Percentage Losses of Weight of Various Ferrous Alloys in Different Gases
Medium of Abrasion—Silicon Carbide

Alloy Number	Carbon Per Cent	Silicon Per Cent	Manganese Per Cent	Chromium Per Cent	Percentage Losses of Weight per Run of 160,000 Revolutions		
					Oxygen (3)*	Air (4)*	Cracked Ammonia (5)*
B-1	0.93	0.62	1.10	....	0.90	0.40	0.15
B-2	1.48	0.60	1.14	....	1.01	0.43	0.15
B-3	1.89	0.80	0.88	....	0.99	0.43	0.16
B-4	2.48	0.81	0.95	....	1.56	0.44	0.16
B-5	3.10	0.81	1.06	....	2.51	0.54	0.15
B-26	1.07	1.29	1.00	15.2	0.15	0.17	0.14
B-27	1.56	1.30	1.08	14.8	0.18	0.20	0.14
B-28	2.05	1.32	0.95	15.1	0.22	0.22	0.16
B-29	2.58	1.30	0.94	14.9	0.25	0.32	0.15
B-30	2.98	1.50	0.95	15.2	1.11	0.48	0.17

*Values in parentheses represent number of runs of 160,000 revolutions in each test.

Gas was now bubbled through the water in the jar by means of a glass tube joined by a rubber tube to the inner end of one of the stopcocks with which the lid was fitted. This glass tube was pulverized during the test which followed, but since the weight of glass tubing used in each of the tests was essentially the same, its effects upon the results of individual tests is likely to have been negligible.

The stopcocks were closed after the jar had been filled and the test, which comprised a number of runs, was then started. The jar was rotated at 60 revolutions per minute for between 42 and 43 hours, 160,000 revolutions. A new charge of abrasive and water was used in each run. The balls were weighed individually before and after each run. The pH of the liquid in the mill was measured

after each run. The test was conducted with each of the gases until a loss of weight of between ½ and ¾ per cent was noted in the least worn ball. The results of the tests in oxygen, air and cracked ammonia are shown in Table V.

The tests show that the high-chromium alloy balls were, on the whole, but slightly affected by changes in the atmosphere in the mill, whereas the iron-carbon balls were materially influenced by alterations in the atmosphere. In cracked ammonia, a mixture of nitrogen and hydrogen, the straight iron-carbon balls behaved in much the same way as the 1 per cent carbon high-chromium alloy balls and variations in the carbon of the high-chromium balls, which were important when the balls were tested in oxygen, were without appreciable effect upon their resistance to abrasion.

With oxygen in the mill, the order of wear of both series of balls was about the same as in previous tests, with the outstanding exception of those in which Lake Shore primary bowl sands were used as the abrading medium. The similarity in behavior of alloys B1, B2 and B3, on the one hand, and alloys B26 to B29, on the other hand, is worthy of note.

These tests show the importance of oxygen in its effect upon the resistance of ferrous alloys to abrasion in the ball mill. In the absence of oxygen, at least under the conditions of test described above, chromium-free alloys behave in practically the same way as chromium-bearing alloys. In other words, the value of chromium in conferring resistance to corrosion is lost in the absence of the corroding agent, oxygen.

In a neutral atmosphere, such as cracked ammonia (average loss of weight is equal to 0.15 per cent), it is not improbable that the average percentage loss of weight per run of these alloys is a measure of the true abrasive effect of carborundum on them. The possibility also exists that the differences between the percentage losses of weight per run of the various alloys in air and in oxygen, respectively, and the average percentage loss of weight per run in a neutral atmosphere indicate very roughly the corrosive effects of the oxygen present in the charge. Such differences, however, cannot be true criteria of the corrosive effects of oxygen, because the conditions of test in a hermetically sealed ball mill are not ideal for obtaining these effects, as will be gathered from what follows.

A small steel mill, 36 inches diameter and 18 inches wide, the main features of which are shown diagrammatically in Fig. 3, was

used in a series of tests designed to check on a somewhat larger scale the results obtained in the rubber lined porcelain jar. It will be seen from Fig. 3 that the ends of this mill were covered inside with ½-inch thick rubber sheets, which served also as gaskets when the ends of the mill were tightened on to the body of the mill. The inner circumferential surface of the mill was left bare. At the center

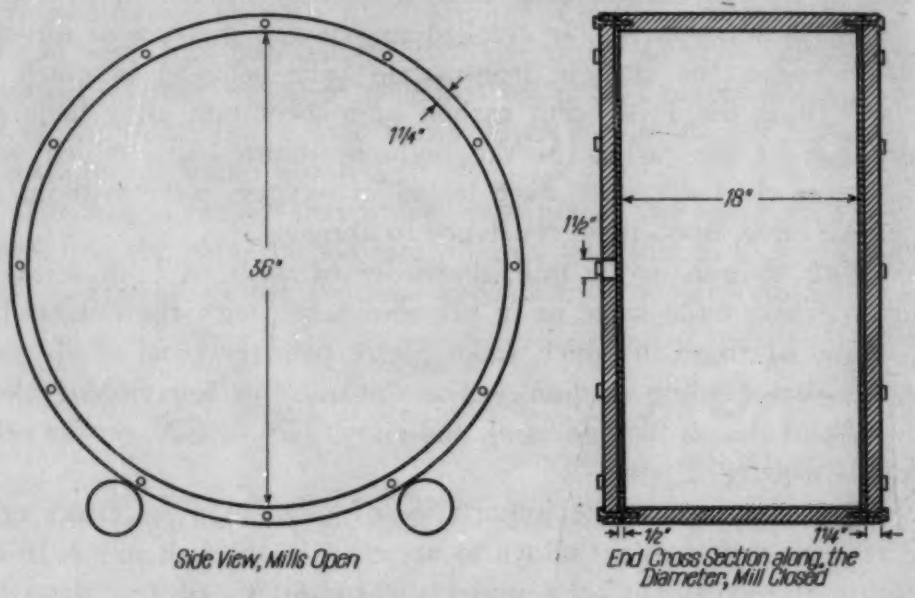

Fig. 3—Diagram of Mill Used in These Tests.

of the steel plate which formed one end of the mill, a hole 1½ inches in diameter was drilled. This hole, the presence of which was more or less accidental, played an important part in deducing the conditions within the mill during the tests which were made therein.

In preparation for each test in this mill, it was charged with 200 pounds of 1½-inch forged steel balls, 50 pounds of silica sand and 50 pounds of water. The gas with which the mill was to be filled was then bubbled through the charge for at least ½ hour before each test was started. The mill was then closed and run for 20 hours at 60 revolutions per minute. The loss in weight of the balls during each run was carefully measured.

The results were most erratic, although the losses in weight of the balls were generally lower when tested in nitrogen than when tested in oxygen. The inner circumferential surface of bare metal in the mill may have had something to do with the inconsistencies observed in the behavior of the balls. Certainly the reaction of such

a surface to the balls and to the medium of abrasion would have an important influence upon both the real and apparent behavior of the balls. This is a point which appears to have been overlooked in some earlier experiments on the resistance of metals and alloys to abrasion in metal ball mills in which the loss of weight of the balls has been the only variable measured.

Two observations of considerable interest were made during these tests. First, when the mill was filled with nitrogen, it was found that, after a time, the pressure of the gas in the mill began to rise as a result of the heat developed in the mill. A point was finally reached where pulp and liquid were expelled from the mill between the rubber sheets and the flanges of the mill. The only way in which this could be prevented was by reducing the weight of the charge, and thus reducing the heat developed in the mill. It invariably occurred with a charge of 200 pounds of balls, 50 pounds of silica and 50 pounds of water. It did not occur when the weight of balls was halved. Second, when the mill was filled with oxygen, it was found that, after a time, the pressure of the gas in the mill fell below that of the outside atmosphere, with the result that the rubber sheet beneath the plate with the 1½-inch hole drilled in it could be seen to bulge inwards into the mill.

A clue is here afforded as to what probably occurs in hermetically sealed mills containing oxygen. The reduction of pressure within the mill in the second case referred to above, despite the fact that heat was being developed in the mill, can only be explained by assuming that oxygen was used up as a result of reaction with iron, so that its pressure, or partial pressure, was lowered.

Because the pressure, or partial pressure, of oxygen falls off as the test proceeds in a hermetically sealed mill, if for no other reason, the rate of wear of the balls must decrease with time. Hence, as has been suggested above, in tests made in such mills, the differences between the percentage losses of weight per run of the various alloys in air or in oxygen, respectively, and the average percentage loss of weight per run in a neutral atmosphere cannot be true criteria of the corrosive effects of oxygen. Only if the pressure, or partial pressure, of the oxygen in the mill were maintained constant could such differences in loss of weight be looked upon as criteria of its corrosive effects.

While experiments were in progress leading to the design of a mill in which (a) the partial pressure of oxygen or other gas could

be maintained constant, or (b) the pressure could be measured—these experiments have occupied much of the spare time of the writer and one or other of his associates during the past 3 years—a number of tests were run in hermetically sealed unlined porcelain jars, using materials other than carborundum as the media of abrasion.

One series of tests involved the use of Lake Shore primary bowl sands in tap water, the other the use of silica sand in tap water to which 0.034 gram potassium cyanide per liter was added, this amount of cyanide being that present in the charge of Lake Shore primary bowl sands and tap water (the bowl sands contained cyanide). Alloys B1 to B5 inclusive (see Tables IV and V) were used in these experiments. The jars were not lined with rubber as in the tests the results of which are quoted in Table V. Ten balls, two of each alloy, were used in each of the tests, which in all other respects were carried out in a manner similar to that described in connection with the tests referred to in Table V. The results of the two series of tests are given in Table VI.

Table VI

Comparison of Abrasive Effects of Silica Sand and Lake Shore Primary Bowl Sands Under Different Atmospheres

Values in Percentage Losses of Weight Per Run of 160,000 Revolutions

Alloy Number	Carbon Per Cent	Silicon Per Cent	Manganese Per Cent	Oxygen (4)		Air (4)		Nitrogen (4)	
				Silica	Sands	Silica	Sands	Silica	Sands
B-1	0.93	0.62	1.10	0.75	1.71	0.33	0.57	0.05	0.37
B-2	1.48	0.60	1.14	0.88	1.80	0.32	0.51	0.03	0.34
B-3	1.89	0.80	0.88	0.88	1.88	0.33	0.52	0.04	0.35
B-4	2.48	0.81	0.95	1.17	2.00	0.35	0.50	0.04	0.34
B-5	3.10	0.81	1.06	1.83	2.29	0.44	0.47	0.04	0.32

These results confirm the profound influence of oxygen upon the wear of ferrous alloys under certain conditions of test.

It is of interest to note that the losses of weight of all the alloys tested were invariably greater in Lake Shore primary bowl sands than in silica sand. In an atmosphere of nitrogen with silica the losses of weight of the balls were very small and did not appear to be related to their composition, whereas with sands, the losses of weight of the balls were relatively high.

In this connection the average results of a number of screen analyses of Lake Shore and silica sands before and after tests in nitrogen may be of interest (Table VII).

The higher losses of weight of the balls when grinding Lake Shore primary bowl sands than when grinding silica sand can doubt-

less be explained in terms of the greater grinding efficiency in the former case.

In an atmosphere of air the order of wear of the alloys in Lake Shore sands was, as in previous cases, roughly opposite to that in

Table VII
Screen Analyses of Lake Shore and Silica Sands Before and After Tests in Nitrogen

Mesh	Lake Shore Primary Bowl Sands		Silica Sand	
	Before	After	Before	After
+20	2.15	....	0.40	0.30
20/40	22.90	....	94.60	81.60
40/60	19.55	....	4.70	12.20
60/80	15.60	1.55	0.10	2.60
80/100	12.90	10.30	0.05	0.95
100/150	9.05	11.10	0.25	0.35
150/200	6.40	10.85		0.20
200/270	4.10	28.25		0.50
−270	6.15	34.85		0.70

silica sand. The screen analyses of the Lake Shore and silica sands before and after the tests in oxygen were similar to those quoted in Table VII and need not be given here. In this case again the higher losses of weight of the balls in the one case than in the other can doubtless be explained in terms of their relative grinding efficiencies.

The results of the tests in oxygen are particularly interesting, because in this case, for the first time, the order of wear of the alloys is the same in both media of abrasion, the losses of weight of the balls increase with increasing carbon content.

It had been hoped that some clue to the reason for the change in the order of wear of the balls in Lake Shore primary bowl sands

Table VIII
Comparison of Alloys A16 and A27 Having Substantially Similar Brinell Hardness Numbers and Microstructures
Values in Percentage Losses of Weight Per Run of 160,000 Revolutions

Alloy No.	Carbon Per Cent	Silicon Per Cent	Manganese Per Cent	Chromium Per Cent	Nickel Per Cent	Oxygen	Air	Nitrogen
A16	1.24	1.24	1.14	2.05	3.94	0.38	0.33	0.16
A27	1.26	0.44	14.83	....	....	1.05	0.44	0.21
B1	0.93	0.62	1.10	....	....	1.26	0.45	0.18
B5	3.10	0.81	1.06	....	....	2.87	0.54	0.24
B26	1.07	1.29	1.00	15.2	....	0.24	0.29	0.18

when tested in oxygen would be forthcoming from the results of the pH tests already referred to, but, unfortunately, the differences in pH were insignificant. The results of these pH tests will, therefore, not be referred to again.

These experiments would seem to indicate, however, that the

presence of oxygen in the mill tends in some manner to counteract the effect of an undiscovered factor. How oxygen may do this is considered below.

The screen analyses of the Lake Shore and silica sands before and after the tests in oxygen were very similar to those quoted in Table VII and need not be given here.

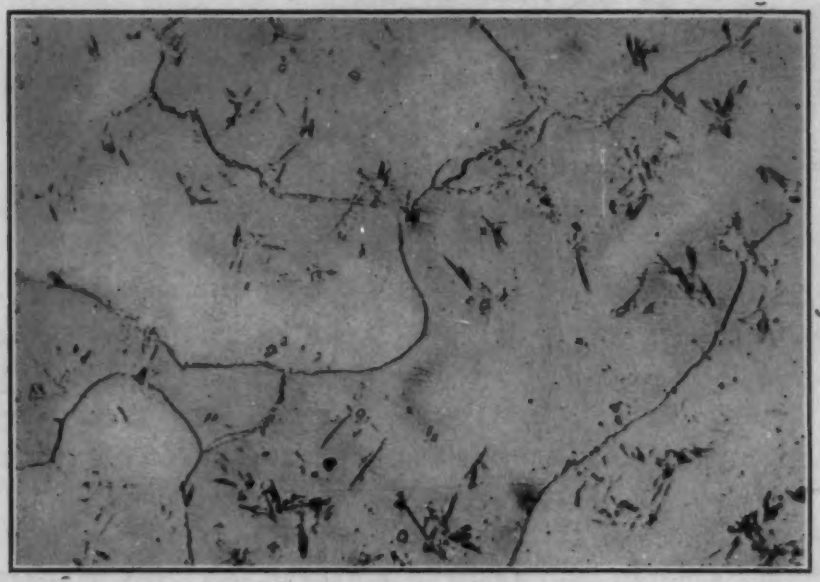

Fig. 4—Microstructure of a Typical Section of Alloy A27.

Another series of tests was made on a group of five alloys, two balls of each of which were submitted to abrasion in carborundum in atmospheres of oxygen, air and nitrogen with the results shown in Table VIII. The conditions of test were similar to those referred to above, except that the pH of the liquid in the mill was not determined. The main object of these tests was to compare alloys A16 and A27. The former was tested in the "as cast" condition, the latter after heat treatment. The alloys in these states had practically the same hardness number, viz., 215, as measured in the Vickers Pyramid Hardness Testing Machine. The microstructure of a typical section of alloy A27 is shown in Fig. 4, at a magnification of 200 diameters. The microstructure of alloy A16 was somewhat similar to, though distinguishable from that of alloy A27.

In the tests in the continuous mill referred to at the beginning of this paper the loss of weight of alloy A27 was 60 per cent greater

than that of alloy A16 after 1021 pounds of Lake Shore sands had been passed through the continuous mill. As a matter of fact, because of their poor showing, the balls made of alloy A27 were replaced by balls of another alloy at this stage in these tests.

The results quoted in Table VIII fall into line with those of the tests in the continuous mill and confirm the opinion that has often been expressed that indentation hardness tests offer little, if any, clue to the behavior of alloys under abrasion. One might hazard the further opinion that the microstructure of alloys is no guide to their resistance to wear. Chemical composition is the all important factor. Of course, these tests, save in so far as they themselves and others like them are concerned, should not be looked upon as placing manganese steel in an unfavorable light. The immense value of manganese steel in situations where its work-hardening properties can be utilized cannot be overlooked.

The next series of tests was designed to give some idea, because, until a mill in which the partial pressure of oxygen or other gas could be held constant, tentative results only could be expected, of:

(I) The effect of varying the ratio of liquid to solid in the charge upon the loss of weight of the balls and their efficiency of grinding.

(II) The effects of varying the atmosphere in the mill upon the efficiency of grinding.

(III) The effects of varying the pH of the charge upon the efficiency of grinding. In all these tests hermetically sealed unlined porcelain jars were used. Ottawa sand was the medium of abrasion.

In these trials no attempt was made to measure the surface of the Ottawa silica sands either before or after the runs. The values quoted by Gross and Zimmerli (American Institute of Mining and Metallurgical Engineers, Milling Methods, Vol. 87, 1930, p. 27-34) for the measured surface per gram of Ottawa sand, Table II of their second paper on "Crushing and Grinding," and for crushed quartz, Table I of this paper, were employed in this connection.

In the first series of tests, five straight carbon steel balls and five 14 per cent chromium steel balls of approximately the same carbon content (1 per cent) were used. The balance of the charge consisted, in all but two tests, of 2000 grams of Ottawa sand and water. When charged, the mill was run at 60 revolutions per minute for 260,000 revolutions. The losses of weight of the two sets of balls were then measured independently. To check the iron losses of the

Table IX

Preliminary Experiments on the Effect of Variations in Liquid/Solid Ratio in the Charge on the Loss of Weight of Balls and the Efficiency of Grinding as Measured by the Production of New Surface in the Medium of Abrasion (Ottawa Sand) (100 Grams)

Test Number	Weight of Charge	Ratio: Water/Sand in Charge	Loss of Weight (Gram) Carbon	Loss of Weight (Gram) Chromium	Total Loss of Weight (Gram)	Percentage Loss of Weight Carbon	Percentage Loss of Weight Chromium	Ratio: Percentage Loss of Weight Carbon to Chromium	Screen Analysis +270 Per Cent	Screen Analysis −270 Per Cent	Calculated New Surface for +270 Material	New Surface +270 (Per Charge)
1	2000	3	2.23	1.07	3.30	0.79	0.37	2.14	68.3	31.7	26,670	53,340
2	2000	2	1.81	0.62	2.43	0.65	0.21	3.10	85.7	14.3	24,170	49,420
3	2000	1	2.62	1.05	3.67	0.93	0.36	2.58	55.8	44.2	27,620	55,240
4	2000	½	3.10	1.59	4.69	1.11	0.54	2.06	8.5	91.5	5,390	10,780
5	1500	1	2.89	2.40	5.29	1.03	0.82	1.26	8.1	91.9	3,266	4,900
6	3000	1	1.21	0.10	1.31	0.43	0.03	14.33	98.7	1.3	14,734	44,200
3 (check)	2000	1	2.61	1.01	3.62	0.94	0.35	....	N.O.	N.O.	N.O.	....

balls, analyses were made of the iron content of the pulp at the end of each run, so that, the iron content of the Ottawa sand being known, it was possible to arrive at the desired figures for iron loss. These loss values, by the way, did not differ materially from the total losses of weights as recorded in column 6 of Table IX. The sieve sizes of the Ottawa sand and of the crushed quartz were determined and estimates of the new surfaces resulting from the grinding operation were obtained therefrom by calculation.

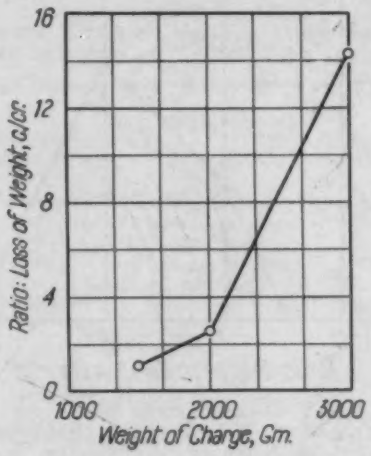

Fig. 5 — Relationship of Rate of Wear of Carbon Steel Balls and Chromium Steel Balls.

The results of the first series of tests are shown in Table IX. The first point in Table IX which merits attention is the relationship shown to exist (1) between the weight of charge and the rates of wear of the two alloys, and (2) between the nature of the charge, i.e., the ratio of water to sand in the charge, and the rates of wear of the two alloys, which is expressed in terms of the ratio: loss of weight (per cent) of carbon to chromium.

The former relationship is described graphically in Fig. 5, which shows clearly that the rate of wear of the carbon steel balls increases much more rapidly than that of the chromium steel balls as the weight of the charge is raised. In the light of the experiments the results of which are given in Table V it would seem reasonable to suggest that the marked change in the ratio: percentage loss of weight, carbon to chromium, with increase of weight of charge, is due to the greater ease with which the oxide film is removed from carbon steel balls than from chromium steel balls. It is here assumed that, in a

mill atmosphere containing oxygen, ferrous alloy balls become coated with a layer of oxide, the physical properties of which are dependent, other things being equal, upon the composition of the alloy. The physical properties of such oxide layers may not only determine the rates of wear of the balls, but their grinding efficiencies as well. A soft, friable film of oxide would tend to reduce the crushing effect of two balls upon a particle of mineral caught diametrically between

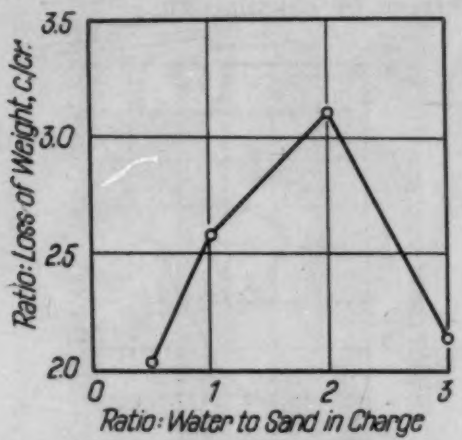

Fig. 6—Diagram Showing Percentage Loss of Weight as the Ratio of Water to Sand in the Charge Increases.

them. A hard, tenacious film of oxide might actually increase this crushing effect over that which would be obtained were clean metal surfaces involved.

There can be no question that in these experiments the grinding efficiency falls off materially as the weight of charge increases (compare tests 3, 5 and 6 in Table IX). The thought arises from this observation that the work of grinding may be divisible into two portions (1) that which is applied to the production of new surface in the medium being crushed, or the medium of abrasion, as it has hitherto been called in this paper, and (2) that which is employed in the production of new metal surface, which ultimately appears in the mill as oxide.

The latter relationship is illustrated in Fig. 6, which shows that, as the ratio of water to sand in the charge increases, so the ratio: percentage loss of weight, carbon to chromium, first increases to a maximum when the weight of water is twice that of the sand and then falls off rapidly again. The actual position of the maximum in this curve could only be arrived at by further experiment.

Another point of some interest in Table IX is the relationship which is shown to exist between the loss of weight of the balls and their grinding efficiency. Given a constant weight of charge, the losses of weight of both the carbon steel and the chromium steel balls are roughly proportional to the new surfaces produced by the medium of abrasion. It is assumed, of course, that the high percentage of −270 mesh material which was produced in test No. 4 (see column

Table X

Preliminary Experiments on the Effect of Various Atmospheres on the Loss of Weight of Balls on the Efficiency of Grinding as Measured by the Production of New Surface

Test No.	Atmosphere	Percentage Loss of Weight of Balls	Alloy	Screen Analysis +270	Screen Analysis −270	Calculated New Surface for +270 Mesh Material (100 Grams)
1	Oxygen	0.034	Carbon Steel	94.0	6.0	14,000
2	Oxygen	0.022	Chromium Steel	87.5	12.5	18,600
3	Air	0.029	Carbon Steel	92.5	7.5	16,200
4	Air	0.019	Chromium Steel	86.0	14.0	19,800
5	Nitrogen	0.019	Carbon Steel	90.0	10.0	17,000
6	Nitrogen	0.022	Chromium Steel	85.0	15.0	19,700

11 in Table IX) would raise the total new surface value well beyond that calculated for the +270 mesh material (see column 12, Table IX).

The fact that the ratio: percentage loss of weight, carbon to chromium, depends so much upon the conditions of test suggests that it is desirable to avoid using mixtures of alloys in such experiments as these.

In the second series of tests, 120 balls of either carbon steel or chromium steel were used. The balance of the charge consisted of 2000 grams of silica and 1000 cubic centimeters of water. The mill was run at 60 revolutions per minute for 5000 revolutions in each test. The loss of weight of the balls was measured and screen analyses of the crushed sand were made. The results of these tests are shown in Table X.

The number of revolutions (5000) in these tests was rather small. It is not surprising, therefore, that the percentage loss of weight of the balls was so low. However, the number of revolutions was kept as low as possible in order to counter-balance some of the effects which might have resulted from the depletion of oxygen in the mill during each test. As has already been pointed out, the conditions in a hermetically sealed ball mill are not such as to allow of the accurate measurement of the corrosive effects of oxygen, because

of the depletion of this gas during test. The values given in Table X must be considered with this thought in mind.

Possibly the most interesting result of these tests is the relationship which has again been shown to exist between percentage loss of weight of balls and grinding efficiency. This relationship is most strikingly brought out in the case of the carbon steel balls, the percentage loss of weight of which falls off considerably as the partial pressure of the oxygen in the mill is reduced. At the same time, the grinding efficiency of the balls increases, whether the grinding efficiency be measured in terms of the new surface of +270 mesh material or of the percentage of —270 mesh material produced.

In nitrogen the greater efficiency of chromium steel is due, in

Table XI

Preliminary Experiments on the Effect of Varying pH on the Loss of Weight of Balls and the Efficiency of Grinding

Test No.	pH		Percentage Loss of Weight	Type of Steel	Screen Analysis		Calculated New Surface for +270 Mesh Material
	Start	Finish			+270	—270	
1	2.5	4.3	0.237	Carbon	92.9	8.1	16,400
2	2.5	3.6	0.050	Chromium	85.0	15.0	18,400
3	6.6	N.O.	0.029	Carbon	92.5	7.5	16,200
4	6.6	7.8	0.015	Chromium	86.0	14.0	18,400
5	11.0	10.4	0.016	Carbon	94.8	5.2	15,500
6	11.0	10.4	0.013	Chromium	88.5	11.5	19,100

all probability, to the greater "crushing effect" of balls made of this alloy. The use of the word "hardness" and reference to any physical or mechanical properties of the alloy are left out of discussion advisedly here, since it may not be the alloy *per se* that determines the efficiency of grinding of the balls made from it, even in a neutral atmosphere, but rather the film which forms on the alloy in the mill as opportunity serves. Then, the fact that chromium steel reacts with nitrogen under certain conditions must not be overlooked in this connection.

There is some evidence in support of the view that the grinding efficiency of chromium steel balls is less in oxygen than in air or nitrogen.

In the third series, except that the chemical character of the pulp was varied from test to test, the general conditions were the same as in the second series. In two of the tests the pH of the solution in the mill was lowered by adding 25 cubic centimeters of acetic acid per liter of water, thus obtaining a value of 2.5. In two

Table XII

Iron Loss and Grinding Efficiency of Carbon and Chromium Steel Balls

Test No.	Solution in Mill	Type of Steel	Number of Revolutions at 60 r.p.m.	Iron Loss (Gram)	Weight Loss (Gram)	Screen Analysis +270	Screen Analysis −270	Calculated New Surface for +270 Mesh Material (Gram)
1	Tap Water	Carbon	5,000	1.94	1.98	92.6	7.4	21,600
2	Tap Water	Carbon	8,000	2.28	2.33	80.0	20.0	28,000
3	Tap Water	Mixed*	5,000	1.96	N.O.	88.6	11.4	23,000
4	Tap Water	Mixed	10,000	3.60	N.O.	61.0	39.0	28,600
5	Tap Water	Chromium	5,000	1.29	1.55	87.0	13.0	25,900
5(a)	Tap Water	Chromium	5,000	1.18	1.42	86.6	13.4	26,000
6	Sodium Sulphite	Carbon	5,200	1.43	1.46	88.1	11.9	23,000
7	Sodium Sulphite	Chromium	5,200	1.28	1.54	86.5	13.5	25,600

*60 carbon steel and 60 chromium steel balls.

of the tests untreated tap water was employed and in two of the tests the pH of the solution was raised by adding 25 cubic centimeters of 3N sodium carbonate solution per liter of water, thus obtaining a value of 11.

The results of the third series of tests are shown in Table XI. The effect of raising the pH, or of increasing the alkalinity of the pulp during grinding, was to reduce the efficiency of grinding quite appreciably. Under acid conditions, however, increased efficiency was obtained at the expense of the metal; even the chromium steel balls lost weight to a marked degree when the pulp was acid.

Finally, a series of tests was run for the purpose of determining the relative grinding effects of carbon steel balls, chromium steel balls and mixtures of equal numbers of two types of balls. The results of some of these tests are given in Table XII.

In each of these experiments, 120 balls were used. In tests 1 and 2, Table XII, one-half of the balls were carbon steel and one-half were chromium steel. The balance of the charge in all cases was 2,000 grams silica and 1,000 cubic centimeters tap water. The total iron loss was arrived at by analyzing the solution in the pulp after the balls had been removed. To the pulp 30 cubic centimeters concentrated hydrochloric acid was added. The pulp was then heated gently until the sand appeared white and the liquid clear. The liquid was now filtered from the sand, the sand then being washed a number of times, first with warm dilute hydrochloric acid solution and finally with hot water. The total solution was carefully measured, after which 2,000 cubic centimeters of it was submitted to chemical analysis for iron. The iron loss of the balls was arrived at by calculation, allowance being made for the iron initially present in the silica sand.

A comparison of the results in tests 1 and 3 in Table XII seems to show that an increase in grinding efficiency results from substituting stainless steel for carbon steel balls in the mill, but that this increase is gained largely, if not entirely, at the expense of the carbon steel balls, otherwise the iron loss in test 3, as compared with that in test 1, is hard to explain. Too much emphasis cannot be placed upon the results of two tests only, but there can be little doubt that an improvement in grinding efficiency results from the partial change from carbon to stainless steel.

A further improvement in grinding efficiency came from entirely

replacing carbon steel by chromium steel (compare test results 5 and 5A with test results 1 and 3).

Two experiments in this series were made with a solution of sodium sulphite in place of tap water. The object of this was to determine whether the use of a relatively powerful deaerator would have a noticeable effect upon the behavior of carbon or chromium

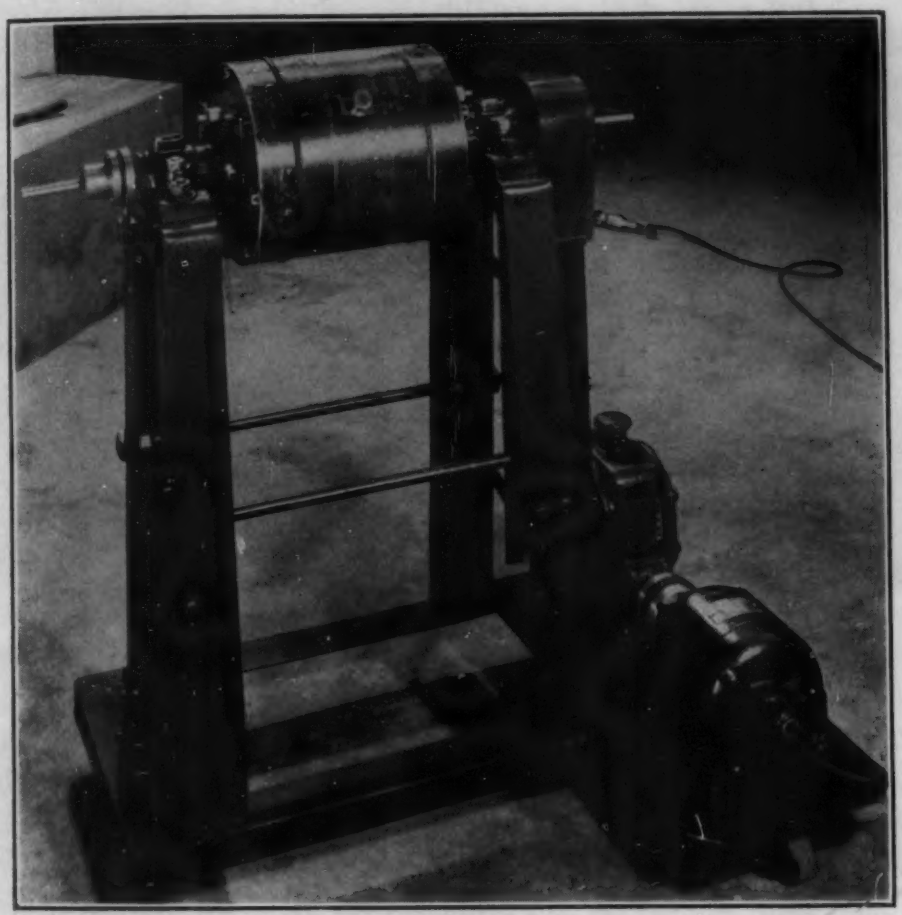

Fig. 7—Photograph of New Mill.

steel balls in the mill, using Ottawa silica sand as the medium of abrasion. A number of experiments in the continuous mill suggested that a deaerator such as sodium sulphite might reduce iron loss, even though it did not improve grinding efficiency. A comparison of the results of tests 1 and 6 in Table XII, which, though they differ in time, test 6 being 4 per cent longer than test 1, suggests that the presence of a deaerator in the mill not only reduces iron loss, but improves grinding efficiency as well. As might have been expected

(cf. tests 5 and 5A with 7) from the results of previous tests, the effect of a deaerator is negligible in the case of stainless steel balls.

We have already referred to the experiments which have been in progress leading to the design of a mill in which (1) the partial pressure of oxygen or other gas could be maintained constant, or (2) the pressure could be measured. Such a mill has at last been

Fig. 8—Showing Mill Knocked Down.

built and preliminary experiments seem to indicate that the design is satisfactory. A photograph of this new mill is shown in Fig. 7. The mill is driven at 60 revolutions per minute by an electric motor through the medium of reducing gear and chain drive. The shafts which support the mill are hollow. Quarter-inch holes extend through them lengthwise and connect with the brass tubes which can be seen at either end of the apparatus. These tubes do not rotate; a seal between them and the rotating shafts being maintained by means of suitable glands. Air or any other gas can be introduced into the mill through one or other of these tubes.

The mill itself is divided into five sections, two relatively heavy end plates, two rubber coated metal diaphragms, and a central portion, which may be looked upon as the mill proper. Each end plate is fitted with a spiral groove of semicircular section. The spiral groove in one end plate can be seen in Fig. 8. At the center of the spiral groove, which corresponds approximately with the center of the end

plate, connection is made with the mill proper through a hole in one of the diaphragms, which, elsewhere, separates it from the mill proper. At the other end of the spiral, a small straight hole, lying parallel to the axis of the mill, meets another which extends to the center of the end plate. This hole is at right angles to the axis of the mill and connects with the hole which extends through one of the shafts which supports the mill. It is through this series of holes and the spiral that communication is maintained between the outside and the inside of the mill. Communication can be interrupted at will at either end of the mill by closing one or other of the valves which can be seen in Fig. 7 fitted into the end plates of the mill. The seats of these valves are situated at the ends of the small holes opposite the spirals. By closing one or other of these valves, the small holes can be closed. If both valves are closed, the mill becomes hermetically sealed. When it is desired to make a run in oxygen, oxygen can be passed through the mill while the mill is standing still or running, until the mill and its contents are saturated with oxygen. The valves can then be closed and the mill hermetically sealed. The pressure inside the mill at the moment the valves are closed will be atmospheric. The mill can be run for any period of time, at the conclusion of which one or other of the valves can be opened so that communication between the inside of the mill and a manometer connected with one of the brass tubes at the end of the mill can be established; the change in pressure in the mill can be immediately determined. Measurements of pressure can be made at intervals throughout a run. It has been found advantageous to do this at intervals rather than to have continuous communication between the inside of the mill and the manometer during a run, because of slight leakage which occurs at the glands. This leakage is, at worst, very slight, even during a long run, hence the loss of pressure occurring during the opening and closing of a valve when measuring pressures is negligible.

The spiral and diaphragm arrangement, which has proved an efficient means of retaining the charge in the mill and at the same time of insuring continuous communication with an atmosphere, developed from a suggestion made by one of the author's colleagues, Mr. J. B. Bassett, who remarked that it might be possible to apply the well known ball mill scoop principle to the solution of the problem which confronted the author.

Using this mill it has already been possible to confirm the fall in pressure which occurs during a run in a hermetically sealed mill with

air or oxygen as the atmosphere. It is hoped that within a relatively short time still further interesting information regarding the wear of metals under ball mill conditions will have been obtained.

Conclusions

To the conclusions quoted in the fourth paragraph of this paper may be added the following:

1. When tested in a small continuous mill, open to the air, and with silica, feldspar, talc or marble as the media of abrasion, the higher the carbon content of ferrous alloys (straight carbon; 2½ per cent nickel; 2½, 7½ and 15 per cent chromium) containing from 1 per cent to 3 per cent of carbon, the lower is the resistance to abrasion.
2. However, under the same conditions of test, but using Lake Shore (Kirkland Lake camp) primary bowl sands as the medium of abrasion, the higher the carbon content of straight iron-carbon alloys, the higher is their resistance to abrasion.
3. The order of wear of iron-carbon alloys when tested under certain specified conditions in hermetically sealed porcelain jars, containing air as atmosphere and Lake Shore primary bowl sands as the medium of abrasion, is the same as that in a continuous mill open to the air, using the same medium of abrasion; the higher their carbon content, the higher is their resistance to abrasion.
4. The order of wear of iron-carbon alloys when tested under the same conditions as above, i.e., with Lake Shore primary bowl sands as the medium of abrasion, but with oxygen as the atmosphere instead of air, is reversed; the higher their carbon content, the lower is their resistance to abrasion. Oxygen in some way counteracts the effect of an as yet undiscovered factor which causes Lake Shore primary bowl sands to behave as an abrasive medium in a somewhat anomalous manner.
5. The mineralogical hardness *per se* of such minerals as silica, feldspar, marble, talc and Lake Shore Primary bowl sands is apparently not the only property which can affect the wear of alloys in ball mills.
6. Whereas the losses of weight of iron-carbon alloy balls of carbon contents varying from 1 per cent to 3 per cent are much greater than that of iron-carbon-chromium (15 per cent chromium)

alloy balls of approximately the same carbon content, when tested in oxygen, and are somewhat greater when tested in air, they are practically the same when tested in an oxygen-free atmosphere, such as cracked ammonia. In tests conducted in hermetically sealed porcelain jars with silicon carbide as the medium of abrasion, the value of chromium in conferring resistance to abrasion on iron-carbon alloys is lost in the absence of oxygen. The outstanding significance of oxygen in controlling the rates of abrasion of ferrous alloys is emphasized by these results, which focus attention on the question whether there are opportunities in mill practice where consideration might be given to the substitution of neutral or oxidizing atmospheres for the purpose of reducing iron loss.

7. In a hermetically sealed mill filled with oxygen at normal temperature and pressure (charge: 200 pounds of balls, 50 pounds of silica and 50 pounds of water) the pressure ultimately falls below atmospheric, despite the elevation of the temperature in the mill due to the work of the grinding, etc. It would appear that this decreased pressure is caused by reaction between iron and oxygen, with resultant formation of iron oxide.
8. In view of the above, the results of abrasion tests conducted in hermetically sealed mills, and particularly such as are lined with ferrous materials, must be interpreted with great care.
9. The indentation hardness of ferrous alloys affords no clue to their resistance to abrasion in ball mills. This is made clear (a) by the results of the tests with Lake Shore primary bowl sands referred to in clauses 3 and 4 above, in which, other things being equal, the atmosphere was changed from air to oxygen, with the result that the order of wear of a series of iron-carbon alloys containing from 1 per cent to 3 per cent of carbon was reversed, and (b) by the results of tests with two alloys of very similar microstructure and almost identical in indentation hardness, the one of which lost about three times as much weight as the other during the same period and under the same conditions of test.
10. When carbon steel balls and chromium steel balls are tested together in a porcelain jar using air as the atmosphere and Ottawa silica sand as the medium of abrasion, the rate of wear of the former increases much more rapidly than that of the latter, as the weight of the charge is raised. This fact, in the light of the statement recorded in clause 6 above, suggests that ferrous alloy

balls, when tested in atmospheres containing oxygen, become coated with layers of oxide whose physical properties are determined, other things being equal, by their compositions. The hypothesis that the physical properties of the oxide layers formed on ferrous alloy balls determines both their grinding efficiencies and their rates of wear will be recognized as worthy of careful consideration by operators of large ball mills. A search for alloys having oxides with suitable physical characteristics might, in certain cases, produce worthwhile economies in mill operation.

11. This fact suggests also that it might be desirable to avoid using mixtures of alloys in ball mill experiments of the general type now under discussion.
12. The physical properties of the oxide layers formed on ferrous alloy balls may not only determine their rates of wear but their grinding efficiencies as well. A soft friable oxide layer would tend to reduce the crushing effect of two balls upon a particle of mineral pinched between them. A hard tenacious layer might well increase the crushing effect over that which would obtain even when clean metal surfaces were involved.
13. It seems not unlikely that the work of grinding in a ball mill may be divisible into two portions (i) that which is applied to the production of new surface in the medium being crushed and (ii) that which is employed in the production of new metal surface, metal surfaces on particles which ultimately appears in the mill as oxide.
14. In experiments involving the use of hermetically sealed porcelain jars (atmospheres—various: medium of abrasion—Ottawa silica sand) a relationship has been shown to exist between percentage loss of weight of balls and grinding efficiency.
15. In similar experiments with air as the atmosphere in the jars, the efficiency of grinding has been found to increase as the result of lowering the pH of the charge, but this increased efficiency is obtained at the expense of the metal of the balls.
16. An improvement in grinding efficiency results from a partial substitution of 15 per cent chromium-carbon for carbon-steel balls, and a still further improvement obtains when 15 per cent chromium-carbon steel balls entirely replace carbon-steel balls in the charge.
17. The results of experiments in which a solution of sodium sulphite was used in place of water, with silica sand as the medium

of abrasion, suggests that the presence of a de-aerator in a ball mill will reduce iron loss and, at the same time, improve grinding efficiency. The question whether aluminum powder, graphite, etc., might not be of value as de-aerators is one which merits consideration.

Acknowledgments

The author wishes to express his appreciation of the encouragement given him in this work by Dr. H. B. Speakman, Director of the Ontario Research Foundation, and the help given him in the prosecution of this work by Mr. T. E. Norman, now with Climax Molybdenum Co., Denver, Colo., Mr. P. Cavanagh, now with the Steel Company of Canada, Hamilton, Ontario, Mr. J. B. Bassett, now with the Otis-Fensom Elevator Company, Limited, of Hamilton, Ontario, and Mr. W. H. Milburn, of the Foundation staff.

DISCUSSION

Written Discussion: By T. E. Norman, metallurgical engineer, Climax Molybdenum Co., Denver, Colo.

The paper Mr. Ellis has presented here today is particularly interesting to us since it described investigations bearing similarity to a number of tests we have conducted during the past two years. We would like to say at this time that the inspiration for many of our tests was obtained from Mr. Ellis' previous papers on this subject.

The tests we have conducted to investigate the wear resistance of grinding balls have employed a technique which is quite similar to that used by Mr. Ellis. An important difference, however, between our tests and his is to be found in the dimensions of the balls and equipment used. Our tests were conducted on balls which were 3 inches in diameter while Mr. Ellis used balls 1 inch in diameter. The mills used in our tests were 3 feet in diameter or larger, while those used by Mr. Ellis were approximately 1 foot in diameter or smaller. In view of this, it may be of interest to make a few comparisons between Mr. Ellis' results and our own.

First, a fundamental difference between rates of wear in small and large mills should be considered. It can be shown by a simple process of mathematical reasoning that where two ball mills of different diameter are operating under comparative conditions, then the rate at which the grinding balls will wear per unit of their weight or surface area will vary directly as the 0.5 power of the mill diameter. Actual experimental evidence indicates this figure more closely approximates the 0.6 to 0.7 power of the mill diameter. On this basis the relative rates of wear of balls (per unit of their weight or surface

area), when operating under comparative conditions in ball mills 1 foot, 3 feet and 9 feet in diameter respectively, will be approximately 1.0, 1.9 and 3.7.

What is the nature of this increased rate of wear which occurs as the mill diameter increases? Does it represent an increase in rate of removal of an oxide film? Or, on the other hand, is the oxide film completely penetrated with the result that metallic particles are also removed? This question will be considered again toward the latter part of this discussion.

An increase in ball size or an increase in the size of the ball mill generally increases the forces of impact created between the balls. It is reasonable to conclude therefore, that the balls in our tests were exposed to greater forces of impact than those in the tests run by Mr. Ellis. This may explain why we fail to check his conclusion that sand cast white iron wears better than chill cast iron. In our tests the opposite result has been consistently obtained. Table A gives a number of results we have obtained on cast iron balls when tested under various abrasive conditions. All tests were conducted with a continuous flow of abrasive passing through the mill. The results in this table indicate rather definite superiority for the chill cast iron balls.

Table A

Relative Abrasion Resistance of 3-Inch Sand Cast and Chill Cast Iron Balls Under Various Conditions of Test

Test No.	49			50			C-3		
Abrasive	Climax Ore			Feldspar			Climax Ore		
Mill Diameter	3′			3′			6′		
Per Cent Solids	75			76			77		
Duration of Test (hours)	24			24			145		
	Hardness	Analysis					Relative		
Type of Ball	B.H.N.	C	Mn	Si	Cr	Mo	Rates of Wear*		
Chill Cast P.C. Iron	460	2.72	0.5	0.3	...	....	140	172	160
Sand Cast P.C. Iron	444	3.05	0.5	0.4	...	....	171	222	...
Chill Cast Cr-Mo Iron	512	3.20	0.6	1.7	0.9	0.25	...	...	144
Sand Cast Cr-Mo Iron	477	3.00	...	0.9	0.8	0.25	...	...	180

*Rates of wear are based on a figure of 100 for forged martensitic steel balls containing 0.88 per cent carbon, 0.50 per cent manganese, 0.20 per cent molybdenum.

Table No. IV of Mr. Ellis' paper contains results on relative rates of wear in various abrasives, which, if duplicable to any reasonable degree in commercial grinding operations, may have great practical value. This table indicates that some abrasives tend to produce relatively small differences in the rates of wear of different types of balls while other abrasives tend to produce relatively large differences. In an attempt to investigate this matter we have run tests of a somewhat similar nature in which over eighty groups of 3-inch balls of various analyses or heat treatments were involved. The tests were run in ball mills three feet or larger in diameter through which a continuous feed of abrasive pulp was passed. The average results from three types of forged steel and one type of cast iron have been selected for presentation here since we believe they illustrate some of the more outstanding information obtained from these tests. The types are as follows:

Group No. 1 is representative of a forged martensitic steel containing 0.70

to 0.85 per cent carbon. In most cases the steel contained 0.20 to 0.30 per cent molybdenum to give it depth hardening properties. Balls of this steel were used in the water-quenched condition.

Group No. 2 is an unalloyed steel similar in carbon content to group No. 1. It was oil-quenched to produce balls having a uniform hardness of approximately 375 Brinell.

Group No. 3 represents a forged steel similar in analysis to group No. 2. It was air-quenched to produce balls having a uniform hardness of approximately 270 Brinell.

Group No. 4 represents unalloyed chill cast iron balls having an analysis range of 2.70 to 3.00 per cent carbon, 0.30 to 0.80 per cent silicon, 0.50 to 0.80 per cent manganese, 0.10 to 0.20 per cent sulphur, 0.10 to 0.20 per cent phosphorus. Their average hardness was approximately 460 Brinell.

The relative performance of these four groups in five types of abrasives is shown in Fig. A. The abrasion factors represent rates of wear relative to a nominally adopted figure of 100 for group No. 1, which in all our tests has been the standard for comparison. In this method of comparison, the lower the abrasion factor, the better is the wear resistance of the group. The Brinell hardness of each of these four groups is also plotted in Fig. A.

The abrasives were, in general, run at pulp densities of 75 to 80 per cent solids. The curve for "sand" represents the results from a washed river sand in which quartz predominated. The sand also contained appreciable quantities of feldspar. The tests with sand were run in a mill 3 feet in diameter operating at 32 revolutions per minute.

The curve for Homestake ore represents the results from a 10-day run in a 5-foot diameter ball mill at the Homestake Mining Company in Lead, South Dakota. The mill operated on a feed of partially ground de-slimed ore coming from the rod mills. The mineral in this ore which creates the predominating abrasive effect is not definitely known but is believed to be quartz.

The curve for Climax ore represents the results of a 7-day run in a 6-foot diameter mill at our operations in Climax, Colorado. The abrasive minerals in this ore are mainly quartz and feldspar in about equal proportions, with minor amounts of pyrite, fluorite and topaz present.

The curves for feldspar and calcite were obtained in the same 3-foot mill as that used for sand. Each of these minerals was relatively pure.

The results from Fig. A illustrate the necessity of considering the character of the abrasive when attempting to evaluate the relative merits of various types of balls. It is interesting to note that we agree with Mr. Ellis in this respect, even though our series of balls was, in general, quite different from his series.

A point which is interesting to note in our Fig. A is the relative performance of pearlitic steels and cast iron when tested in each of the five abrasives. The reversal of the trend for cast iron when run in feldspar or calcite bears some resemblance to the reversal Mr. Ellis noted for cast iron when run in Lake Shore sands.

The results from groups 1 to 3 of our Fig. A serve to illustrate that indentation hardness does have a pronounced influence on the wear resistance of balls, particularly when run in feldspar or calcite. We would like to qualify

this conclusion, however, by stating that so far as we have been able to determine, it applies only to steels and does not apply with any degree of reliability to cast irons. Also, in the case of steels, compositional changes or changes in quenching temperatures may often overshadow the effect of high indentation hardness. Another condition in which we have found that indentation hardness offers no clue to wear resistance is where the ball contains high proportions of retained austenite.

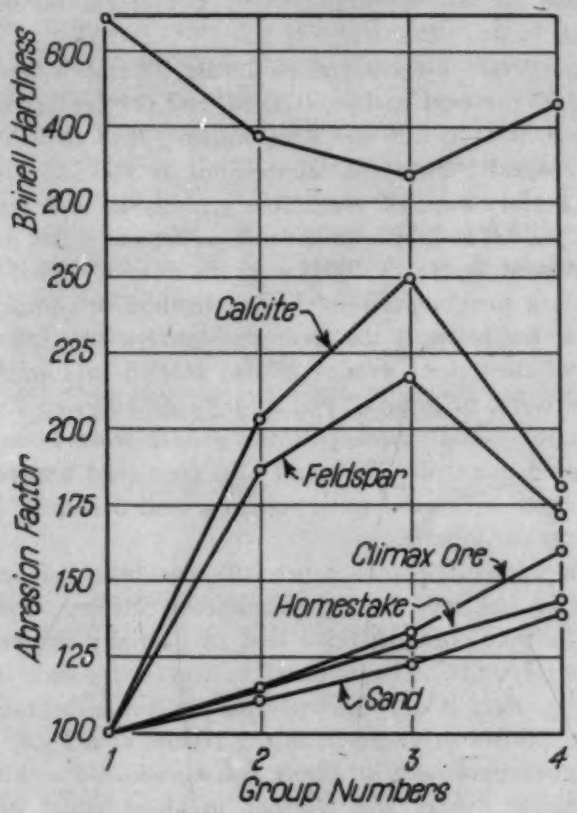

Fig. A—Relative Rates of Wear of Four Types of Balls in Various Abrasives.

Mr. Ellis' data on the effect of the oxygen concentration on rates of abrasion is decidedly interesting. We suspect, however, that when small balls are tested in a laboratory jar mill an abrasive condition exists which favors the removal of the continuously reforming oxide film, together with only minor proportions of metallic iron. We have previously pointed out that when the diameter of the ball mill is increased, the rate of wear per unit of exposed area also increases. We suspect that much of this increased rate of wear takes place by removal of iron as metallic particles. If this is the case, then a point may soon be reached, as the diameter of the ball mill is increased, where the removal of iron as metal greatly overshadows its removal as oxide film.

We have made a brief study of the relative importance of oxide films on the wear of 3-inch balls when run in a mill 3 feet in diameter. A test

was run in which a series of batches of crushed Climax ore (diluted with tap water to 70 per cent solids) was ground in an atmosphere estimated to contain 85 to 95 per cent oxygen. The tests were run with both ends of the mill sealed except for small inlets and outlets to allow a continuous flow of oxygen to pass through the mill. Each batch of pulp was saturated with oxygen before the balls were charged into the mill.

The percentage of increase in rate of wear of two commercially produced types of balls which resulted from this oxygen atmosphere is shown in Table B. This increase is as compared with the normal wear in an air atmosphere with all other conditions remaining the same.

It is generally recognized that alkaline pulps tend to reduce the rate of oxidation of ferrous materials in a ball mill. This effect is quite noticeable when we compare the results of Tests 1, 3 and 5 in Table XI of Mr. Ellis' paper. To investigate this, our 3-foot mill was used to run a series of batch tests, in an air atmosphere, with Climax ore as abrasive. The pulp was made alkaline by the addition of 18 pounds of $Ca(OH)_2$ and 5 pounds of $Na(CN)$ per ton of water in the pulp. The results with this alkaline pulp were compared to results with a "natural pulp" (ore and tap water) run under the same conditions. The reduction in rate of wear as a result of making the pulp alkaline is given in Table B.

Table B
Changes in Rates of Wear Caused by Changes in the Oxidizing Conditions in a 3-Foot Ball Mill*

Type of Steel	Carbon Per Cent	Hardness B.H.N.	Wear in Oxygen Per Cent Increase	Wear in Alkaline Pulp Per Cent Decrease
Pearlitic Forged Steel	0.75	370	39	10.7
Martensitic Forged Steel	0.85	685	19	7.4

*Rates of wear were compared with those from tests run in an atmosphere of air with a neutral pulp. All other conditions of test remained the same.

It is interesting to note from Table B that the changes in rates of wear which we obtained by use of an oxygen atmosphere or by making the pulp alkaline were not nearly as great as those obtained in any of Mr. Ellis' tests. It is suggested the reason for this may be that in our tests the removal of oxide film did not represent nearly as great a proportion of the total wear as it did in Mr. Ellis' much smaller jar mills.

Additional evidence is available from commercial ball mill practice to indicate that iron is often removed from the balls as metallic particles. The ground pulp obtained from wet grinding operations will, when allowed to stand, generate surprisingly large volumes of hydrogen. This hydrogen is believed to come from the decomposition of water by metallic iron. Often these particles of iron can actually be separated from the pulp by use of concentrating tables.

The value of Mr. Ellis' studies on the relation of oxide films to wear should not be under-emphasized. There seems to be little doubt that the formation and physical characteristics of oxide films have a pronounced influence on many

types of wear. We believe, however, that before Mr. Ellis' findings can be properly applied to commercial grinding problems, it would be advisable to investigate the nature of the increase in rate of wear which occurs as the mill diameter is increased.

The data presented by Mr. Ellis on the relative grinding efficiencies of carbon and chromium steel balls is very interesting. It is difficult to imagine an oxide film having a thickness of probably not more than half a micron as being capable of "cushioning" the grinding of particles having diameters between 75 and 1000 microns. However, another explanation for the better grinding efficiency of chromium steel may be that this chromium oxide film develops a greater coefficient of friction, between itself and mineral particles, than is obtainable from films of iron oxide. This in turn may allow the mineral particles to be "nipped" more effectively when caught between the spherical surfaces of two balls. Whatever the explanation may be, the results are such that they may have valuable commercial significance. In view of this it would be desirable to see if these results could still be obtained when the grinding is done in larger mills.

Written Discussion: By J. S. Vanick, development and research division, International Nickel Co., New York.

In 1935 I had the privilege of discussing the results of 5 years of wear testing which Mr. Ellis and his Associates reported in a paper to the American Foundrymen's Association.[1] Since then, Mr. Ellis has answered every question I raised at that time and I should be satisfied with the thorough, comprehensive results which he has presented here. But the wear of milling equipment is so complex a problem that its many angles offer unlimited inducements for further research.

In this work Mr. Ellis has uncovered important evidence that abrasion and corrosion go hand in hand in determining the wear rate of grinding balls. The fact that relatively pure minerals like quartz, feldspar and talc follow a rational course while the Lake Shore Mining Company's sands upset the schedule seems convincing evidence that mineral aggregates must be individually tested to establish their wearing rates upon the materials used in the grinding circuits. This comment represents the mill man's point of view, and Mr. Ellis is aware, I am certain, of the many factors which influence the final result.

Most ores are aggregates containing widely varying quantities of different minerals. From the practical standpoint one of the problems in ore milling is to adjust the feed of these minerals to arrive at a uniform end product. The ore may vary from mine to mine, and indeed from face to face in the same mine. Factors contributing to the abrasion result may vary between wide extremes. We might qualitatively attempt to describe the solids as hard or soft, round or angular, sharp or dull, smooth or rough, greasy or sticky, and fine as dust or coarse enough to include ¾ inch and possibly 1 to 2-inch sizes. Liquids might be corrosive or inert, decomposable or stable, abrasion neutralizing, like oil, or abrasion aggravating, like water, and the temperatures involved might vary between hot or cold. Combinations of operating conditions in milling in-

[1] "The Wear Resistance of White Cast Iron," *Transactions*, American Foundrymen's Association, 1935, Vol. XLIII, p. 511.

volving the size of the mills, design of the liners, size of balls or rods, the ball or rod load, size of feed and discharge product, kind of water, quantity and level of overflow, whether the mill is run with a full load, underfed or overfed, etc., introduce additional factors. Ore milling is an integration of these numerous factors. The effects are so difficult to isolate that in most cases we have approached this type of abrasion problem along the same lines that we approach the corrosion problem and attempt to evaluate the materials employed by making them part of the mill circuit or subjecting them as nearly as possible to the conditions prevailing in service.

Mr. Ellis' work has ably demonstrated the importance of the corrosion factor in affecting ball mill wear. There is hope in these results that tests made in small mills or porcelain jars will offer a guide to the results which might be expected in large production mills. One factor upon which more emphasis might be needed is the measure of grinding efficiency which reports the amount of new surface formed, representing the amount of grinding done upon each product. The screen tests in Tables VII and IX represent this type of work and emphasize the need for following a standard procedure in achieving a result which should be of interest to the grinding mill operators.

Complex metallurgical factors seem to add to the difficulty of evaluating the performance of different materials. For instance, in Fig. 2 the Ni-Hard composition seems to excel the steel composition of similar alloy content. The results for iron-carbon alloys showing an increase in abrasion loss for the higher carbon unalloyed compositions would suggest that Ni-Hard might similarly show a higher abrasion loss than its low carbon nickel-chromium (A-17) companion composition. In Fig. 2 the results are exactly opposite and may be due to the austenitic condition of the relatively low carbon steel alloy.

Actually, steels of the austenitic nickel-chromium alloy type such as Mr. Ellis has reported upon in Fig. 2 and in Table VIII have been made and are expected to show encouraging results against competing high alloy steels. Their use has been brought about mainly through the need for a higher degree of toughness in the Ni-Hard type of product rather than through the expectation of greater abrasion resistance. If, however, the results which Mr. Ellis presents indicate that this austenitic nickel-chromium alloyed steel may excel a corresponding austenitic manganese steel by as much as 3 to 1, then some relation between these steels and the white iron end of the series of alloyed grinding ball compositions might be ventured from such production tests as are available.

Reports[2] upon five sets of Marcy rod mill liners matching Ni-Hard against austenitic manganese steel showed a three to two performance in terms of tons ground in favor of the Ni-Hard. Another 6 by 5-foot ball mill, grinding gold ore with 4-inch balls, developed a 2.8 to 1 advantage over chilled white iron in terms of tons of ore milled.

Where white iron grinding balls have been matched against the nickel-chromium alloyed Ni-Hard type, the Ni-Hard has confirmed the above results showing an advantage of 2½ to 3 times the wear resistance of white iron. C.

---

[2]J. E. Kerr, "Nickel's Role in Milling Equipment," *Engineering and Mining Journal*, Dec. 1939, Vol. 140, No. 12, p. 56.

H. Benedict,[3] Calumet and Hecla Mining Company, reported the results of this order obtained on mills grinding copper conglomerates in the Lake Superior area.

These comparisons taken from production milling of ores are offered to lend some emphasis to the importance of Mr. Ellis' work. There are fine details in the metallurgy of some of the products tested which might be discussed at length without assurance that the final results would be significantly altered. As instances: (1) the impression that chill cast white iron is inferior to sand cast (Fig. 1); (2) the possibility that the performance of the alloys shown in Table IV could be upset if the materials were processed with the object of developing them into their best condition for the intended test; and (3) the possibility that microstructures of materials of identical composition might be important in effecting their performance (page 263).

The work which Mr. Ellis and his associates have engaged in is bound to penetrate the fog which so completely obscures the function of the many factors which enter into abrasion wear. His work offers the prospect that a test procedure may be devised which can be applied for any specific conditions involving the production milling of ores to develop the most suitable material for use in the grinding mill.

Oral Discussion

NEIL METCALF:[4] The company with which I am associated is a large producer of forged steel grinding balls used extensively in the Canadian Gold Mining fields and other industries.

In regard to the ninth conclusion in Mr. Ellis' paper, it is our experience that users very quickly note increases in their grinding costs if indentation hardness falls off. In this premise we are in agreement with Mr. Norman. It should be noted that a steel and not a cast iron ball is being referred to.

Author's Reply

It affords me great pleasure to reply to the contributions which Messrs. Vanick and Norman have made to the discussion of my paper. The former is to be congratulated on the clear, concise picture which, in paragraph three of his contribution, he has presented of the numerous factors which enter into the process of ore milling. Among these he has included the sizes of balls or rods, and the ball or rod load, and it is of interest to observe that Mr. Norman has laid stress on the importance of these factors. That I have not overlooked their importance and that of other factors enumerated by Mr. Vanick is known to both these gentlemen. It is well, however, that attention should be directed anew to their importance, because they should be borne in mind by all those who have occasion to consider such results as are presented in the author's paper.

I am glad that Mr. Vanick has emphasized the value of measuring grinding efficiency in such tests as I have reported. We at the Ontario Research

[3] "Ore Concentration and Milling," *Mining and Metallurgy*, Feb. 1941, p. 70.
[4] Metallurgist, Burlington Steel Co., Hamilton, Ont.

Foundation are only at the beginning of work along these lines. As has been pointed out on page 263 of the paper, tentative results only could be expected until a correctly designed mill was available for use.

Mr. Vanick has picked out an interesting point regarding the high and low carbon alloys of Ni-Hard composition. I believe, however, that he has misinterpreted the information given in the paper. Fig. 2, which shows Ni-Hard to be superior to A 17 (a low carbon alloy of Ni-Hard analysis), refers to tests in Lake Shore sands. Now, in Lake Shore sands (continuous mill) the higher the carbon content of straight iron-carbon alloys, the *higher* is their resistance to abrasion, as is stated in conclusion 2 on page 274 of the paper. In Lake Shore sands, therefore, the Ni-Hards, as we may call them, behave relatively, one to the other, as do the straight iron-carbon alloys. It certainly would be interesting to determine how they would behave in these media of abrasion (silica, etc.) wherein the higher the carbon content of the straight iron-carbon alloys, the *lower* is their resistance to abrasion.

Another point which Mr. Vanick has dealt with in his discussion is that of the relative resistance to abrasion of austenitic manganese steel and austenitic nickel-chromium alloy steel. In this connection the author intends to add, in the final proof of his paper, to that part of the abstract which deals with the tests on these austenitic alloys, the words "when tested in an atmosphere of oxygen". The statement relating to these alloys as it stands in the preprint is quite misleading. When tested in air (see Table VIII) the Ni-Hard steel lost three-quarters of the weight of the manganese steel under the same conditions of test which caused the former to lose only one-third of the weight of the latter when tested in oxygen.

The results of the large scale experiments reported by Kerr and by Benedict and referred to by Mr. Vanick are most interesting. Mr. Vanick refers to the impression created by Fig. 1 that chill cast white iron is inferior to sand cast white iron. It is of interest to note that Mr. Norman has failed to check the author's results when using heavier balls and larger mills. We are inclined to accept his view that the greater impact forces involved in his tests account for the difference between his results and ours. It is probable that the coarser structure of the sand cast balls may render them, in the absence of impact, more resistant to abrasion than the chill cast balls, while the coarser structure might cause them to disintegrate more readily when impact forces begin to predominate. We use the word "disintegrate" advisedly, because we are sure that something more than abrasion occurs under the conditions of Mr. Norman's tests. In his tests, wear comprises both loss of weight due to abrasion and loss of weight due to disintegration. In our tests, disintegration approaches a minimum, though it is not entirely absent.

The results of Mr. Norman's tests, which are illustrated in his Fig. A, deserve special attention. The anomalous, if such it can be called, behavior of cast iron when tested in calcite and feldspar naturally attracts one's attention. One is prompted to inquire what would happen if similar tests were run in oxygen.

Mr. Vanick hints at, and Mr. Norman emphasizes, the importance of indentation hardness in determining resistance to abrasion. I still feel that my remark that "indentation hardness tests offer little, if any, clue to the behavior

of alloys under abrasion" should stand, but I am prepared to qualify it by stating that the resistance to abrasion of an alloy can, in many instances, be increased by treatments which cause an increase in indentation hardness. I have been surprised, however, at the relatively small improvement in resistance to abrasion which, in many tests, has resulted from hardening steel alloys by quenching in water. I have sometimes questioned whether the increase in cost of balls due to heat treatment does not more than counterbalance the decrease in cost of milling due to the reduction in loss of weight as a result of abrasion. Mr. Norman's tests with large balls (see his Fig. A) suggest that quenched balls of suitable analysis are definitely superior to normalized balls of small carbon content. It would be interesting to know the actual over-all savings which have resulted from the use of martensitic in place of pearlitic balls, etc.

The results of Mr. Norman's experiments on the effects of oxygen and alkalinity serve to support the author's findings. Mr. Norman's suggestion, that the differences between his results and those described in the paper are, in all probability, related to what I have described above as "disintegration", seems logical. The author is impressed by the thought that what should be sought for in this connection are alloys which will not readily disintegrate and whose oxide film will not readily abrade.

The alternative explanation which Mr. Norman offers for the greater grinding efficiency of chromium steel balls as compared with straight carbon steel balls is worthy of attention. A comparative test of straight carbon and chromium balls on a large scale would be well worth while. It may be asking too much to suggest that Mr. Norman consider the use of his mill in this connection. Nevertheless, I throw out the hint.

Replying to Mr. Metcalf, we are aware that in a given steel, or, for that matter, a cast iron, of given composition, variations in hardness resulting from variations in heat treatment will affect the rate of wear of the balls—the harder the steel or cast iron the greater, generally speaking, the resistance to abrasion. I say "generally speaking" advisedly, however, because I have yet to be convinced that cases will not arise where, for example, heat treated (hard) steel, or iron, balls of the same composition as unheat treated (soft) steel, or iron, balls will wear more rapidly than the unheat treated (soft) steels, or iron, balls. In other words, I still believe that certain abrasives will sooner or later be found that will affect hard ferrous materials as seriously as, if not more seriously than, soft ferrous materials of the same composition, though such cases may be rare.

In closing, I wish to remark that I am happy to know that the work which has been carried out at the Ontario Research Foundation has served to inspire others to work along these same lines.

MICROSTRUCTURAL CHARACTERISTICS OF HIGH PURITY ALLOYS OF IRON AND CARBON

By Thomas G. Digges

Abstract

A study was made of the microstructural characteristics of slowly cooled high purity alloys of iron and carbon of hypereutectoid composition and of the influence of certain impurities (oxygen, aluminum, and hydrogen) on the structures of the slowly cooled alloys. The alloys were prepared from 17 irons, varying in degrees of purity, by carburizing in a mixture of hydrogen and benzene vapor. The structure of the carburized irons of highest purity, free from aluminum and with a total of less than 0.009 per cent identifiable impurities, contained free ferrite in the hypereutectoid zone. If oxygen were responsible for this structural feature, then a minute amount was sufficient and as effective as larger quantities. Aluminum in excess of about 0.001 per cent prevented the formation of free ferrite and alumina was not the factor responsible for its formation in these alloys. The hydrogen dissolved in the irons during carburization had no detectable effect on the divorcement of ferrite. The experimental results indicate that a structure containing free ferrite is characteristic of very high purity alloys of iron and carbon of hypereutectoid composition that have been slowly cooled from the austenitic condition.

Introduction

THE existence of free ferrite adjacent to coalesced masses of cementite in the hypereutectoid zone of carburized specimens from certain heats of plain carbon steel was reported in 1922 by McQuaid and Ehn (1).[1] Steels showing this lack of perfection in the crystallization of pearlite after carburizing were designated as "abnormal". Such steels usually have relatively fine-grained austenite at the carburizing temperature. In "normal" steels the austenitic

[1]The figures appearing in parentheses refer to the references appended to this paper.

A paper presented before the Twenty-third Annual Convention of the Society held in Philadelphia, October 20 to 24, 1941. The author, Thomas G. Digges, is metallurgist, National Bureau of Standards, U. S. Department of Commerce, Washington, D. C. Manuscript received May 23, 1941.

grain size usually is relatively large and, after slowly cooling from the carburizing temperature, the pearlite extends continuously to thin envelopes of cementite in the hypereutectoid zone. In McQuaid and Ehn's practice, the surfaces of the normal steels were completely hardened whereas the surfaces of the abnormal steels frequently contained soft spots after the quenching treatment. Abnormality was attributed to the presence of oxides, either in solution or as submicroscopic particles.

The choice of the words "normal" and "abnormal" to designate the differences in structure and hardenability of these carburizing steels appeared to be reasonable and suited to this specific use. The terms are clear to all when they are restricted to their original application, namely, to plain carbon steels of the carburizing type, but confusion results when the terms are applied to other grades of alloys and steels. This nomenclature has been the concern of many metallurgists as shown by the comments of Epstein and Rawdon (2), Davenport and Bain (3), and others. To eliminate confusion in the present report the terms "normal" and "abnormal" will be retained only for reference to previous investigations. The structures produced in the slowly cooled alloys may be completely identified by representative micrographs and by naming all the constituents therein observed, such as free ferrite, massive cementite, or cementite and pearlite. The structure containing free ferrite (divorced ferrite) corresponds to that previously designated as abnormal.

The present study was made primarily to determine the influence of small amounts of impurities, particularly oxygen, aluminum, and hydrogen, in different irons, on the structures produced by oxygen-free carburizing followed by cooling slowly and at a constant rate through the transformation range.

Previous Investigations

McQuaid and Ehn's work with commercial steels was followed by numerous investigations carried out by carburizing both commercial steels and high purity irons. A survey of some of the publications on this subject shows wide differences in opinions regarding the factors responsible for normality and abnormality. In 1928, Epstein and Rawdon (2) pointed out that many cases of abnormality in commercial steels seemed to be associated with the use of aluminum for deoxidizing, although abnormal steels could be produced in

other ways. Nothing arose during their experiments to disprove Ehn's theory that abnormality was due ordinarily to the presence of oxides, perhaps dissolved but more probably undissolved. Several years later, Grossmann (4) was of the opinion that abnormality was due to oxygen dissolved during carburization.

In 1932, Duftschmid and Houdremont (5) reported the presence of abnormal structures at the surfaces of electrolytic and carbonyl irons after carburizing. They contended that a prerequisite to abnormal structure was a rapid rate of crystallization which occurred when the Ar_1 transformation took place at a very high temperature. The regions of highest purity were believed to be responsible for abnormality in carburized structures.

Bain (6) reported, in 1932, the results of carburizing experiments with a variety of irons obtained from widely different sources. These irons developed abnormal structures in pack carburizing and, with one exception, in oxygen-free carburizing. The exception was a hydrogen-treated iron which was almost entirely normal after carburizing in pure hydrogen and hydrocarbon. This iron contained 0.005 per cent carbon, 0.003 per cent sulphur, 0.028 per cent manganese, 0.004 per cent phosphorus, 0.0012 per cent silicon, 0.003 per cent oxygen, and 0.0001 per cent nitrogen. With other irons containing aluminum in excess of 0.4 per cent, normal structures were produced by carburizing in hydrocarbon and abnormal structures were developed in the outer portion of the hypereutectoid zone by pack-carburizing. Bain at that time was of the opinion that pure oxygen-free iron (perhaps with hydrogen in solution) would be normal after oxygen-free carburizing and that dissolved oxygen lowered the critical point, Ae_1, and at the same time provided the high reaction rate and high carbon-diffusivity responsible for abnormality. To secure a normal structure by the standard McQuaid-Ehn procedure required the presence of an element such as silicon or aluminum, which contributed to deep hardening, or at least materially reduced oxygen solubility. However, in 1934, Davenport and Bain (3) were of the opinion that carburized high purity iron was abnormal.

In 1937, Brophy and Parker (7) reported the results of carburizing experiments with irons containing 0.001, 0.01, 0.1 and 1 per cent aluminum. Normal structures were produced in the cases of all the irons when carburized in a mixture of hydrogen and benzene vapor and abnormal structures when pack-carburized. They con-

cluded that extremely small amounts of aluminum were sufficient to cause abnormality if oxygen was available. However, in the discussion McMullan pointed out that normality or abnormality in steel was a function of composition and cooling rate and that any of the common steels might have their apparent normality or abnormality greatly changed by varying the rate of cooling from the carburizing temperature. Aluminum by itself increases normality and grain size but when both aluminum and oxygen were present in the right amounts the steel was fine-grained, and hence might show an abnormal structure after carburizing. McQuaid was of the opinion that Brophy and Parker's results would have been more conclusive had a definite hypereutectoid case been obtained in both methods of carburizing and that the presence of hydrogen might have affected the final structure obtained by carburizing in hydrogen-benzene atmosphere.

Derge, Kommel and Mehl (8), in 1938, reported the results of carburizing experiments with irons containing aluminum or silicon. All the irons had abnormal structures after pack-carburizing, and normal structures after carburizing in oxygen-free hydrocarbon vapor. This was interpreted as indicating that abnormality under these conditions was due to dissolved oxygen obtained from the carburizing gas rather than to aluminum, Al_2O_3, or oxides already existing in the metal. In the discussion McQuaid reported that his results indicated that steels carburized in a hydrogen-hydrocarbon atmosphere were normal due to the presence of hydrogen and not to the absence of oxygen and that silicon, with or without the presence of aluminum, was an important factor that affected the results obtained after carburizing.

The present writer, in discussing the paper by Derge and coworkers, submitted micrographs showing that abnormal structures were obtained in specimens of iron (total identifiable impurities less than 0.031 per cent) which were carburized, to contents of 1.01, 1.14, and 1.21 per cent carbon, respectively, in oxygen free hydrocarbon vapor, homogenized, and subsequently heated at 1700 degrees Fahr. (925 degrees Cent.) in vacuo and slowly cooled in vacuo. Analyses of duplicate specimens indicated that there was no change in the oxygen content of the specimen (0.003 per cent) during the carburizing treatment and it was difficult to believe that oxygen could have been picked up anywhere in the cycle, to cause the abnormal structures. Derge, however, suggested that oxygen might have

entered the specimen during the vacuum treatments and cited experiments by Wells in which abnormal structures never were obtained when specimens of comparable purity were carburized in pure, oxygen-free hydrocarbon mixtures. In his closure, Derge expressed the opinion that the whole question of abnormality, in general, is one of relative rates which may be influenced by a great many factors.

A review of the literature shows that abnormality has been attributed to:

(1) Oxides, perhaps dissolved but more probably undissolved.
(2) Alumina.
(3) Oxygen dissolved during carburization.
(4) Oxygen in solid solution in the original material.
(5) High Ar_1 temperature.
(6) High purity.
(7) High carbon diffusivity.
(8) High transformation rate (rapid rate of recrystallization).
(9) Fine grain size.
(10) Aluminum in small amounts, if oxygen is present.

Normality has been attributed to:

(1) Aluminum.
(2) Hydrogen.
(3) Silicon.
(4) Coarse grain size.
(5) Low transformation rate.
(6) Alloying elements of the deep hardening type.
(7) Alloying elements which reduce oxygen solubility.

Obviously some of the items listed as influencing either normality or abnormality are interrelated. It is now generally recognized that normality and abnormality are functions of composition and cooling rate.

Materials and Experimental Procedure

Specimens from 17 irons were used in the present investigation. These irons were prepared by different methods and some differences existed in the identifiable impurities as listed in Table I. The irons of highest purity, designated by the numbers 1, 2, 5, 6, 11, 15, and 18, respectively, were prepared by Thompson and Cleaves as described in detail in a previous report (9). The procedure consisted essentially of converting purified iron oxide to sponge iron followed by melting under a vacuum, treating with hydrogen while molten, and solidifying in a vacuum.

Table I
Impurities Determined in the Irons

Iron No.	Element—Per Cent by Weight																	Total Identifiable[3]
	Mn	P	S	Si	Cr	Al	Cu	Ni	Co	Ca	Pb	Mg	Be	Ge	O_2[2]	N_2	H_2	
	Before Carburizing																	
1	ND[1]	....	0.002	0.001	ND	ND	<0.002	ND	ND	ND	ND	ND	<0.001	ND	0.002_2	0.000_1	0.000_1	$<0.009_2$
2	ND	<0.0005	0.002	0.001	ND	ND	<0.002	ND	ND	ND	ND	ND	<0.001	ND	0.001_2	0.000_2	0.000_2	$<0.008_4$
5	ND	....	0.001	0.003	ND	<0.001	<0.002	ND	ND	ND	ND	ND	ND	ND	0.004_9	0.000_2	0.000_2	$<0.012_8$
6	ND	....	0.001	0.001	ND	ND	<0.002	ND	ND	ND	ND	ND	<0.001	ND	0.005_4	0.000_2	0.000_2	$<0.011_6$
11	ND	....	0.001	ND	ND	ND	<0.002	ND	ND	ND	ND	ND	ND	ND	0.005_4	0.000_2	0.000_1	$<0.009_7$
15	ND	....	0.001	ND	ND	<0.001	<0.002	ND	ND	ND	ND	ND	ND	ND	0.002_8	0.000_6	0.000_2	$<0.008_4$
18	ND	....	0.001	ND	ND	ND	<0.002	ND	ND	ND	ND	ND	ND	ND	0.004_3	0.000_1	0.000_2	$<0.008_2$
J[4]	0.013	ND	0.000_2	0.003	0.0005	ND	0.013	0.006	ND	ND	ND	ND	ND	ND	0.001	0.003	0.000_5	<0.045
D[5]	0.002	<0.001	0.004	0.002	ND	ND	<0.001	0.007	0.007	<0.001	<0.001	<0.001	ND	ND	0.003	0.000_5	0.000_1	<0.031
	After Carburizing[6]																	
A[7]	<0.001	....	....	<0.001	0.002	ND	0.003	0.02	<0.01	...	...	...	ND	...	0.010 to 0.017	....	0.000_1	
B	<0.001	....	....	<0.001	0.003	ND	0.002	0.02	<0.01	ND	ND	ND	FT[1]	T[1]	0.007_5	0.000_7	0.000_3	
C	<0.001	....	....	<0.001	<0.001	0.1	<0.001	0.06	<0.01	ND	ND	ND	T	ND	0.002_1	0.000_4	0.000_2	
E	<0.001	....	....	0.008	0.003	0.025	0.003	0.02	<0.01	ND	ND	ND	FT	T	0.002 to 0.005	0.000_3	0.000_2	
F[7]	<0.001	....	....	<0.001	<0.001	0.1 to 0.2	0.001	0.06	<0.01	ND	ND	ND	T	ND	0.001_5	ND	....	
G[7]	<0.001	....	....	0.015	0.002	<0.005	0.002	0.01	<0.01	ND	ND	ND	FT	ND	0.001_6	0.000_2	0.000_2	
H[7]	<0.001	....	....	0.004	0.002	0.3	0.003	0.01	<0.01	ND	ND	ND	W[1]	ND	0.002_8	0.000_3	0.000_3	
I[7]	....	....	....	0.015	<0.001	0.2	0.001	0.01	<0.01	ND	ND	ND	T	T	0.001_8	ND	0.000_2	

(1) ND means not detected; T means trace; FT means faint trace; W means weak.
(2) Includes surface oxygen.
(3) Carbon was not included.
(4) This iron also contained 0.004 per cent molybdenum and traces of vanadium and tin.
(5) Some of the values reported were obtained on specimens after carburizing.
(6) Values for manganese were obtained by chemical analysis on specimens that were not carburized. Values reported for all of the other elements except gases for the irons after carburizing were determined by spectrochemical analysis.
(7) Values for gases obtained on specimens that were not carburized.

Chemical analyses were made by H. A. Bright, J. L. Hague, and W. H. Jukkola; spectrochemical analyses by B. F. Scribner and H. R. Mullin; and vacuum fusion analyses by V. C. F. Holm.

Iron "J" was carbonyl iron subsequently treated with hydrogen. The remaining irons were prepared from different lots of electrolytic iron melted and solidified under a vacuum. In some of the latter melts, a small amount of carbon was added to deoxidize the iron, and to iron "I" sufficient carbon was added (in the form of an iron-carbon alloy) to produce a carbon content of 1.12 per cent in the final product.

The impurities, other than carbon, that were identified by spectrochemical and chemical methods, and the gas content as determined by the vacuum fusion method are listed in Table I. The arc spectrum for each iron, except A, was examined for the sensitive lines of Ag, Al, As, Au, B, Ba, Be, Bi, Ca, Cb, Cd, Co, Cr, Cu, Ga, Ge, Hf, Hg, In, Ir, Mg, Mn, Mo, Na, Ni, Os, Pb, Pd, Pt, Re, Rh, Ru, Sb, Si, Sn, Ta, Th, Ti, U, V, W, Zn and Zr. The sensitive lines of Ce, K, Li, Sc, Sr, Tl and Y were sought in the spectra of all the irons of highest purity and of iron D. The elements identified, other than iron and carbon, are given in the table. The aluminum which is present as an impurity in some of the irons was obtained principally from the alumina crucibles used in preparing these particular heats.

The impurities were determined either on specimens from the original ingots or on specimens after the carburizing treatment, and the specimens used for carburizing were not necessarily taken from the same part of the ingot as the specimens used for analyses. However, in some instances, determinations of manganese, silicon, oxygen, nitrogen and hydrogen were made on the same iron before and after carburizing, and the results, summarized in Table II, show that there was no appreciable change in these impurities incident to the carburizing treatment.

Specimens of the different irons, usually between 0.04 and 0.05 inch in thickness, were carburized at about 1700 degrees Fahr. (925 degrees Cent.) for 3 hours in a mixture of hydrogen and benzene vapor, followed by cooling in this atmosphere through the Ar_1 transformation at approximately 4 degrees Fahr. per minute. Time in the carburizing temperature range was sufficient to produce a hypereutectoid zone throughout the cross section of the specimen. The benzene used was thiophene-free and conformed to American Chemical Society specifications. The hydrogen was purified and dried by passing in succession through Ascarite, silica gel heated to 1300-1350 degrees Fahr. (705-730 degrees Cent.), magnesium perchlorate, and phosphorus pentoxide. The dry hydrogen next passed through the

Table II

Impurities Determined in Irons Before and After Carburizing in a Mixture of Hydrogen and Benzene Vapor

Iron No.	Condition[1]	Impurities—Per Cent by Weight				
		Mn	Si	O_2	N_2	H_2
2	Before carburizing	ND[2]	0.001	0.001_2	0.000_2	0.000_2
2	After carburizing	ND	ND	0.002_6	0.000_3	0.000_2
5	Before carburizing	ND	0.003	0.004_9	0.000_2	0.000_2
5	After carburizing	ND	<0.001	....	....	....
15	Before carburizing	ND	ND	0.002_8	0.000_6	0.000_2
15	After carburizing	ND	ND	....	....	....
B	Before carburizing	...	...	0.007_5	0.000_7	0.000_4
B	After carburizing	...	...	0.007_5	0.000_7	0.000_3
B	After carburizing	...	<0.001	0.007_3	0.000_7	0.000_2
C	Before carburizing	...	...	0.003	0.000_2	0.000_2
C	After carburizing	...	<0.001	0.002_1	0.000_4	0.000_2
D	Before carburizing	0.002	0.002	0.004_4	0.000_3	0.000_2
D	After carburizing	...	<0.001	0.003_2	0.000_5	0.000_1
E	Before carburizing	...	...	0.003_8	0.000_3	0.000_2
E	After carburizing	...	0.008	0.004_1	0.000_2	0.000_3
E	After carburizing	...	...	0.002	ND	0.000_2
E	After carburizing	...	...	0.002_0	0.000_2	0.000_2
E	After carburizing	...	...	0.005	0.000_3	0.000_3

(1) For each iron, the different specimens were not always from the same part of the original ingot.

(2) ND means not detected.

benzene and then into the quartz tube where the specimens were suspended vertically by a wire of high purity iron or iron-carbon alloy. The hydrogen finally passed into the air at the exit end of the train. The quartz tube was contained within an electrically heated furnace. The hot junction of a chromel-alumel thermocouple was located outside of the carburizing chamber between the quartz tube and the furnace tube in the uniformly heated zone.

The gas flow was not accurately determined or maintained constant during the carburization of the various irons, but the average flow was believed to be about 100 milliliters per minute. The vapor not used in carburizing was burned at the exit end of the train.

The specimens were cleaned by washing in xylene or benzene and were then suspended in the cold zone of the quartz tube near the outlet. The tube was thoroughly flushed with the mixture of hydrogen and benzene vapor before lowering the specimens from the cold zone to the uniformly hot or carburizing zone.

Measurements of the austenitic grain size of the carburized specimens were made by the method described by Jeffries (10) and by comparison with the grain-size chart of the American Society for Testing Materials (11).

Structures of the Carburized Irons

The structures obtained by carburizing the various irons at 1700 degrees Fahr. (925 degrees Cent.) for 3 hours in the hydrogen-benzene atmosphere, followed by cooling in this atmosphere through the Ar_1 transformation at 4 degrees Fahr. per minute, are summarized in Table III and Figs. 1 to 6.

It is well known that the rate of cooling through the thermal critical range influences the divorcement of ferrite in hypereutectoid steels. Rejection of free ferrite could be entirely prevented in the present iron-carbon alloys by cooling at sufficiently high rates from the temperature used in carburizing. As pointed out by Davenport and Bain (3) cooling rates of 4 to 5 degrees Fahr. per minute are considered satisfactory for obtaining consistent results in normality studies. Obviously, the relative amounts of free ferrite in the alloys might have been different had the cooling rates differed widely from that used.

The impurities present in alloys of iron and carbon may be without effect or may act either to increase or to decrease the transformation rate of austenite or the diffusivity of carbon in the temperature range of the Ar_1 transformation and accordingly influence the divorcement of ferrite in the final structures. Since in this study it was difficult to isolate the effect of an individual impurity, it must be borne in mind that the structure produced in any alloy may have resulted from the combined effects of all of its impurities.

Influence of Impurities

(a) *Oxygen*—The aluminum-free irons of highest purity (total identifiable impurities less than 0.012 per cent) with oxygen content ranging from about 0.001 to 0.005 per cent, had appreciable amounts of free ferrite in the final structures as illustrated in Fig. 1, A and B. However, this difference in oxygen content had no detectable effect on the amount of free ferrite. If oxygen, either in the form of oxides or more probably in solution, were responsible for this structural condition then a minute amount of the element evidently was sufficient and as effective as larger amounts. Furthermore, in the aluminum-free irons of intermediate purity (B and D, Table I) more free ferrite was obtained in the carburized structure of the iron containing 0.003 per cent oxygen (Fig. 2 A) than in the iron containing 0.007 per cent oxygen (Fig. 2 B).

Table III

Structure and Austenitic Grain Size of Iron-Carbon Alloys. Specimens were Carburized at 1700 Degrees Fahr. for 3 Hours in a Hydrogen-Benzene Atmosphere and Cooled in this Atmosphere Through the Ar_1 Transformation at 4 Degrees Fahr. Per Minute

Iron					Impurities—Per Cent by Weight					Austenitic Grain Size	
		Preparation									
No.	Base	Deoxidizer	Fabrication	Treatment with Hydrogen after Solidification	Al	O_2[2]	N_2	H_2	Total Identified	Av. Grain/in.^{2} at ×100	ASTM No.
1	Sponge	Hydrogen	As cast	None	ND[1]	0.002	0.0001	0.0001	<0.010	0.5	0
2	Sponge	Hydrogen	As cast	None	ND	0.001	0.0002	0.0002	<0.009	1.0	1
5	Sponge	Hydrogen	As cast	None	<0.001	0.005	0.0002	0.0002	<0.013	0.2	−1
6	Sponge	Hydrogen	As cast	None	ND	0.005	0.0002	0.0002	<0.012	0.8	1
11	Sponge	Hydrogen	As cast	2000° F. for 1 hour and water quenched	ND	0.005	0.0002	0.0001	<0.010	1.6	2
15	Sponge	Hydrogen	Hot and cold worked	None	<0.001	0.003	0.0006	0.0002	<0.009	0.6	0
18	Sponge	Hydrogen	As cast	None	ND	0.004	0.0001	0.0002	<0.009	0.6	0
A	Electrolytic	None	As cast	None	ND	0.010 to 0.017	....	0.0001	....	1.1	1
A	Electrolytic	None	As cast	2000° F. for 1 hour and water quenched	...	....	....	....	....	1.0	1
B	Electrolytic	None	As cast	None	ND	0.007	0.0007	0.0003	....	0.9	1
C	Electrolytic	None	As cast	None	0.1	0.002	0.0004	0.0002	....	2.6	2
D	Electrolytic	None	Hot and cold worked	None	ND	0.003	0.0005	0.0001	<0.031	5.6	3
E	Electrolytic	Carbon	As cast	None	0.025	0.004	0.0003	0.0002	....	5.0	3
F	Electrolytic	Carbon	As cast	None	0.1 to 0.2	0.001	ND	....	....	6.5	4
G	Electrolytic	Carbon	Hot and cold worked	None	<0.005	0.002	0.0002	0.0002	....	0.9	1
H	Electrolytic	Carbon	As cast	None	0.3	0.003	0.0003	0.0003	....	9.5	4
H	Electrolytic	Carbon	As cast	2000° F. for 1 hour and water quenched	...	....	....	....	....	7.6	4
H	Electrolytic	Carbon	Hot and cold worked	2000° F. for 1 hour and water quenched	...	....	....	....	....	2.8	2
H	Electrolytic	Carbon	Hot and cold worked	None	...	0.002	0.0004	0.0002	....	1.0	1
I	Electrolytic	Carbon	As cast (1.12% C)	None	0.2	0.002	ND	0.0002	....	2.1	2
J	Carbonyl	Not melted	Hot worked	Treated. Exact treatment unknown	ND	0.001	0.003	0.0005	<0.045	0.3	−1

(1) ND means not detected.
(2) Includes surface oxygen.

Table III—Continued

Structure and Remarks	
No. 1—Free ferrite, massive cementite network and pearlite as shown in Fig. 1A.	No. C—Cementite network and pearlite as shown in Fig. 3A.
No. 2—Free ferrite, massive cementite network and pearlite as shown in Figs. 6A and B.	No. D—Free ferrite, cementite network and pearlite as shown in Fig. 2A.
No. 5—Very small amount of free ferrite, cementite network and pearlite as shown in Fig. 1D. Mixed size with some very large austenitic grains.	No. E—Cementite network and pearlite with a very small amount of free ferrite in some areas as shown in Fig. 2D. Mixed size austenitic grains.
No. 6—Free ferrite, massive cementite network and pearlite as shown in Fig. 5A.	No. F—Cementite network and pearlite as shown in Fig. 3B. Marked difference in austenitic grain size. Some No. −2 grains.
No. 11—Free ferrite, massive cementite network and pearlite as shown in Fig. 5B.	No. G—Cementite network and pearlite as shown in Fig. 2C. Marked difference in austenitic grain size. Some No. −2 grains.
No. 15—Free ferrite, massive cementite network and pearlite as shown in Fig. 1C. Mixed size austenitic grains.	No. H—Cementite network and pearlite as shown in Fig. 3C.
No. 18—Free ferrite, massive cementite network and pearlite as shown in Fig. 1B.	No. H—Cementite network and pearlite similar to Fig. 3C. Some elongated austenitic grains.
No. A—Free ferrite, massive cementite network and pearlite as shown in Fig. 5C. Some elongated austenitic grains.	No. H—Cementite network and pearlite similar to Fig. 3C.
No. A—Free ferrite, massive cementite network and pearlite as shown in Fig. 5D.	No. H—Cementite network and pearlite as shown in Fig. 3D. Some elongated austenitic grains.
No. B—Free ferrite, massive cementite network and pearlite as shown in Fig. 2B. Elongated austenitic grains.	No. I—Cementite network and pearlite as shown in Fig. 4D. Mixed size austenitic grains.
	No. J—Small amount of free ferrite, cementite and pearlite. Cementite principally in plates. Only a few austenitic grains delineated by cementite.

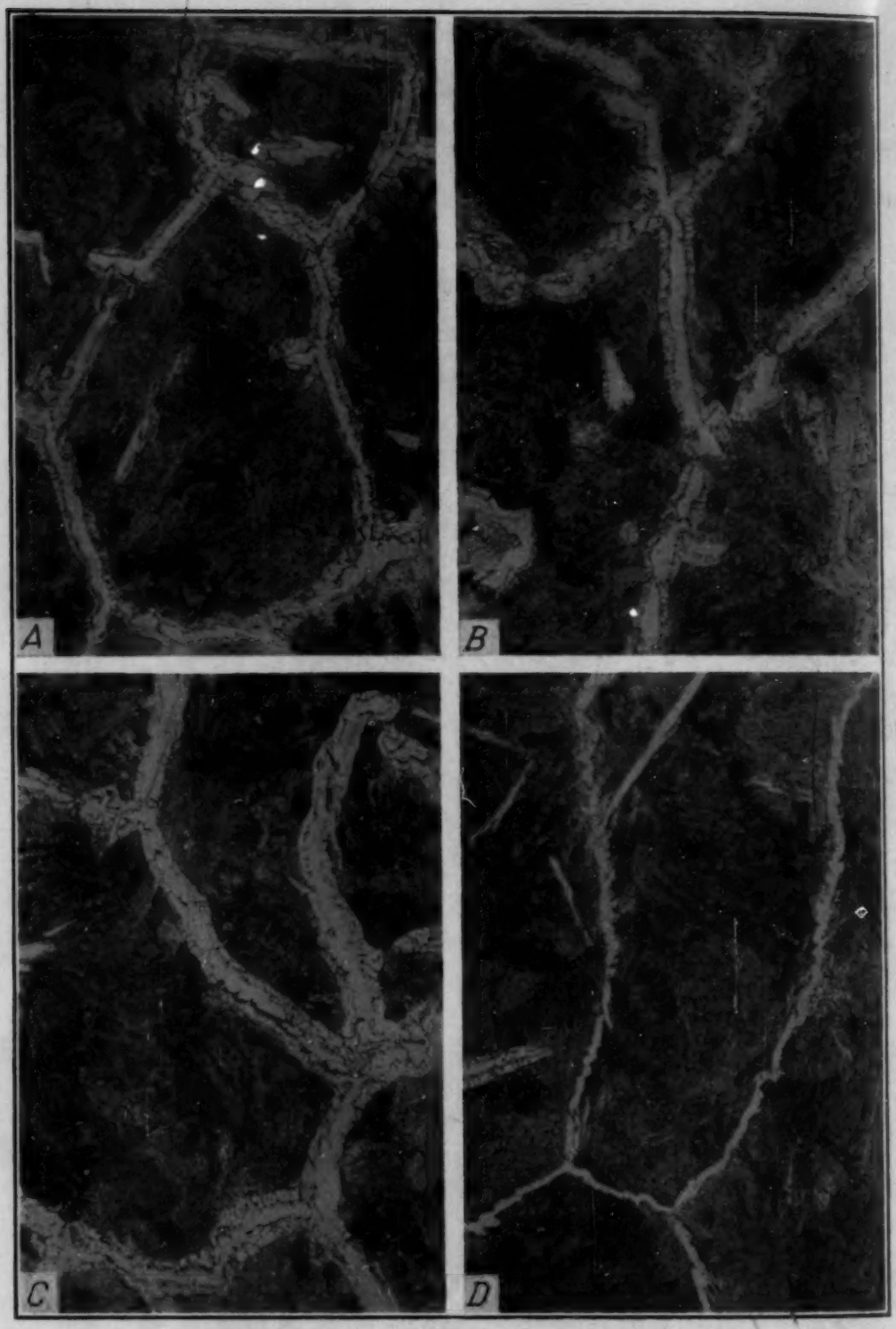

Fig. 1—Structure of High Purity Irons After Carburizing.

A—Iron 1, with 0.002 Per Cent O_2, no Aluminum and <0.010 Per Cent Total Identifiable Impurities. B—Iron 18 with 0.004 Per Cent O_2, no Aluminum and <0.009 Per Cent Total Identifiable Impurities. C—Iron 15 with 0.003 Per Cent O_2, <0.001 Per Cent Aluminum and <0.009 Per Cent Total Identifiable Impurities. D—Iron 5 with 0.005 Per Cent O_2, <0.001 Per Cent Aluminum and <0.013 Per Cent Total Identifiable Impurities. Etched with 1 Per Cent Nital. × 100.

Oxygen contents of about 0.001 per cent as determined by the vacuum fusion method represent a close approximation to oxygen-free material. The vacuum fusion method determines the total oxygen content, i.e., the film of oxides on the surface of the specimen as well as the oxygen in the interior of the specimen. Evidence has been obtained indicating that the surface film on certain specimens amounts to about 0.001 per cent. For these reasons vacuum fusion determinations of less than 0.001 per cent of oxygen are seldom obtained, even for the most carefully deoxidized material.

The oxygen content, from 0.001 to 0.007 per cent, could not be correlated with the divorcement of free ferrite in the final structure of these alloys, which were free from aluminum but some of which contained appreciable amounts of other impurities. A structure containing free ferrite is characteristic of very high purity alloys of iron and carbon of hypereutectoid composition, with very low oxygen content, that have been cooled slowly from the austenitic condition through the thermal critical range.

(b) *Aluminum and Alumina*—The carburized structures of all of the irons which were free from aluminum contained free ferrite. All of the irons which contained more than 0.001 per cent aluminum had carburized structures that were practically free from ferrite.

Of the two carburized irons which contained a trace of aluminum (less than 0.001 per cent), number 15 had an appreciable amount of free ferrite in the hypereutectoid zone (Fig. 1C) and number 5 had only a small amount of free ferrite (Fig. 1D). The values obtained by analyses indicated that sufficient oxygen was available in each of these carburized irons (0.003 and 0.005 per cent oxygen, respectively) to combine with all of the aluminum to form alumina, provided the greater portion of the oxygen reacted in this manner. Thus it appears probable that both alloys were free from metallic aluminum and each had approximately the same amount of alumina. Evidently the differences in amounts of free ferrite in the final structures were not due to differences in metallic aluminum or alumina. A noteworthy feature is that, when a trace of aluminum was present, the carburized specimens from the iron with lower oxygen content had the greater amount of free ferrite, a fact which is contrary to the prevailing opinion.

The carburized structure of iron G with less than 0.005 per cent aluminum (0.015 per cent silicon) was essentially free from ferrite (Fig. 2C), and that of iron E with 0.025 per cent aluminum (0.008

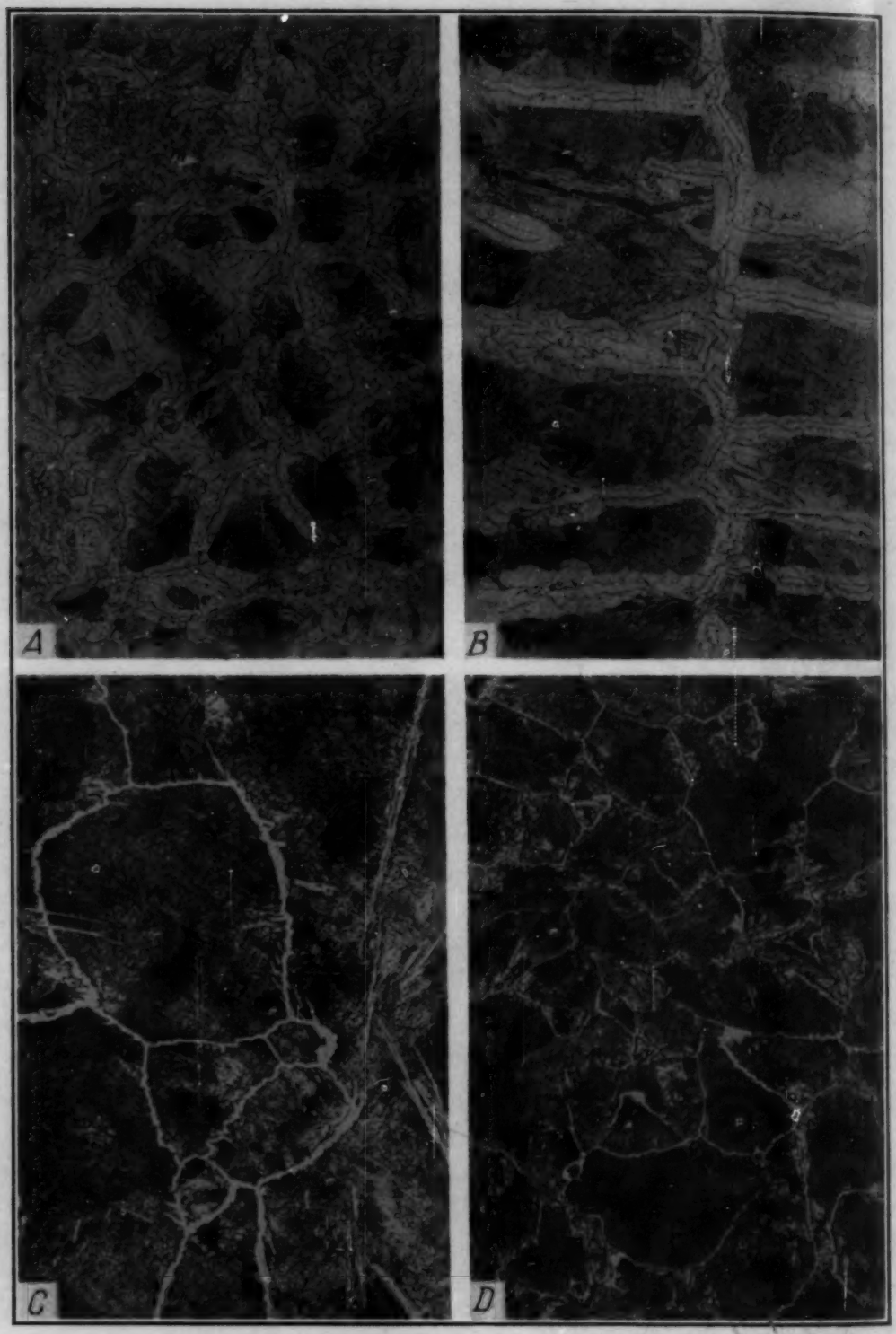

Fig. 2—Structure of Intermediate-Purity Irons After Carburizing.

A—Iron D with 0.003 Per Cent O_2 and no Aluminum. B—Iron B with 0.007 Per Cent O_2 and no Aluminum. C—Iron G with 0.002 Per Cent O_2 and <0.005 Per Cent Aluminum. D—Iron E with 0.004 Per Cent O_2 and 0.025 Per Cent Aluminum. Etched with 1 Per Cent Nital. × 100.

Irons D and G were Hot and Cold-Worked Prior to Carburizing Whereas Irons B and E were As Cast.

per cent silicon) contained only a small amount of free ferrite in some areas (Fig. 2D). The relatively high silicon content was perhaps a factor in preventing the formation of ferrite in these alloys, especially in the one with the lower aluminum content. However, the carburized structures (Fig. 3) of the irons with aluminum ranging from 0.1 to 0.3 per cent (silicon from trace to 0.004 per cent) contained no free ferrite. It should be pointed out that the two alloys with a trace of silicon also contained relatively high nickel (0.06 per cent) but the amount of nickel in the other alloy (0.01 per cent) was only slightly higher than that of the aluminum-free alloy of Fig. 2A (0.007 per cent nickel) which contained a large amount of free ferrite.

The values for oxygen ranged from approximately 0.001 to 0.005 per cent in the alloys containing aluminum and, as already stated, from 0.001 to 0.007 per cent in the aluminum-free alloys which contained appreciable amounts of free ferrite in the final structures. In the alloys of low aluminum content, the aluminum should be present almost entirely as the oxide (alumina) and, while the alloys of high aluminum content also contained alumina, the greater portion should be present as the metal. It is generally believed that alumina increases the decomposition rate of austenite to ferrite and carbide by acting as centers for transformation whereas metallic aluminum enters into solid solution in the austenite and thereby decreases its transformation rate. The present results show that aluminum in excess of about 0.001 per cent inhibits the divorcement of ferrite, and alumina was not the factor responsible for its formation in these hypereutectoid alloys.

(c) *Hydrogen*—Carburized and homogenized specimens prepared from iron D (12) containing 1.01 and 1.21 per cent carbon were annealed in an atmosphere of dry hydrogen at 1700 degrees Fahr. (925 degrees Cent.) for 1 hour and cooled through the Ar_1 transformation at 4 degrees Fahr. per minute. Other specimens of these same alloys, with the same initial structure of fine pearlite, were given a similar thermal treatment in vacuo. During the time of cooling from the annealing temperature through the transformation range the former specimens were saturated with hydrogen whereas the specimens annealed in vacuo were relatively free from hydrogen. The surfaces of the specimens annealed in hydrogen were decarburized but a hypereutectoid zone was retained in the center of some of the specimens. The hypereutectoid zones contained free ferrite

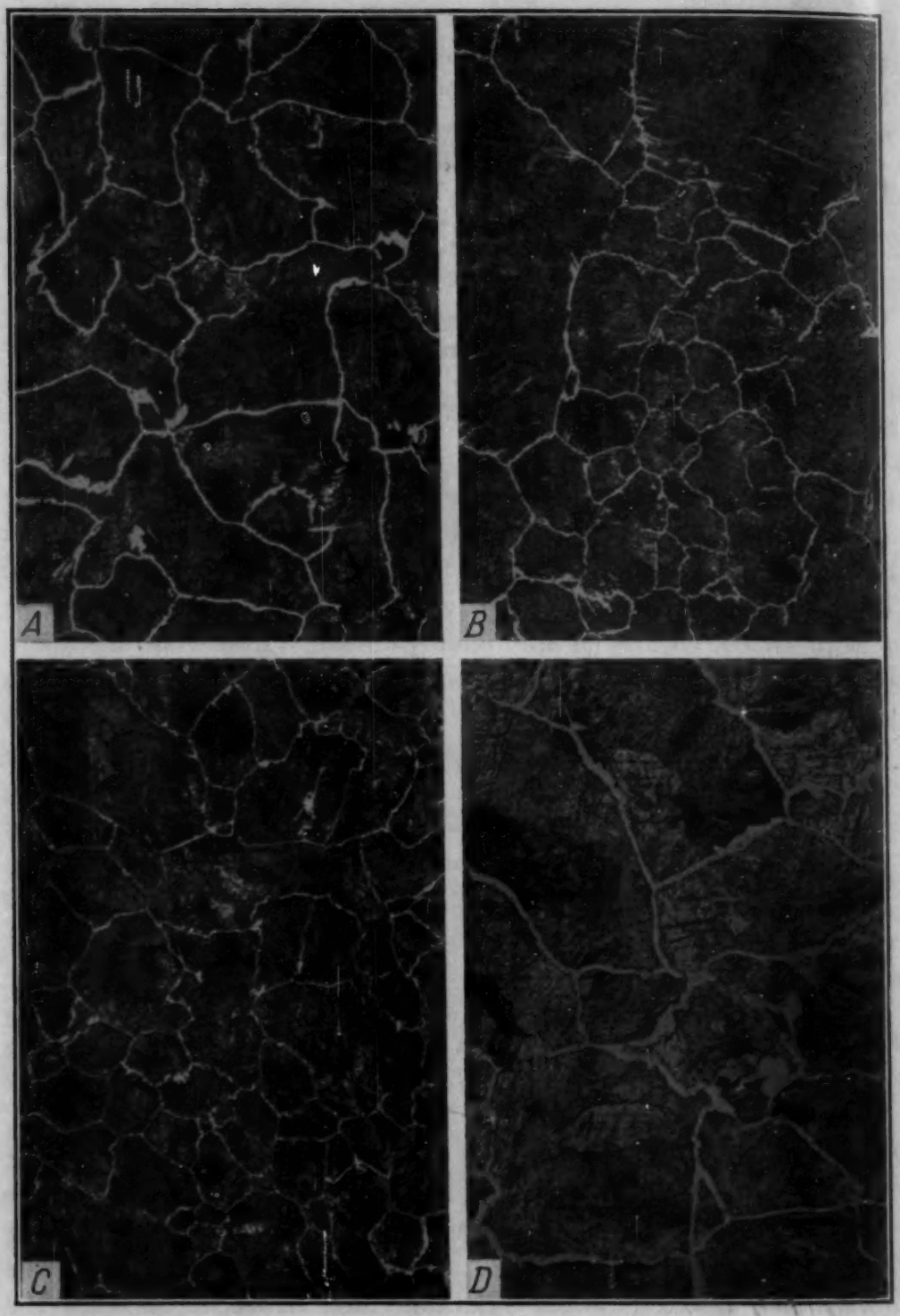

Fig. 3—Structure of Irons Containing Aluminum After Carburizing.

A—Iron C with 0.002 Per Cent O_2 and 0.1 Per Cent Aluminum; Initial Structure As Cast. B—Iron F with 0.001 Per Cent O_2 and 0.1 to 0.2 Per Cent Aluminum; Initial Structure As Cast. C—Iron H with 0.003 Per Cent O_2 and 0.3 Per Cent Aluminum; Initial Structure As Cast. D—Iron H with 0.002 Per Cent O_2 and 0.3 Per Cent Aluminum; Initial Structure as Hot and Cold Worked. Etched with 1 Per Cent Nital. × 100.

and had a structure similar to that of the vacuum-annealed specimens shown in Figs. 4A and 4B. Furthermore, the amount of free ferrite obtained in the latter specimens was of the same order of magnitude as that of specimens of the same iron D carburized at 1700 degrees Fahr. (925 degrees Cent.) in a mixture of hydrogen and benzene vapor and cooled at a similar rate directly from the carburizing temperature in an atmosphere containing hydrogen (see Fig. 2A). Thus this structural feature of free ferrite in slowly cooled hypereutectoid alloys was produced with equal facility either by cooling directly from the carburizing temperature or by subsequently annealing in vacuo or in hydrogen.

The structure of alloy I (containing 1.12 per cent carbon as cast) after the annealing treatment in vacuo (Fig. 4C), and the structure of the same alloy after the carburizing treatment (Fig. 4D), consisted of cementite network and pearlite. A marked increase in austenitic grain size resulted from the carburizing treatment in which the specimen was held at 1700 degrees Fahr. (925 degrees Cent.) for 3 hours in an atmosphere containing hydrogen. Free ferrite was not produced in the structure of alloy I either by annealing in hydrogen or in vacuo.

Specimens from several different irons were treated in dry hydrogen at approximately 2000 degrees Fahr. (1095 degrees Cent.) and quenched in water (Table III). Although the time at high temperature was sufficient for the hydrogen to diffuse throughout the cross section of the specimens, it was not sufficient to cause an appreciable reduction in the oxygen content as shown by determinations made on similarly treated specimens. The hydrogen content of the specimens immediately after quenching varied; the maximum value was about 0.0005 per cent. The hydrogen was extracted by heating at about 1500 degrees Fahr. (815 degrees Cent.) for 6 to 15 minutes (13) before carburizing in the hydrogen-benzene atmosphere in the usual manner. The structures produced by carburizing untreated high purity iron 6, and hydrogen-treated iron 11 of equivalent purity, and untreated and hydrogen-treated iron A are shown in Fig. 5. Free ferrite was present in all of these specimens and no difference in the amount of free ferrite was obtained as a result of the hydrogen treatment (compare Fig. 5A with Fig. 5B and Fig. 5C with Fig. 5D).

These results show that hydrogen had no influence on the final structures obtained in the slowly cooled alloys.

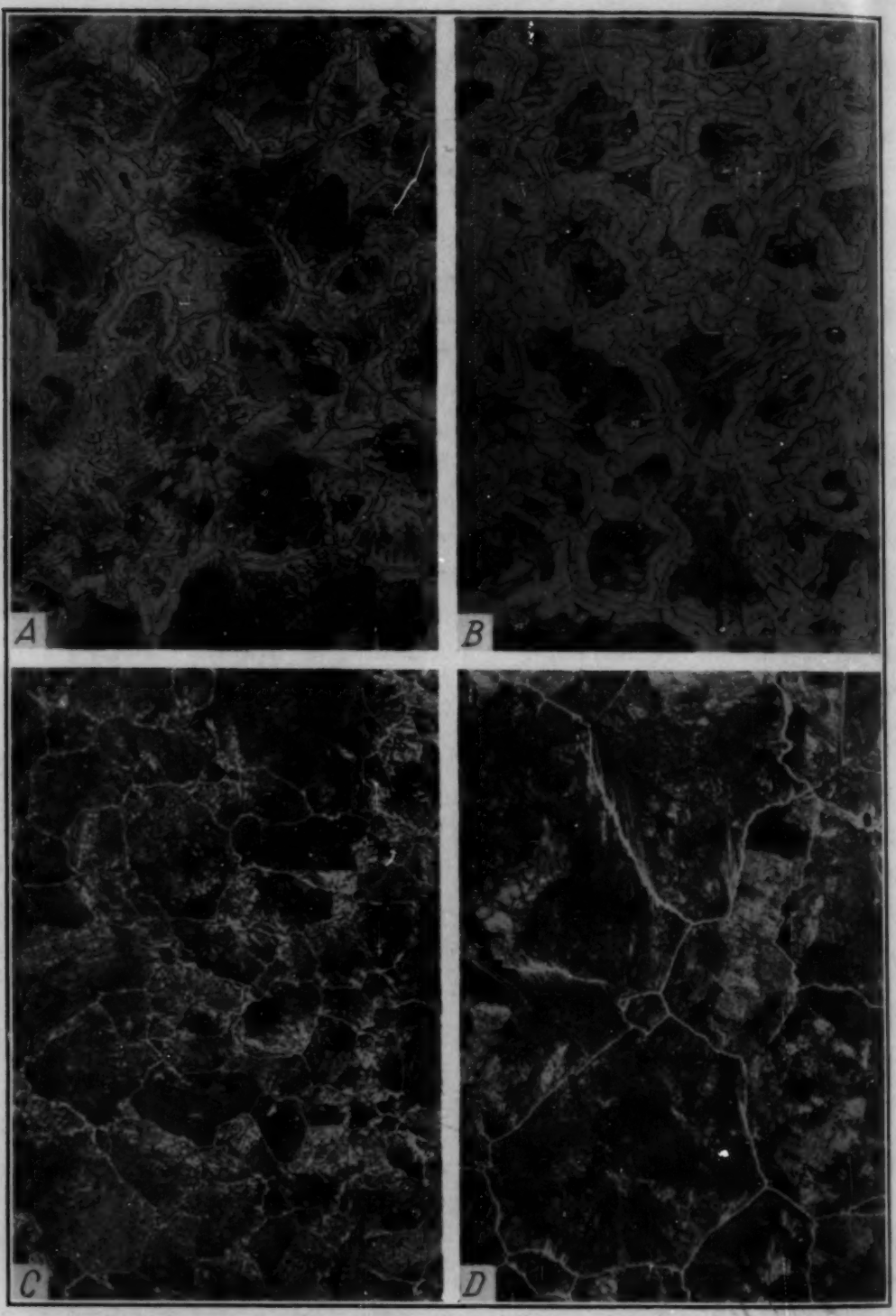

Fig. 4—Structure of Iron-Carbon Alloys After Annealing in Vacuo or as Carburized. A—1.01 Per Cent Carbon, Prepared from Iron D, After Annealing in Vacuo. B—1.21 Per Cent Carbon, Prepared from Iron D, After Annealing in Vacuo. C—1.12 Per Cent Carbon, Prepared from Iron-Carbon Alloy I, After Annealing in Vacuo. D—Iron-Carbon Alloy I, After Carburizing. The Annealing Treatment Consisted of Heating in Vacuo at 1700 Degrees Fahr. for 1 Hour and Cooling Through the Ar_1 Transformation at 4 Degrees Fahr. Per Minute. Etched with 1 Per Cent Nital. × 100.

Influence of Total Impurities

The results summarized in Table III show, in general, that the irons of highest purity (total identifiable impurities less than about 0.010 per cent) had structures containing free ferrite in the hypereutectoid zone after carburizing and slowly cooling in an oxygen-free atmosphere. However, the carburized structure of iron 5 (total impurities less than 0.013 per cent) contained only a relatively small amount of free ferrite (Fig. 1D) as compared with the carburized structure (Fig. 1C) of iron 15 (total impurities less than 0.009 per cent). Since specimens from these two irons were carburized at the same time the different amounts of free ferrite in the final structures must be attributed to differences in composition and not to the carburizing conditions. As shown in Table I, the identifiable impurities for the original ingots of irons 5 and 15 differed mainly in silicon (0.003 per cent and nil, respectively) and oxygen (0.005 and 0.003 per cent, respectively), but these differences are of doubtful significance because of the uncertainty of analytical determinations of this order of magnitude. Spectrochemical analysis showed that no definite change in the amounts of impurities occurred during the carburizing treatment and it has already been shown that the carburizing treatment did not change appreciably the amounts of the gaseous elements. It is difficult, therefore, to explain satisfactorily the observed differences in the percentages of free ferrite on the basis of such minute variations in these detectable impurities.

Different amounts of free ferrite were obtained in the carburized structures of the irons of intermediate purity (0.03 to 0.05 per cent identifiable impurities), whereas the carburized structures were essentially free from ferrite for the irons of relatively low purity (appreciable amounts of aluminum).

These results show that the presence of free ferrite in the hypereutectoid zone of very high purity alloys of iron and carbon is characteristic of the structures obtained after slowly cooling from the carburizing temperature. As the amounts of impurities are increased, the final structures obtained in the alloys by slowly cooling after carburizing may or may not contain free ferrite in the hypereutectoid zone, depending on whether the added impurities are of the type which increase or decrease the reaction rate of austenite or the diffusivity of carbon in the Ar_1 transformation range.

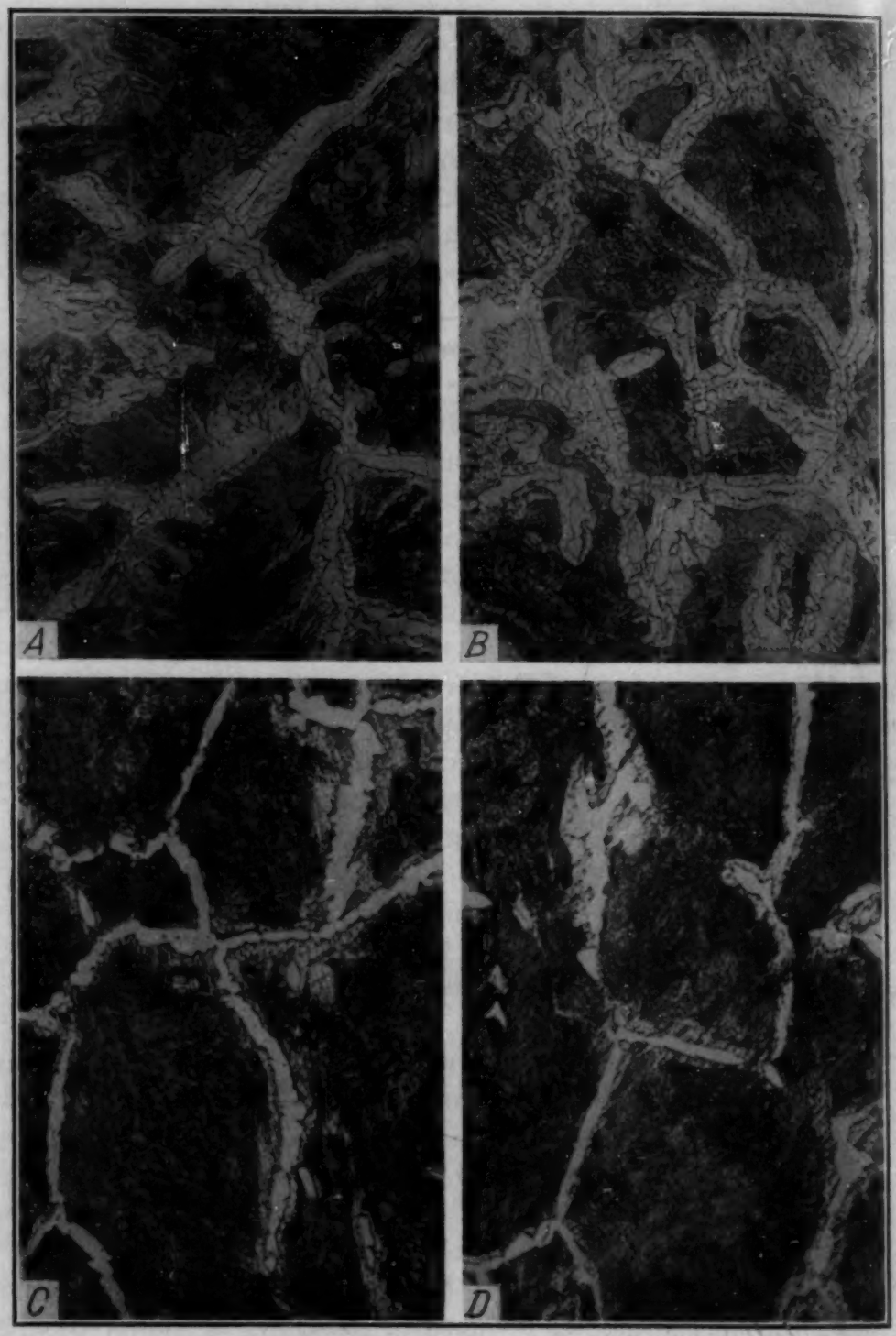

Fig. 5—Structure of Irons After Carburizing.

A—Iron 6, Not Treated with Hydrogen Before Carburizing. B—Iron 11, Treated with Hydrogen Before Carburizing. C—Iron A, Not Treated with Hydrogen Before Carburizing. D—Iron A, Treated with Hydrogen Before Carburizing. The Hydrogen Treatment Consisted of Heating Specimens of the Irons As Cast in Dry Hydrogen at 2000 Degrees Fahr. for 1 Hour and Quenching in Water. Etched with 1 Per Cent Nital. × 100.

Influence of Other Factors

(a) *Carbon*—Divorcement of ferrite was not observed in the eutectoid zone of any of the carburized specimens. As illustrated in Fig. 6, the presence of a proeutectoid constituent (carbide in this case) in austenite appears to be essential for the production of free ferrite in the structure of iron-carbon alloys cooled at 4 degrees Fahr. per minute through the thermal critical range. With slowly cooled alloys of eutectoid content the austenite transformed entirely to pearlite (Fig. 6C). However, variations may exist in the carbon content in excess of the eutectoid without appreciably influencing the amount of free ferrite in the final structure of the slowly cooled alloys, as illustrated in Figs. 4A and B.

(b) *Annealing Treatment*—It has already been pointed out that carburized and homogenized specimens containing 1.01 and 1.21 per cent carbon (prepared from iron D) and subsequently annealed in vacuum had approximately the same amount of free ferrite in the final structures (Figs. 4A and B) as specimens of the same iron carburized to produce a hypereutectoid alloy in the hydrogen-benzene atmosphere followed by cooling in this atmosphere at the same rate (Fig. 2A).

No increase in oxygen content of the iron-carbon alloys occurred during the time of annealing in vacuo as shown by the values obtained for oxygen as follows:

Iron or Alloy No.	Condition	Oxygen Per Cent by Weight
D	As carburized	0.003
D	As carburized and annealed	0.003
I	As cast (1.12 per cent carbon)	0.002
I	As cast and annealed	0.001

The structural feature consisting of free ferrite in slowly cooled hypereutectoid alloys was produced with equal facility either by cooling directly from the carburizing temperature or by subsequently annealing in vacuo.

(c) *Initial Structure*—For most of the irons, the structure prior to carburizing was that of the cast metal. In several irons, however, the initial structure was that obtained by hot and cold working the cast metal, and the carbonyl iron had been hot-worked after sintering. As shown by the results summarized in Table III, Figs. 2A and 2B, and Figs. 3C and 3D, the amount of free ferrite obtained in the car-

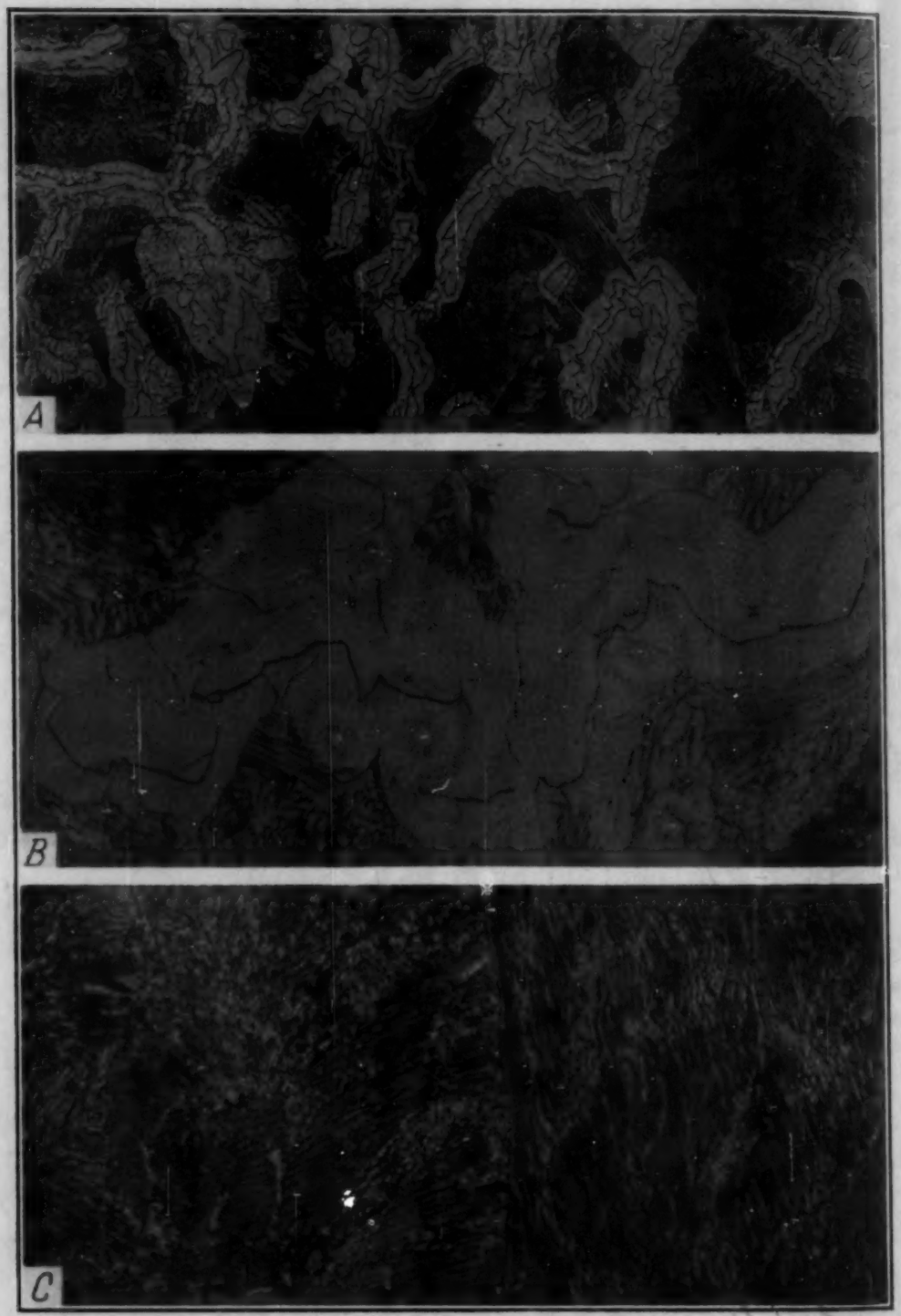

Fig. 6—Structure of the Hypereutectoid and Eutectoid Zones Produced in High Purity Iron by Carburizing.

A—Iron 2, Hypereutectoid Zone. × 100. B—Iron 2, Hypereutectoid Zone. × 500. C—Iron 2, Eutectoid Zone. × 500. Etched with 1 Per Cent Nital.

burized structure was independent of the initial structure of the irons, whether as cast or as hot and cold-worked.

Influence of Austenitic Grain Size

In a previous report (14) it was shown that the austenitic grain size affected the rate of decomposition of austenite in the Ar′ temperature range of high purity alloys of iron and carbon. The critical cooling rate progressively decreased (hardenability increased) as the austenitic grain size increased in alloys containing 0.80 to 0.85 per cent carbon. Davenport, Grange and Hafsten (15) recently reported that with an increase in austenitic grain size the isothermal transformation of austenite in an S.A.E. 4140 steel was retarded in the temperature levels (about 1050 degrees Fahr. and above) where soft lamellar structures form.

The grain sizes established in the various irons by carburizing at 1700 degrees Fahr. (925 degrees Cent.) were determined and the results are summarized in Table III. Variations existed in the average size of the austenitic grains and in some cases grains of mixed sizes were obtained in the same alloy, but no correlation was found between austenitic grain size and divorcement of ferrite in the final structures of the slowly cooled hypereutectoid alloys. For example, two of the alloys which had structures free from ferrite had average American Society for Testing Materials grain number 4 (Fig. 3C) and grain number 1 (Fig. 2C, mixed size grains containing some number —2), whereas two other alloys with the same average grain sizes had structures containing appreciable amounts of free ferrite (Figs. 2A and 6A, respectively). An interesting feature is the large austenitic grains and a structure containing free ferrite which was obtained in the alloys of highest purity, as shown in Fig. 1.

Summary

Seventeen irons, varying in degrees of purity, were carburized in a mixture of hydrogen and benzene vapor at 1700 degrees Fahr. (925 degrees Cent.) for 3 hours followed by cooling in this atmosphere through the transformation range at 4 degrees Fahr. per minute. The time at the carburizing temperature was sufficient to produce hypereutectoid zones in all of the irons.

The presence of free ferrite in the hypereutectoid zones is characteristic of the structures obtained in irons of very high purity under these conditions. As the amounts of impurities in the irons are increased the final structures obtained after carburizing may or may not contain free ferrite in the hypereutectoid zone, depending

upon whether the added impurities are of the type which increase or decrease the reaction rate of austenite or the diffusivity of carbon in the Ar_1 transformation range. Differences in oxygen content from about 0.001 to 0.007 per cent could not be correlated with the amount of free ferrite in the final structure of the alloys. Some of the irons represent a close approximation to oxygen-free material. The precise role of oxygen in the development of ferrite in the final structure is not entirely clear. However, if oxygen were responsible for this structural feature in the hypereutectoid alloys of highest purity, then a minute amount was sufficient and as effective as larger amounts.

The carburized structures of all the irons which were free from aluminum contained free ferrite. Aluminum in excess of about 0.001 per cent inhibits the formation of free ferrite in the hypereutectoid zone and alumina was not the factor responsible for its formation.

The presence of hydrogen in the carburizing and annealing atmospheres had no detectable effect on the formation of free ferrite.

Free ferrite was not detected in the eutectoid zone of any of the alloys. However, variations might exist in amounts of proeutectoid carbide without markedly affecting the formation of free ferrite on slowly cooling from the austenitic condition.

Free ferrite in hypereutectoid alloys was produced with equal facility either by cooling directly from the carburizing temperature or by annealing in vacuo. The initial structures of the irons, either as cast or after working, had no effect on the formation of free ferrite in the final structures.

The average grain size established in carburizing the various irons at 1700 degrees Fahr. (925 degrees Cent.) ranged from American Society for Testing Materials grain number 4 to —1, but there existed no correlation between austenitic grain size and the formation of free ferrite. A noteworthy feature was the large austenitic grains of the alloys of highest purity which contained relatively large amounts of free ferrite.

Acknowledgments

Grateful acknowledgment is due H. E. Cleaves and J. G. Thompson for specimens of the highest purity irons, and V. C. F. Holm, for specimens of some of the irons and for the determinations of the gas content of the irons and alloys.

References

1. H. W. McQuaid and E. W. Ehn, "Effect of Quality of Steel on Case-Carburizing Results," *Transactions,* American Institute of Mining and Metallurgical Engineers, Iron and Steel Division, Vol. 67, 1922, p. 341.
2. S. Epstein and H. S. Rawdon, "Steel for Case Hardening—Normal and Abnormal Steel," *Journal of Research,* Bureau of Standards, Vol. 1, Sept. 1928, p. 423; RP14.
3. E. S. Davenport and E. C. Bain, "General Relations between Grain Size and Hardenability and the Normality of Steels," TRANSACTIONS, American Society for Metals, Vol. 22, Dec. 1934, p. 879.
4. M. A. Grossmann, "Oxygen in Steel," TRANSACTIONS, American Society for Steel Treating, Vol. 18, 1930, p. 601.
5. F. Duftschmid and E. Houdremont, "Purest Steels Develop Soft Spots if Carburized and Quenched," METAL PROGRESS, Vol. 21, May 1932, p. 30.
6. E. C. Bain, "Factors Affecting the Inherent Hardenability of Steel," TRANSACTIONS, American Society for Steel Treating, Vol. 20, Nov. 1932, p. 385.
7. G. R. Brophy and E. R. Parker, "Influence of Aluminum on the Normality of Steel," TRANSACTIONS, American Society for Metals, Vol. 25, March 1937, p. 315.
8. G. Derge, A. R. Kommel and R. F. Mehl, "Some Factors Influencing Austenitic Grain Size in High Purity Steels," TRANSACTIONS, American Society for Metals, Vol. 26, March 1938, p. 153.
9. J. G. Thompson and H. E. Cleaves, "Preparation of High Purity Iron," *Journal of Research,* Bureau of Standards, Vol. 23, July 1939, p. 163.
10. Zay Jeffries, American Society for Testing Materials, Standards, Part I, Metals, Designation E 2-36 (Note 2), 1936, p. 763.
11. Standard Grain Size Chart for Classification of Steels. American Society for Testing Materials, Standards, Part I, Metals, Designation E 19-33, 1936, p. 761.
12. T. G. Digges, "Effect of Carbon on the Hardenability of High Purity Iron-Carbon Alloys," TRANSACTIONS, American Society for Metals, Vol. 26, June 1938, p. 408. Also, "Effect of Carbon on the Critical Cooling Rate of High Purity Iron-Carbon Alloys and Plain Carbon Steels," *Journal of Research,* Bureau of Standards, Vol. 20, May 1938.
13. V. C. F. Holm and J. G. Thompson, "Determinations of Hydrogen in Ferrous Materials by Vacuum Extraction at 800 Degrees Cent. and by Vacuum Fusion," *Journal of Research,* Bureau of Standards, Vol. 26, March 1941, p. 245; RP1373.
14. T. G. Digges, "Influence of Austenitic Grain Size on the Critical Cooling Rate of High Purity Iron-Carbon Alloys," *Journal of Research,* Bureau of Standards, Vol. 24, June 1940, p. 723; RP1308.
15. E. S. Davenport, R. A. Grange and R. J. Hafsten, "Influence of Austenite Grain Size Upon Isothermal Transformation Behavior of S.A.E. 4140 Steel," *Metals Technology,* Vol. 8, Jan. 1941; TP1276.

DISCUSSION

H. ROSE:[1] As the experiments were conducted on high purity materials, I should like to ask Mr. Digges about free ferrite distribution in materials of less purity.

C. D. FOULKE:[2] I should like to ask Mr. Digges whether or not any attempt was made to determine aging characteristics of any of the alloys prepared for this investigation.

---

[1]Assistant metallurgist, Ranger Aircraft Engines, Farmingdale, Long Island, N. Y.
[2]Senior metallurgist, Weirton Steel Company, Weirton, West Virginia.

CYRIL WELLS:[3] As a result of Dr. Derge's work done on high purity steels some years ago and on a basis of my own work, I believe that oxygen diffusing into a steel containing aluminum is at least one factor which contributes to abnormality. Dr. Derge discussed this point very ably I thought in answering a discussion by Mr. Digges.[4]

More recently in my diffusion studies I diffused oxygen from a rather pure Armco iron into a 1.1 per cent carbon steel containing 0.05 per cent or so of aluminum. Carbon of course was also diffused from higher to lower carbon concentrations during the diffusion period. The structures across the diffusion zones were as follows: (1) the carbon and oxygen-rich large-grained Armco iron showed a normal structure, (2) the zone of diffusion involving carbon, oxygen, and aluminum in which alumina could form gave a much more abnormal structure, and (3) the structure of the steel removed from the farthest oxygen penetration was again normal.

It is true that high purity hypereutectoid steels show under certain conditions of cooling a certain degree of abnormality especially in the vicinity of former austenite grain boundaries. This I believe is partly due to the presence of proeutectoid cementite nuclei and absence of proeutectoid ferrite nuclei. The cementite having a nucleating effect probably causes the austenite surrounding it to lose carbon to such an extent that when ferrite subsequently appears close to the carbide-austenite interface the austenite has in it much less carbon than is present in the eutectoid. Under these conditions a rapid separation of ferrite on the newly formed ferrite nuclei present is to be expected with the remaining austenite approaching the eutectoid composition. At distances sufficiently removed from the influence of proeutectoid cementite more normal structures would of course be expected.

Author's Reply

In reply to the inquiry of Mr. Rose, the distribution of free ferrite in the structures of the alloys of both highest and intermediate purity was quite similar to that obtained in abnormal structures of commercial steels. That is, the free ferrite usually existed adjacent to a network of cementite and in the case of extreme conditions certain areas consisted almost entirely of free ferrite and coalesced cementite. A similar distribution of free ferrite in abnormal structures, therefore, would be expected in materials of less purity than the present alloys. With regard to Mr. Foulke's inquiry, tests have not been carried out to determine the aging characteristics of these alloys.

The structures obtained by Dr. Wells in the zone of diffusion of Armco iron and carbon steel containing aluminum and his view regarding the formation of free ferrite in high purity alloys of iron and carbon of hypereutectoid composition are indeed interesting. The mechanism of this transformation has also received some attention by the author. In this study, however, only a few preliminary tests have been completed and definite conclusions cannot be stated at this time.

---

[3]Metals Research Laboratory, Carnegie Institute of Technology, Pittsburgh.

[4]G. Derge, A. R. Kommel, and R. F. Mehl, TRANSACTIONS, American Society for Metals, Vol. 26, 1938, p. 153.

THE SELF-DIFFUSION OF COPPER

By C. L. Raynor, L. Thomassen and L. J. Rouse

Abstract

This paper presents a method for obtaining rates of diffusion, particularly self-diffusion, by employing artificially produced radioactive elements. Experiments were carried out with copper. A mixture of ordinary and radioactive copper was plated onto copper blocks which were then heated at three temperatures for various lengths of time. The diffusion coefficients were calculated directly from intensity measurements of the beta rays emerging from the plated surface before and after heating. The development of the equations for the computation and the method of calculation are given. The dependence of the diffusion coefficient upon temperature was thus established. The values obtained are lower than those anticipated by Rhines and Mehl by extrapolation from binary alloy systems containing copper, but are not as low as those obtained by Rollin and by Steigman, Shockley, and Nix. A possible explanation why the values obtained by direct measurements are lower than those expected by extrapolation is suggested.

A SUITABLE technique for the study of self-diffusion of radioactive metals was first perfected in 1925 by von Hevesy and Obrusheva (4).[1] At the time of its development its use was limited to the naturally occurring radioactive substances and the initial work was carried out on lead which has the naturally occurring radioactive isotope, thorium B. The continuation of this study by von Hevesy (3), (7) and his collaborators gave one of the most complete sets of data now available, and with the series performed by Seith (7) on silver has furnished most of our fundamental conceptions concerning the theory of metallic diffusion. In view of the fact, that series of correlated experiments are the most fruitful for aiding the

[1]The figures appearing in parentheses refer to the bibliography appended to this paper.

This paper is an abstract of a dissertation presented by C. L. Raynor in partial fulfillment of the requirements for the Degree of Doctor of Science at the University of Michigan, Ann Arbor, Mich.

Of the authors, C. L. Raynor is associated with the engineering department, Hoskins Manufacturing Co., Detroit, L. Thomassen is associate professor of metallurgical engineering and L. J. Rouse is assistant professor of mathematics, University of Michigan, Ann Arbor, Mich. Manuscript received August 23, 1940.

progress of our understanding of diffusion, Rhines and Mehl (10) carried out their investigation of the copper-aluminum, copper-beryllium, copper-cadmium, copper-silicon, copper-tin, and copper-zinc systems. A significant result of this latter investigation was the estimation of the self-diffusion coefficient of copper by the extrapolation of their data to zero concentration of solute. By this method self-diffusion coefficients could be estimated when the absence of a radioactive isotope eliminated the possibility of direct determination. The validity of the extrapolation had to await the direct determination of the self-diffusion coefficient of copper.

The availability of artificially induced radioactive metals has made possible the wider application of the von Hevesy (4) method and the continuation of self-diffusion studies. This paper describes a method for obtaining data on self-diffusion which uses artificially produced radioactive substances. The method is illustrated by the determination of the self-diffusion coefficient of copper.

Procedure

Samples for study are prepared in a manner similar to that for a two-component system. The usual method of electrodeposition may be employed and it was chosen for this work. The radioactive copper was prepared by bombarding ordinary copper with deuterons in a cyclotron. The piece of copper to be made radioactive in the cyclotron is called a target and the target after bombardment is then a source of radioactive atoms.

The experimental method consisted of plating the radioactive copper onto a copper block, heating the block to allow diffusion to take place, and calculating the diffusion coefficients from intensity measurements of the beta rays emerging from the plated side of the block before and after diffusion took place.

The following characteristics of the target after removal from the cyclotron had to be considered in choosing the plating technique to be used. The source did not consist of 100 per cent radioactive copper atoms. Only a very small percentage were radioactive, and these were concentrated in that section of the target which was the focal spot for the deuteron beam and to the depth of maximum penetration of the deuterons. This was a volume approximately one-half inch in diameter by 0.005 inch deep. Its position could not be definitely located and how the radioactive atoms were distributed

in it was not determined. Using a source of this nature and plating it directly onto the sample block would result in a plate in which the distribution would be the reverse, top to bottom, of the source.

The distribution of the radioactive atoms in the plate had to be known for the purposes of calculation. This requirement was met by completely dissolving the source and converting the solution into a suitable plating bath. In solution, the distribution became uniform and when this copper was plated, using an insoluble anode, the concentration of radioactive atoms at all sections in the plate was a constant.

The desirability of having as high a concentration as possible of radioactive atoms in the plate made the following target size the most suitable to use. Because atoms at a depth greater than 0.005 inch could not be made radioactive, the targets were cut from a strip 0.005 inch in thickness. The strip was one-half inch in width which would take the entire focal spot. A sufficient length was taken for each target so that it could be easily clamped onto the target holder. The target after bombardment was cut into one-half inch by one-sixteenth inch sections and from these sections those containing the radioactive copper were selected by means of the electroscope. The selected ones were dissolved and the plating bath prepared.

A cyanide bath (1) with a platinum anode was used. The bath was stirred and low current densities were used to insure the obtaining of smooth plates of uniform thickness. The thickness of the plates used varied from 0.00015 to 0.003 inch. The plates of less than 0.001 inch in thickness were not touched after plating. The heavier ones were smoothed on 3/0 emery paper. Before plating, the blocks were annealed in vacuum at 750 or 850 degrees Cent. (1380 or 1560 degrees Fahr.) for 24 hours to prevent any major changes in the grain size during the subsequent diffusion anneal.

The plated blocks, in an evacuated tube, were placed in a cold furnace, heated to 400 degrees Cent. (750 degrees Fahr.), and given a 1-hour soak to remove any occluded hydrogen. The agreement of intensity measurements before and after this treatment showed that no appreciable diffusion took place during this short and low temperature anneal.

For the diffusion anneal all but two of the blocks were heated in vacuum by sealing them in quartz vials. The vials were made

from quartz tubing. A length of 1 to 2 inches was used which just sufficed to enclose the blocks. In this way a temperature gradient along the vial was eliminated. The block dimensions were ½ by ⅜ by $\frac{3}{16}$ inches. No allowance was made in the time at temperature for heating and cooling of the samples. They were always placed in a furnace which was at temperature and as their heat capacity was small they rapidly reached the temperature of their surroundings. Two blocks were not heated in vacuum but in a tube through which hydrogen was continuously passed.

The plate thickness was determined by a measurement of its image at × 1000 on the view plate of a metallographic camera. The average of several readings was used. The blocks treated at 650 and 750 degrees Cent. (1200 and 1380 degrees Fahr.) were measured after the diffusion anneal. This made it possible to cut and measure these blocks along two axes which crossed at right angles at the center of the block. The blocks treated at 850 degrees Cent. (1560 degrees Fahr.) had to be measured before the diffusion anneal since grain growth obliterated the plate boundary in this case. For this latter case, as the blocks had to be preserved, readings of the plate thickness were limited to one edge.

The radioactivity was measured by means of a Lauritsen (6) electroscope. Normal decay of the intensity of the source was allowed for by correcting all readings to a common base time for comparison. This was done by means of the normal decay curve for copper. Radioactive copper has a half-life period of 12.8 hours (13). This value was confirmed in the present investigation. The intensities used were the average of at least two measurements.

The copper used throughout the work was oxygen-free high conductivity copper and a spectrographic analysis showed it to be of excellent purity.

Method of Calculation

The diffusion coefficient is defined by Fick's Law,

$$dm = DA\frac{dc}{dx}dt \qquad (1)$$

From equation (1) we may derive the differential equation,

$$\frac{dc}{dt} = \frac{d}{dx}\left(D\frac{dc}{dx}\right) \qquad (2)$$

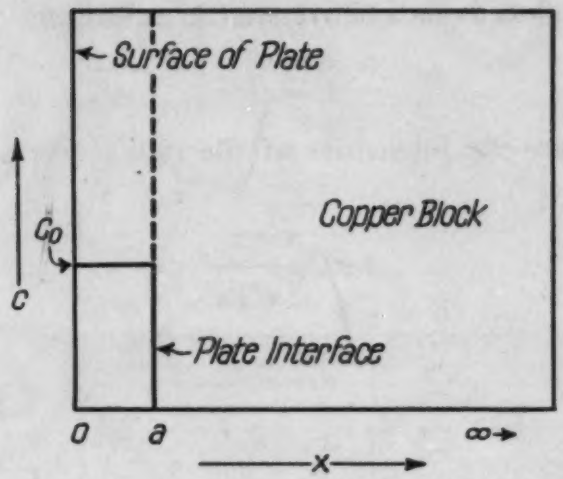

Fig. 1—Graph Showing the Initial Distribution of Solute.

For self-diffusion D may be taken out of the differential,

$$\frac{dc}{dt} = D\frac{d^2c}{dx^2} \tag{3}$$

In the solution of this equation the following limits, which apply to the experimental procedure used, must be considered:

1) At $t = 0$, Fig. 1,
$c = c_o$ for $0 < x < a$
and
$c = 0$ for $x > a$

2) For $t > 0$,
$c = 0$ at $x = \infty$

The integration of equation (3) according to these limits yields the equation of the concentration depth curve.

$$c = \frac{c_o}{\sqrt{\pi}} \int_{-\frac{a+x}{2\sqrt{Dt}}}^{\frac{a-x}{2\sqrt{Dt}}} e^{-\beta^2} d\beta \tag{4}$$

c is the concentration at the depth x after the time t.
c_o is the initial concentration.
a is the plate thickness.
D is the diffusion coefficient.
β is an integration variable.

When the solute is radioactive we can substitute

$$i_o = c_o$$
$$i = c$$

where i_o and i are the intensities of the radioactive solute per unit volume.

$$i = \frac{i_o}{\sqrt{\pi}} \int_{-\frac{a+x}{2\sqrt{Dt}}}^{\frac{a-x}{2\sqrt{Dt}}} e^{-\beta^2} d\beta \qquad (5)$$

The intensity of beta rays emerging from a given surface of a block of copper which contains a given amount of radioactive copper is a function of the distribution of the radioactive copper in the block. This is due to the stopping power of copper for beta rays. The stopping power was determined by measuring the intensity of a source after various thicknesses of copper had been interposed between it and the electroscope. The data are shown in Fig. 2 and the equation of this curve is:

$$I = I_o e^{-\mu x} \qquad (6)$$

I is the intensity passing through the thickness x.

I_o is the initial intensity.

μ is the absorption coefficient. Its value was found to be 786 inches^{-1}.

The intensity i′ emerging from one side of the block due to an intensity i at x is given by

$$i' = A\, i\, e^{-\mu x} \qquad (7)$$

A is the area of the surface.

The total intensity is the summation of all such terms as equation (7) or,

$$I = \Sigma\, i' = \int_0^\infty A\, i\, e^{-\mu x}\, dx \qquad (8)$$

I, the total intensity emerging from the given surface can be measured.

Combining equations (5) and (8)

$$I = A \int_0^{\infty} \left[\frac{i_o}{\sqrt{\pi}} \int_{-\frac{a+x}{2\sqrt{Dt}}}^{\frac{a-x}{2\sqrt{Dt}}} e^{-\beta^2} d\beta \right] e^{-\mu x} dx \qquad (9)$$

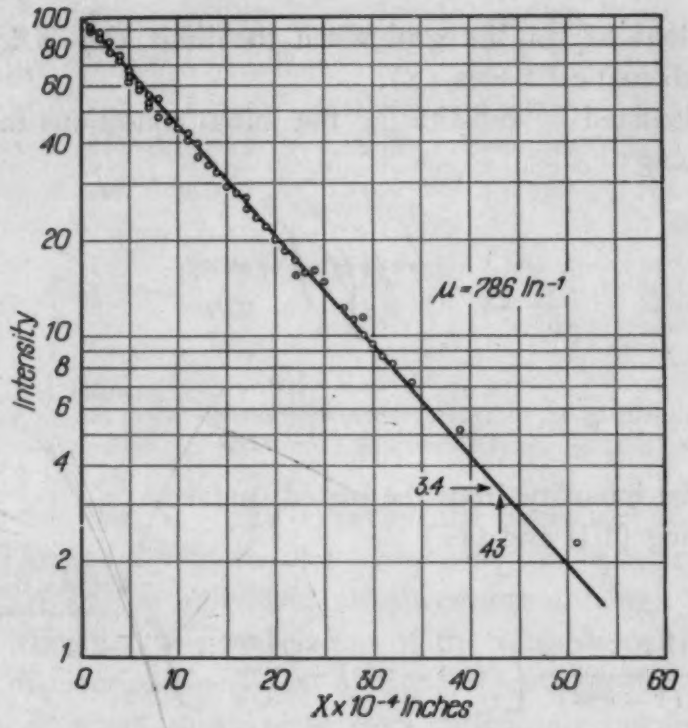

Fig. 2—The Measured Intensity (I), Expressed as Per Cent of the Initial Intensity (I_o), Passing Through Copper of Varying Thicknesses (x).

and integrating

$$\frac{1}{A} = \frac{i_o}{2\mu} e^{\mu^2 tD} \left[(e^{\mu a} - e^{-\mu a}) - \frac{2 e^{\mu a}}{\sqrt{\pi}} \int_0^{\frac{a+2\mu tD}{2\sqrt{tD}}} e^{-\beta^2} d\beta \right.$$

$$\left. + \frac{2 e^{-\mu a}}{\sqrt{\pi}} \int_0^{\frac{-a+2\mu tD}{2\sqrt{tD}}} e^{-\beta^2} d\beta \right] + \frac{2 i_o}{\mu \sqrt{\pi}} \int_0^{\frac{a}{2\sqrt{tD}}} e^{-\beta^2} d\beta \qquad (10)$$

we have the equation for calculating D from intensity measurements of the beta rays emerging from the plated side of the block.
I can be measured at any time (t) by means of the Lauritsen electroscope.

$$\frac{2}{\sqrt{\pi}} \int_0^y e^{-\beta^2} d\beta \quad \text{is the probability integral.}$$

The values of this integral when the limit (y) is known are given in mathematical tables (8).
i_o can be calculated by substituting the initial conditions in equation (8) and solving:

$$I_1 = A\, i_o \int_0^a e^{-\mu x}\, dx$$

$$i_o = \frac{I_1 \mu}{A\,(1 - e^{-\mu a})} \tag{11}$$

I_1 is the initial intensity from the plated surface.
Combining (10) and (11)

$$I = \frac{I_1 e^{\mu^2 tD}}{2\,(1 - e^{-\mu a})} \left[(e^{\mu a} - e^{-\mu a}) - \frac{2 e^{\mu a}}{\sqrt{\pi}} \int_0^{\frac{a + 2\mu tD}{2\sqrt{tD}}} e^{-\beta^2} d\beta \right. \tag{12}$$

$$\left. + \frac{2 e^{-\mu a}}{\sqrt{\pi}} \int_0^{\frac{-a + 2\mu tD}{2\sqrt{tD}}} e^{-\beta^2} d\beta \right] + \frac{2 I_1}{\sqrt{\pi}\,(1 - e^{-\mu a})} \int_0^{\frac{a}{2\sqrt{tD}}} e^{-\beta^2} d\beta$$

The diffusion coefficient D may be calculated from this equation, using the data of Table I, by the method of trial and error.

Results and Discussion

The self-diffusion coefficient for copper was determined at three temperatures and the effect of temperature on the rate of diffusion

Table I
Data Used and the Diffusion Coefficients Determined

Sample No.	Block Annealing Temp. Degrees Cent.	Diffusion Temperature Degrees Cent.	Plate Thickness Inch	Initial Intensity I_1 Sec.$^{-1}$	Final Intensity I Sec.$^{-1}$	Time at Temperature Hours	Diffusion Coefficient Cm.^{2}/Sec.
10	850	650	0.00023	$1.83\cdot10^{-2}$	$1.53\cdot10^{-2}$	85.6	$2.03\cdot10^{-12}$
11	850	650	0.00015	$1.26\cdot10^{-2}$	$9.75\cdot10^{-3}$	85.6	$3.17\cdot10^{-12}$
17	850	650	0.00015	$1.18\cdot10^{-2}$	$8.90\cdot10^{-3}$	69.9	$4.57\cdot10^{-12}$
22	850	650	0.00058	$8.85\cdot10^{-2}$	$7.44\cdot10^{-2}$	93.9	$3.68\cdot10^{-12}$
23	850	650	0.00050	$8.76\cdot10^{-2}$	$7.57\cdot10^{-2}$	93.9	$2.53\cdot10^{-12}$
						Av. =	$3.20\cdot10^{-12}$
1	750	750	0.0014	$9.16\cdot10^{-2}$	$5.94\cdot10^{-2}$	96.2	$3.35\cdot10^{-11}$
4	750	750	0.0028	$6.41\cdot10^{-2}$	$5.97\cdot10^{-2}$	103.0	$1.34\cdot10^{-11}$
6	750	750	0.0016	$6.06\cdot10^{-2}$	$4.40\cdot10^{-2}$	106.0	$2.29\cdot10^{-11}$
18*	850	750	0.0015	$1.84\cdot10^{-2}$	$1.31\cdot10^{-2}$	77.0	$2.96\cdot10^{-11}$
19*	850	750	0.0014	$1.94\cdot10^{-2}$	$1.43\cdot10^{-2}$	77.0	$2.53\cdot10^{-11}$
						Av. =	$2.49\cdot10^{-11}$
20a	850	850	0.0017	$3.54\cdot10^{-2}$	$2.24\cdot10^{-2}$	24.0	$2.79\cdot10^{-10}$
20b**	...	...	.....	$3.54\cdot10^{-2}$	$1.81\cdot10^{-2}$	46.0	$2.35\cdot10^{-10}$
21a	850	850	0.0020	$3.66\cdot10^{-2}$	$2.42\cdot10^{-2}$	24.0	$2.90\cdot10^{-10}$
21b	...	...	.....	$3.66\cdot10^{-2}$	$1.98\cdot10^{-2}$	46.0	$2.44\cdot10^{-10}$
						Av. =	$2.62\cdot10^{-10}$

*Annealed in hydrogen.
**The same sample as 20a but put back in the furnace for an additional 22 hours.

was obtained, Fig. 3. The experimental variation of the data is shown. The validity of the data, however, can best be shown by a consideration of the individual measurements although the accuracy of D is subject to the interrelation of the variables with each other.

The Absorption Coefficient of Copper for Beta Rays—The magnitude of D is not sensitive to even rather large changes μ. The value of μ is given by Steigman, Shockley and Nix (12) as 700 inches^{-1}, but when this value is used instead of that determined in this work no appreciable change in D is noted.

Intensity Measurements—The average deviation of the intensity measurements, from the mean of all readings for that intensity determination, was 1.5 per cent. A maximum error of this amount in both intensity measurements or a 3 per cent error in the ratio would show an average error of 14 per cent in D. It is thought that the error from this source was considerably less.

The Plate Thickness—Great care had to be taken in the plating operation. This is necessary when the entire width of a plate and thus the outside edge is used. Every precaution was taken to have as smooth a surface as possible. Some individual measurements varied as much as 50 per cent from the mean. However, the aver-

age was much better as shown by the following. All of the samples except those treated at 850 degrees Cent. (1560 degrees Fahr.) were repolished at least once and the average variation of the reading for each polish from the mean was only 8 per cent. Hence, the error from this source was less than 10 per cent.

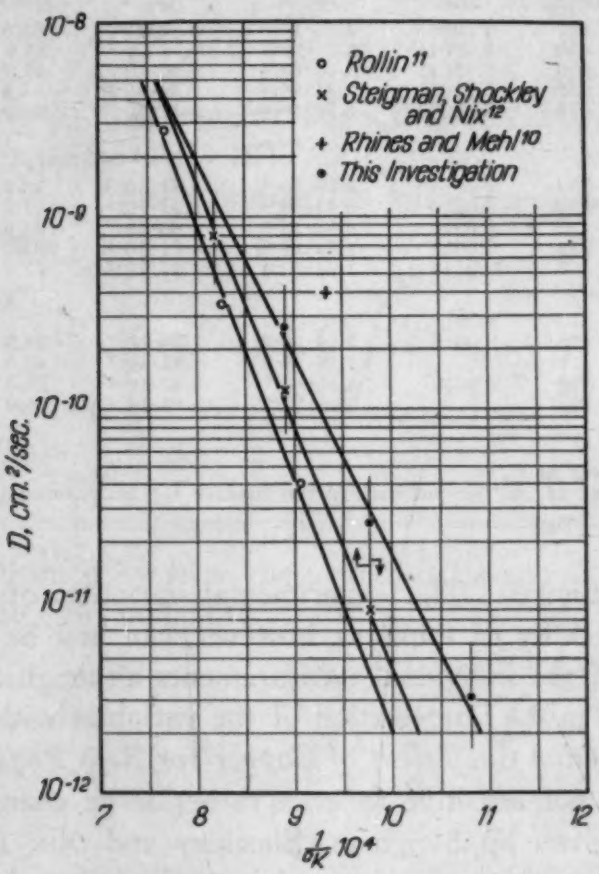

Fig. 3—The Self-Diffusion Coefficient of Copper Versus Temperature.

Temperature—Small variations in temperature are not distinguishable on the scale used for the plot.

Time—There was no uncertainty in this measurement.

It is to be noted that the depth-concentration curve was not used for the calculation and thereby the uncertainties associated with its use were avoided.

The determination of the self-diffusion coefficient of copper renders more complete Rhines and Mehl's (10) series of measurements on the copper-aluminum, copper-beryllium, copper-cadmium, copper-silicon, copper-tin and copper-zinc systems. Their extrapo-

lated value of 4.10^{-10} centimeter per second squared at 800 degrees Cent. (1470 degrees Fahr.) seems to be too high. This is shown in Fig. 3. This is undoubtedly due to the inaccuracy of their data at the concentration limits, as mentioned by them, and the necessity of extrapolation from the regions of rather high concentration. At very low concentrations it is likely that the diffusion coefficient does decrease and approach the self-diffusion coefficient of copper. Or, starting with pure copper, for solute additions of very much less than 1 atomic per cent the diffusion coefficient increases rapidly. The rate of increase then falls off and only increases slightly until the limit of solubility is reached. Close to the limit of solid solubility the rate of increase of the diffusion coefficient is again rapid.

This conception of the shape of the curve at low concentrations can be understood from the following considerations. Whatever the crystal form of the solvent is, the introduction of a foreign, solute atom into this lattice disarranges it. This condition allows for the more rapid penetration of additional solute atoms through the solvent lattice. However, for solute atoms to aid each other in this way, there must be enough present so that the effect of one is noticeable to another. Or, the solute atoms must be close enough together so that the disorder caused by one is not smoothed out in the interval between it and another solute atom. The effect at low concentrations is therefore that a rapid increase in the rate of diffusion results from small increases in the amount of solute added. The slope of the curve falls off as soon as there is enough solute present to make the disorder of the solvent lattice practically continuous. The lower values of concentration for which Rhines and Mehl (10) determined the coefficients were on the plateau portion of the curve. The extrapolation, therefore, gave an incorrectly high value of the self-diffusion coefficient.

Also shown in Fig. 3 are the results of two other investigations (11, 12) on copper which were published after the inception of this work. The methods were sufficiently different and this work had advanced so far it was decided that it was worthy of completion.

A modification of the Dushman-Langmuir equation (2),

$$D = A e^{-\frac{Q}{RT}},$$

was used to represent the data. The Q values, Table II, show that the slope of the curve representing the data obtained in this investi-

gation is in closer agreement with the expected value as given by Rhines and Mehl (10) and by Kanter (5, 9). The extrapolated value of Rhines and Mehl (10), however, would be expected to be low due to the same considerations as discussed for the diffusion coefficient. As the diffusion coefficient decreases and the total amount of diffusion is less, slight variations in the handling and measurement of the samples have greater weight. Thus a greater variation in the data is to be expected at the lower temperatures.

Table II

Summary of the Q Values for the Dushman-Langmuir Equation,

$$D = A e^{-\frac{Q}{RT}}$$

Rhines and Mehl (10)	44,000 cal./mol.
Kanter*	39,000 " "
Rollin (11)	61,400 " "
Steigman, Shockley and Nix (12)	57,200 " "
This investigation	46,800 " "

*Private communication to Rhines and Mehl (10). The method is given in reference 5.

Many times the question of interference to diffusion by the interface between the electrodeposited layer and the body of the sample has been mentioned. The agreement between the data of Rollin (11), and Steigman, Shockley and Nix (12), and this work show that electrodeposition is a satisfactory method for preparing diffusion samples. Rollin (11) used a direct method for preparing his samples which eliminated such an interface.

In Table I it is noted that two samples were run in hydrogen. No effect due to this was noted in the coefficients calculated from these samples. Also, no difference was observed by a change in the block anneal from 750 to 850 degrees Cent. (1380 to 1560 degrees Fahr.), although the grain size was somewhat larger at 850 degrees Cent. (1560 degrees Fahr.). During the 650 and 750 degrees Cent. (1200 and 1380 degrees Fahr.) diffusion anneals, the grain size remained practically constant. However, during diffusion at 850 degrees Cent. (1560 degrees Fahr.) there was continuous grain growth. This was why the plate thickness on these blocks had to be measured before the anneal as the grains grew across the boundary and obliterated it. This also did not produce a noticeable effect in the results of this test.

Summary

A method for obtaining data on diffusion which uses artificially produced radioactive substances has been presented.

The self-diffusion coefficient for copper was determined at three temperatures and the dependence upon temperature obtained. The rate of diffusion is lower than was expected from the value given by Rhines and Mehl (10).

The method of calculation is presented and it is shown that assumptions which are inherent in other methods may be eliminated.

Acknowledgment

The helpful assistance of Professor J. M. Cork and his collaborators of the Physics Department of the University of Michigan is gratefully acknowledged.

Bibliography

1. W. Blum and G. B. Hogaboom, "Principles of Electroplating and Electroforming," 1924, McGraw-Hill Book Co., New York.
2. S. Dushman and I. Langmuir, *The Physical Review,* Vol. 20, 1922, p. 113.
3. G. von Hevesy, *Transactions,* Faraday Society, Vol. 34, 1938, p. 841.
4. G. von Hevesy and A. Obrusheva, *Nature,* Vol. 115, 1925, p. 674.
5. J. J. Kanter, *Metals Technology,* Dec., 1937.
6. C. C. Lauritsen and T. Lauritsen, *Review of Scientific Instruments,* Vol. 8, 1937, p. 438.
7. R. F. Mehl, *Transactions,* American Institute of Mining and Metallurgical Engineers, Vol. 122, 1936, p. 11. See bibliography.
8. B. O. Pierce, "A Short Table of Integrals," 1910, Ginn and Co.
9. Private communication to R. F. Mehl (7).
10. F. N. Rhines and R. F. Mehl, *Transactions,* American Institute of Mining and Metallurgical Engineers, Vol. 128, 1938, p. 185.
11. B. V. Rollin, *The Physical Review,* Vol. 55, 1939, p. 231.
12. J. Steigman, W. Shockley and F. C. Nix, *The Physical Review,* Vol. 56, 1939, p. 13.
13. S. N. van Voorhis, *The Physical Review,* Vol. 50, 1936, p. 895.

THE OVER-ALL LINEAR EXPANSION OF THREE FACE-CENTERED CUBIC METALS (Al, Cu, Pb) FROM —190 DEGREES CENT. TO NEAR THEIR MELTING POINTS

By John W. Richards

Abstract

Direct measurements of length were made for aluminum, copper, and lead at liquid air temperatures and at intervals up to temperatures close to the melting points of these metals. By extrapolation to 0 degrees Kelvin and to the melting points, the total linear expansion of aluminum from absolute zero to its melting point was found to be 2.66 per cent of its length at absolute zero, of copper 2.78 per cent, and of lead 1.61 per cent.

The expression $L=L_0(1+at+bt^2+ct^3)$ *was found to express the relationship between length and temperature; where L is the length at the centigrade temperature t, and* L_0 *is the length at zero degrees centigrade. For aluminum* $a=2.02\times10^{-5}$, $b=1.4\times10^{-8}$, $c=5.9\times10^{-12}$, *for copper* $a=1.67\times10^{-5}$, $b=3.8\times10^{-9}$, $c=1.5\times10^{-12}$, *and for lead* $a=2.63\times10^{-5}$, $b=1.4\times10^{-8}$, $c=3.1\times10^{-12}$.

IT is the purpose of this paper to present a series of direct measurements of length for aluminum, copper, and lead, in which a whole series of measurements ranging from close to the melting point down to liquid air temperatures were made on a single specimen for each metal. Since an expansion curve of a material must necessarily be very flat at temperatures approaching 0 degrees Kelvin, it is easy to extrapolate the data back to 0 degrees Kelvin. The highest temperatures used for each metal were so close to the melting points that extrapolation to the melting points could be made safely. This gives, for the three metals investigated, reliable values of their over-all expansions from 0 degrees Kelvin to their melting points.

Apparatus and Technique

Because of the variations in the data found in the literature it is desirable to give a rather detailed description of the apparatus used

A paper presented before the Twenty-third Annual Convention of the Society held in Philadelphia, October 20 to 24, 1941. The author, John W. Richards, is professor of physics, Mt. St. Mary's College, Emmitsburg, Maryland. Manuscript received April 26, 1941.

in this work so that the data presented here may be properly assayed. The furnace is shown in Fig. 1. The outer shell was a cast iron pipe 20 inches long and 11 inches in diameter. The ends of the furnace were disks of boiler plate bolted to flanges which in turn were brazed to the ends of the pipe. Gaskets made of soft copper tubing were used between the ends and the flanges. Co-axial with this pipe was an alundum tube 15 inches long with an internal diameter of 4 inches. The ends were capped with transite plates. A heating

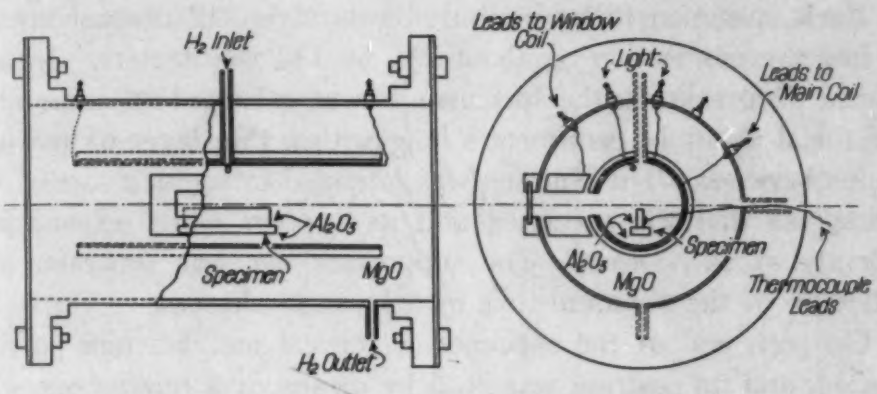

Fig. 1—The Furnace Used in this Investigation.

unit made of 0.025-inch molybdenum wire was wound on the tube. An asbestos-magnesia mixture, such as is ordinarily used on steam pipes, served partly as heat insulation between the tube and the pipe, and partly as support for the tube. The furnace was long enough so that, with this insulation, the middle 4 inches were of substantially uniform temperature. It was this middle portion that was used in these experiments.

The pipe and the alundum tube were each provided with a viewing slot about 4½ inches long so that the central portion of the furnace could be seen directly from the outside. The two slots were connected by a transite box covered with a thin layer of alundum cement. To prevent heat loss and possible condensation of vapors this box was wound with an auxiliary heater of molybdenum wire. The pipe was provided with a pyrex window opposite the viewing slot. The window was sealed with a water glass-asbestos mixture. An accessory heater was placed outside the window during the high temperature part of the runs on copper to prevent condensation of vapor. A second window was added during the low temperature part of each run to prevent condensation of moisture. The connec-

tions of the heating elements were made by means of spark plugs screwed into the furnace shell. Insulated thermocouple leads were brought in through ½-inch pipes screwed into the shell. These pipes were about 5 inches long. They were sealed at the outside end with alundum cement and water glass. Two additional pipes were screwed into the furnace shell, one on the top—and one on the bottom as shown in Fig. 1. The upper pipe served as an inlet for liquid air and for hydrogen or nitrogen. The lower pipe served as an outlet for evaporated liquid air and hydrogen or nitrogen.

Each specimen to be measured was about 12 centimeters long and had a cross section of about 2½ by 1¼ centimeters. In order to avoid distortions in the specimen, it was mounted on a bar of the same metal about 14 centimeters long with a thin layer of powdered alumina between. The alumina was intended to act as a sort of "ball bearing" so that the specimen and its support could expand independently of each other. The supporting bar was separated from the bottom of the alundum tube by a layer of alumina.

On each end of the specimen a vertical molybdenum post was mounted, and its position was read by means of a microscope which traveled on a track provided with a scale and a vernier (Cenco No. 72935). The travelling microscope measured the actual length of the specimen at each reading, not just the expansion or contraction from the previous reading.

All temperatures were measured by means of thermocouples embedded in the specimen. A chromel-alumel thermocouple was used. It was checked against a standardized copper-constantan thermocouple over the range in which the latter could be used and was further calibrated by noting the potentials at the melting points of little posts of silver and lead placed in a porcelain boat fastened to the top of the specimen by means of alundum cement. The potentials due to the thermocouples were measured in the usual way with a potentiometer.

The aluminum was furnished through the courtesy of J. A. Nock, Jr., of the Aluminum Company of America. The following analysis was given: Silicon, 0.004 per cent, iron, 0.003 per cent, copper, 0.004 per cent, and aluminum, 99.989 per cent.

C. A. Hall of the Electric Storage Battery Company kindly furnished the lead. It was Doe Run lead with the following spectrographic analysis: Copper 0.0001 per cent, silver, 0.0001 per cent,

iron, 0.0001 per cent, with no cadmium, bismuth, nickel, cobalt, antimony, or tin.

The copper was "bus-bar" copper and therefore was of high purity. Its chief impurities are usually at crystal boundaries where they have the least effect on the coefficient of expansion.

At the beginning of each run the length of the specimen at room temperature was measured; then liquid air was forced into the furnace until a constant temperature was obtained, at which time another length measurement was made. The furnace was then allowed to come to room temperature where the length was again read. The

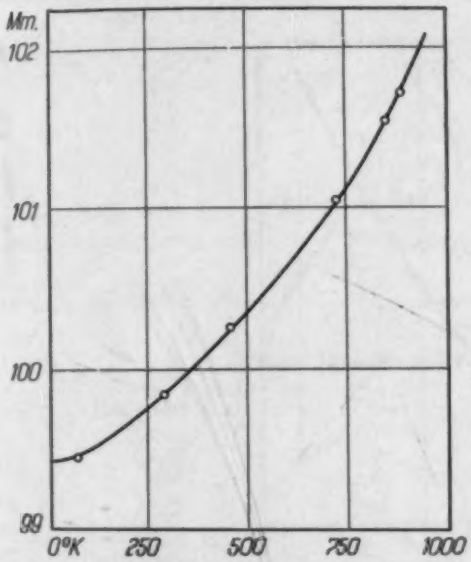

Fig. 2—Expansion Curve of Aluminum.

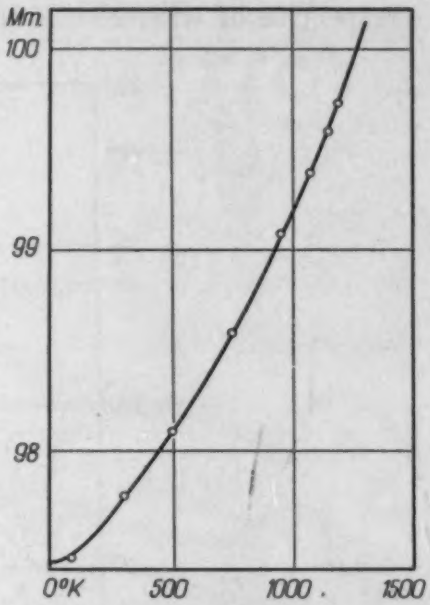

Fig. 3—Expansion Curve of Copper.

furnace temperature was then slowly raised. While the furnace was above room temperature hydrogen or nitrogen was passed in to prevent oxidation of the specimen and the heating elements. At each point where a measurement was made the furnace was kept at one temperature for several hours to insure the establishment of thermal equilibrium.

Once the reading of the highest temperature was taken the power was shut off and the furnace allowed to cool. The cooling was halted at various temperatures and length measurements made. When room temperature was reached the length was checked against that at the start of the run. Several measurements of the length were made at each point.

With aluminum and lead, hydrogen or nitrogen was used as an

atmosphere in the furnace. With copper, however, it was found necessary to use hydrogen exclusively at high temperatures because the nitrogen used contained enough oxygen to oxidize the specimen and thermocouple above 800 degrees Cent.

Results

Tables I, II, and III and Figs. 2, 3, and 4 give the expansions for typical specimens of aluminum, copper and lead from liquid air temperature to temperatures near their melting points. Within the precision of plotting identical data were obtained time after time irrespective of whether the specimen was being cooled or heated.

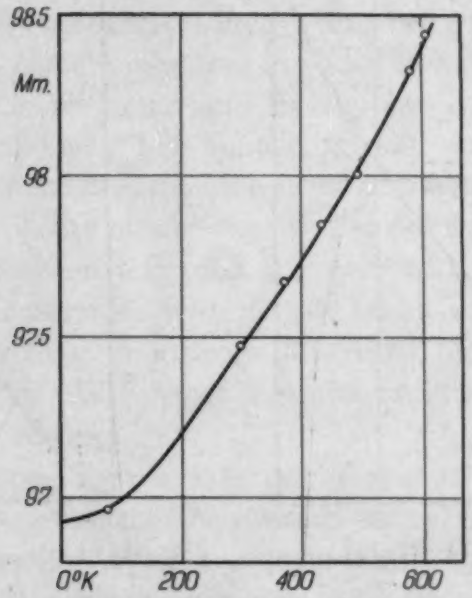

Fig. 4—Expansion Curve of Lead.

If the data of Tables I, II, and III are expressed in terms of the customary equation

$$L = L_o (1 + at + bt^2 + ct^3)$$

the following coefficients are found:—

for aluminum, $a = 2.02 \times 10^{-5}$
$b = 1.4 \times 10^{-8}$
$c = 5.9 \times 10^{-12}$

for copper, $a = 1.67 \times 10^{-5}$
$b = 3.8 \times 10^{-9}$
$c = 1.5 \times 10^{-12}$

for lead, $a = 2.63 \times 10^{-5}$
$b = 1.4 \times 10^{-8}$
$c = 3.1 \times 10^{-12}$

Table I
Change in Length of Aluminum with Temperature

Degrees Cent.	Length in mm.
−191	99.44
27	99.84
193	100.27
463	101.05
588	101.54
623	101.72
M.P. 658.7	

Table II
Change in Length of Copper with Temperature

Degrees Cent.	Length in mm.
−190	97.47
28	97.77
223	98.09
476	98.59
685	99.09
808	99.39
890	99.59
934	99.73
M.P. 1083	

Table III
Change in Length of Lead with Temperature

Degrees Cent.	Length in mm.
−190	96.96
27	97.47
103	97.68
160	97.85
223	98.02
309	98.33
325	98.42
M.P. 327.5	

For purposes of comparison, the values of the expansion coefficients to be found in the literature are shown in Tables IV, V, and VI.

It will be noted that the data in the literature do not agree among themselves over similar temperature ranges, and that they differ considerably from the values reported in this paper. It is felt that the technique described above for mounting the specimens, for protecting the specimens from oxidation, and for measuring total lengths of single specimens over the whole temperature range, should lend considerable weight to the present data.

Figures 1, 2, and 3 show by extrapolation what the length of typical specimens would have been at 0 degree Kelvin and at the melting point. The total linear expansions of these specimens from

0 degree Kelvin to their melting points (expressed as percentage of the 0 degree Kelvin lengths), are therefore as follows:

for aluminum 2.66 per cent
for copper 2.78 per cent
for lead 1.61 per cent

Table IV
The Expansion Coefficients in the Literature for Aluminum

Range in degrees Cent.	$a10^5$	$b10^8$	$c10^{12}$	Number of Reference
100	2.36			(38)
180	2.50			(38)
260	2.66			(38)
340	2.84			(38)
420	2.96			(38)
500	3.11			(38)
530	3.23			(38)
−253 to 0	1.47			(39)
−190 to 0	1.80			(39)
0 to 100	2.37			(39)
20 to 300	2.57			(29)
20 to 500	2.77			(29)
20 to 600	3.01			(29)
−200 to 0	2.265	1.675	3.667	(22,23)
0 to 600	2.265	0.95		(16,18,21,24, 25,26,27)
0 to 600	2.258	0.989		(19)
0 to 600	2.190	1.20		(21)
−78 to 500	2.29	0.9		(17)
−191 to 623	2.02	1.4	5.9	This paper

Table V
The Expansion Coefficients in the Literature for Copper

Range in degrees Cent.	$a10^5$	$b10^9$	$c10^{12}$ ($d10^{15}$)	Number of Reference
−100 to 400	1.62	9.5	−20 d 23	(24,23,16,20)
−250 to −193	0.39			(34)
−193 to −183	0.68			(34)
−183 to 19	1.23			(34)
0 to 1000	2.00			(25)
−253 to −185	0.49			(37)
−185 to −103	1.21			(37)
−103 to 0	1.54			(37)
0 to 101	1.62			(37)
110	1.68			(38)
140	1.68			(38)
180	1.69			(38)
220	1.77			(38)
260	1.73			(38)
300	1.75			(38)
20 to 1083	2.13			(42)
−193 to 1083	2.35			(41)
	2.24			
12 to 39	1.709	40.4		(43)
	(used t-30 in place of t)			
−190 to 934	1.67	3.8	1.5	This paper

It is of interest to note that the total expansion found for aluminum and for copper are consistent with the theoretical minimum

Table VI
The Expansion Coefficients in the Literature for Lead

Range in degrees Cent.	$a10^5$	$b10^9$	$c10^{12}$ ($d10^{15}$)	Number of Reference
−200 to 150	2.83	12	−13.3 d 75	(31,32,24 33,34,36)
0 to 320	3.3			(35)
14 to 94	2.726	7.4		(40)
−253 to 0	2.47			(39)
−190 to 0	2.61			(39)
0 to 100	2.89			(39)
80	2.90			(38)
120	2.95			(38)
160	3.02			(38)
200	3.12			(38)
240	3.20			(38)
280	3.43			(38)
−190 to 325	2.63	14	3.1	This paper

value of 2.6 per cent (15)[1]. The low value found for lead cannot be explained by assuming distortion of the specimen, for measurements of length could be duplicated on successive runs with the same specimen. It may possibly be accounted for by assuming that the melting point assigned to lead is really the temperature at which sub-microscopic crystal fragments are washed off the surface by molten lead from the grain boundaries. Improbable as such an explanation seems at first sight, it is consistent with the experimental work of Goetz (44) and of Mueller (45) on bismuth and on paraffin.

Summary

Measurements of length have been made on rather pure specimens of aluminum, copper, and lead from liquid air temperatures to temperatures close to their melting points, using, for a given run, the same specimen over the whole temperature range. The customary three expansion coefficients have been determined for the three metals. By extrapolation of the L-t curves, their over-all linear expansions from 0 degree Kelvin to the melting points have been found to be 2.66 per cent for aluminum, 2.78 per cent for copper, and 1.61 per cent for lead.

Bibliography

1. Lindemann, *Physik. Zeit.*, Vol. 11, 1910, p. 609.
2. Grüneisen, *Ann. d. Physik*, Vol. 39, 1912, p. 257.
3. Braunbeck, *Zeit. f. Physik*, Vol. 38, 1926, p. 549.
4. Raschevsky, *Zeit. f. Physik*, Vol. 40, 1927, p. 214.

[1]The figures appearing in parentheses refer to the bibliography appended to this paper.

5. Herzfeld and Goeppert-Mayer, *Physical Review*, Vol. 46, 1934, p. 995.
6. Born, *Journal of Chemistry and Physics*, Vol. 7, 1939, p. 591.
7. Born, "Atomtheorie des festen Zustandes," Leipzig, 1923.
8. Lennard-Jones and Devonshire, *Proceedings of the Royal Society*, Vol. A169, 1939, p. 317.
9. Bragg and Williams, *Proceedings of the Royal Society*, Vol. A145, 1934, p. 699; Vol. 151, 1935, p. 540; Vol. 152, 1935, p. 230.
10. Brillouin, *Physical Review*, Vol. 54, 1938, p. 916.
11. Brillouin, "La Structure des Corps Solides" (A. S. I., No. 549, Hermann, Paris, 1937).
12. Stern, *Ann. d. Physik*, Vol. 51, 1916, p. 237.
13. Williams, *Physical Review*, Vol. 46, 1934, p. 1011.
14. Rice, *Journal of Chemistry and Physics*, Vol. 7, 1939, p. 883.
15. Davey, "A Study of Crystal Structure and Its Applications" (McGraw-Hill, 1934), p. 410-412.
16. Dittenberger, *Zeit. ver. de. ing.*, Vol. 46, 1902, p. 1532.
17. Scheel, *Zeit. f. Physik*, Vol. 5, 1921, p. 167.
18. Jaeger and Scheel, *Electrotechnische Zeit.*, Vol. 40, 1919, p. 150.
19. Hidnert, Bur. of Standards, Scientific Paper, No. 497 (1925).
20. Hidnert, Bur. of Standards, Scientific Papers, No. 410 (1922).
21. Souder and Hidnert, Bur. of Standards, Scientific Papers, No. 426 (1921).
22. Ayres, *Physical Review*, Vol. 20, 1905, p. 38.
23. Henning, *Annal. d. Physik*, Vol. 22, 1907, p. 631.
24. Fizeau, *Comptes Rendus*, Vol. 68, 1869, p. 1125.
25. Le Chatelier, *Comptes Rendus*, Vol. 108, 1889, p. 1096.
26. Lussana, *Nuovo Cimento*, Vol. 19, 1910, p. 182.
27. Schulze, *Physik. Zeit.*, Vol. 22, 1920, p. 402.
28. Schulze, *Zeit. Phys., Vol.* 47, 1928, p. 712-122.
29. Schulze, *Zeit. Phys.*, Vol. 49, 1928, p. 146-154.
30. Brislee, *Chemical News and Journal of Industrial Science*, Vol. 105, 1912, p. 3.
31. Dorsey, *Physical Review*, Vol. 25, 1907, p. 88.
32. Dorsey, *Physical Review*, Vol. 27, 1908, p. 1.
33. Grüneisen, *Ann. d. Physik*, Vol. 33, 1910, p. 65.
34. Lindemann, *Physik. Zeit.*, Vol. 12, 1911, p. 1197.
35. Vincentini and Omodei, *Atti della reale accademia nazionale dei Lincei*, Vol. 31, 1887, p. 235, 294, 321.
36. Rauramo and Saarilko, *Översicht av Finska Veterschaps-Scoietetens Förhandinger*, Vol. 54A: No. 24, 1912.
37. Keesom, van Agt, and Jansen, *Proceedings of Amsterdam*, Vol. 29, 1926, p. 1786-1791.
38. Uffleman, *Philosophical Magazine*, Vol. 10, 1930, p. 633-659.
39. Ebert, *Zeit. Phys.*, Vol. 47, 1928, p. 712-722.
40. Matthiessen, *Proceedings of the Royal Society*, Vol. 15, 1866, p. 220; *Pogg. Ann.*, Vol. 130, 1867, p. 50; *Philosophical Magazine*, Vol. 32, 1866, p. 472.
41. Haring, M. S. Thesis, The Penna. St. College (1934).
42. Davey and Wilson, *Physical Review*, Vol. 27, 1926, p. 819.
43. Voigt, *Gött. Nachr.* (1893) 177. *Wied. Ann.*, Vol. 49, 1893, p. 697.
44. Goetz, *Physical Review*, Vol. 35, 1930, p. 193.
45. Mueller, *Proceedings of the Royal Society*, Vol. 127, 1930, p. 417.

DISCUSSION

Written Discussion: By Peter Hidnert, U. S. Department of Commerce, National Bureau of Standards, Washington, D. C.

From the data presented in Tables I to III, it appears that the lengths of

the samples were determined to the nearest 0.01 millimeter per 10 centimeters. If so, this does not represent a high degree of precision for thermal expansion determinations. This may also account for the fact that the author apparently obtained identical data irrespective of whether the samples were being cooled or heated. It would be of interest to know whether the data in these tables were derived from several different runs and if so, the magnitude of the variations for the different runs.

The probable error of the length computed from Richards' equation for aluminum is ±0.022 per cent, whereas the probable error of the length from Hidnert's second-degree equation (Scientific Paper, Bureau of Standards, Vol.

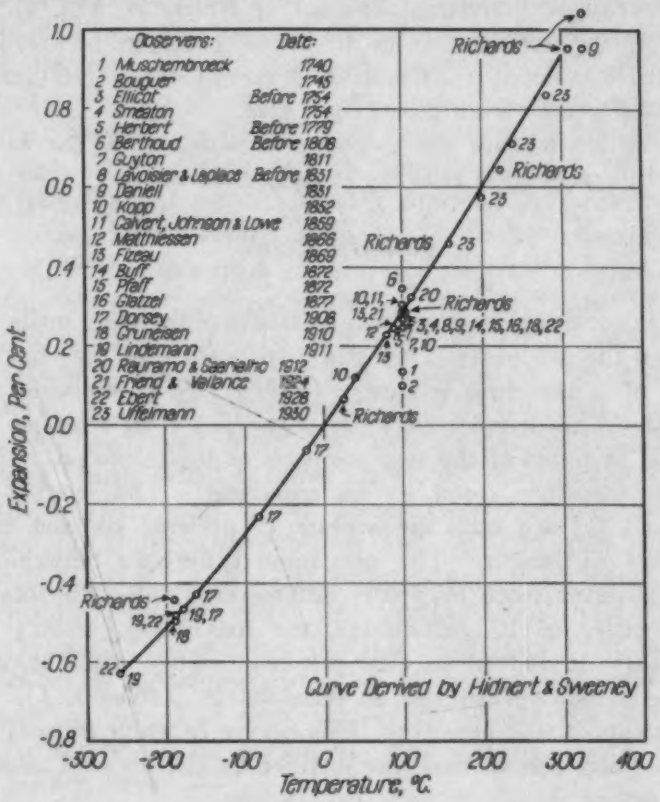

Fig. A—Comparison of Richard's Expansion Data on Lead With Those of Previous Observers.

19, 1923-24, p. 697; S497) for cast aluminum (99.95 per cent) is only ±0.002 per cent. For example, Richards' error corresponds to an error of 5 per cent of the linear expansion from −191 to 27 degrees Cent. (−310 to 80 degrees Fahr.) A comparison of the average coefficients of expansion computed from these equations for various temperature ranges between 20 and 600 degrees Cent. (70 and 1110 degrees Fahr.) shows differences from 1 to 22 per cent.

The probable error of the length computed from Richards' equation for copper is ±0.023 per cent. The probable error of the lengths from Hidnert's second-degree equations (Scientific Paper, Bureau of Standards, Vol. 17, 1922, p. 91; S410) for hot-rolled copper and for hot-rolled and drawn copper (99.97 per cent) is less than ±0.001 per cent. A comparison of the average coefficients

of expansion computed from these equations for various temperature ranges between −50 and 300 degrees Cent. (−60 and 570 degrees Fahr.) shows that Richards' values for copper are in good agreement (within 2 per cent) with those reported by Hidnert. We note with much interest that the extraordinarily high coefficients of expansion reported by Davey and Wilson (42) and Haring (41) have not been confirmed by Richards.

Fig. A shows a comparison of Richards' expansion data on lead with those obtained by previous observers. The probable error of the length determined from Richards' equation for lead is ±0.012 per cent. A comparison of the coefficients of expansion given in the summary of Hidnert and Sweeney's publication (Bureau of Standards, *Journal of Research,* Vol. 9, 1932, p. 703; RP500), with those computed from Richards' equation for lead for various temperature ranges between −100 and 300 degrees Cent. (−150 and 570 degrees Fahr.), shows differences from 1 to 11 per cent.

Can the author indicate the previous treatments of the samples he investigated and the reference relating to reference number (47) in Table V?

Author's Reply

At each temperature, independent measurements were made of the total distance between the Mo posts. The setting for each post was made by making the cross hair of a traveling telescope (Cenco 72935) coincide with the top of the Mo post. The distance between posts was then read on a scale, outside the furnace, in terms of the two positions of the telescope. Each measurement of length therefore stood on its own feet. The lengths recorded in Tables I, II, and III are each the average of at least six and usually of ten separate readings of length. The maximum difference between readings in any one set was never more than 0.04 millimeter. Since the total length was always of the order of 10 centimeters, the maximum variation was of the order of four parts in 10,000, i.e. 0.04 per cent. This would indicate that the averages of the separate readings, as recorded in Tables I, II, and III, are probably good to about 0.02 per cent. This degree of accuracy was sufficient for our main purpose and was all that was justified by the scale on which Figs. 1, 2, 3, and 4 were drawn.

Since the same specimens were used in several consecutive runs, they may be regarded as having been thoroughly annealed.

SOME PROPERTIES OF PHOSPHORUS-TITANIUM STEELS

By George F. Comstock

Abstract

In this paper the mechanical properties of low-carbon steels containing 0.08 to 0.80 per cent phosphorus, up to 0.70 per cent titanium, and small amounts of other alloys, are reported and discussed. The steels were all melted in a small induction furnace, cast in the form of 17-pound ingots, and rolled to 7/8-inch rounds which were heat treated in various ways. The object was to determine the composition, using alloying elements of the lowest cost, that would have a yield point above 50,000 pounds per square inch, and an Izod impact value above 20 in all conditions of heat treatment, including normalized at 1650 degrees Fahr. (900 degrees Cent.), and water-quenched from 1850 and 2000 degrees Fahr. (1010 and 1095 degrees Cent.). Low temperature impact values, and weldability, were also investigated. Copper, chromium, nickel, tin, and molybdenum additions were tried, as well as the substitution of vanadium, zirconium, columbium, or aluminum for the titanium in the steel. The conclusion reached was that the steel should contain about 0.08 to 0.11 per cent carbon, 0.85 to 1.25 per cent manganese, 0.15 to 0.25 per cent silicon, 0.10 to 0.15 per cent phosphorus, 0.45 to 0.60 per cent copper, and 0.40 to 0.60 per cent titanium to meet most economically the requirements mentioned, and that this steel is not subject to temper-hardening or temper-brittleness, is weldable, and tough at 22 degrees Fahr. below zero.

Introduction

DURING the past few years considerable interest has been stimulated in the effects of phosphorus on low-carbon steel.[1] Phosphorus has been shown to be very useful for raising the yield strength and improving resistance to corrosion, without detrimental

[1] "Phosphorus Iron Alloys," Bulletins No. 1, No. 2, and No. 3, Monsanto Chemical Company, St. Louis, Missouri, 1938-1940.

A paper presented before the Twenty-third Annual Convention of the Society held in Philadelphia, October 20 to 24, 1941. The author, George F. Comstock, is chief metallurgist, associated with the Titanium Alloy Mfg. Co., Niagara Falls, N. Y. Manuscript received April 5, 1941.

effects on ductility or impact resistance unless present in excessive amounts. Other alloying elements have been investigated in conjunction with phosphorus in low carbon steels, but relatively little work has been reported with titanium in this connection. Lorig and Krause[2] have reported a few test data on steels containing 0.35 to 0.45 per cent phosphorus and 0.15 per cent titanium. Their results, however, did not seem very conclusive as to the influence of titanium, which was considered to be "possibly beneficial" in small amounts.

In the Monsanto Bulletin No. 3,[1] a list is given of 51 U. S. Patents dealing with cast iron or steel containing phosphorus as an intentional alloy addition. Five of these also mention titanium. Of these five, two, namely 590,239 and 1,662,158, describe the use of titanium, with other elements, for correcting the brittleness and weakness due to high phosphorus in cast iron. The other three are more pertinent to the present investigation.

No. 171,183, issued in 1875 to F. J. Slade, covers the process of regulating the contents of various elements including titanium to "supplement the steelifying action of the phosphorus" in alloys of iron, manganese, and phosphorus. No specific effect of titanium is described.

No. 2,026,390, issued in 1935 to H. Kamura, shows how the addition of a little silicon and titanium does not impair the beneficial effect of phosphorus on certain magnetic properties of carbonless iron, and improves the machinability and electrical resistance.

No. 2,137,945, issued in 1938 to Mathesius, is the most interesting and pertinent, as it is stated therein that "anticorrosion steels" containing less than 0.1 per cent carbon and about 0.5 per cent titanium "may be given a content of 0.5 to 1 per cent of phosphorus without cold brittleness occurring, since the action of the titanium carbides in making the granule finer exceeds the contrary action of the iron phosphides." It was decided to investigate the properties of steels of that nature to see if this claim could be substantiated.

Preliminary Experiments

For this purpose some low carbon steels were made in a small induction furnace with 0.17 to 0.81 per cent phosphorus and 0.10 to 0.70 per cent titanium. The 3-inch square ingots were rolled to ⅞-

[2]Lorig and Krause, "Phosphorus as an Alloying Element in Low Carbon, Low Alloy Steel," *Metals and Alloys*, February, 1936, Vol. 7, p. 51.

inch rounds, and tensile, hardness, and Izod impact tests were made on specimens heat treated in various ways. Since steel of this nature would probably be used for structural purposes without heat treatment, the properties were determined in the as-rolled condition as well as normalized to simulate a standard rolled condition of larger

Table I
Properties of Phosphorus-Titanium Steels with Low Manganese

Heat No.	Chemical Analysis, Per Cent C	Mn	Si	P	Ti	Normalizing Temp. °F.	Lbs. Per Sq. In. Yield Point	Lbs. Per Sq. In. Tensile Strength	Per Cent Elongation in 2 In.	Per Cent Reduction of Area	Brinell Hardness No.	Izod Impact Resistance Ft.-Lbs.
Air-Cooled Specimens												
1	0.08	0.30	0.19	0.216	0.112	None	54000	70700	36.5	68.7	146	103-115-57
						1650	45800	65800	37.5	67.5	140	15-12-13
						1850	46400	67800	36.0	67.2	138	11-16-12
2	0.14	0.34	0.14	0.195	0.308	None	66800	81000	33.5	65.0	159	90-90-87
						1650	60200	77500	34.0	67.8	163	80-80-78
						1850	61700	78600	33.5	66.6	156	76-93-70
3	0.15	0.36	0.20	0.196	0.600	None	70100	80800	32.0	65.6	170	95-90-80
						1650	56500	75300	33.0	68.0	158	40-41-40
						1850	60300	78000	31.0	65.9	158	55-60-75
4	0.09	0.39	0.20	0.515	0.120	None	70000	88500	31.5	58.8	192	15-11-16
						1650	59200	84500	33.0	57.8	179	2-1-1
						1850	58300	83600	35.0	62.5	174	1-1-1
5	0.13	0.42	0.23	0.503	0.705	None	72800	88500	30.0	60.0	192	6-6-5
						1650	50200	80200	32.0	59.7	166	1-1-1
						1850	46700	78300	31.0	53.1	163	0-1-1
Water-Quenched Specimens						Quenching Temp. °F.						
1	0.08	0.30	0.19	0.216	0.112	1650	54200	74600	36.0	71.8	195	11-10-10
						1850	66000	91500	25.0	67.8	245	16-15-18
						2000	65700	90600	23.0	65.0	248	11-12-12
2	0.14	0.34	0.14	0.195	0.308	1650	67100	86700	32.0	69.4	181	74-65-65
						1850	70200	99500	28.5	66.3	232	53-55-61
						2000	111500	147000	12.5	43.3	326	7-7-7
3	0.15	0.36	0.20	0.196	0.600	1650	57200	77700	33.0	66.0	179	51-44-55
						1850	61000	81500	26.0	65.8	197	39-35-43
						2000	74200	105000	24.0	60.0	232	20-21-25
4	0.09	0.39	0.20	0.515	0.120	1650	67400	97200	31.0	59.4	235	1-2-2
						1850	64900	89500	31.0	57.7	200	1-2-2
						2000	66500	101000	26.0	52.3	201	2-2-2
5	0.13	0.42	0.23	0.503	0.705	1650	50100	80700	34.0	57.9	170	1-1-1
						1850	54900	83500	29.0	53.3	190	2-1-1
						2000	99300	138000	17.0	40.6	281	1-2-1

shapes. Since structural steels should be capable of heating and rapid cooling without excessive hardening or embrittlement, in order to be classed as weldable, specimens of the 7/8-inch rounds were also water-quenched from 1650, 1850, and 2000 degrees Fahr. before testing. Some of the results obtained in this way are reported in Table I. All the steels with about 0.8 per cent phosphorus were extremely brittle in all conditions of heat treatment, even with as much as 0.69 per cent titanium, and some even broke in machining. The steels with about 0.5 per cent phosphorus were also very low in im-

pact value, so that the statement quoted from the Mathesius patent is evidently in disagreement with the present findings. Some of the steels with about 0.2 per cent phosphorus and high titanium, however, showed rather interesting properties as noted in Table I.

Steel No. 1 showed low yield point and tensile strength as normalized, owing to its low carbon and manganese; it also showed poor impact values, evidently due to its phosphorus content and low titanium. Steels 2 and 3 were better in all respects, except for the ductility and impact value of the former after quenching from 2000 degrees Fahr. (1095 degrees Cent.). Apparently with 0.14 or 0.15 per cent carbon and about 0.20 per cent phosphorus, more than 0.30 per cent titanium, as in steel No. 3, is necessary to maintain reasonably low hardness, good ductility, and impact values above 20 after quenching from such a high temperature.

General Program

The combination of properties exhibited by steel No. 3 seemed sufficiently interesting to warrant further work on modified analyses. A number of other ingots were made to show the advisable limits for carbon and phosphorus. The effects of higher manganese or silicon, of added copper, chromium, nickel, tin and molybdenum, and of substituting vanadium, zirconium, columbium, or aluminum for the titanium, were also investigated. As the chief criteria of value of the various compositions, a yield point above 50,000 pounds per square inch, and impact values above 20, were considered essential both as normalized at 1650 degrees Fahr. (900 degrees Cent.), and after quenching in water from 1850 and from 2000 degrees Fahr. (1010 and 1095 degrees Cent.). This combination should assure satisfactory service in welded structures, and is not too easy to secure.

Effects of Manganese, Copper, and Silicon

Some tests of a series with phosphorus contents between 0.10 and 0.30 per cent and titanium around 0.6 per cent indicated that the phosphorus should not exceed 0.20 per cent. It also appeared that with increasing carbon contents above approximately 0.11 per cent, the impact requirements necessitated correspondingly higher titanium contents. On the other hand, with carbon as low as 0.08 per cent the strength was low, even with low titanium, as shown by

steel No. 1 in Table I. Thus some other strengthening agent such as manganese, copper, or silicon, seemed to be required. Some of the results obtained with the aid of these alloy additions are reported in Table II.

Table II

Properties of Phosphorus-Titanium Steels with Higher Manganese, Copper, or Silicon

Heat No.	Chemical Analysis Per Cent C	Mn	Si	P	Cu	Ti	Heat Treatment, °F.	Lbs. Per Sq. In. Yield Point	Tensile Strength	Per Cent Elongation in 2 In.	Reduction of Area	Brinell Hardness No.	Izod Impact Resistance, Ft.-Lbs.
							1650, air	49200	67100	36.5	77.2	134	140-135-136
6	0.102	0.83	0.15	0.147	0.07	0.585	1850, water	71500	89100	26.0	68.8	200	147-130-143
							2000, water	80400	98500	24.0	67.9	217	60-50-45
							1650, air	51300	69700	35.5	77.5	144	150-140-139
7	0.10	1.34	0.16	0.145	0.07	0.585	1850, water	80400	97600	24.5	67.3	207	138-130-138
							2000, water	82100	102000	21.0	61.5	232	60-45-36
							1650, air	48900	66000	36.5	75.4	131	145-140-142
8	0.098	0.43	0.17	0.145	0.58	0.600	1850, water	63900	84200	26.5	70.3	197	150-140-141
							2000, water	88500	107300	19.0	57.4	241	20-25-25
							1650, air	52600	71000	33.0	74.8	138	150-139-143
9	0.102	0.33	0.18	0.147	1.01	0.540	1850, water	69900	89500	25.5	69.2	195	130-145-150
							2000, water	89900	107200	19.0	64.5	241	41-41-40
							1650, air	51900	71000	34.5	74.0	141	152-128-127
10	0.092	0.87	0.21	0.147	0.58	0.570	1850, water	74900	91700	25.0	66.6	207	147-145-145
							2000, water	89200	111400	20.0	60.2	238	48-34-25
							1650, air	57000	76500	31.5	73.0	149	154-145-145
11	0.092	1.22	0.20	0.142	0.44	0.480	1850, water	81200	102400	21.0	58.7	255	95-90-125
							2000, water	100300	123000	18.0	55.0	302	36-40-56
							1650, air	58500	75800	34.5	75.0	156	150-148-144
12	0.095	1.35	0.54	0.144	0.07	0.465	1850, water	75200	100400	25.0	65.8	232	100-123-119
							2000, water	101100	124900	17.5	55.5	302	2-2-30
							1650, air	64700	76000	35.0	73.2	159	150-140-141
13	0.094	0.88	0.50	0.149	0.47	0.465	1850, water	74600	99800	22.0	63.0	226	110-128-97
							2000, water	94900	123800	17.0	54.6	302	5-5-5

From Table II it can be seen that steel No. 6 with only 0.83 per cent manganese, and steel No. 8 with only 0.58 per cent copper, had yield points below 50,000 pounds per square inch when normalized at 1650 degrees Fahr. With higher manganese (steel No. 7) or higher copper (steel No. 9), or both copper and manganese as in steels Nos. 10 and 11, the results were more acceptable. Higher silicon, however, gave poor impact values after quenching from 2000 degrees Fahr. (1095 degrees Cent.), as can be seen by comparing steels Nos. 12 and 7, or steels Nos. 13 and 10. The combination of properties shown by steel No. 11 seems quite satisfactory.

Effects of Chromium, Nickel, Tin, and Molybdenum

A number of other steels were made and tested in the same conditions of heat treatment to see whether small amounts of chro-

Table III

Properties of Phosphorus-Titanium Steels with Nickel, Chromium, Molybdenum or Tin

Heat No.	Chemical Analysis, Per Cent C	Mn	Si	P	Cu	Ti	Others	Heat Treatment °F.	Lbs. Per Sq. In. Yield Point	Lbs. Per Sq. In. Tensile Strength	Per Cent Elongation in 2 In.	Per Cent Reduction of Area	Brinell Hardness No.	Izod Impact Resistance, Ft.-Lbs.
								1650, air	56600	77300	32.5	72.9	156	152-140-147
14	0.10	1.28	0.18	0.14	....	0.480	0.70 Ni	1850, water	74600	97800	26.0	66.1	202	140-140-136
								2000, water	94900	121000	17.0	56.0	241	66-58-39
								1650, air	59200	79200	31.5	70.4	156	152-145-149
15	0.09	1.11	0.16	0.14	....	0.435	1.04 Ni	1850, water	74900	100200	22.5	65.4	215	138-120-115
								2000, water	99200	123100	17.0	57.7	255	2-4-4
								1650, air	59900	76000	34.0	72.3	156	151-141-140
16	0.09	0.83	0.17	0.14	0.49	0.420	0.58 Ni	1850, water	75200	98700	25.0	64.0	229	119-122-125
								2000, water	104900	130400	15.5	49.2	281	3-2-3
								1650, air	54100	69800	35.0	77.8	137	147-135-140
17	0.088	0.46	0.20	0.142	0.46	0.450	0.77 Cr	1850, water	75500	98600	22.0	65.7	229	135-132-140
								2000, water	95700	117000	17.5	59.5	289	40-43-70
								1650, air	53000	69700	37.5	77.0	143	155-152-150
18	0.08	0.49	0.19	0.145	0.49	0.405	0.87 Cr	1850, water	85500	101000	20.5	67.0	245	65-64-48
								2000, water	99400	115100	17.5	64.0	289	45-40-16
								1650, air	52300	73200	37.0	74.6	143	155-146-138
19	0.08	1.05	0.21	0.136	0.46	0.412	0.78 Cr	1850, water	84900	105200	21.0	68.4	255	90-100-95
								2000, water	112100	127300	14.0	56.8	302	20-32-44
								1650, air	55600	74100	33.5	73.0	149	151-140-145
20	0.082	0.48	0.22	0.14	0.45	0.450	{0.60 Ni {0.80 Cr	1850, water	75200	99400	22.0	64.1	241	122-117-135
								2000, water	100200	121800	19.5	54.5	321	65-60-32
								1650, air	55000	73500	34.0	73.1	149	146-137-140
21	0.096	0.91	0.19	0.151	0.45	0.480	0.21 Mo	1850, water	79900	99700	25.0	61.7	229	131-140-137
								2000, water	90600	115800	20.0	60.8	302	60-37-31
								1650, air	35900	66800	35.0	76.5	126	16-17-12
22	0.104	0.83	0.16	0.105	0.57	0.585	0.17 Sn	1850, water	81100	94300	24.0	67.3	197	102-135-134
								2000, water	94900	112300	18.0	61.3	248	20-20-20

mium, nickel, tin, or molybdenum could be used advantageously as strengtheners for this phosphorus-titanium steel. Some typical examples of the results obtained with these additions are presented in Table III.

The substitution of nickel for copper in these steels seems to be permissible, as shown by steel No. 14 in Table III. Too much nickel with over 1 per cent manganee, however, as in steel No. 15, gave low impact resistance after the 2000 degrees Fahr. (1095 degrees Cent.) quench. Nickel with copper and as much as 0.83 per cent manganese in steel No. 16 had the same effect. Thus nickel must be used carefully in these steels, and in general does not seem to show an advantage commensurate with its comparatively high cost.

The use of chromium replacing some of the manganese used for strengthening this phosphorus-titanium steel, as in steel No. 17, gave excellent results. In the similar heat 18, however, the impact resistance after quenching was not as good. Heat 19 with chromium and higher manganese was surprisingly similar in properties, and heat 20 with chromium, copper, nickel, and low manganese was also very good. Compared with steel No. 11 of Table II, however, these chromium steels do not seem to offer sufficient advantage to justify their slightly higher cost.

The same conclusion can be drawn from the use of molybdenum in steel No. 21. The properties of this steel were good, but it is not apparent that the molybdenum produced an improvement proportional to its high cost.

The substitution of a little tin for some of the phosphorus in steel No. 22 caused surprisingly low impact values in the normalized steel, although the quenched steels were not so bad. This curious result was checked by other tests, and was certainly not due to any accidental injury to the test specimens. Presumably some embrittling tin compound is held harmlessly in solution when the steel is quenched from high temperatures.

Variations in Phosphorus and Titanium

The work so far reported indicates that phosphorus-titanium steel to meet the requirements of at least 50,000 pounds per square inch yield point when normalized, and at least 20 foot-pounds Izod impact value after quenching in water from 1850 or 2000 degrees

Fahr. (1010 or 1095 degrees Cent.), should contain about 0.08 to 0.11 per cent carbon, 0.85 to 1.25 per cent manganese, 0.15 to 0.25 per cent silicon, and 0.45 to 0.60 per cent copper, in addition to phosphorus up to possibly 0.15 per cent and titanium around 0.40 to 0.60 per cent. This, of course, involves the assumption that the lowest alloy costs, as well as the best properties, are desired. To

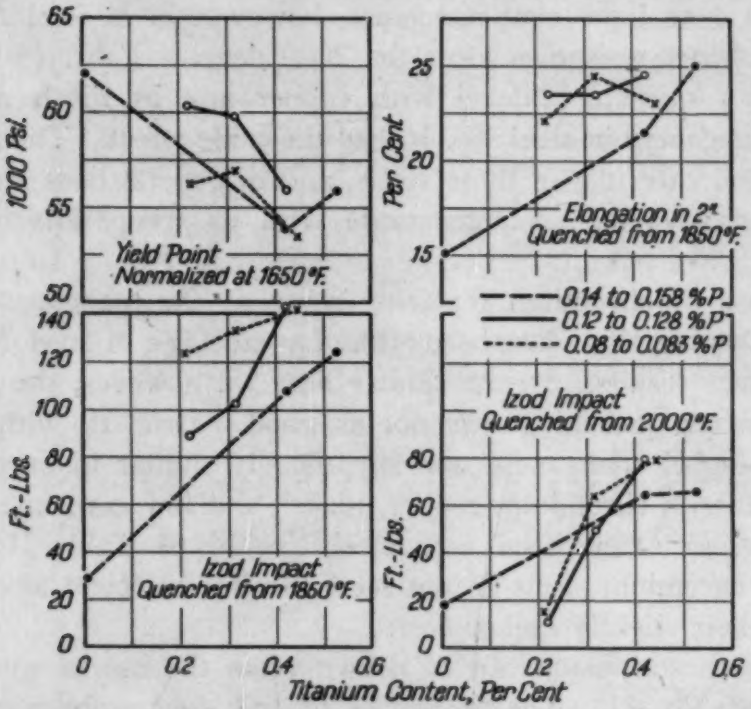

Fig. 1—Some Properties of Phosphorus-Titanium Steels Containing About 0.09 Per Cent Carbon, 1.1 Per Cent Manganese, 0.2 Per Cent Silicon and 0.5 Per Cent Copper, Except the Steel With Only 0.003 Per Cent Titanium, Which Contained 0.4 Per Cent Manganese and 1.16 Per Cent Copper.

check more definitely the preferred or permissible phosphorus and titanium limits, the latter of which would have a marked influence on costs, another series of steels involving those variables was prepared and tested.

The most interesting and important properties of this series of steels, with approximately constant carbon, manganese, silicon and copper contents, are shown on Fig. 1 in the form of curves plotted against the titanium content. Separate curves are plotted for each of three ranges of phosphorus contents, as noted in the legend on Fig. 1. These curves indicate that the steels with about 0.14 per cent phosphorus have a tendency toward lower elongation and impact values, in the quenched condition, than those with about 0.12 or 0.08 per cent phosphorus having the same titanium content. Also

the higher phosphorus steels show no consistent advantage in yield point. Thus about 0.12 per cent phosphorus seems in general most satisfactory. The yield points are shown to decrease with higher titanium contents but do not drop below 50,000 pounds per square inch. At the same time the impact values in the quenched condition rise sharply, so that around 0.3 to 0.4 per cent titanium seems definitely preferable to lower values since toughness after rapid cooling from 2000 degrees Fahr. is one of the desired objectives.

Temper Hardening

The susceptibility of a number of these steels to precipitation hardening on tempering was investigated by quenching small specimens from 1700 degrees Fahr. in water and measuring the Rockwell hardness before and after tempering for 3 hours at 400, 600, 800, 1000 and 1200 degrees Fahr. (205, 315, 425, 540 and 650 degrees Cent.) respectively. No appreciable increase in hardness was found on tempering any of the steels in this way, except in steel No. 9 (Table II) containing 1 per cent copper. This steel hardened from 85 to 94 Rockwell B on tempering at 1000 degrees Fahr. (540 degrees Cent.) only. Most of the steels softened slightly on tempering, especially at 1200 degrees Fahr. (650 degrees Cent.).

Temper Brittleness and Low-Temperature Impact

The susceptibilities to temper brittleness, and to low temperature embrittlement, were also investigated as far as the available stock left from the small ingots would permit. The results of these tests are given in Table IV. The temper brittleness tests were made by quenching test specimens in water after 1½ hours at 1700 degrees Fahr. (925 degrees Cent.), and then reheating them 1½ hours at 1150 degrees Fahr. (620 degrees Cent.) after which they were cooled either in cold water or slowly inside the furnace. After final machining and notching these specimens were tested for hardness by the Rockwell method between notches, and their impact resistance was determined with an Izod machine at three notches and the results averaged. The low temperature tests were made with a Charpy machine using the highest speed. The specimens were standard size, but had the Izod-type V notch. They were normalized at 1650 degrees Fahr. (900 degrees Cent.), and tested within a few seconds after having been held at —22 degrees Fahr. (—30

Table IV
Results of Temper Brittleness and Low Temperature Impact Tests

Heat No.	Chemical Analysis Per Cent C	Mn	Si	P	Cu	Ti	Others	Av. Izod Impact Resistance at Room Temperature, Ft.-Lbs. Quenched from 1150° F.	Slowly Cooled from 1150° F.	Decrease Due to Slow Cooling	Charpy Impact Resistance at Minus 22° F. Kgm.-M.
15	0.09	1.11	0.16	0.14	....	0.435	1.04 Ni	...	...	.....	14.8-16.2-15.9
18	0.08	0.49	0.19	0.145	0.49	0.405	0.87 Cr	85	91	Minus 6	11.3-17.9
19	0.08	1.05	0.21	0.136	0.46	0.412	0.78 Cr	126	92	34	19.7-14.4
20	0.082	0.48	0.22	0.14	0.45	0.450	0.60 Ni, 0.80 Cr	139	128	11	Not tested
21	0.096	0.91	0.19	0.151	0.45	0.480	0.21 Mo	122	131	Minus 9	Not tested
23	0.088	1.13	0.26	0.146	0.5	0.525	.....	132	136	Minus 4	Not tested
24	0.098	1.11	0.23	0.14	0.56	0.420	.....	131	141	Minus 10	14.6-19.1-18.2
25	0.088	1.12	0.24	0.128	0.5	0.420	.....	140	140	None	20.8-19.2-17.5
26	0.07	0.99	0.15	0.12	0.5	0.315	.....	137	140	Minus 3	19.3-7.0
27	0.08	1.09	0.18	0.127	0.52	0.218	.....	141	143	Minus 2	19.2

degrees Cent.) for at least 15 minutes. These results are reported individually in Table IV.

Table IV shows that only the chromium steels Nos. 19 and 20 were susceptible to temper embrittlement, and that all the phosphorus-titanium steels of the preferred composition were not susceptible. No trouble of that kind need therefore be anticipated with this steel, in which chromium is not used. The slowly cooled specimens were from 1 to 6 Rockwell points softer than the quenched specimens, but the differences in hardness did not seem to be related to the differences in impact value.

The low temperature impact values were satisfactory, except for one result on steel No. 26 which contained only 0.315 per cent titanium. The preferred steel with about 0.4 per cent titanium may, therefore, be relied on to maintain its notch-toughness at —22 degrees Fahr. A steel containing nickel instead of copper (No. 15) was found to be no better in low temperature impact resistance.

Welding Tests

Weldability tests were attempted on these steels, but the value of these tests suffered from the fact that no larger stock than ⅞-inch rounds was available. These rounds were forged flat to secure strips about 1½ inches wide and ¼ inch thick, which were normalized at 1650 degrees Fahr. (900 degrees Cent.). Weld beads

were then deposited from $\frac{5}{32}$-inch coated rods on the cold strips, and cooled rapidly. Sections were cut through these beads for hardness tests, and the welded strips were also machined smooth, and bent. Some of the weld deposits cracked after bending 105 degrees or more, but no cracks occurred in the steel base of any of the samples except at two seams which were not located in or near the metal affected by the heat of welding.

The cross sections for hardness testing were filed smooth and roughly polished and etched to show the outline of the weld penetration, and Rockwell hardness tests were made in lines across them so as to include several determinations at the weld boundaries. The unaffected base metal of these sections was of about 77 to 82 Rockwell B hardness, and the weld deposits were about 83 to 89. The higher readings obtained at and near the weld boundaries are summarized in Table V.

Table V
Results of Hardness Tests on Cross Sections of Welded Strips

Heat No.	Chemical Analysis Per Cent C	Mn	Si	P	Cu	Ti	Others	Welding Rate, Inches Per Minute	Rockwell B Hardness Maximum	Rockwell B Hardness Average of 3 Middle Tests
2	0.14	0.34	0.14	0.195	....	0.308	.....	Not measured	102	95
3	0.15	0.36	0.20	0.196	....	0.600	.....	Not measured	105	95
11	0.092	1.22	0.20	0.142	0.44	0.480	.....	11.0	101	99
14	0.10	1.28	0.18	0.14	....	0.480	0.70 Ni	10.9	100	94
17	0.088	0.46	0.20	0.142	0.46	0.450	0.77 Cr	11.4	96	93
18	0.08	0.49	0.19	0.145	0.49	0.405	0.87 Cr	10.9	101	99
19	0.08	1.05	0.21	0.136	0.46	0.412	0.78 Cr	11.5	102	97
23	0.088	1.13	0.26	0.146	0.5	0.525	.....	11.4	101	98
24	0.098	1.11	0.23	0.14	0.56	0.420	.....	6.9	95	91
25	0.088	1.12	0.24	0.128	0.5	0.420	.....	11.5	97	96
26	0.07	0.99	0.15	0.12	0.5	0.315	.....	10.9	95	92
27	0.08	1.09	0.18	0.127	0.52	0.218	.....	11.9	93	91

The hardness values in Table V show that all these steels were readily weldable (except possibly No. 3) without undue hardening at the weld, at least in the form of ¼-inch strips. More conclusive tests of weldability, made with thicker sections of steel, must unfortunately be deferred until such sections are available. It may be noted that steels Nos. 25, 26, and 27, all with less than 0.13 per cent phosphorus, showed less weld-hardening than the others, except No. 17. No. 24 is hardly comparable on account of the accidentally slower rate of welding.

Substitutes for Titanium

A final series of these steels was made to indicate the effects of columbium, zirconium, vanadium, and aluminum when substi-

tuted for the titanium in them. The amounts of the first three elements added were computed so as to form Cb_4C_5, ZrC, or VC with the same amount of carbon that 0.45 per cent titanium would unite with to form TiC. One zirconium heat was made, however, with only about half as much zirconium. The heat in which only aluminum was used received an addition about 5 times larger than any of the others. All the titanium steels were deoxidized with about 0.05 per cent aluminum before the ferrotitanium was added, in accordance with usual commercial practice, and the aluminum content of that alloy contributed about another 0.05 per cent. The plain aluminum steel was treated with 0.50 per cent aluminum. The results from these steels, rolled, heat treated, and tested in the usual ways, are reported in Table VI, where their analyses are also given. The phosphorus contents came a little lower than was desired, but this should not interfere with the comparison between the various additions.

The results in Table VI show that the columbium steels Nos. 30 and 31 were superior to the titanium steels Nos. 28 and 29 in room temperature impact resistance and lack of hardening after quenching from 2000 degrees Fahr. (1095 degrees Cent.), and were quite similar in strength and ductility. The columbium steels, however, would be decidedly more expensive unless the columbium content was greatly decreased, and then the superiority over the titanium steels would probably be lost. In low temperature impact resistance the titanium steels were better than the columbium steel No. 30, but not so good as No. 31. It should be noted, however, that the latter had an abnormally low phosphorus content, and this probably affected the low temperature impact resistance favorably.

The zirconium steels were decidedly inferior to the titanium steels in impact value in all conditions of heat treatment and at both temperatures, and were also slightly inferior in ductility. Evidently zirconium is not suitable for use in place of titanium in this kind of steel.

The vanadium steel was stronger than any of the others, especially after quenching, and also was harder and less ductile, as would be expected. The impact values at room temperature were surprisingly high for such a strong steel, but at low temperature this steel was brittle. On account of cost, as well as low temperature brittleness, this otherwise interesting steel does not seem commercially attractive.

Table VI

Comparison of Phosphorus-Titanium Steels with Those Containing Columbium, Zirconium, Vanadium or Merely Aluminum

Heat No.	Chemical Analysis, Per Cent					Heat Treatment °F.	Lbs. Per Sq. In.		Per Cent		Brinell Hardness No.	Izod Impact Resistance at Room Temp. Ft.-Lbs.	Charpy Impact Resistance at Minus 22° F. Kgm.-M.
	C	Mn	Si	P	Cu	Others		Yield Point	Tensile Strength	Elongation in 2 In.	Reduction of Area			
28	0.082	1.21	0.21	0.101	0.47	0.431 Ti	1650, air	54500	70900	34.5	73.0	137	128-126-129	9.2-13.5-14.6
							1850, water	75900	98300	26.0	69.4	217	72-79-90	
							2000, water	96500	112000	17.5	62.5	255	42-40-43	
29	0.088	1.10	0.23	0.110	0.43	0.394 Ti	1650, air	54000	70800	35.0	76.4	143	133-130-129	12.7-4.1-19.6
							1850, water	75000	96800	25.5	71.8	207	130-114-136	
							2000, water	92800	110400	20.0	65.9	255	35-34-37	
30	0.084	1.13	0.30	0.100	0.51	0.72 Cb	1650, air	52600	71100	34.5	74.8	137	129-123-127	11.2-4.5-6.3
							1850, water	72700	91000	26.0	64.5	187	122-120-122	
							2000, water	95200	112900	19.5	63.2	215	94-99-107	
31	0.088	1.18	0.21	0.085	0.47	0.58 Cb	1650, air	55500	71700	34.5	73.0	140	117-121-120	20.0-20.8-21.5
							1850, water	73700	90300	24.0	63.9	192	114-127-120	
							2000, water	86000	99200	20.0	64.9	226	77-61-78	
32	0.084	1.14	0.22	0.106	0.52	0.569 Zr	1650, air	54000	70600	38.0	69.0	149	95-98-95	5.0-4.4-2.3
							1850, water	63700	87700	22.0	54.2	179	40-36-30	
							2000, water	80900	97900	19.5	57.5	217	13-15-12	
33	0.082	0.94	0.39	0.103	0.43	0.275 Zr	1650, air	52400	70000	36.5	68.0	137	93-94-109	1.5-2.3-2.4
							1850, water	85600	112000	18.5	56.1	269	23-21-23	
							2000, water	91300	106000	19.5	55.3	241	23-25-27	
34	0.090	1.04	0.16	0.092	0.40	0.52 V	1650, air	59700	81200	32.0	67.5	163	132-128-135	1.0-0.8-1.4
							1850, water	116500	151000	15.0	53.4	321	60-74-89	
							2000, water	127300	154300	14.0	50.1	321	64-66-70	
35	0.090	1.20	0.28	0.111	0.43	0.5 Al Added	1650, air	56600	74500	38.0	73.2	149	127-122-118	25.9-25.1-23.5
							1850, water	91700	121000	16.0	51.0	255	73-79-43	
							2000, water	107000	128600	15.0	47.2	302	26-21-22	

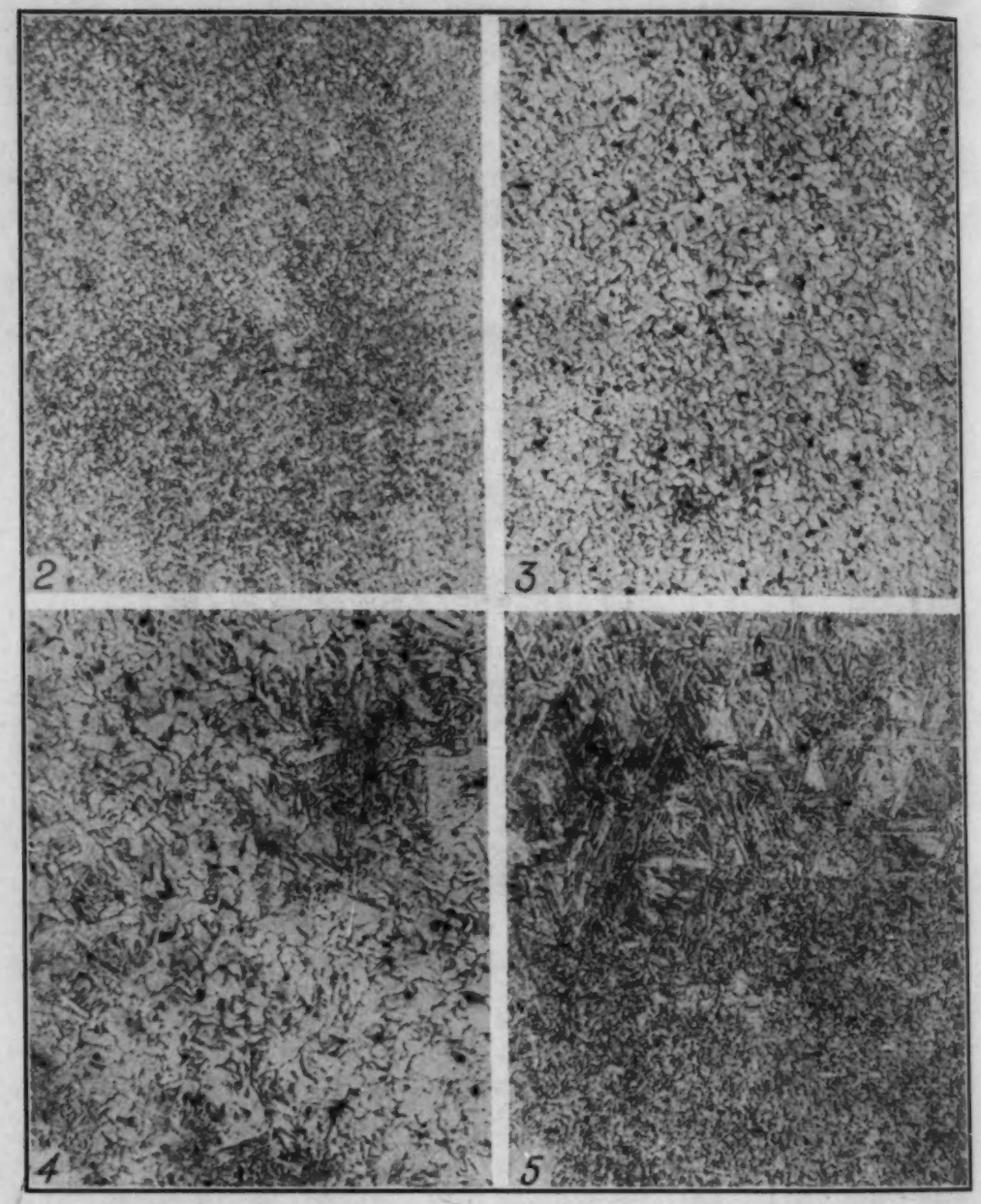

Fig. 2—Heat No. 3, As-Rolled. Very Fine-grained Ferrite. 0.15 Per Cent Carbon, 0.36 Per Cent Manganese, 0.196 Per Cent Phosphorus, 0.60 Per Cent Titanium. 170 Brinell. 88 Izod Impact Value.

Fig. 3—Heat No. 3, Quenched from 2000 Degrees Fahr. Fine-grained Ferrite. 232 Brinell. 22 Izod Impact Value.

Fig. 4—Heat No. 1, Quenched from 2000 Degrees Fahr. Moderately Coarse Ferrite with Some Martensite. 0.08 Per Cent Carbon, 0.30 Per Cent Manganese, 0.216 Per Cent Phosphorus, 0.112 Per Cent Titanium. 248 Brinell. 12 Izod Impact Value.

Fig. 5—Heat No. 11, Quenched from 2000 Degrees Fahr. Ferrite and Martensite, Partly Fine and Partly Coarse. 0.09 Per Cent Carbon, 1.22 Per Cent Manganese, 0.142 Per Cent Phosphorus, 0.45 Per Cent Titanium. 302 Brinell. 38 Izod Impact Value.

All Etched with Nital, and Magnified 100 Diameters.

The aluminum steel No. 35 was stronger than any of the others except the vanadium steel, and was also harder and less ductile after

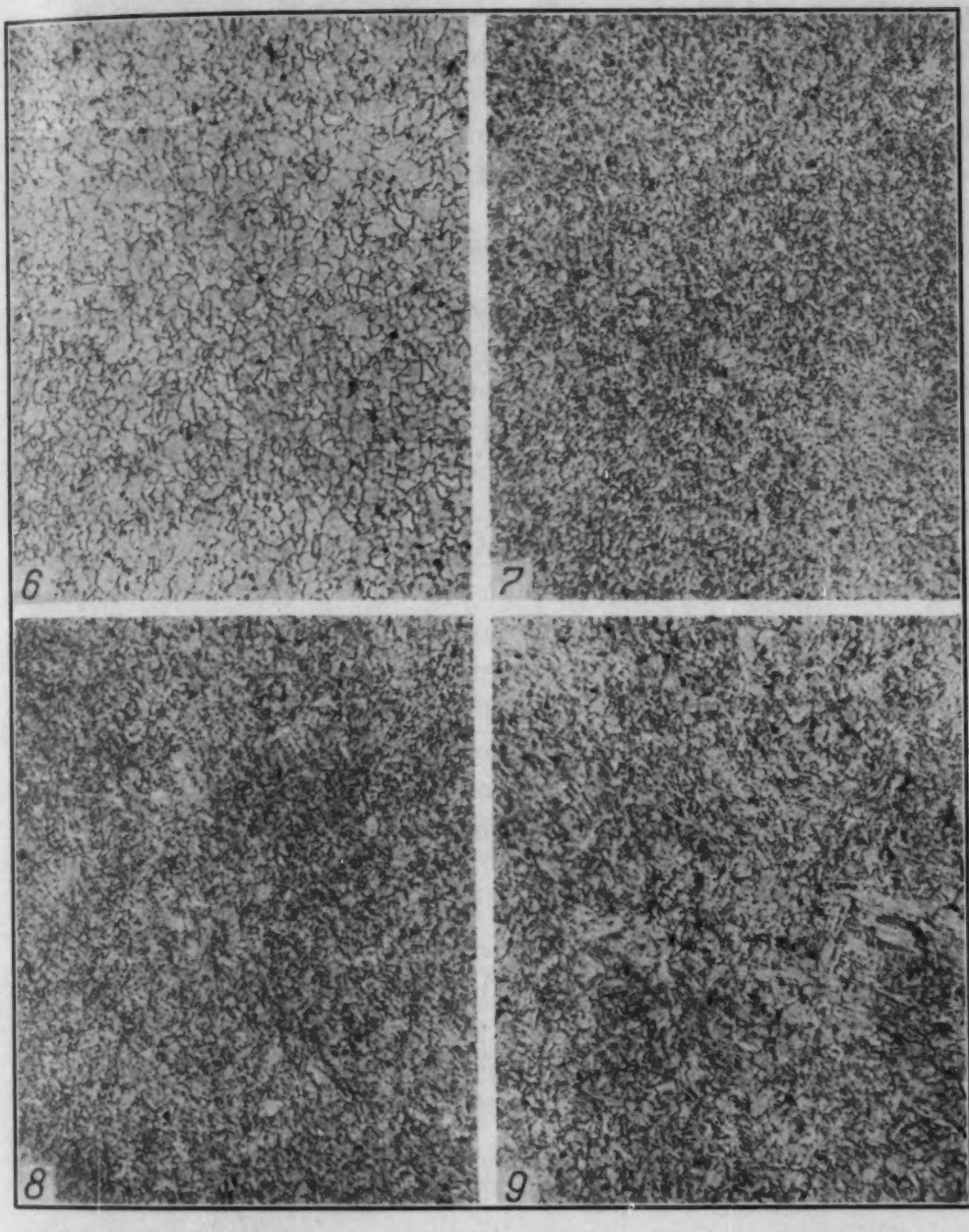

Fig. 6—Heat No. 25, Normalized at 1650 Degrees Fahr. Fine-grained Ferrite. 0.088 Per Cent Carbon, 1.12 Per Cent Manganese, 0.128 Per Cent Phosphorus, 0.42 Per Cent Titanium. 143 Brinell. 150 Izod Impact Value.

Fig. 7—Heat No. 25, Quenched from 1850 Degrees Fahr. Very Fine Ferrite and Martensite. 217 Brinell. 143 Izod Impact Value.

Fig. 8—Heat No. 28, Quenched from 2000 Degrees Fahr. Very Fine Ferrite and Martensite. 0.082 Per Cent Carbon, 1.21 Per Cent Manganese, 0.101 Per Cent Phosphorus, 0.431 Per Cent Titanium. 255 Brinell. 42 Izod Impact Value.

Fig. 9—Heat No. 32, Quenched from 2000 Degrees Fahr. Moderately Fine Ferrite and Martensite. 0.084 Per Cent Carbon, 1.14 Per Cent Manganese, 0.106 Per Cent Phosphorus, 0.569 Per Cent Zirconium. 217 Brinell. 13 Izod Impact Value.

All Etched with Nital, and Magnified 100 Diameters.

quenching. Although its impact values at room temperature were inferior to those of the titanium steels, it was tougher than any of

the other steels at sub-zero temperature. This agrees with the results of previous work, which showed aluminum to be in a class by itself for promoting low temperature impact resistance in steel, but it should be noted that the titanium steels, especially Nos. 24 and 25 (Table IV), were also tough at the same low temperature.

Microstructures

The microstructures of many of these steels were examined, mostly as quenched from 2000 degrees Fahr. (1095 degrees Cent.), and some photomicrographs are presented as Figs. 2 to 9 to illustrate them. In the as-rolled and normalized conditions the steels consisted of fine-grained ferrite and very fine titanium carbide crystals that were barely perceptible at 100 diameters magnification. After quenching from 2000 degrees Fahr. (1095 degrees Cent.), the structures of the steels containing over 0.9 per cent manganese and less than 0.5 per cent titanium were in some instances partly acicular and presumably martensitic. Such structures were harder than ferritic structures, but the toughness of these steels did not vary inversely with the amount of acicular martensite present as might have been expected. For instance, steel No. 11, which was partially martensitic after the high temperature quench, had better impact resistance than steel No. 3 which showed no martensite. This indicates that even if some hardening and coarsening of the structure occurred in welding these steels, the welds would not necessarily lack toughness. Martensite was not formed to any noticeable extent when the quenching temperature was only 1850 degrees Fahr. (1010 degrees Cent.). The zirconium steel, in spite of its low impact resistance, seemed to have a satisfactory microstructure with only traces of coarsely acicular martensite after quenching from 2000 degrees Fahr. (1095 degrees Cent.).

Practical Possibilities

Obviously these high phosphorus steels should be suitable for manufacture by the Bessemer process, where the desired phosphorus contents could readily be recovered from the pig iron used. Manganese and copper could be added in the ladle, but the titanium would probably have to be added in a second ladle out of contact with the converter slag, or in the molds, to secure a reasonable recovery. Preliminary deoxidation with aluminum would also be advisable for

the sake of better titanium recovery. Mold additions, using low carbon 40 per cent ferrotitanium, should not be impractical, though re-ladling would doubtless be better from a quality standpoint. The amount of titanium required for satisfactory properties might be less when larger ingots are made that would be reduced more in rolling. It is admitted that the results here shown are not conclusive, but require checking with steel made by large-scale operations.

Conclusions

It is indicated by this work that a steel having about the following composition should be useful for structural purposes, especially where welding is involved:

	Per Cent
Carbon	0.08 to 0.11
Manganese	0.85 to 1.25
Silicon	0.15 to 0.25
Phosphorus	0.10 to 0.15
Copper	0.45 to 0.60
Titanium	0.40 to 0.60

Such steel has been shown to have a yield point above 50,000 pounds per square inch as normalized, and good ductility and notched-bar impact resistance even after water quenching from 2000 degrees Fahr. (1095 degrees Cent.). It is not subject to temper hardening or temper brittleness, is weldable, and tough at —22 degrees Fahr. Previous investigations have shown that the phosphorus content would provide excellent resistance to atmospheric corrosion. Trials of this steel in practical service should be of interest.

Acknowledgments

The thanks of the author are due to the Titanium Alloy Manufacturing Company for providing the facilities required for this investigation, and to numerous members of that organization who helped with the work. Special credit should be given to Mr. A. S. Yocco, of the metallurgical research staff, who melted all the steels used and made most of the mechanical tests. The author also appreciates the valuable assistance of Dr. Morris Cohen, of Massachusetts Institute of Technology, with some of the heat treatment, and in the preparation of the report.

DISCUSSION

Written Discussion: By R. W. Simon, assistant manager, metallurgical division, Carnegie-Illinois Steel Corporation, Pittsburgh.

Mr. Comstock's paper provides a substantial addition to the knowledge of manganese-phosphorus steels of low carbon content in which the hardenability to be expected is opposed by a considerable addition of a strong carbide-forming element (titanium) acting presumably to form a special stable carbide of low solubility even at high temperatures. Such information is welcome since there is by no means an abundance of data of this character in the literature. The relatively low hardness developed in the compositions after water quenching small sections (¾-inch rounds) strongly suggests that the titanium does exert some of the influence mentioned above, at least at temperatures below about 2000 degrees Fahr. (1095 degrees Cent.). The uncertainty as to the degree of this influence arises from the lack of comparison data, that is, measurements of the properties developed in titanium-free steels otherwise similarly constituted and treated.

As a broad preliminary exploration of the field the paper serves its purpose well, and it is no criticism therefore to point out that welding may induce, in the heavier sections particularly, rates of cooling which may induce greater hardness than does water quenching, when it is recalled that temperatures up to the fusion point are inevitably involved. At such temperatures titanium will be dissolved in considerable proportion and this element, as dissolved, is doubtless one contributing to hardenability. Of greater interest than quenching in water therefore, are the actual bead welding tests as employed with considerable assurance abroad. Since the coarsened zone of maximum hardness may be fairly thin, an exploration of hardness with the Vickers hardness test is preferable to the less discerning Rockwell measurements.

It is reassuring to note that the preferred composition as outlined by Mr. Comstock carries a half of one per cent of copper because the contribution of phosphorus to corrosion resistance is apparently much enhanced by a moderate copper content.

It should be emphasized that a need for normalizing is a great handicap to any high-strength structural steel and that, generally speaking, testing should therefore be performed upon experimental compositions in the as-rolled state. Relatively little commercial interest attaches to the characteristics of these particular steels as normalized. Furthermore, both longitudinal and transverse bend tests, in which the bend itself is of considerable length, are prime criteria of the usefulness of compositions contending for general structural applications. Finally, it cannot be overlooked that merits commensurate with the cost of a steel must be clearly established to justify its manufacture.

The author suggests that his steel might well be made by the Bessemer process, using a reladling procedure to obtain a satisfactory titanium yield. Most Bessemer plants of today do not have reladling facilities available but regardless of this the mass of material to be added in one or two ladles, or even in the molds, does seem to set up a formidable problem. To obtain a 0.50 per cent titanium content in the steel might require up to 50 pounds of 40 per cent low carbon ferrotitanium per ton of steel based on 50 per cent effi-

ciency as a ladle addition, plus a rather large manganese addition to meet the 1.00 per cent specification. High vessel temperatures would be necessary which would result in lower alloy efficiency and a very possible detriment to steel quality. Mold additions to the Bessemer steel would result in higher alloy efficiency, possibly 60 per cent, but still an addition of about 42 pounds per ton of steel would indicate probably poor titanium distribution.

Written Discussion: By Walter Crafts, research metallurgist, Union Carbide and Carbon Research Laboratories, Inc., Niagara Falls, N. Y.

The author is to be congratulated on presenting such a thorough and comprehensive survey of low carbon-phosphorus-titanium structural steels. It would appear that titanium is effective in reducing the embrittling effect of phosphorus under the conditions tested. Swinden and Reeve[1] found excellent properties in low phosphorus-0.15-0.25 per cent carbon-titanium steels with a 3 to 1 ratio of titanium to carbon. In an independent survey conducted at the Union Carbide and Carbon Research Laboratories, Inc., before publication of the Swinden and Reeve paper, a titanium content of 0.20 to 0.40 per cent was found to be desirable in 0.15 per cent carbon-1.5 per cent manganese steels. In view of this, Mr. Comstock's conclusion, that 0.40 to 0.60 per cent titanium should be present in 0.08-0.11 per cent carbon-0.10-0.15 per cent phosphorus steel, indicates that a somewhat higher ratio of titanium to carbon is required in high phosphorus steel.

The reduced tendency of high titanium steels to harden in welding confirms our results. It was found that titanium and columbium were quite effective in this respect and they should be of material assistance in reducing the tendency toward cracking during welding of steels having tensile strengths in excess of 75,000 to 80,000 pounds per square inch. However, titanium was not found to be effective in extending the range of steels with "fool proof" welding characteristics in the un-stress relieved conditions to ranges of tensile strength above 80,000 pounds per square inch. For example, many steels, including the high titanium type, having tensile strengths of less than 80,000 pounds per square inch tensile strength can be submitted to the U. S. Navy welded Tee-bend test without failure, but the high titanium types, like the others, have not given good results when the initial tensile strength exceeded a ceiling of about 80,000 pounds per square inch.

The embrittling effect of phosphorus may also be reduced by chromium as shown by Lorig and Krause,[2] Jones,[3] and the present writer.[4] As indicated in the latter paper, the phosphorus effect may also be minimized by grain refinement using relatively small additions of grain refining elements. Particularly good properties have resulted from adding balanced combinations of grain refining elements. As Mr. Comstock has shown, titanium has a tendency to lower the yield point and it has been observed that this effect becomes evident with quite small additions in certain types of steel.

Mr. Comstock has discarded the advantages of chromium on account of the slightly higher cost, even though the chromium steels of properly balanced

[1]T. Swinden and L. Reeve, The Institute of Welding, Vol. 1, 1938, p. 7.
[2]C. H. Lorig and D. E. Krause, *Metals and Alloys*, Vol. 7, 1936, p. 9, 51, 69.
[3]J. A. Jones, The Iron and Steel Institute, Vol. 135, 1937, No. 1, p. 113.
[4]W. Crafts, American Institute of Mining and Metallurgical Engineers, Vol. 135, 1939, p. 473.

composition, Nos. 17 and 18, had good properties. Steels Nos. 19 and 20, which were subject to temper brittleness, were unbalanced by high manganese or nickel contents, whereas the balanced chromium steel, No. 18, suffered no embrittlement. The general criticism of chromium on page 346 is, therefore, unsupported by the data. It has been shown that chromium improves the general corrosion resistance of phosphorus-copper steels[5] and in our work[4] chromium has been found to have a specific influence in changing the character of rust to a more protective fine-grained adherent type. It would seem more rational to use chromium and lower the phosphorus somewhat without loss and probably with improvement of corrosion resistance. This would make it unnecessary to use such a large amount of titanium and would result in a substantially less expensive steel. It would also minimize the possibility of abnormal brittleness that sometimes develops in very high phosphorus steels.

In conclusion we wish to commend Mr. Comstock for presenting valuable information on the characteristics of high titanium structural steels. It is felt that the advantages of high titanium contents are even more useful in the higher strength structural steels and it is to be hoped that Mr. Comstock will continue his research in that direction where the need for improved weldability is great.

Written Discussion: By E. C. Wright, chief metallurgist, National Tube Co., Pittsburgh.

We believe that the publication of this paper by Mr. Comstock is of timely interest, as it gives further corroboration to the beneficial effects of moderate additions of phosphorus to low carbon steels. This feature is being gradually recognized by the work of several investigators and it seems likely that in the near future the old rigid restriction of 0.04 per cent phosphorus maximum in most all commercial steels may be considerably changed.

From the description of the melting and deoxidation practice given for the various analyses discussed in Mr. Comstock's paper, we assume that all of the heats were thoroughly deoxidized. During the past three years we have realized very definitely the highly beneficial effects of phosphorus additions up to 0.15 per cent in low carbon steel when the heats have been thoroughly killed or thoroughly deoxidized with additions of silicon and aluminum. We have been successful in manufacturing thousands of tons of regular acid bessemer steel which is thoroughly deoxidized and finished with the approximate analysis tabulated below:

	Per Cent
Carbon	0.15-0.30
Manganese	0.40-0.70
Silicon	0.15-0.30
Sulphur	0.06 max.
Phosphorus	0.11 max.

This steel has been deoxidized exactly like thoroughly killed open-hearth steel, teemed successfully in hot topped ingots, and rolled into bars of satisfactory forging quality.

---

[5]G. N. Schramm, E. S. Taylerson and A. F. Stuebing, *Iron Age*, Vol. 134, 1934, Dec. 6, p. 33.

Many thousands of tons of seamless pipe in a wide range of commercial sizes have been produced from this thoroughly deoxidized acid Bessemer steel with steel mill yields and pipe mill yields closely approximating those obtained with standard killed basic open-hearth steel. We have been surprised at the definitely superior properties of these steels as compared to basic open-hearth steels of the same tensile strength. The average physical properties of this material as-rolled in the form of seamless pipe have been 54,000 pounds per square inch yield point, 74,000 pounds per square inch tensile strength, 35 per cent elongation in 2 inches. There would be little difficulty in producing this deoxidized acid Bessemer steel to a minimum yield point of 50,000 pounds per square inch, which was the aim in producing the heats described in Mr. Comstock's paper.

As indicated by the tensile properties given above, this steel has excellent ductility. A study of the impact toughness on hundreds of heats has shown that satisfactory Charpy impact values, such as 20 foot-pounds, can be regularly obtained at temperatures as low as 0 and —50 degrees Fahr. This result is obviously due to the very thorough aluminum deoxidation which is employed in the manufacture of this steel. The high physical properties are generally the result of the silicon and phosphorus additions shown in the analysis, above that which is normal for basic open-hearth steel of similar carbon and manganese content.

It has been thoroughly demonstrated in making this large quantity of steel on a regular production basis, that toughness and ductility at low temperature are largely influenced by oxygen content and are little affected by phosphorus if the oxygen content of the steel is reduced to a low value. The past occurrences of extreme brittleness at low temperatures in bessemer steel must certainly have been due to the fact that the steel was of the open or undeoxidized type, and the high phosphorus combined with the oxygen contributed to the brittle condition.

In addition to the high ductility and high tensile strength for the low carbon-manganese analysis, these steels have been found to exhibit an extremely high elastic limit. In many of the tensile tests which have been made, a stress-strain curve has been plotted and the elastic limit has been within 95 per cent of the 0.2 per cent set yield point, a situation which rarely occurs in open-hearth steel of the same tensile strength. The ratio of the yield point to tensile strength is also of the order of 74 per cent as against a common ratio in seamless pipe of 63 per cent for basic open-hearth seamless pipe of the same tensile strength.

Fatigue tests run on this type of steel have also exhibited an endurance limit in air of approximately 45,000 pounds per square inch for bessemer steel of 70,000 pounds per square inch tensile strength. Fatigue tests on basic open-hearth steel in the same type of pipe with 75,000 pounds per square inch tensile strength exhibit a fatigue limit in air of 35,000 pounds per square inch.

One further advantage of this steel with a minimum yield point of 50,000 pounds per square inch is its definitely superior weldability as compared to open-hearth steel of the same tensile strength. Spot bead tests made on this steel do not develop any martensite adjacent to the bead, and have not shown

Vickers hardness numbers above 285. Spot bead tests on carbon-manganese basic steels of 75,000 pounds per square inch tensile strength have shown considerable martensite with Vickers hardness numbers as high as 500. The actual welding of large quantities of this seamless pipe has shown that the high phosphorus content of 0.09 to 0.10 per cent has not been detrimental in any way to the welding characteristics. This, however, is not odd, in spite of the considerable prejudice among arc welders to phosphorus, since thousands of tons of Bessemer lap-weld pipe containing the same phosphorus have been successfully arc welded and acetylene welded in the past in the laying of long pipe lines.

The characteristics of the deoxidized acid Bessemer steel described herein have been checked and thoroughly duplicated on heats made to a similar analysis in the basic open-hearth, acid open-hearth, and laboratory electric induction melting furnaces. With the same levels of carbon, silicon, manganese, and phosphorus with similar deoxidizing treatments, practically the same range of physical properties has been obtained. We feel this represents a very thorough demonstration of the value of phosphorus additions up to 0.15 per cent for many varieties of structural steels.

We believe the work which we have done in the past three years on a large commercial scale verified the results which Mr. Comstock has described for the beneficial effects of phosphorus. It seems quite obvious from our experience that high strength structural steels of good welding quality can be made without resorting to any expensive alloys.

Written Discussion: By J. W. Halley, metallurgist, Inland Steel Co., East Chicago, Indiana.

Mr. Comstock's paper is particularly welcome because of the small amount of published work on low alloy steels despite their general use.

The physical properties of the steel recommended are very interesting and in order to check them in a slightly larger melt, a 300-pound induction heat was made to the following analysis:

	Per Cent
Carbon	0.12
Manganese	1.15
Phosphorus	0.118
Sulphur	0.011
Silicon	0.220
Copper	0.53
Titanium	0.31

The steel was forged to a slab and rolled to 5/8-inch plate. The as-rolled physical properties were as follows:

	Yield Strength Lbs./Sq.In.	Tensile Strength Lbs./Sq.In.	Per Cent Elongation 2 Inches	Per Cent R. A.
Longitudinal	69,920	90,680	26.5	71.4
Transverse	69,520	89,600	26.0	64.3

The lack of directional properties and high percentage reduction of area are particularly desirable.

The impact properties, particularly at low temperature, were, however,

somewhat disappointing, being 49 foot-pounds Charpy at room temperature and 3.5 foot-pounds at —40 degrees Fahr. For general service, a low alloy steel should have at least 15 foot-pounds Charpy at —40 degrees Fahr.

The 300-pound heat had much higher tensile strength than the smaller heats made by Mr. Comstock. We have found that steel from larger heats usually have somewhat higher strength, but discrepancy in this case is considerably more than we would have anticipated.

It is very probable that titanium has a place in low alloy steels but the analysis recommended does not meet all the requirements for this type of steel. In view of the high cost of titanium, it would be desirable to lower the titanium content as much as possible.

Author's Reply

I wish to thank the gentlemen who have been kind enough to discuss this paper. The thoughtful and valuable discussions submitted were all very much appreciated.

In regard to Mr. Wright's question as to whether the steels were thoroughly deoxidized, it is true that the steels that I used were all treated with a small amount of aluminum before the titanium was added. He has shown that these steels can be made without titanium with fairly acceptable properties, but according to our own work, it seems that the toughness after rapid cooling was definitely improved by the titanium content, and I believe that in the higher strength steels of that nature when welded, the titanium would show a definite improvement in commercial applications. As to just how much titanium would be necessary, we need further data on heats made on a larger scale, because all of my work has been done on very small ingots and probably in larger scale practice, less titanium would be effective.

This is also pertinent to Mr. Simon's remarks in regard to the difficulties of recovering that amount of titanium in Bessemer practice. I believe that if the steel were made on a larger scale, probably it would be found that smaller amounts of titanium would be sufficient. This is also borne out by the data reported by Mr. Crafts, showing that small additions of titanium have been found to be beneficial to the welding properties of high-strength steels.

In reply to Mr. Crafts, I did not mean to criticize chromium particularly, but simply reported what we found, that the chromium that we added to our experimental heats did not seem to afford any particular advantage over what could be obtained, without chromium, but very likely, if the corrosion resistance was investigated, chromium might be found to be useful. I'm afraid that Mr. Crafts, in referring to a "general criticism of chromium on page 346" has imagined an implication which was not intended or actually expressed.

It is gratifying to note that Mr. Simon recognizes the influence of titanium in decreasing the hardenability of the steels described in the paper. Comparison data on steel practically free from titanium are not entirely lacking, however, as may be seen by referring to Fig. 1, which was inserted expressly for the purpose of supplying such a comparison, and which Mr. Simon apparently has overlooked.

It is admitted that welding tests and bend tests on larger samples of these steels would be desirable, and on as-rolled rather than on normalized specimens. Such tests will have to wait, however, until the steel has been made on a larger scale than in 17-pound laboratory heats, and the chief purpose of the paper was to indicate that such larger-scale trials would be worth while. Normalized rather than as-rolled specimens were chosen for the test-results reported in the paper in order to avoid abnormally high yield points which might have been developed in some of the steels by too low a finishing temperature at the small mill where they were rolled. The results reported on the steels in the quenched condition were thought to furnish sufficient evidence that normalizing is not *needed* for these steels as Mr. Simon suggests.

With adequate preliminary deoxidation of Bessemer steel it should be possible to secure, through re-ladling or mold additions, much better recovery of alloy additions of titanium than 50 or 60 per cent, which is the basis of Mr. Simon's computations. Also with large-scale practice it may be found that less titanium is needed. It seems very probable that after a little experience has been acquired in the commercial production of these steels, the necessary ferrotitanium addition may be even less than 30 pounds per net ton.

It is gratifying to note that Mr. Halley has made a heat of this steel on a slightly larger scale, and secured good transverse properties in a ⅝-inch plate. The high strength and poor low-temperature impact resistance may be due to the carbon being on the high side and the titanium slightly low. Less titanium would be necessary with lower carbon, and it appears from Mr. Halley's results that the carbon could have been reduced several points without decreasing the strength to an undesirable value. Probably better impact values, as well as economy in the use of titanium, would be attained if the carbon were held below 0.10 per cent. The author is especially grateful to Mr. Halley for reporting the results he obtained from the 300-pound heat.

EFFECT OF GRAIN SIZE AND HEAT TREATMENT UPON IMPACT TOUGHNESS AT LOW TEMPERATURES OF MEDIUM CARBON FORGING STEEL

By Samuel J. Rosenberg and Daniel H. Gagon

Abstract

A study was made of the effect of grain size and heat treatment upon the impact toughness of S.A.E. 1050 steel, as judged by the temperature range wherein cold brittleness occurred. There was no relation between grain size and impact toughness in the hot-rolled steels. Normalizing improved this property and in this condition the fine-grained steels proved superior to the coarse-grained steels. The toughness of the steels, either as hot rolled or as normalized, was relatively low, but was markedly increased by hardening and tempering. Normalizing prior to heat treatment had no effect upon the impact properties. When heat treated, there was no relation between grain size and impact toughness. Each individual heat of steel appeared to have an inherent resistance to impact, dependent upon factors not at present recognized. Impact toughness at room temperature was no criterion of impact toughness at lower temperatures.

Introduction

THE purpose of this study was to determine the influence of grain size and heat treatment upon the impact properties at low temperatures of medium carbon forging steels and the determination of the temperature range in which brittleness of the steel occurs. This range is characterized by a marked decrease in the observed impact values accompanied by a change in the appearance of fracture from a fibrous one to a granular one. The study was made in co-operation with the Bureau of Aeronautics, Navy Department.

The technical literature contains numerous references on the impact toughness of steel. Most data presented appear to substan-

A paper presented before the Twenty-third Annual Convention of the Society held in Philadelphia, October 20 to 24, 1941. Of the authors, S. J. Rosenenberg is metallurgist, and D. H. Gagon is assistant scientific aid, National Bureau of Standards, Department of Commerce, Washington, D. C. Manuscript received May 23, 1941.

tiate the conclusion that fine-grained steel is superior in toughness to coarse-grained steel (1) to (6)[1], although a contrary opinion has been expressed (7).

Materials and Methods of Test

Six heats of S.A.E. 1050 steel, furnished by the Bethlehem Steel Corporation in the form of hot-rolled 1-inch diameter rods, were used in this study. The chemical compositions of these steels, as determined at this Bureau, are given in Table I. The microstructures and grain sizes of the steels in the as-received condition are shown in Fig. 1.

Table I
Chemical Composition of the Steels(1)

Steel	Per Cent									
	C	Mn	P	S	Si	O_2	N_2	H_2	Al	Al_2O_3
A	0.49	0.79	0.023	0.023	0.22	0.005	0.004	0.0003	0.002	0.001
						0.004	0.005	0.0001		
B	0.45	0.80	0.019	0.023	0.19	0.006	0.004	0.0001	0.002	0.001
						0.006	0.004	0.0001		
C	0.52	0.85	0.021	0.031	0.29	0.004	0.005	0.0002	0.002	0.005
						0.005	n.d.(2)	n.d.(2)		
D	0.49	0.80	0.022	0.028	0.21	0.003	0.003	n.d.(2)	0.016	0.007
						0.003	0.004	0.0003		
E	0.46	0.55	0.040	0.039	0.20	0.005	0.006	0.0003	0.019	0.004
						0.003	0.005	0.0003		
F	0.45	0.59	0.021	0.028	0.24	0.002	0.003	0.0002	0.013	0.004
						0.003	0.004	0.0002		

(1) Chemical analyses were made by W. H. Jukkola, junior chemist; gas analyses by V. C. F. Holm, assistant chemist.
(2) n.d. = not detected.

Steels A, B and C were submitted by the manufacturer as having a coarse McQuaid-Ehn grain size and steels D, E and F a fine grain size. However, tests made by carburizing at 1700 degrees Fahr. (925 degrees Cent.) for 18 hours (the usual procedure for McQuaid-Ehn tests) showed that steel C was a medium fine-grained steel. The grain sizes developed in the McQuaid-Ehn tests are shown in Fig. 2 and Table II.

Each steel was tested in eight conditions of heat treatment and the hardness for each was determined (Table III).

The austenitic grain sizes (Table II) were determined on bars 3 inches long, after heating at 1475 and 1600 degrees Fahr. (800 and 870 degrees Cent.) and quenching one end into water. To eliminate variables in grain size, the procedure (rate of heating, time at tem-

[1] The figures appearing in parentheses refer to the bibliography appended to this paper.

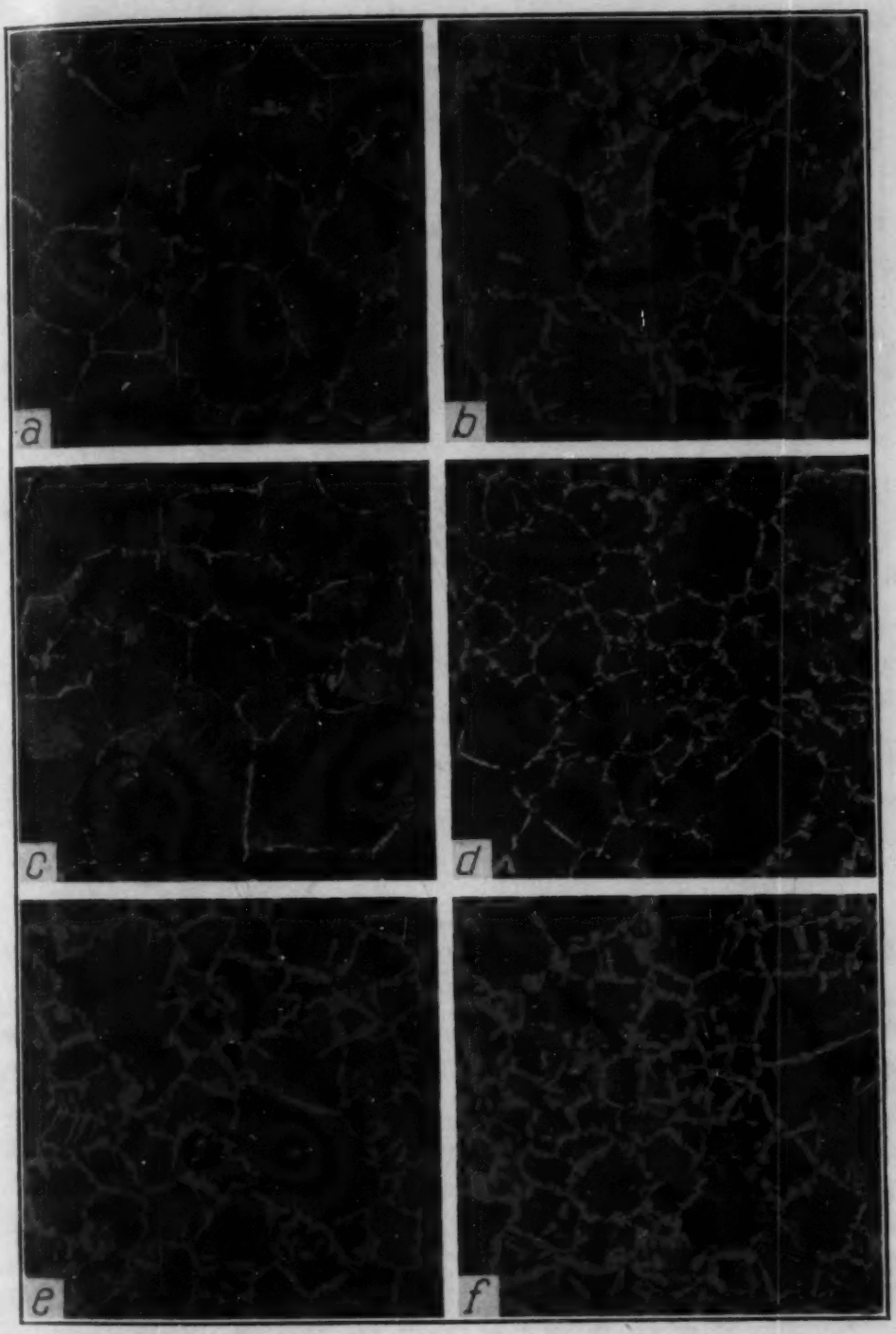

Fig. 1—Microstructures of the Steels as Hot-Rolled. Etched with 1 Per Cent Nital. × 100. The Letters on the Photomicrographs Correspond with the Designations Used for the Individual Steels.

perature, etc.) was approximately the same as that employed during the heat treatment of the steels.

The specimens used for impact tests were 10 millimeter square

Table II
Austenitic Grain Size of the Steels

Steel	At 1475° F. Grains per sq. in. at × 100	At 1475° F. ASTM Grain Size No.	At 1600° F. Grains per sq. in. at × 100	At 1600° F. ASTM Grain Size No.	As hot rolled Grains per sq. in. at × 100	As hot rolled ASTM Grain Size No.	(McQuaid-Ehn) As carburized Grains per sq. in. at × 100	(McQuaid-Ehn) As carburized ASTM Grain Size No.
A	50	7	19	5	7	4	3.5	3
B	50	7	9	4	9	4	3.5	3
C	110	8	95	7	8	4	37	6
D	150	8	140	8	14	5	100	8
E	150	8	130	8	16	5	110	8
F	130	8	110	8	17	5	105	8

Table III
Heat Treatment and Hardness of the Steels

Heat Treatment [a]	Rockwell Hardness Number Steel A	Steel B	Steel C	Steel D	Steel E	Steel F
As-received (hot rolled)	B 95	B 91	B 97	B 94	B 88	B 89
As-received, water quenched from 1475° F., tempered at 1000° F.	C 32	C 30	C 33	C 32	C 28	C 26
As-received, water quenched from 1475° F., tempered at 1150° F.	C 23	C 21	C 24	C 22	C 19	C 19
As-received, water quenched from 1475° F., tempered at 1300° F.	C 14	C 12	C 14	C 15	C 11	C 11
As-normalized (air cooled from 1600° F.)	B 97	B 93	B 96	B 93	B 89	B 88
Normalized, water quenched from 1475° F., tempered at 1000° F.	C 32	C 29	C 32	C 31	C 28	C 28
Normalized, water quenched from 1475° F., tempered at 1150° F.	C 22	C 20	C 23	C 22	C 20	C 18
Normalized, water quenched from 1475° F., tempered at 1300° F.	C 13	C 13	C 15	C 14	C 11	C 11

[a] All steels were held for 1 hour at normalizing and tempering temperatures and ½ hour at hardening temperatures. Bars were shaped to ½-inch square and cut to lengths of about 15 inches prior to heat treatment.

by 55 millimeter long with a 45-degree "V" notch 2 millimeters deep having a root radius of 0.25 millimeter. Since the shape of the notch can influence the impact properties of a specimen, particular care was exercised in grinding the cutter used for this work. All impact tests were made in quadruplicate at test temperatures of +212 degrees Fahr. (+100 degrees Cent.), room temperature, 32, −4, −40 and −108 degrees Fahr. (0, −20, −40 and −78 degrees Cent.) in a Charpy machine having a capacity of 224 foot-pounds. The constants of this machine and details of test procedure have been given in a previous paper (8).

Results of the Tests and General Discussion

Before proceeding to a discussion of the results of the tests, it

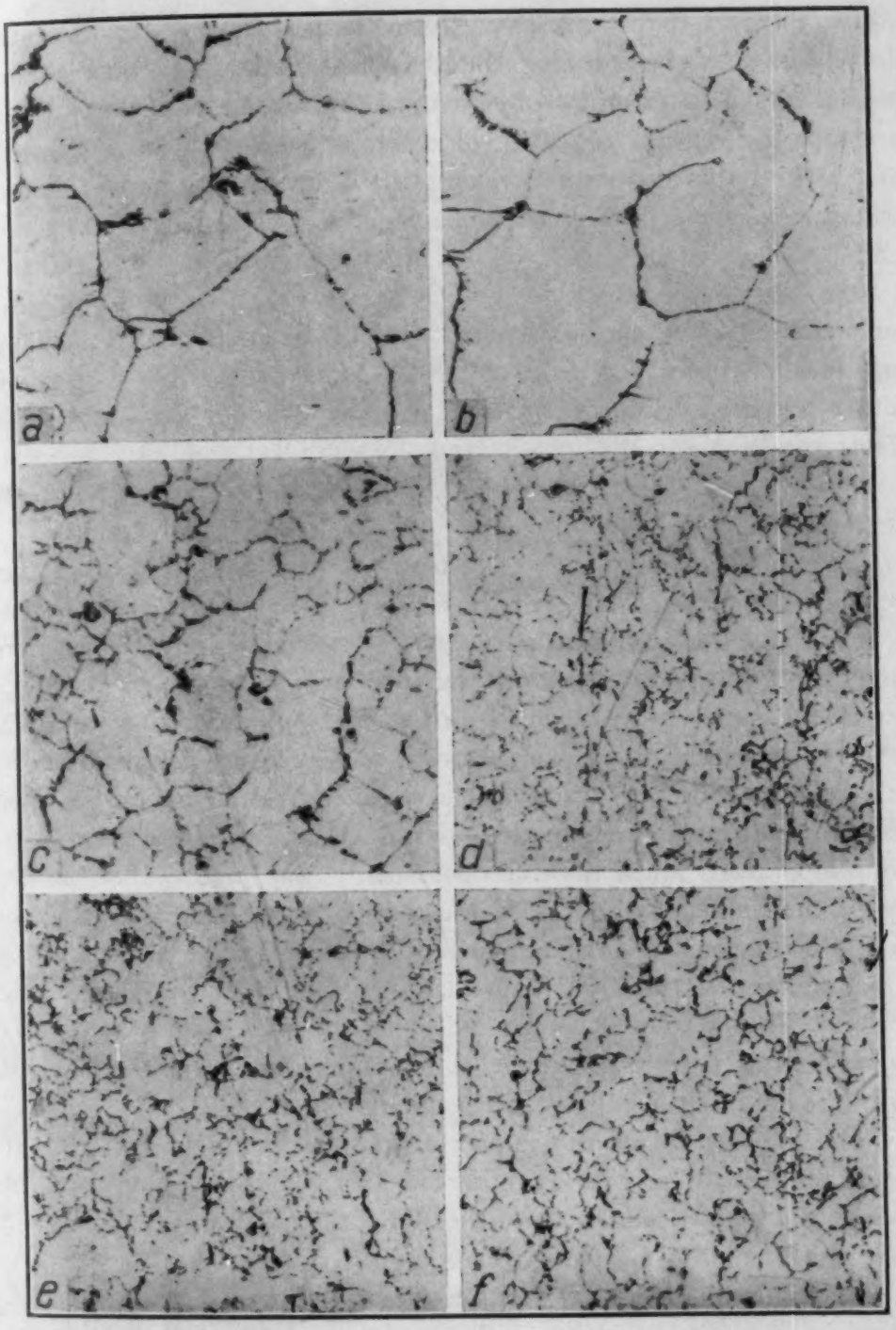

Fig. 2—Grain Size of the Steels as Developed by the McQuaid-Ehn Test. Etched with Boiling Sodium Picrate. × 100. The Letters on the Photomicrographs Correspond with the Designations Used for the Individual Steels.

is advisable to consider the meaning of the results of impact tests, particularly as modified by test temperatures.

It should be pointed out that any impact test is only qualitative,

despite the fact that results are given numerical values indicative of the energy absorbed during the deformation and fracture of test specimens. The primary objective of impact tests of steels is to ascertain the relative tendency of different steels to fail in a brittle fashion and this cannot be accomplished by making a few impact tests under one set of conditions. Slight changes in the size and shape of the test specimen, in the depth or sharpness of the notch, in total energy or velocity of the hammer, or in temperature, may cause disproportionate changes in the results of impact tests. At least one of these factors must be varied in order to obtain a true picture of the impact deformation characteristics of any steel. The effects of these various factors and the interpretation of the results of impact tests are discussed by McAdam and Clyne (9) and by Hoyt (10).

The location of the temperature range, wherein impact values are markedly decreased and the type of fracture changes from fibrous to granular (the cold brittle range), is not a definite temperature range for any special steel. It may be moved to higher or lower temperatures merely by changing any one of numerous test variables. The relative tendency of a steel towards cold brittleness may, however, be established by studying the effect of test temperature upon the results of impact tests made under a certain set of test conditions. The temperature range in which cold brittleness occurs is an indication of the impact toughness of the steel being tested. Under comparable conditions of test, the lower the temperature at which this transition occurs, the more dependable is that steel for engineering service. This statement is true despite the fact that a steel may absorb greater energy in impact at a temperature above and at one below the cold brittle range than does another steel.

The appearance of the impact fractures obtained over a range of test temperatures, with all other factors constant, is an excellent guide to the impact toughness of the steel under study. Typical fractures, shown in Fig. 3, are of three types. That shown in Fig. 3A, the fibrous or tough type, is accompanied by appreciable deformation and high energy absorption, and occurs at temperatures above the cold brittle range. That shown in Fig. 3D is of the granular or brittle type, is accompanied by little or no deformation and low energy absorption, and occurs below the cold brittle range. Those shown in Fig. 3B and C are typical of breaks which occur within the cold brittle range. The relative areas of fibrous and granular

appearance may vary widely, with concomitant variations in the impact energy absorbed. The theory underlying the discontinuity of the transition from fibrous to granular fracture has been discussed by McAdam and Clyne (9).

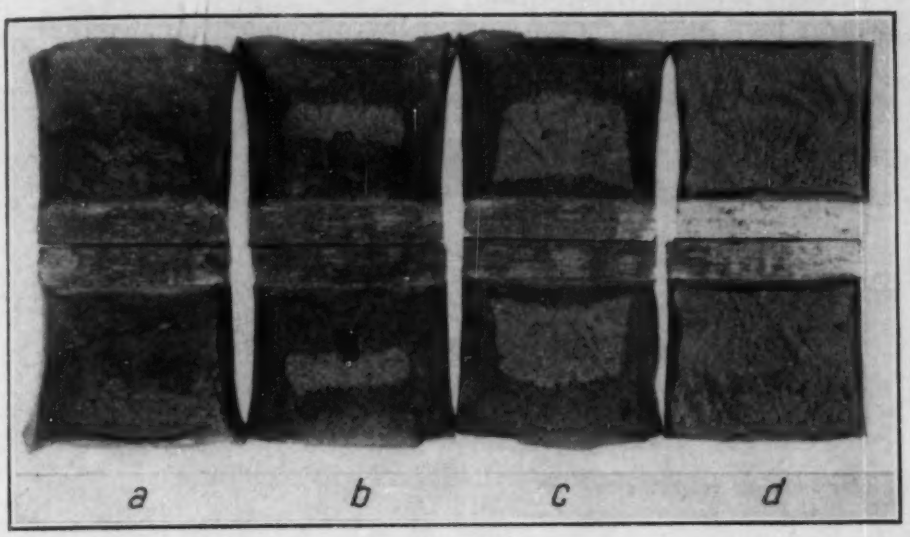

Fig. 3—Appearance of Typical Charpy Impact Fractures. × 2. a—Fibrous Fracture Obtained by Testing Specimen at a Temperature Above the Cold Brittle Range. Fracture Was Accompanied by Considerable Deformation and the Energy Absorbed Was High; b—Partly Fibrous, Partly Granular Fracture Obtained by Testing Specimen at a Temperature Within the Cold Brittle Range; c—Partly Fibrous, Partly Granular Fracture Obtained by Testing Specimen at a Temperature Within the Cold Brittle Range; d—Granular Fracture Obtained by Testing Specimen at a Temperature Below the Cold Brittle Range. Fracture Was Accompanied by But Little Deformation and the Energy Absorbed Was Low.

The values obtained in impact tests at various temperatures are presented in several ways to show a comparison:

(a) Between steels in the as-received condition and after normalizing at 1600 degrees Fahr. (870 degrees Cent.) (Fig. 4).

(b) Of the effect of tempering at 1000, 1150 and 1300 degrees Fahr. (540, 620 and 705 degrees Cent.) on steels quenched from 1475 degrees Fahr. in both as-received and normalized conditions (Figs. 5 to 7).

(c) Of the effect of the various heat treatments on each steel individually (Figs. 8 to 13).

Fig. 4 shows that there was no significant difference between the impact resistance of the as-received and normalized steels at room temperature or below. The impact resistance was low, the fractures were granular, and the cold brittle range, as determined under the specific conditions of test, occurred above room temperature.

In the as-received condition all of the steels exhibited granular, or mostly granular, fractures at +212 degrees Fahr. (+100 degrees Cent.). In this condition, therefore, the cold brittle range of all the steels occurred above +212 degrees Fahr. (+100 degrees Cent.).

In the normalized condition, steels D, E and F at +212 degrees Fahr. (+100 degrees Cent.) had fibrous fractures, high impact

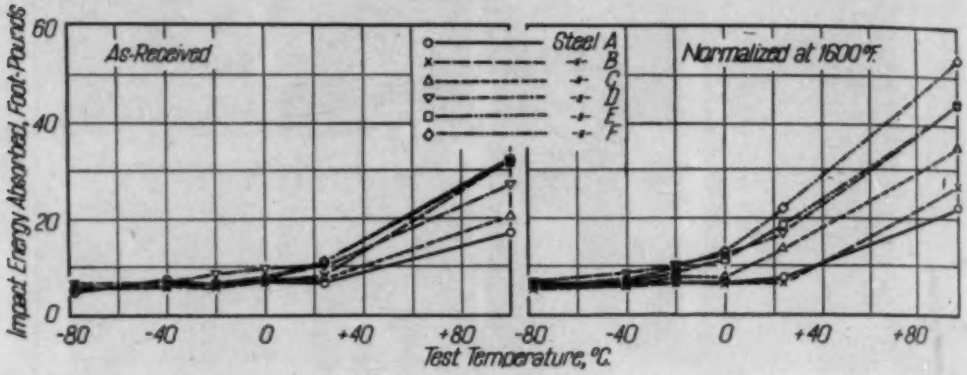

Fig. 4—Effect of Test Temperature Upon the Impact Toughness of the Steels as Hot-Rolled and as Normalized.

values, and the cold brittle range, therefore, occurred between room temperature and +212 degrees Fahr. (+100 degrees Cent.). These steels had fine McQuaid-Ehn grain sizes (No. 8), as well as fine grain sizes at the normalizing temperature (also No. 8). Steel C, as normalized, had somewhat lower impact resistance at +212 degrees Fahr. (+100 degrees Cent.), the fractures were partly fibrous and partly granular; and the cold brittle range occurred in the neighborhood of +212 degrees Fahr. (+100 degrees Cent.). This steel had a medium fine McQuaid-Ehn grain size (No. 6), and at the normalizing temperature its grain size was No. 7. Steels A and B, both of which had coarse McQuaid-Ehn grain sizes (No. 3), exhibited granular fractures at +212 degrees Fahr. (+100 degrees Cent.) and the cold brittle range, therefore, must be located at some temperature above +212 degrees Fahr. (+100 degrees Cent.). At the normalizing temperature steels A and B had grain sizes of No. 5 and No. 4, respectively.

It is apparent that (a) normalizing caused an improvement in the impact toughness of fine-grained S.A.E. 1050 steel as compared with the same steel as hot rolled, and (b) the impact toughness of the normalized steels was related to both the McQuaid-Ehn and the austenitic grain size, the finer the grain size the greater the toughness. No relation between grain size and impact toughness was apparent

in the hot-rolled steels under the specific conditions of test. This type of steel (S.A.E. 1050) does not, however, have appreciable impact toughness in either the as-rolled or as-normalized conditions. This deficiency can be remedied by suitable heat treatment.

The effect of quenching from the proper temperature and tempering at relatively high temperatures was to lower markedly the

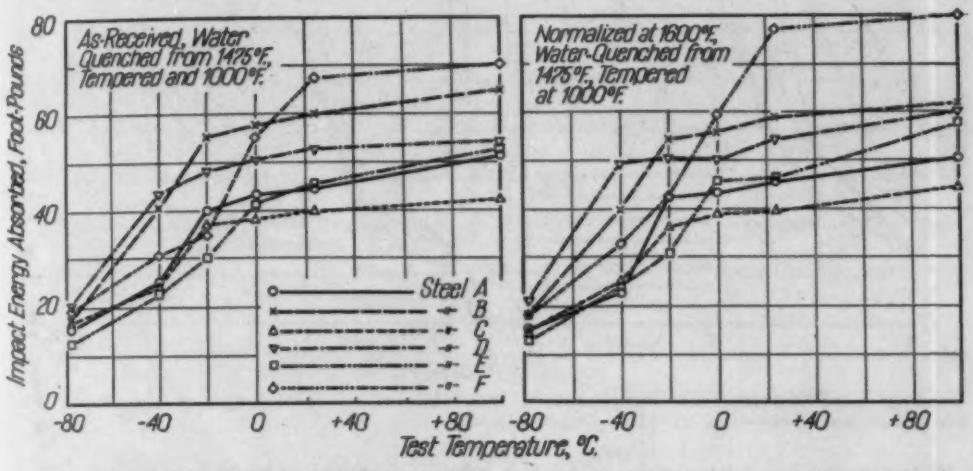

Fig. 5—Effect of Test Temperature Upon the Impact Toughness of the Steels As-Hardened and Tempered at 1000 Degrees Fahr.

temperature range within which cold brittleness occurred (Figs. 5, 6 and 7). None of the steels was cold brittle at room temperature. In a few instances, cold brittleness was manifested between room temperature and 32 degrees Fahr. (0 degrees Cent.), but usually it did not occur above 32 degrees Fahr. (0 degrees Cent.), and in many cases was observed only at temperatures lower than —40 degrees Fahr. (—40 degrees Cent.).

From Figs. 5, 6, and 7, it is obvious that the cold brittle range of steel D, in all conditions of heat treatment, occurred at lower temperatures than in any of the other steels. This steel may therefore be considered to have the best impact toughness, even though other steels sometimes had higher impact values at temperatures above the cold brittle range. Steel D had a fine McQuaid-Ehn grain size and a fine austenitic grain size at the heat treating temperature 1475 degrees Fahr. (800 degrees Cent.). Steel E, however, with the same grain size as steel D, consistently exhibited the minimum impact toughness, as measured by the location of the cold brittle range, in all conditions of heat treatment.

Steel B, which generally showed the second best impact toughness, had a coarse McQuaid-Ehn grain size and a fine austenitic

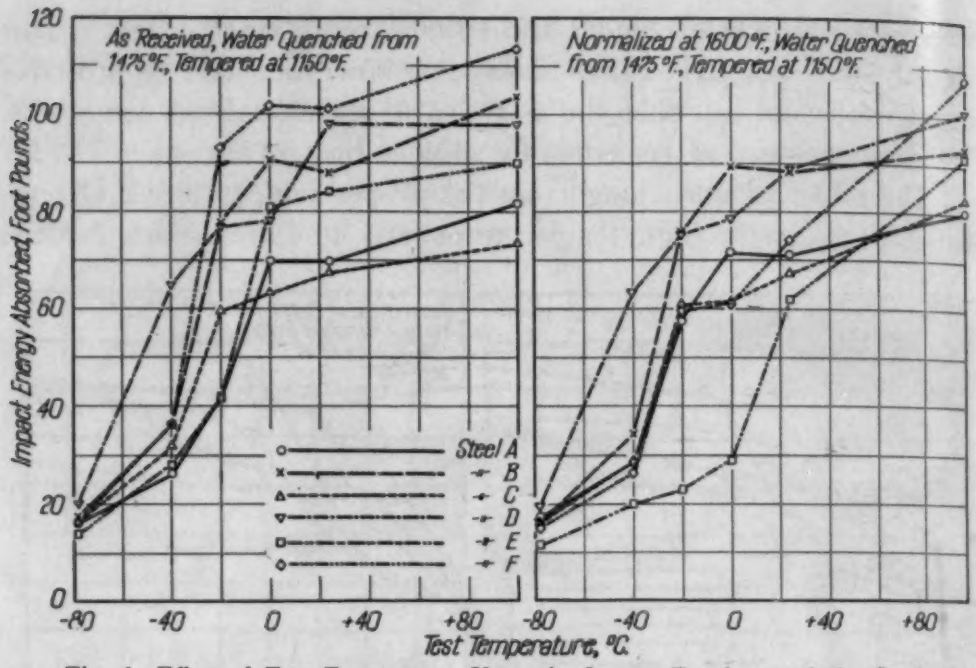

Fig. 6—Effect of Test Temperature Upon the Impact Toughness of the Steels As-Hardened and Tempered at 1150 Degrees Fahr.

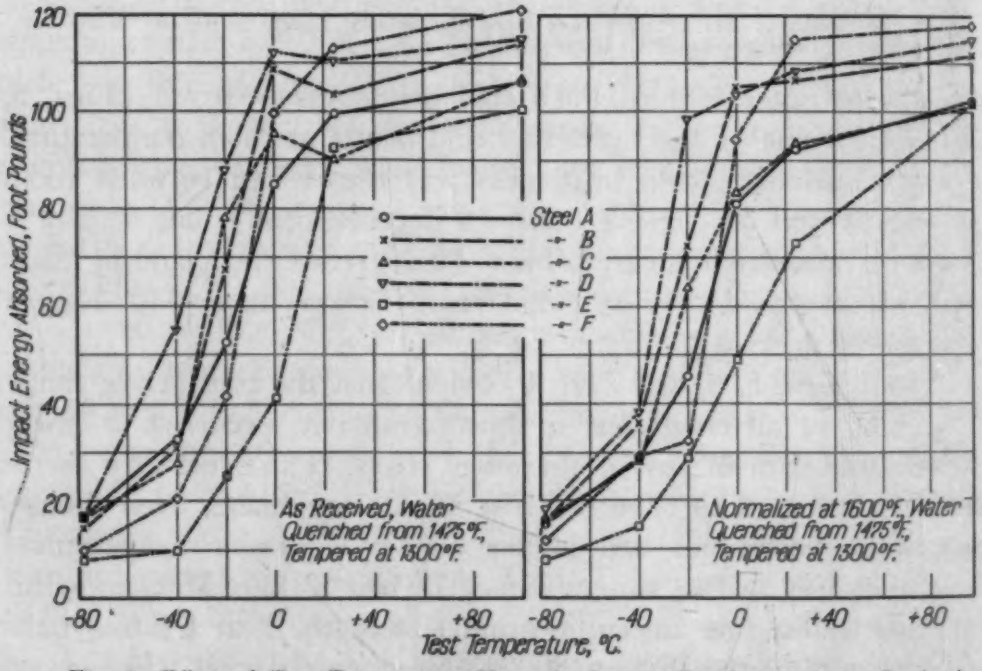

Fig. 7—Effect of Test Temperature Upon the Impact Toughness of the Steels As-Hardened and Tempered at 1300 Degrees Fahr.

grain size (on the low side of No. 7) at the hardening temperature. Steel A, with the same grain size as steel B, however, had decidedly lower impact toughness than steel B in the various conditions of heat treatment.

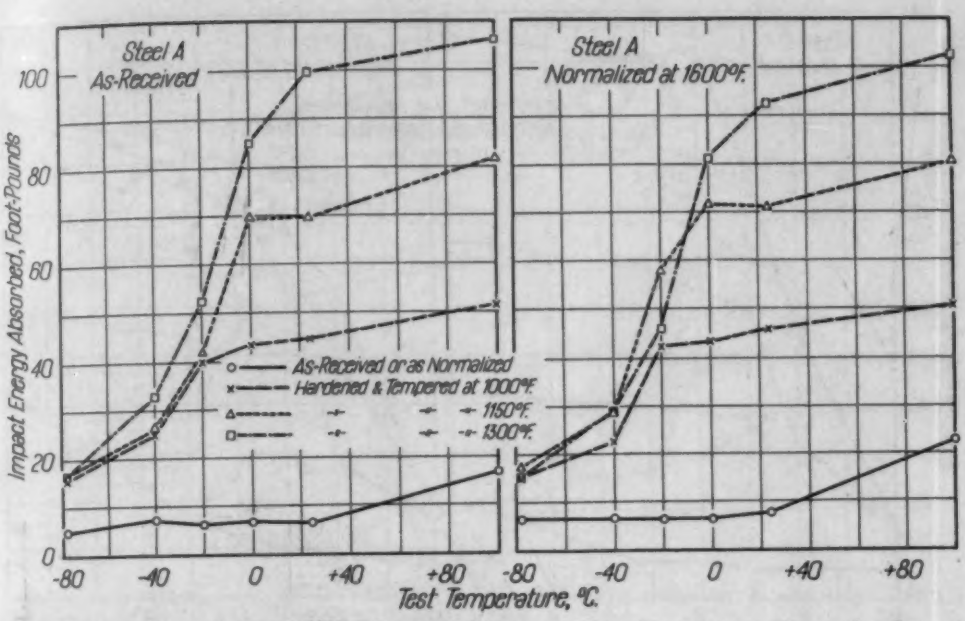

Fig. 8—Comparison of the Effect of Different Heat Treatments Upon the Impact Toughness of Steel A at Different Temperatures.

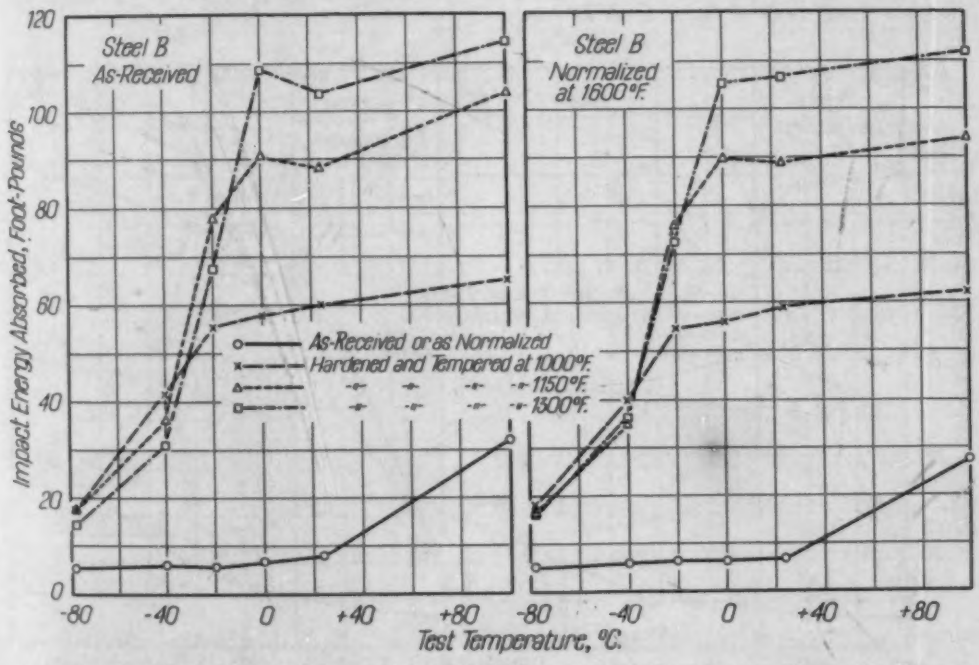

Fig. 9—Comparison of the Effect of Different Heat Treatments Upon the Impact Toughness of Steel B at Different Temperatures.

From the foregoing discussion it may be concluded that when heat treated (a) there was no significant relation between grain size and impact toughness in S.A.E. 1050 steel, and (b) each heat of S.A.E. 1050 steel had its own characteristic resistance to impact. Another point to be emphasized is that high impact toughness at room

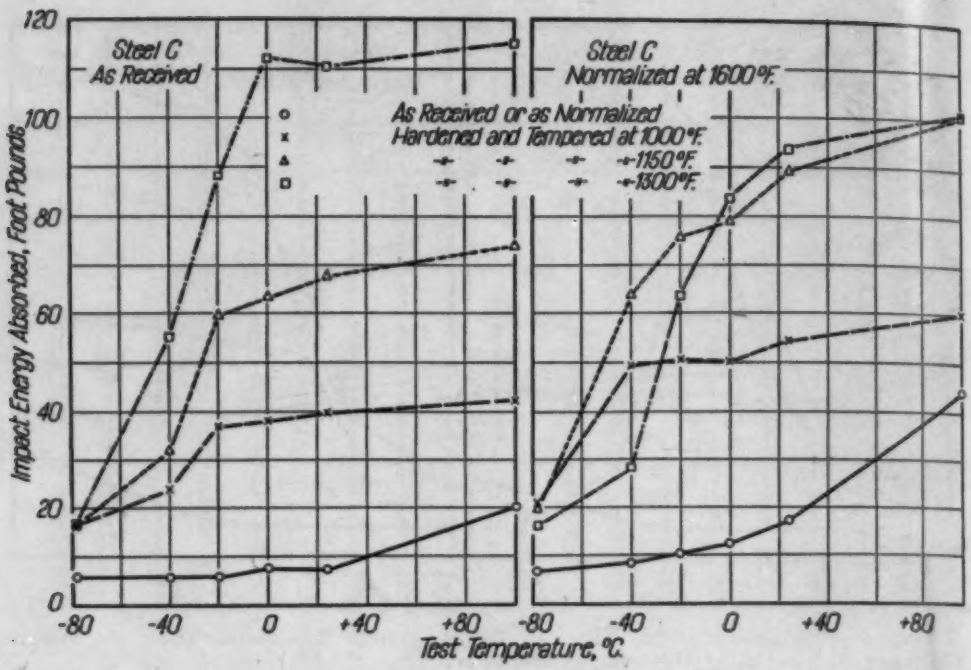

Fig. 10—Comparison of the Effect of the Different Heat Treatments Upon the Impact Toughness of Steel C at Different Temperatures.

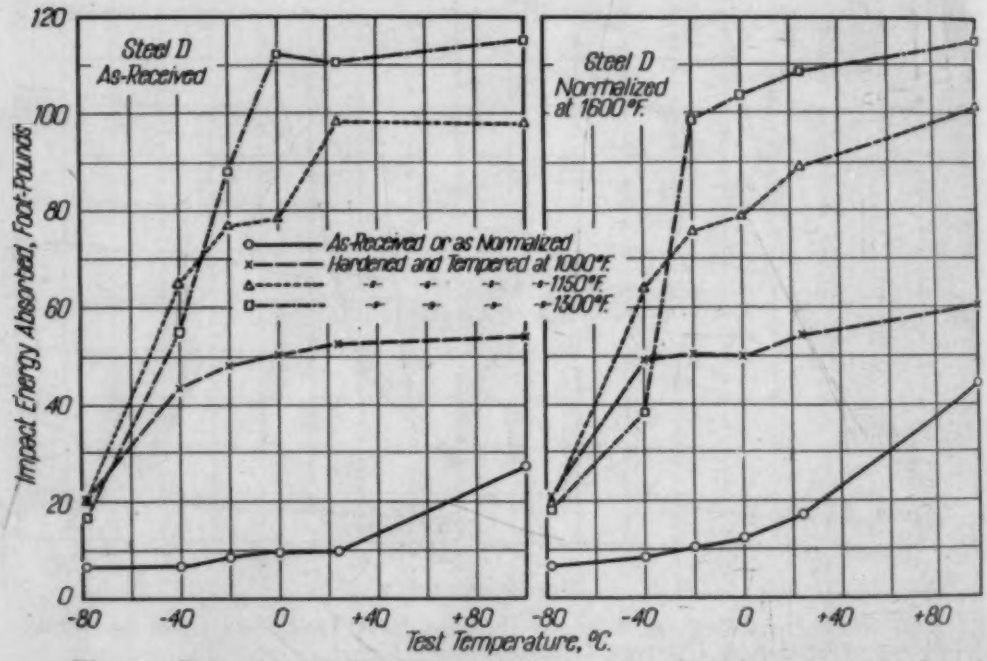

Fig. 11—Comparison of the Effect of Different Heat Treatments Upon the Impact Toughness of Steel D at Different Temperatures.

temperature was no assurance of superior impact toughness at lower temperatures. This is particularly well illustrated by the curves in Fig. 5, which show that steel F had higher numerical values for impact resistance when tested at room temperature than any of the

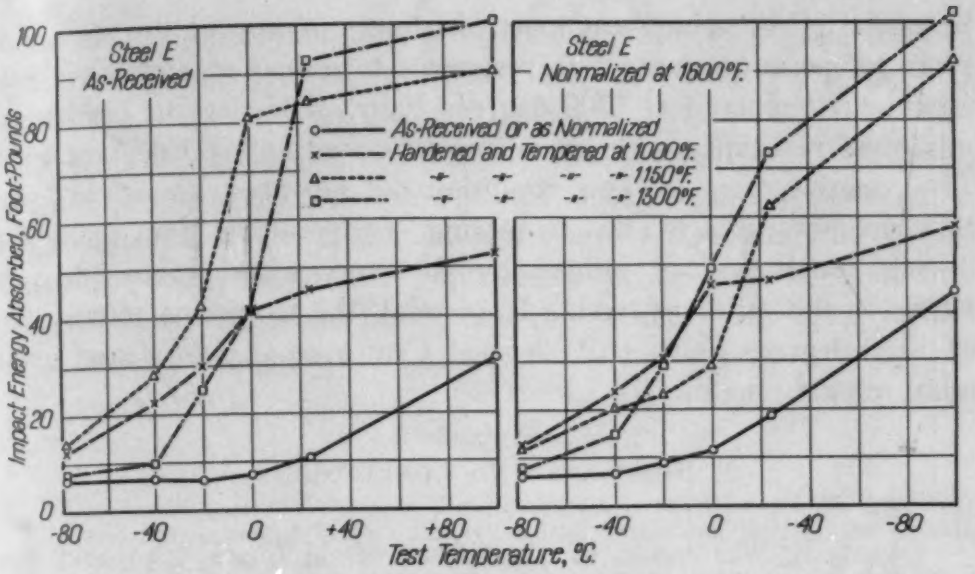

Fig. 12—Comparison of the Effect of Different Heat Treatments Upon the Impact Toughness of Steel E at Different Temperatures.

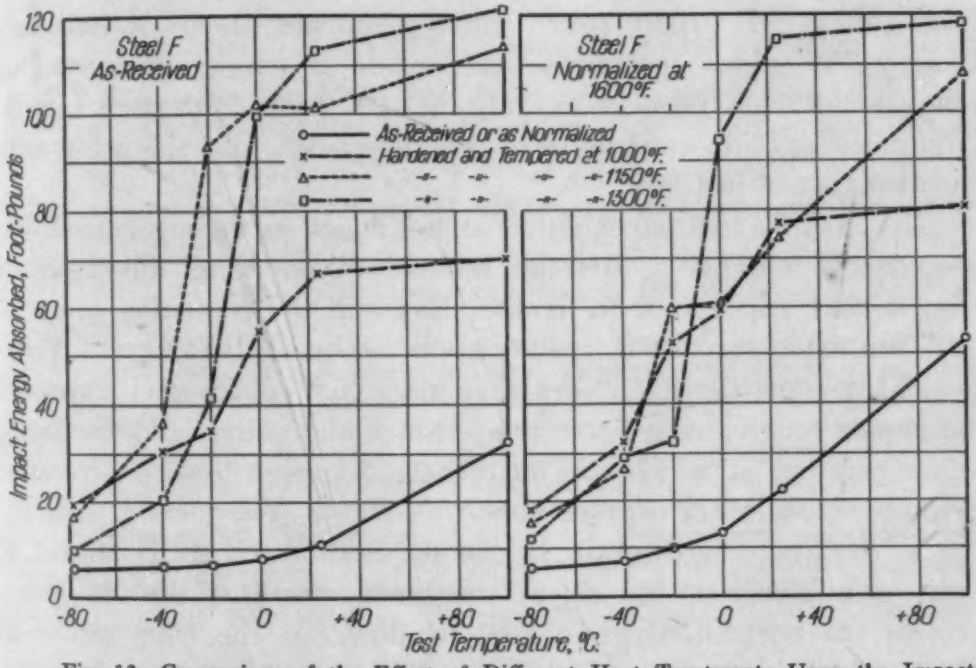

Fig. 13—Comparison of the Effect of Different Heat Treatments Upon the Impact Toughness of Steel F at Different Temperatures.

other steels. When the impact temperature curve is examined, however, it may be seen that cold brittleness was manifested at higher temperatures in steel F than in steels B and D.

The curves in Figs. 8 to 13 illustrate the effect of heat treatment upon the impact toughness of the individual steels at the various test temperatures. Normalizing prior to heat treatment had no

beneficial effect upon the impact toughness of any of the steels. At room temperature, maximum resistance to impact was obtained with specimens tempered at 1300 degrees Fahr. (705 degrees Cent.) and minimum resistance with specimens tempered at 1000 degrees Fahr. (540 degrees Cent.). This condition did not always exist at lower test temperatures. The tempering temperature for maximum impact toughness, as judged by the impact temperature curves, varied in the different steels. In general, the tempering temperature of 1150 degrees Fahr. (620 degrees Cent.) seemed to impart maximum impact toughness.

Summary and Conclusions

A study was made of the effect of McQuaid-Ehn and austenitic grain sizes at heat treating temperatures and of different heat treatments upon the low temperature impact toughness of six heats of S.A.E. 1050 steel. Charpy impact tests, of standard Charpy "V" notch specimens, were made at temperatures ranging from +212 to −108 degrees Fahr. (+100 to −78 degrees Cent.). Under the specific conditions of test described, the following conclusions appear justified:

1. S.A.E. 1050 steel, either as hot rolled or as normalized, has low impact toughness. In the hot-rolled condition, this type of steel is cold brittle at room temperature and the transition range to cold brittleness occurs at temperatures above +212 degrees Fahr. (+100 degrees Cent.). Normalizing the hot-rolled steel improves the impact toughness at room temperature and above, and the range of temperature at which cold brittleness occurs is lowered, in some cases, to below +212 degrees Fahr. (+100 degrees Cent.).

2. Differences in grain size in the normalized steels appear to exert an influence on the impact toughness; the finer the McQuaid-Ehn or the normalized grain size, the lower is the temperature at which cold brittleness is manifested. This trend was not observed, however, with the hot-rolled steels.

3. Impact toughness is markedly improved by hardening and tempering, but normalizing prior to heat treatment has no effect upon this property.

4. Impact toughness at room temperature is no criterion of impact toughness at lower temperatures.

5. Fine grain size, either McQuaid-Ehn or austenitic, is no

assurance of impact toughness superior to that of coarser-grained steel similarly heat treated (quenched and tempered), particularly as regards the occurrence of cold brittleness.

6. S.A.E. 1050 steel, in various conditions of heat treatment, does not have a characteristic resistance to impact in the same sense, for instance, as it has a characteristic tensile strength. Each individual heat, when heat treated, apparently has an inherent resistance to impact between certain limits, and this is dependent upon factors not at present recognized.

Bibliography

1. Philip Schane, Jr., "Effects of McQuaid-Ehn Grain Size on the Structure and Properties of Steel," TRANSACTIONS, American Society for Metals, Vol. 22, 1934, p. 1038.
2. H. W. McQuaid, "Effect of McQuaid-Ehn Grain Size on Hardness and Toughness of Automotive Steels," TRANSACTIONS, American Society for Metals, Vol. 22, 1934, p. 1017.
3. Howard Scott, "Factors Determining the Impact Resistance of Hardened Carbon Steels," TRANSACTIONS, American Society for Metals, Vol. 22, 1934, p. 1142.
4. E. S. Davenport and E. C. Bain, "General Relations Between Grain Size and Hardenability and the Normality of Steels," TRANSACTIONS, American Society for Metals, Vol. 22, 1934, p. 879.
5. S. Epstein, J. H. Nead, and T. S. Washburn, "Grain-size Control of Open-hearth Carbon Steels," TRANSACTIONS, American Society for Metals, Vol. 22, 1934, p. 942.
6. C. H. Herty, Jr., "The Effect of Deoxidation on Some Properties of Steel," TRANSACTIONS, American Society for Metals, Vol. 22, 1934, p. 113.
7. F. B. Foley, "Resume of Round-table Discussion on Effect of Subatmospheric Temperatures on the Properties of Metals," *Proceedings,* American Society for Testing Materials, Vol. 39, 1939, p. 637.
8. Samuel J. Rosenberg, "Effect of Low Temperatures on the Properties of Aircraft Metals," *Bureau of Standards Journal of Research,* Vol. 25, 1940, p. 673 (Research Paper RP 1347).
9. D. J. McAdam, Jr., and R. W. Clyne, "The Theory of Impact Testing: Influence of Temperature, Velocity of Deformation, and Form and Size of Specimen on Work of Deformation," *Proceedings,* American Society for Testing Materials, Vol. 38, part II, 1938.
10. S. L. Hoyt, "Notched Bar Testing," *Metals and Alloys,* Vol. 7, 1936, p. 5, 39, 102, 140.

DISCUSSION

Written Discussion: By S. L. Hoyt, technical advisor, Battelle Memorial Institute, Columbus, Ohio.

The authors seem to have built up a good case for the proposition that a purchaser of steel cannot rely solely upon composition and grain size to secure a desired level of notch toughness. The authors use the term "impact tough-

ness" in this connection, but since there is an active interest these days in true impact testing, that terminology without reference to the text is bound to be misleading.

The writer would also like to inquire if the authors have studied the effect of varying the normalizing temperature on grain size of an individual steel to find out if under those circumstances there is a definite effect of grain size on toughness. The conclusion seems to be stated in broad enough terms to include the effect of variable normalizing temperature.

It is interesting to compare the alumina contents of Table I with the grain sizes of Fig. 1. Though Steel C has more alumina than Steel F, for example, it is definitely coarser grained. The same would hold true for Fig. 2 which gives the grain sizes developed by the McQuaid-Ehn test. The total oxygen contents reported do not seem to help much, but when one considers melting and deoxidation practice there does not seem to be any reason why they should. Even the fractional oxygen might not provide the solution to the riddle but they are the only determinations of this kind which hold forth promise. It would be of interest to have the authors report complete fractional vacuum fusions on all six steels and also include an adequate microscopic study of the foreign inclusions of each steel.

The authors have wisely studied their steels over a range of temperature, but I should like to inquire why they use the Izod "V" notch instead of the Charpy keyhole notch. The former is so shallow that the deformation of notch tough steels spreads to the outer face of the bar and gives a test which is part simple bending and part notch bending, and the energy values may be said to be artificially high. This must have a pronounced effect on the slope and position of the "energy absorption versus test temperature" curves and it is my impression that the standard Charpy keyhole notch is more satisfactory than the Izod notch of the authors for these purposes.

Written Discussion: By R. J. Hafsten, metallurgist, Firestone Tire and Rubber Co., Falls River, Mass.

The authors are to be complimented on the excellent data presented in their paper.

I wish to comment on the authors' conclusions as to the association of grain size, of steels tested as hot-rolled and as quenched and tempered, with impact toughness. The effect of the austenitic grain size on physical properties should be readily evident in the hot-rolled and normalized treatments as there are two points to consider, the influence of the austenitic grain size and the bearing this size has on the structure. It has been observed that in a specific steel where the austenitic grain size can be varied by temperature or time, the per cent of proeutectoid constituent increases as the grain size becomes smaller. From the authors' data the austenitic grain size of the steels as received were all approximately the same, 4 and 5 A.S.T.M. which probably accounts for the poor relationship between the austenite grain size and impact toughness. If the rolling practice had been such that some of the steels were fine-grained and others coarse-grained, would the authors have an opinion as to whether or not the fine-grained steel would be superior to the coarse-grained steel with respect to impact values?

It would appear difficult to conclude from the data that the austenite grain

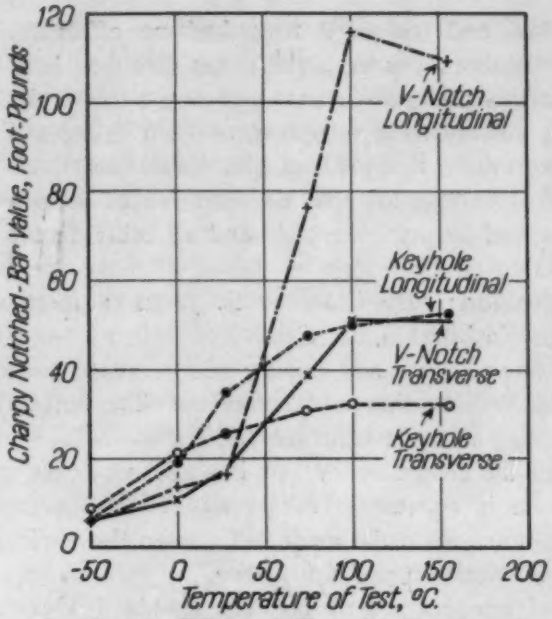

Fig. A—Effect of Type of Notch and Direction of Rolling on the Standard Charpy Notched-Bar Value of a Low-Alloy High-Tensile Steel.

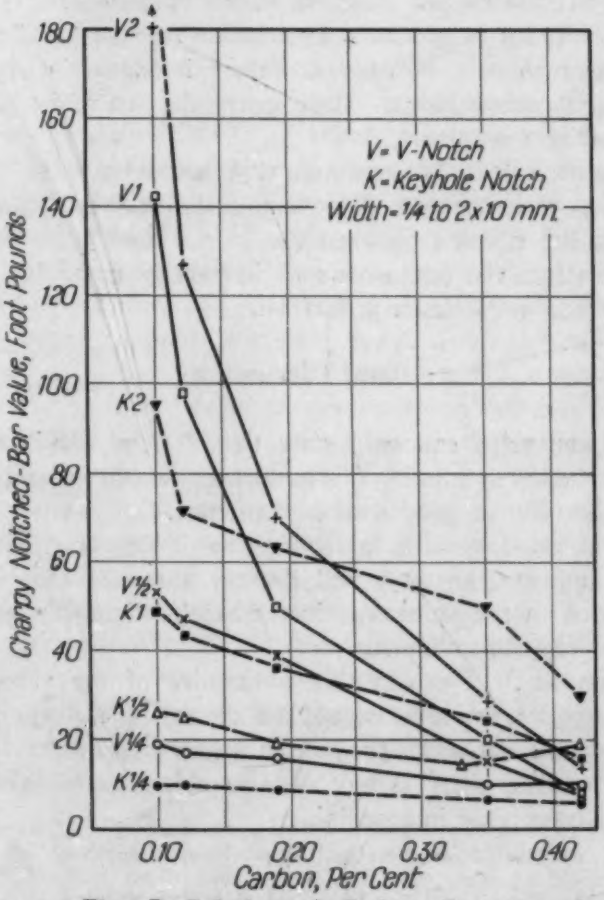

Fig. B—Relation of Carbon Content and Width of Specimen to Charpy Notched-Bar Value for Hot-Rolled Carbon Steels.

size of the quenched and tempered tests had no effect on impact toughness inasmuch as in the authors' research the grain size was held constant and such factors as chemical analysis and furnace practice were variables.

At the chosen austenitizing temperature 1475 degrees Fahr. (800 degrees Cent.) all the steels were fine-grained and hence not too adapted to a grain size study. Would it be possible that the data would be more conclusive if the austenite grain size had been the variable and all other factors such as chemical analysis, constants?

Written Discussion: By Clarence E. Jackson, metallurgist, Naval Research Laboratory, Washington, D. C.

Rapid strides have been made during recent years toward untangling the mysteries of notched-bar testing and behavior. The excellent data presented by Rosenberg and Gagon are a welcome addition.

The question of the choice of "V" or keyhole notch for the Charpy type of notched-bar specimen is constantly recurrent. A comparison of the behavior of the two types of notches can be made only when the variables of temperature of test and width of specimen are considered.

The relation of temperature of test for standard V-notched and keyhole-notched specimens of a low-alloy high-tensile steel is shown in Fig. A. The greater sensitivity of the V-type of notch is to be noted; the low temperature drop is steeper and the overall range of values is greater.

The effect of width of specimen and carbon content on Charpy notched-bar values (temperature of test, 70 degrees Fahr.) is shown in Fig. B for a series of hot-rolled plain carbon steels. Here again the sensitivity of the V-notched specimens is readily recognized.

It has been repeatedly pointed out that the relation of the resistance to fracture and the resistance to deformation determine notched-bar behavior. In other words, the relation between the forces tending to deform and those which tend to fracture the test piece may in part be controlled by the size and shape of the particular specimen under test.

Oral Discussion

A. V. de FOREST:[1] I can only state that I firmly believe that Dr. Hoyt has all these variables in mind. We have many more variables than we have equations and, therefore, a good deal of confusion.

It requires a great deal of knowledge to define, first, what we mean by notch impact toughness, anyway, and second, a tremendous amount of work to correlate that with the unknowns in the steel. Certainly grain size is only one of a number of such unknowns.

G. F. COMSTOCK:[2] I would like to inquire of the authors whether the use of round impact specimens would be of any advantage in helping their machine shop to turn out more product in a given time, and whether that has been considered, and if there is any definite objection to using round impact test specimens to save time in machining.

[1]Professor of mechanical engineering, Massachusetts Institute of Technology, Cambridge, Mass.

[2]Metallurgist, The Titanium Alloy Manufacturing Co., Niagara Falls, N. Y.

JOHN M. LESSELLS:[3] Some reference has been made in previous discussions of this paper to the round type of Izod impact specimen. Might I point out that British specifications for aircraft steels allow either the round type or square type, the values being more or less comparable. The round type is cheaper to machine, although due to the nature of the fracture, it does not offer the same opportunity for an examination of the appearance of the fracture as the square type.

With regard to the remarks which have been made on the "V" notch and the keyhole notch, it is worthy of note that the "V" notch has been found by Moser[4] to be necessary for ductile steels. Such test bar types are used with the Charpy type of machine.

Since our ideas of brittle and sliding types of failure stem from Moser's basic work, these conclusions arrived at by him possibly should be considered.

Authors' Closure

The authors wish to thank all those who were kind enough to offer some discussion of this paper.

Dr. Hoyt questions the advisability of using the "V" notch instead of the keyhole notch in this work. It is realized that the use of the "V" notch usually gives higher values for notch-tough steels than are obtained with the keyhole notch. For notch-brittle steels, however, the use of the "V" notch usually results in lower values than are obtained with the keyhole notch. Some data on this very subject are fortunately submitted in the discussion by Mr. Jackson. The net result of the use of the "V" notch is, therefore, to accentuate the location of the temperature-sensitive range which, after all, is the prime measure of the toughness of steels, rather than the absolute impact values obtained.

It would undoubtedly have been wise to have studied the effects of higher normalizing and hardening temperatures, as suggested by Dr. Hoyt and Mr. Hafsten, since this would have given a range of grain sizes in each individual steel. This was, indeed, actually included in the original plan of study. Unfortunately, however, because of the press of other work and because of the difficulty of securing the machining of so many specimens (about 1200 were tested in the work reported), it was not possible to do this.

Mr. Hafsten notes that the austenitic grain sizes of all the steels were approximately the same in the hot-rolled condition. In the normalized condition, however, steels A and B were definitely coarser than the other four, as well as more brittle. It would appear, therefore, as noted in the paper, that the grain size resulting from normalizing does have an influence upon the toughness. In response to Mr. Hafsten's inquiry, the authors are of the opinion that if the rolling practice had been such that some of the steels were fine-grained and some coarse-grained, the fine-grained steels would have shown superior impact resistance to that of the coarse-grained steels if tested as hot-rolled.

---

[3]Associate professor of mechanical engineering, Massachusetts Institute of Technology, Cambridge, Mass.

[4]Max Moser, "Notched Bar Tests", *Transactions*, American Society of Mechanical Engineers, 1933.

It is apparent from the curves that the impact resistance of the heat treated steels varied considerably. As pointed out by Mr. Hafsten, the austenitic grain size of all six heat treated steels was about the same. Quite definitely, then, the grain size was no guide to the toughness of these steels as heat treated. Variations in chemical composition are of minor importance, since all steels were representative of the S.A.E. 1050 class. The only significant difference in the steels was in the method of manufacture, that is, three of the steels were controlled and three noncontrolled. And although this difference was reflected in the McQuaid-Ehn test, it apparently had no influence on the results of the impact tests on the heat treated steels.

The use of round impact specimens was never considered in this work. It is likely that these could be made with greater ease than the square specimen. However, a considerable amount of data on the effect of low temperatures on the toughness of various metals, both ferrous and nonferrous, has been accumulated at this Bureau and a square specimen with a "V" notch was used in all cases. If only for the sake of uniformity, it would seem wise to continue using the same type of specimen.

THE STRUCTURE OF PEARLITE

By Frederick C. Hull and Robert F. Mehl

Abstract

This paper is a discussion of the structure and mechanism of formation of pearlite. The literature on pearlite has been reviewed with particular reference to the theory of the formation of pearlite. The genesis of pearlite by a combination of sidewise and edgewise growth is accepted as the theory which furnishes the best explanation for the lamellar nature of pearlite, the constancy of pearlite spacing, the variation of spacing with temperature, and the curvature of cementite lamellae. The mechanism by which pearlite nodules are formed is discussed and attention is called to a mode of transformation, not previously described, in which pearlite nodules grow many times larger than the austenite grains.

Introduction

A KNOWLEDGE of the structure of pearlite is important for several obvious reasons; (a) the development of a sound theory of the formation of pearlite requires detailed information on the structural disposition of the component ferrite and cementite phases (1)[1]; (b) the rate of formation of pearlite, which at the knee of the S-curve determines the hardenability of plain carbon steels, can be understood only if the structural mode of growth of pearlite is known (1), (2); and (c) the correlation of the mechanical properties of pearlite formed isothermally with the temperature of formation can be understood only if full information on the structure of pearlite is at

[1]The figures appearing in parentheses refer to the bibliography appended to this paper.

This paper is part of a thesis submitted by Frederick C. Hull in partial fulfillment of the requirements of the degree of Doctor of Science at the Carnegie Institute of Technology, Pittsburgh, June, 1941. Other parts of this thesis will appear later.

A paper presented before the Twenty-third Annual Convention of the Society held in Philadelphia, October 20 to 24, 1941. Of the authors, Frederick C. Hull is Research Engineer, Westinghouse Electric and Manufacturing Co., East Pittsburgh, Pa., formerly Westinghouse Graduate Fellow in Metallurgical Engineering, Carnegie Institute of Technology, and Robert F. Mehl is Director, Metals Research Laboratory, and Head, Department of Metallurgical Engineering, Carnegie Institute of Technology, Pittsburgh. Manuscript received July 7, 1941.

hand (3). The term structure as used in this paper will be understood to refer not only to the distribution and orientation relationships of the ferrite and cementite in a single pearlite colony, but to the size and shape of colonies, the size and shape of pearlite nodules, and the sites of nucleation.

The voluminous literature on the subject of pearlite is exceedingly contradictory, especially with regard to the theory of formation of pearlite. Although the general outlines of an acceptable theory have begun to emerge from the investigations of the past, some aspects of the theory have been unnecessarily confused by recent writers.

The present paper has a three-fold purpose: (a) to subject past knowledge to a critical inspection, (b) to report the results of experiments that were designed to check the validity of old and new concepts, and (c) to rationalize well attested facts into a consistent theory of formation of pearlite. Attention will be called to a mode of transformation, not previously described, in which pearlite nodules grow many times larger than the austenite grains. Since all eutectoid structures appear to be lamellar and appear to form in the same manner as pearlite, the principles set forth here should find general application in the study of the genesis of lamellar eutectoid aggregates.

The Nature of Pearlite

The structure of the "pearly compound" in steel was first described by Sorby (4), in 1886, as a series of fine straight or curved parallel lines on the surface of polish caused by the presence of alternating thin plates of varying hardness. Sorby suggested that a stable compound of iron with a small amount of carbon exists at high temperatures and that at lower temperatures it decomposes into iron combined with more carbon and iron free from it. He also proposed that the direction of the alternating plates was determined by the previous crystalline structure, though he observed that in some cases the plates were less well marked and the structure was more granular.

The compound of iron and carbon in unhardened steel was identified as Fe_3C in 1885 by Abel (5) and Müller (6). This carbide of iron, which is one of the two constituents of pearlite, was named "cementite" by Howe, and the term was introduced in a paper by Howe and Sauveur (7) that appeared in 1896. The terms "ferrite,"

"pearlite," and "eutectoid" were also proposed by Professor Howe.

The constituent of hardened steel which was originally believed to be a compound of hardening carbon with iron was called "hardenite" by Howe (8), but "martensite," chosen in honor of Martens by Osmond (9) in 1895, has become the accepted term. In the same year, Osmond (10) discovered, in partially hardened steel, a dark etching constituent which he named "troostite" in honor of the eminent French chemist Troost. The term "austenite," named after Roberts-Austen, was used by Osmond (11) in 1896 to describe the high temperature phase in carbon steels and the microconstituent of high alloy nickel and manganese steels.

Theories of Formation of Pearlite

The first theory of formation of pearlite proposed that pearlite formed from martensite through the agglomeration of the carbides. Osmond introduced the concept that troostite was a transition form between martensite and pearlite.[2] After austenite had been established as the high temperature phase in steel, the theory was modified to include the allotropic transformation of austenite to martensite, and pearlite was held to result from the resolution of carbide through the intermediate stages troostite and sorbite. The theory in this form was supported by Arnold and McWilliam, Sauveur, Honda, and Lucas.

In 1905, Benedicks (12) pointed out that troostite was observed by Heyn (13) and Kourbatoff (14) to form preferentially in contact with ferrite or cementite. From these and his own experiments Benedicks concluded that ferrite and cementite act as "germs" for the resolution of martensite into ferrite and cementite. This statement appears to be the first that suggests that pearlite may be formed by a process of nucleation and growth. H. Le Chatelier, in the discussion of Benedick's paper, proposed for the first time that "pearlite developed itself at the direct expense of the nonmagnetic solid solution" [austenite]. The details of the mechanism of formation were not stated clearly, but it appears that Le Chatelier considered the cementite lamellae to form by agglomeration of ultra-

[2]When steels are quenched during $A_{r'}$ transformation at rates somewhat less than the critical, a border of fine pearlite will form about the coarse pearlite as the steel passes through the knee of the S-curve. The intervention of this layer of irresolvable pearlite (troostite) between the martensite and coarse pearlite led the early investigators to believe that troostite was a transition phase between martensite and pearlite.

microscopic particles of carbide, just as was supposed in the older theory.

Howe and Levy (15), in 1916, described the direct transformation of austenite to pearlite as taking place by a process of nucleation and growth. They predicted the fact that the rate of nucleation increases with the degree of undercooling, but did not mention a similar variation in the rate of growth. The theory that proposed the successive stages austenite, martensite, troostite, sorbite, pearlite, was questioned by Howe and Levy, who observed that lamellar pearlite cannot be produced from martensite, troostite, or sorbite by a tempering treatment. They state: "Thus while lamellar pearlite readily spheroidizes and so turns into granular pearlite, it cannot be derived from granular pearlite or any other transformed constituent, but only from the transformation of austenite."

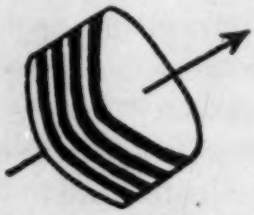

Fig. 1 — Sidewise Growth of Eutectics by Alternate Solidification of the Two Constituents as Depicted by Vogel in 1905.

During this period, the theory of the formation of lamellar eutectics was developed, and some of the concepts used in this connection apparently influenced thinking with respect to the genesis of pearlite. As early as 1905, Vogel (16) had proposed that the growth of a lamellar eutectic structure takes place by alternate precipitation of the two constituents, upon one another, in the form of parallel plates, as illustrated in Fig. 1. Portevin (17), in 1923, described the factors which operate to produce such sidewise growth in terms of the equilibrium diagram. "The crystallization of one of the constituents of the eutectic increases the degree of surfusion of the liquid in relation to the other, and in this way it may be stated that the crystallization of one constituent of the eutectic determines that of the other; this phenomenon being reciprocal, it is possible to conceive an alternate crystallization first of one and then of the other constituent." Portevin observed that in the tin-lead eutectic there was no inter-

penetration of constituents in different colonies. From this fact he concluded that a type of growth was possible in which alternate lamellae extend edgewise into the melt with their velocities of crystallization synchronized. Brady (18) also concluded that lamellar eutectics form by the simultaneous solidification of two metals separating side by side.

In 1922, Hallimond (19) described the edgewise growth of pearlite as taking place by the diffusion of carbon through austenite to the exposed surface of each carbide lamella. According to Hallimond if "two lamellae approach too closely, their growth will be arrested; if on the other hand, the lamellae are too far apart, the cementite in the intervening region must be deposited on a fresh nucleus. Thus for each condition of formation there will be a characteristic average spacing which gets closer as the rate of growth increases."

Belaiew (20) briefly outlined two theories of formation of pearlite in 1922. In one of these he assumed that crystallization starts with the precipitation of cementite, thus increasing the supersaturation of the remaining austenite with respect to ferrite. The mechanism of reciprocal supersaturation then leads to alternate precipitation of ferrite and carbide lamellae in a series of successive parallel plates. This appears to be the first reference to sidewise nucleation and growth of pearlite, while Hallimond was the first to describe the edgewise growth of pearlite.

Belaiew's second theory proposed that nuclei are formed on cooling, and from these a crystallographic rearrangement proceeds with a certain linear velocity. Simultaneously with that rearrangement, cementite lamellae are thrown out of solution and the formation of pearlite goes on apace. The interpretation to be placed upon these statements is not wholly certain. One viewpoint is that austenite transforms to supersaturated ferrite by a process of nucleation and growth. Precipitation of carbide follows very soon after the crystallographic rearrangement of γ to α. This mode of growth differs from that described by Hallimond, since it is assumed that carbon segregates in the α after γ has transformed, whereas Hallimond assumed that the diffusion of carbon to the cementite lamellae takes place through austenite from the advancing ferrite interface.

In 1935 and 1938 Belaiew (21) amplified his theories of the genesis of pearlite. He cites Whiteley, and Carpenter and Robertson

as showing that quenching of pearlite during formation never produces isolated lamellae, but that there are always grains (colonies) of pearlite surrounded by martensite. Belaiew concludes that "in order that the formation of pearlite operate in this fashion, grain by grain, it must be admitted that the transformation of the γ-lattice into the α-lattice is produced in an instantaneous manner in the whole volume which will become the α-grain (colony). By abruptly increasing the supersaturation with respect to carbon, such a transformation necessitates and produces the deposition of carbon in the whole

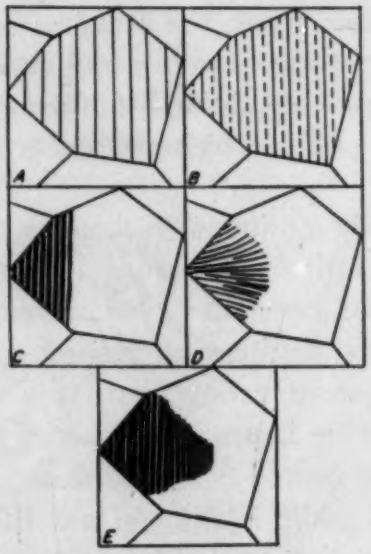

Fig. 2—Modes of Formation of Pearlite as Suggested by Carpenter and Robertson. E Shows Pearlite Produced by a Combination of Sidewise and Edgewise Growth.

grain." Belaiew visualizes the whole α-grain as forming in a fraction of a second (similar to formation of martensite plates); the precipitation of cementite from the supersaturated ferrite is assumed to take place with great linear crystallization velocity, as in proeutectoid deposits, and may lead to a Widmanstätten pattern of carbide plates if cementite is precipitated in α from several points at the same time. Belaiew considers lamellar troostite to form by radial growth, while pearlite forms by the pulsating process.

Carpenter and Robertson (22) reviewed the theories of formation of pearlite prevalent in 1932. The theory that austenite transforms to pearlite by proceeding through the intermediate stages martensite, troostite, and sorbite was excluded on the basis of the

microscopic evidence that, though precipitation and coalescence of globules do occur when quenched steels are tempered, the ultimate product of the coalescence is not pearlite. On the basis of experimental observations, Carpenter and Robertson concluded that most pearlite forms by a process of edgewise growth in which the plates of ferrite and carbide form simultaneously and advance together, edge first, into the austenite. This type of growth is illustrated in Fig. 2D. A certain amount of pearlite was believed to form as shown in Fig. 2E. This is the first recognition of the fact that the genesis of pearlite actually involves the co-operation of both sidewise and edgewise growth, with new lamellae of ferrite and cementite produced by a process of sidewise nucleation and growth, while the subsequent development of these plates proceeds by a process of edgewise growth. During radiating edgewise growth, as illustrated schematically in Fig. 2D, the pearlite spacing increases until new carbide plates appear by a process of sidewise nucleation in accordance with a tendency to maintain a spacing characteristic of the temperature of formation.

Ellis (23) has attempted to account for the lamellar nature of pearlite on the basis of an assumed carbon lattice interpenetrating the face-centered cubic gamma iron lattice. Owing to the questionable nature of the basic assumption, this theory has not been generally accepted.

Mehl (1) described the edgewise growth of pearlite as taking place by the diffusion of carbon through austenite from a high carbon concentration in advance of the ferrite lamellae to a low concentration at the cementite:austenite interfaces. It was demonstrated in a semi-quantitative fashion that the interlamellar spacing decreases sufficiently rapid with undercooling to overcompensate for the decrease in the rate of diffusion of carbon, thus causing the rate of growth of pearlite to increase as the reaction temperature is lowered. The concentration gradients governing diffusion are not only increased by the decrease in spacing, as proposed by Mehl, but also by a change in the interface concentrations with temperature, as pointed out by Hultgren in the discussion to Mehl's paper.

The most recent description of the formation of pearlite is that given by Jolivet (24). According to Jolivet a nodule of pearlite is made up of a number of "zones" (colonies) in which the alternate layers of ferrite and carbide are roughly parallel to a given direction. The formation of a zone is initiated by the crystallization of cement-

ite which involves the indirect formation of an adjacent ferrite lamella. The latter grows sidewise until another carbide lamella forms, and then the sequence is repeated. This process gives rise to a succession of elementary lamellae exhibiting definite crystallographic relationships among themselves and with the parent austenite. These lamellae are further developed edgewise by the simultaneous precipitation of ferrite and carbide.

From time to time attention has been given to the direct transformation of austenite to granular pearlite without passing through a lamellar state.[3] It is to be understood that spheroidite is a direct transformation product only of nonhomogeneous austenite, that is, austenite containing undissolved carbides or residual concentration gradients, while lamellar pearlite is the normal decomposition product of austenite.

The Pearlite Colony

The pearlite colony,[4] as originally defined by Belaiew (20), is a volume of pearlite in which the alternating ferrite lamellae are all of one orientation. Jolivet (24) considers that the cementite within a colony has a single orientation, and Belaiew draws the same conclusion from the alignment of cleavage fractures of cementite plates, lying nearly parallel to the surface, which have been broken during

Table I

Steel	Composition in Per Cent						
	Carbon	Silicon	Manganese	Phosphorus	Sulphur	Chromium	Nickel
A	0.78	0.18	0.63	0.014	0.030	....	....
B	0.80	0.24	0.74	0.019	0.029	0.01	0.11
C	0.79	0.21	0.62	.....	.....	....	....
D	0.78	0.23	0.63	.....	.....	....	....
E	1.02	0.13	0.19	0.013	0.010	0.03	0.03
F	1.01	0.16	0.15	0.011	0.011	0.05	0.03
G	1.02	0.31	0.26	0.014	0.012	0.06	0.02
H[1]	0.89	0.22	0.29	0.014	0.010	0.07	0.03
I	1.10	0.24	0.26	0.014	0.011	0.04	0.02
J	0.57	(0.1)	0.46	0.025	0.030	....	....
K	0.57	0.15	1.56	0.025	0.031	....	....
L[2]	0.93	0.002	<0.004	<0.005	0.0001	<0.0005	0.006

[1]Vanadium 0.22. [2]Slightly hypereutectoid.

polishing. Both Belaiew (20) and Rosenhain (25) state that pearlite colonies may be distinguished by a uniformity in the orientation of the etch pits in the ferrite, though neither submitted photomicrographs to substantiate the observation.

[3]The possibility of such a transformation was suggested by Howe and Levy in 1916. Reference 15.

[4]The terms grain, zone, and parcel have also been used in place of colony.

A technique has now been developed that yields satisfactory photomicrographic evidence on the point. If specimens of high purity eutectoid steel[5] are electrolytically polished and then etched with Vilella's martensite reagent, the ferrite of pearlite is attacked differentially in the several colonies. The etch pits in the ferrite between parallel carbide lamellae appear to have the same orientation, but are too small to be clearly resolved. The photomicrographs in Fig. 3 are typical of the results obtained. The lower Figures show a sub-boundary structure in the ferrite similar in appearance to alpha veining. Although the cementite plates in a given ferrite colony are usually approximately parallel, Jolivet (24) has pointed out that the cementite lamellae may assume two directions as illustrated in the photomicrograph on the right.

Theory of Formation of the Pearlite Colony

The most satisfactory theory of formation postulates that pearlite forms directly from austenite by a process of nucleation and growth, and that the genesis of pearlite requires both sidewise and edgewise growth. These points will now be considered in detail.

Nucleation of Pearlite

As pearlite is composed of two constituents—ferrite and cementite—the possible constituents which may serve to nucleate pearlite are (a) ferrite, (b) cementite, or (c) ferrite and cementite simultaneously. Direct experimental evidence was obtained by Mehl and D. W. Smith (26) that the orientation relationship between the ferrite of pearlite and the parent austenite is different from that found between proeutectoid ferrite and austenite, or between martensite and austenite (27). This finding has recently been confirmed by Mehl and G. V. Smith (28) for both coarse and fine pearlite. As Mehl (1) reasons in the "Physics of Hardenability," "if pearlite were nucleated by ferrite, it would be expected that the orientation of ferrite in pearlite with respect to the austenite from which it forms would be that which occurs when proeutectoid ferrite forms from austenite in hypoeutectoid steels, and in other Widmanstätten figures in which the types of co-operating lattices are the same, but the orientation of ferrite in pearlite is in fact an entirely different one and for this rea-

[5]Steel L. The compositions of all steels referred to in this paper are listed in Table I.

son it is a fair presumption that ferrite does not nucleate pearlite, and, since only ferrite and cementite are present in pearlite, that cementite does."

If cementite nucleates pearlite and if the first cementite plates

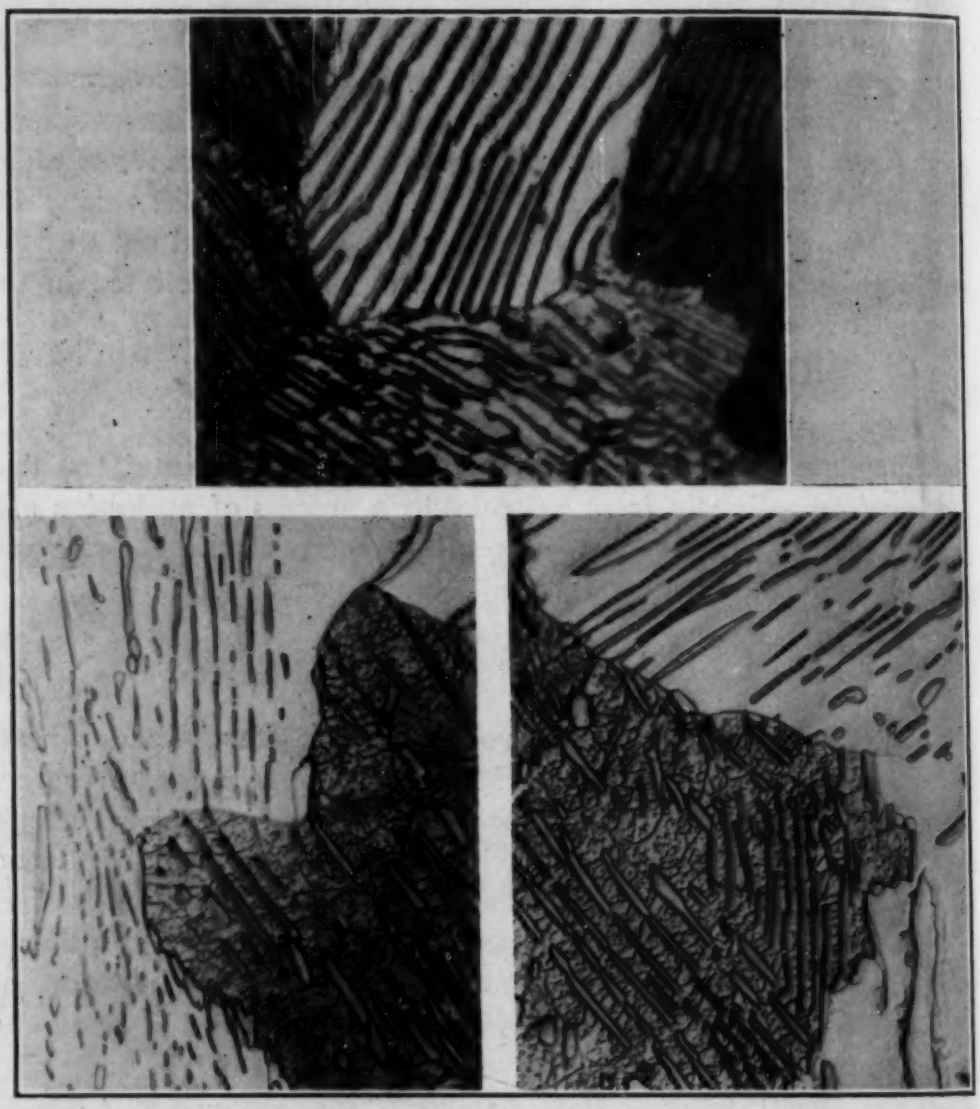

Fig. 3—Differential Etching of the Ferrite of Pearlite. High Purity Eutectoid Steel (Steel L) Electrolytically Polished and Etched with Vilella's Martensite Reagent. Upper—Austenitized ½ hour at 875 Degrees Cent. (Grain Size No. 1), and transformed at 716 Degrees Cent. × 2500. Lower Left and Right—Austenitized ½ Hour at 875 Degrees Cent. and Transformed at 722 Degrees Cent. × 1500. Note the Etch Pits and Sub-boundary Structure in the Ferrite in Lower Photomicrographs, and the Two Directions of Cementite Lamellae in a Single Colony in Lower Right Photomicrograph. (Reduced 50 Per Cent in Reproduction.)

are truly Widmanstätten, they should be parallel to $\{hkl\}_\gamma$ observed for proeutectoid cementite. Mehl, Barrett, and Smith (*27*) did not succeed in determining $\{hkl\}_\gamma$ for proeutectoid cementite, but it

appeared to be a 24-family plane. R. Colton (29) recently measured cementite trace directions in pearlite on a specimen for which the austenite orientation had been determined by G. V. Smith. Only straight plates were considered, and moreover, only those which were nearly perpendicular to the surface of polish. It was found that the

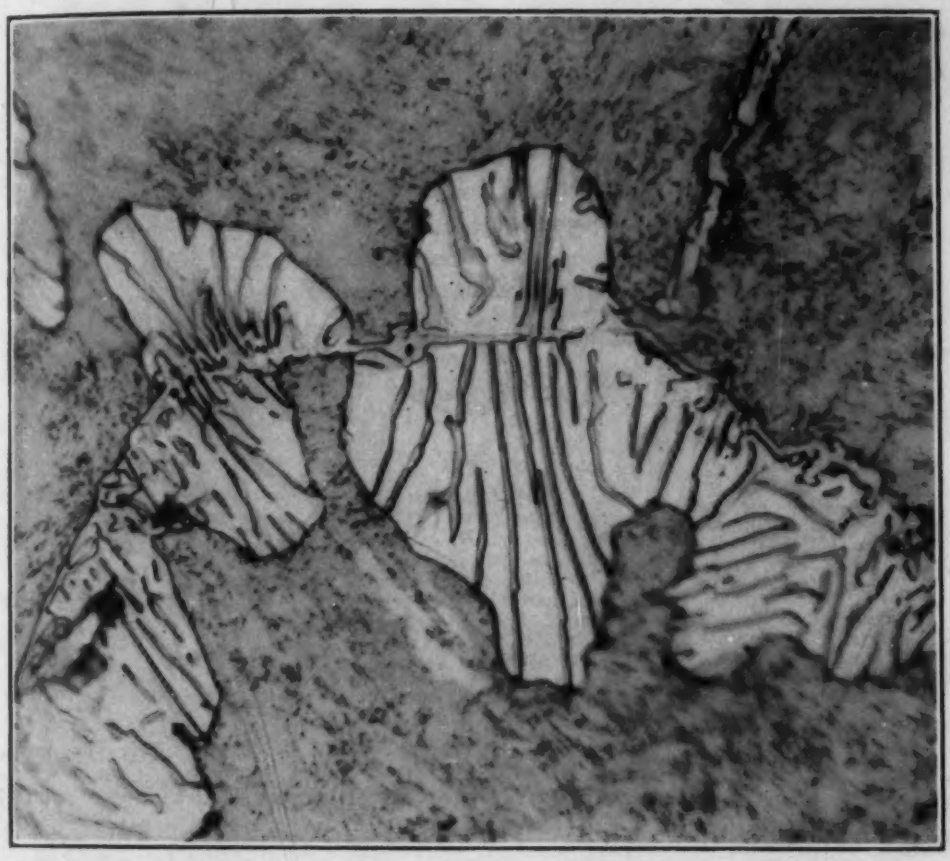

Fig. 4—Continuity of Proeutectoid Cementite With the Cementite of Pearlite. Partial Transformation of Steel I (1.1 Per Cent Carbon). Austenitized ½ Hour at 915 Degrees Cent.; Reacted 30 Minutes at 720 Degrees Cent. Electrolytically Polished; Etched With 4 Per Cent Picral. × 1500.

plates were necessarily parallel to some $\{hkl\}_\gamma$ of high index—a 24-family rather than a 12-family plane. This observation is in conformity with the observation on proeutectoid Fe_3C and thus constitutes further evidence that cementite nucleates pearlite.

Fig. 4 shows that proeutectoid cementite in a pearlite matrix may give rise to dendrite-like branches that appear to be continuous with the carbide lamellae of pearlite and may indeed be an integral part of the pearlite structure. The case is never observed, however, in which proeutectoid ferrite is continuous with the ferrite of

pearlite. It is interesting to note that in Fig. 15 (right) fine pearlite was nucleated at the coarse pearlite: austenite interface during the gradient quench, but that proeutectoid ferrite served to nucleate upper bainite. That ferrite nucleates bainite is further indicated by the orientation relationship between the ferrite of bainite and austenite which is identical to that obtaining for proeutectoid ferrite and austenite (28).

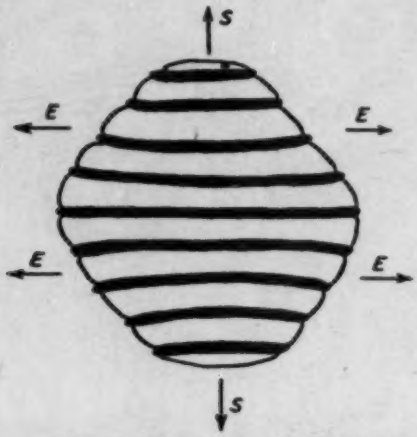

Fig. 5—Diagrammatic Representation of the Development of a Pearlite Colony by Simultaneous Sidewise and Edgewise Growth. New Lamellae of Ferrite and Cementite are Produced by Sidewise Nucleation and Growth (S) and Further Transformation Involves the Edgewise Extension (E) of These Elements.

The crystallographic relationships cited and the micrographic evidence presented both indicate that cementite is the active nucleus in the formation of pearlite.[6] The combination—ferrite and cementite—might operate as the nucleus of pearlite, but for lack of direct evidence in support of this possibility it seems better to assume the operation of the simpler and thus more probable mechanism.[7]

Sidewise Nucleation and Growth of Pearlite

It seems inescapable that pearlite colonies originate as a result of edgewise growth and of sidewise nucleation and growth. It has been clear for some time that edgewise growth is essential to explain the development of colonies and nodules as these structures are

[6]These orientation relationships are the most convincing evidence that the mechanism of formation of pearlite postulated by Belaiew (21) and the older sequence—austenite, martensite, pearlite—cannot be correct.

[7]In referenees 30, 31, 32 cementite has been assumed as the active nucleus in the formation of pearlite.

viewed under the microscope; and since colonies may readily be observed constituted of nearly parallel lamellae, a structure which could not arise from edgewise growth alone, sidewise nucleation and growth must also occur.

The crystallization of ferrite or cementite from supercooled austenite is controlled by the same factors that operate in determining the crystallization velocity of any substance precipitating from solution. At constant temperature the crystallization velocity of a given

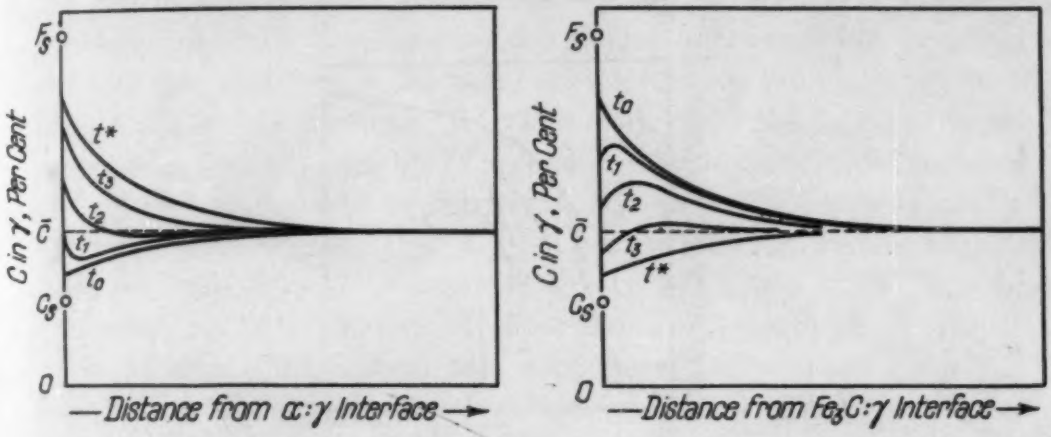

Fig. 6A Fig. 6B

Fig. 6—Variation of Carbon Concentration in Austenite During Sidewise Growth of Pearlite. The Compositions F_s and C_s Are Obtained by Extrapolating the Ferrite and Cementite Solubility Curves to the Reaction Temperature. The Figures Refer to the Concentration Changes Along the Lines Marked S in Fig. 5; Similar Curves Could Be Drawn for Different Portions of the Interface. Concentration Fluctuations During Sidewise Growth of Ferrite (Left Curves) and Cementite (Right Curves).

crystal face depends only upon the interface concentration; from the experiments of Marc (33) it appears that this velocity increases proportionally to the square of the supersaturation. The interface concentration does not remain constant, however, during the precipitation of substances from solution under ordinary conditions.

During sidewise nucleation and growth the crystallization of the outermost ferrite lamellae, as, for example, of the colony shown in Fig. 5, proceeds at a velocity controlled at the interface by the interface concentration. Starting with a rate of growth which is high because of the low carbon concentration established during the growth of the preceding cementite lamella, the velocity decreases as carbon is rejected into austenite; and, as the carbon concentration gradient becomes flatter, the interface concentration rises—throughout the whole period of sidewise growth of ferrite the interface concentration adjusts itself so that carbon is rejected into austenite by

the kinetic process at the interface which involves the transformation of γ to α, at the rate at which it may be carried away by the existing concentration gradients.

The concentrations in austenite as measured from the ferrite interface are shown in Fig. 6A starting with the time at which the ferrite was nucleated (t_o) and ending with the concentrations at the time of nucleation of the adjoining cementite lamella (t^*). Fig. 6B follows the concentration changes during the sidewise growth of a cementite lamella from the time at which it was nucleated in Fig. 6A.

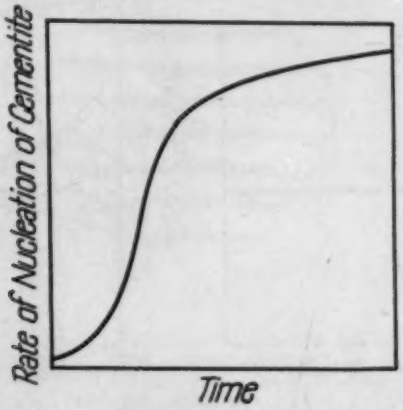

Fig. 7—Variation in the Rate of Nucleation of Cementite Per Unit Area of Ferrite: Austenite Interface Versus Time. The Rate of Nucleation Increases With the Degree of Supersaturation. See Fig. 6A.

The concentration at the cementite interface tends to approach C_s, as given by the Hultgren extrapolation of the A_{cm} line to the temperature of reaction, but never reaches it. The carbon concentration at the ferrite interface likewise never reaches F_s.

Hultgren assumed in his discussion to the "Physics of Hardenability" (1) that the austenite concentrations at the ferrite and cementite interfaces were "related to the metastable equilibrium conditions for austenite at the temperature of transformation." The extrapolation of solubility curves into metastable regions may be carried out with some confidence, judging from the work of Miers and Isaac (34); but during the growth of ferrite or cementite the interface concentrations cannot be those predicted by Hultgren, for even under conditions of metastable equilibrium there can be no net change in the amount of substance present, and hence no growth. Accordingly, the concentration extremes must be somewhat less than Hultgren assumed, though the variation in the concentrations with lowering temperature must occur and this in turn must be one of the factors

which determines an increasing rate of growth of pearlite as the temperature of formation is lowered, as Hultgren proposed.

The growth of either ferrite or cementite increases the supersaturation of austenite with respect to the other. During the sidewise nucleation and growth of pearlite, the concentration fluctuations are localized in a region near the interface; the austenite a distance of five to ten interlamellar spacings away is probably unaffected by the variations occurring at the interface.

The probability of nucleation of cementite at the ferrite: austenite interface must increase as the supersaturation becomes greater. The variation in the rate of nucleation of cementite per unit area of the ferrite: austenite interface with time, $N_{Fe_3C}(t)$, is represented schematically in Fig. 7.[7a] There is an initially rapid increase during the early growth of ferrite, but the rate then becomes nearly constant. The ferrite area, $A_{\alpha:\gamma}(t)$, available for nucleation also increases with time. Starting with a very small area at the time of nucleation, there is a period of rapid edgewise growth as the ferrite tends to cover the exposed side surface of the previous cementite lamella. A steep concentration gradient and a short diffusion distance make this possible. The thin ferrite sheet then grows more slowly, both edgewise and sidewise, and the whole course of the area versus time curve is very similar to the variation in $N_{Fe_3C}(t)$ with time.

Pearlite Spacing as Established by Sidewise Nucleation and Growth

The thickness of the ferrite lamella and hence the pearlite spacing established by sidewise nucleation and growth depends upon the length of time during which ferrite grows before cementite is nucleated. The probable nucleation time (t^*) is a measure of the pearlite spacing for a given reaction temperature, and may be defined as the time required for the probable number of nuclei to equal unity. The probable number of nuclei (P) formed in a given increment of time is given by

$$P = N_{Fe_3C}(t) \cdot A_{\alpha:\gamma}(t) \cdot \Delta t.$$

t^* is defined by the expression:

$$\int_0^{t^*} N_{Fe_3C}(t) \cdot A_{\alpha:\gamma}(t)\, dt = 1.$$

[7a] For a given degree of supersaturation the rate of nucleation of cementite at a ferrite interface is so much greater than in homogeneous austenite in advance of the interface that the possibility of the latter may be neglected.

The conditions governing the formation of a ferrite nucleus on a growing cementite plate are similar in principle to those outlined in the foregoing.

It has been experimentally observed by Pellissier (35) that the apparent pearlite spacings within a single colony show a distribution of spacings about some mean value as illustrated in Fig. 8. The

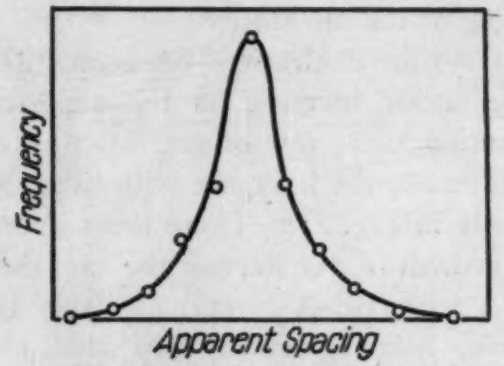

Fig. 8—Distribution of Apparent Spacings Within a Single Colony of Pearlite. Steel B Reacted at 694 Degrees Cent. Pellissier.

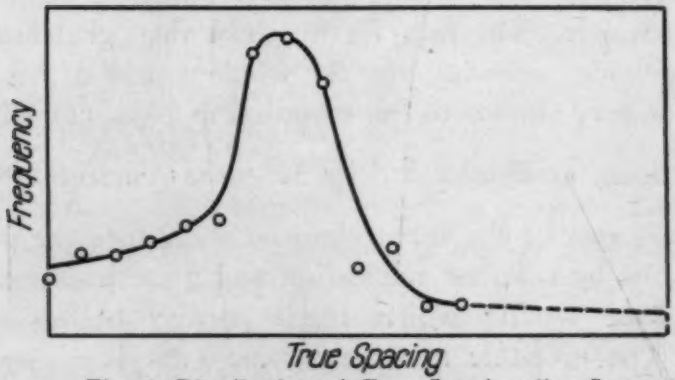

Fig. 9—Distribution of True Interlamellar Spacings in Steel B Reacted at 694 Degrees Cent. Pellissier.

explanation for the observed deviation of spacing from absolute constancy is readily found in this theory of the formation of pearlite. The value of t* for ferrite or cementite is an averaged value, a probability value. Nuclei will occasionally form sooner, sometimes later, and the result is a series of spacings statistically distributed about some average value characteristic of the reaction temperature.

The equations which define the conditions under which ferrite and cementite are nucleated contain a term representing the area

of the effective interface. The size and shape of a pearlite colony may thus have some influence upon the pearlite spacing established by sidewise nucleation and growth.

Pearlite Spacing Versus Temperature

An explanation for the decrease in pearlite spacing as the reaction temperature is lowered may be found from a consideration of the mechanism of formation of pearlite as outlined above, starting with the appearance of the original cementite nucleus[8]. Indeed, one

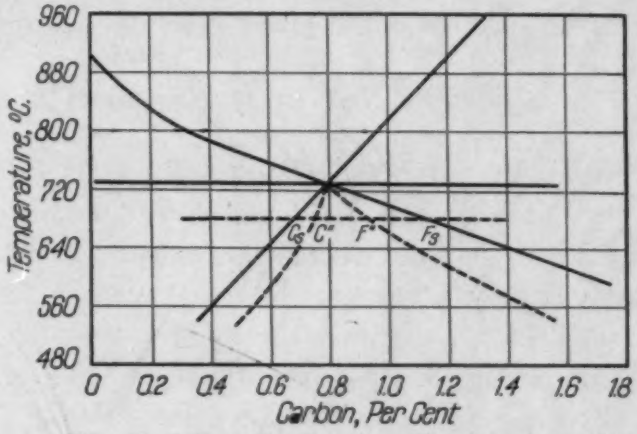

Fig. 10—Schematic Drawing Showing Austenite Interface Concentrations at Which Ferrite (C″) and Cementite (F″) are Nucleated, on the Average, During Sidewise Growth of Pearlite. C_s and F_s Are Compositions Obtained by the Hultgren Extrapolation.

of the most cogent reasons for adopting the point of view that in large measure pearlite nucleates sidewise lies in the readiness with which this will explain the decrease in interlamellar spacing with decreasing temperature. As the reaction temperature is lowered, the supersaturation of austenite with respect to carbide is increased, and a higher rate of spontaneous crystallization (nucleation) of cementite results.[8a] The growth of the original nucleus is a kinetic process whose rate is controlled by the interface concentration, as stated above. The interface composition decreases rapidly at first from $\overline{C}$ (the average composition of the austenite) and then more slowly to some point C″ between $\overline{C}$ and C_s as given by the Hultgren extrapola-

[8]This discussion constitutes an extension and correction of the idea proposed by Mehl in reference 1.

[8a]The effect of supersaturation in decreasing the size of the stable nucleus, and thus the work of nucleation, overbalances the effect of the lower temperature upon rate of diffusion. The application of classical nucleation theory to reactions in solid metals has been reviewed by Mehl (1) and Mehl and Jetter (36).

tion. See Fig. 10. The supersaturation of austenite with respect to ferrite is $(F_s - \overline{C})$ at zero time and increases to $(F_s - C'')$ by the time ferrite is nucleated. This supersaturation increases with decreasing temperature, and results in a markedly increased rate of nucleation of ferrite at the cementite interface. The rate of nucleation of ferrite increases more rapidly with supersaturation than does the crystallization velocity of cementite so that ferrite is nucleated before cementite has grown to the same thickness it attained at a higher temperature.[9] The nucleation of cementite on the ferrite layer that results is likewise accelerated with a resultant decrease in pearlite spacing at the lower reaction temperature.[10]

Edgewise Growth of Pearlite

The cementite and ferrite lamellae produced by sidewise nucleation and growth are further developed by edgewise growth. Although the volume of pearlite actually produced by sidewise nucleation and growth is only a fraction of that resulting from edgewise growth, this fact does not diminish the importance of the concept of sidewise nucleation. Fig. 5 is a schematic representation of an early stage in the development of a pearlite colony nucleated in the interior of an austenite grain. When pearlite is nucleated at a grain boundary, as is usually the case, a variety of colony shapes is possible.

Curvature of Pearlite Lamellae

If cementite lamellae in pearlite were precipitated in completely developed form from austenite, they would be expected to form a Widmanstätten pattern of precise geometry, as in the precipitation of proeutectoid cementite (*27*). Belaiew's contention that the plates are initially straight but are curved after formation by transformation stresses is not wholly satisfactory (*20*). It appears more likely that the nuclei of cementite are accurately formed plates and that the curvature observed in pearlite occurs during the growth process.[11]

---

[9]Rates of nucleation appear in general to increase more rapidly with undercooling than rates of growth, as is evidenced by the grain refinement resulting from chill casting. The rates of nucleation and growth of pearlite have been found to vary in this fashion. Data supporting this statement will be published in the near future. (cf. ref. 1.)

[10]If the maximum in the curve of the rate of nucleation versus undercooling were passed at a temperature higher than that of the maximum in the growth curve for either ferrite or cementite, it would be possible for the pearlite spacing to begin increasing with further undercooling. No experimental evidence is now available supporting this inference.

[11]The orientation of the lattice of single lamellae is a constant, even though the external surfaces are curved. This is not unusual in solid-solid transformations (*37*).

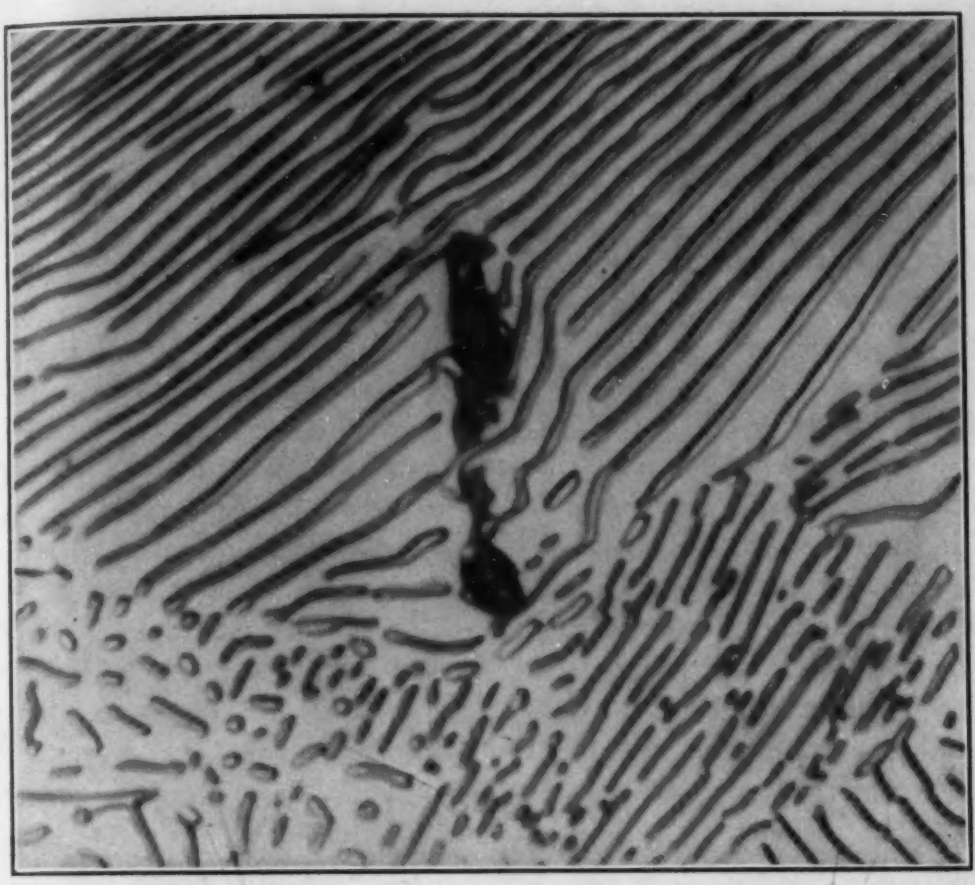

Fig. 11—Curvature of Cementite Lamellae in the Vicinity of an Inclusion. Eutectoid Steel Reacted at 715 Degrees Cent. Electrolytically Polished; Etched With 4 Per Cent Picral. × 2500.

A number of possibilities exist for the explanation of the curvature of the lamellae, any one of which appears adequate. It may be that the transformation stresses arising from the volume change accompanying the formation of pearlite from austenite cause displacement of the pearlite: austenite interface with respect to concentration gradients that had been established at the previous moment of growth, and thus induce curvature. Furthermore, the concentration gradients around the growing colony, shown in Fig. 5, may cause the lamellae to curve in an effort to maintain the lamellae edges perpendicular to the growing interface. The curvature of cementite plates around an inclusion as seen in Fig. 11 appears to be caused by a disruption of carbon concentration gradients in austenite, suggesting that a nonuniform carbon distribution might likewise serve to produce waviness.

Edgewise Growth of Pearlite and Pearlite Spacing

As the plates curve during growth, as described above, the spacing increases, and new cementite plates are nucleated at the centers of ferrite lamellae. (See Fig. 16A for example). This nucleation of cementite results from the fact that as the spacing increases and rate of growth decreases, the supersaturation of austenite with respect to cementite at the ferrite interface increases.

As the concentration gradients and geometry of the interface are different for sidewise and edgewise growth, there is no reason for expecting the spacing established by sidewise growth to be maintained exactly, even though the same basic factors operate to determine the spacing in both cases. The experimental work of Pellissier (35) has established the fact that the distribution of true spacings in a steel is not wide, as may be seen in Fig. 9; it follows, therefore, that the difference between the average spacings for sidewise and edgewise growth, respectively, cannot be large. Once the plates are perpendicular to the pearlite:austenite interface, there should be little tendency for the mean spacing to change during subsequent edgewise growth.

Concentration Gradients in Austenite During Edgewise Growth

The important features of the edgewise growth of pearlite have been described by Hallimond (19), Hultgren (38), (1), Carpenter and Robertson (22) and Mehl (1). As first pointed out by Hallimond, it appears that the rate of edgewise growth is controlled by two factors: "the diffusion of material into the approximately saturated layer in contact with the growing face, and also a definite heterogeneous reaction-velocity [at the interface] conditioning the deposition of material."

During the edgewise growth of pearlite, if the lamellae maintain their spacing and are perpendicular to the interface, the carbon concentrations in austenite as measured from the interface become nearly independent of time, provided there is no lateral displacement of the colony with respect to austenite by reason of the volume change accompanying transformation. The probable concentrations obtained are indicated schematically in a photograph of a three-dimensional model (Fig. 12). Carbon diffuses through austenite from a high concentration at the ferrite interface to a low concen-

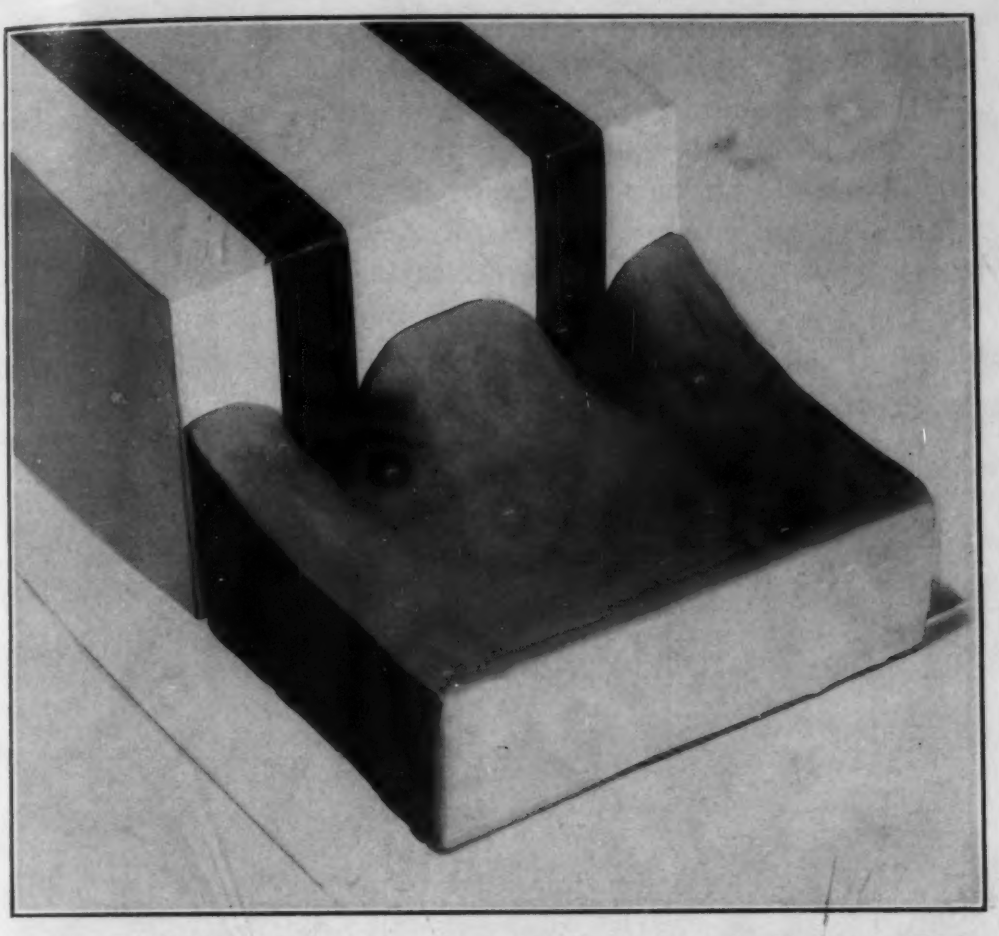

Fig. 12—Model Depicting Carbon Concentrations in Austenite During the Edgewise Growth of Pearlite. Carbon Diffuses in Austenite From a High Concentration at the Ferrite:Austenite Interface (White) to a Low Concentration at the Cementite:Austenite Interface (Black).

tration at the cementite interface. A short distance in advance of the interface the carbon concentration in austenite is not affected by the approaching pearlite.

A mathematical solution of the differential equation for two-dimensional diffusion that would fulfill the boundary conditions for the edgewise growth of pearlite would be highly desirable. A quantitative relationship between the rate of growth, pearlite spacing, rate of diffusion of carbon, and interface concentrations could thus be established, and the austenite carbon concentration gradients could be calculated. Basic information is lacking on two, and perhaps on three points. (a) The average ferrite and cementite interface concentrations are not known; (b) the concentration probably varies across each interface in an undeterminable manner; and (c) the shape of the interface is the object of further uncertainty.

Determination of Interface Concentrations During Edgewise Growth

The mechanism by which the average interface concentrations are established during edgewise growth may be explained with the aid of Fig. 13 in which are plotted the crystallization velocities of ferrite and cementite as functions of the austenite interface concentration for a given reaction temperature. The conditions for edgewise growth are that the composition of the residual austenite remains unchanged, the pearlite spacing remains constant, and ferrite

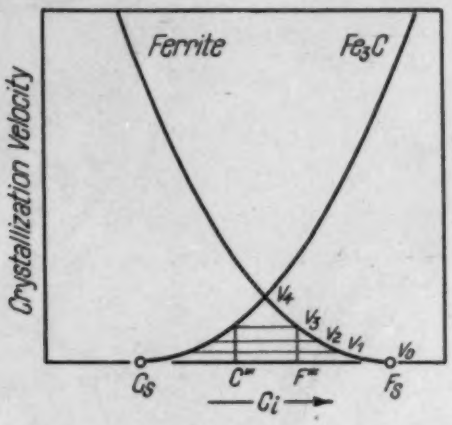

Fig. 13—Crystallization Velocities of Ferrite and Cementite as Functions of the Austenite Interface Concentration. If the Metastable Equilibrium Concentrations, C_s and F_s, Prevailed at the Interfaces, the Growth Velocity Would be Zero.

and cementite grow with equal velocities. The requirement that ferrite and cementite grow at the same rate does not fix both interface concentrations; but, if one of them is selected, the other is determined as shown by the horizontal lines labeled v_1, v_2, and v_3 in Fig. 13.

The crystallization velocity of pearlite cannot be equal to or greater than v_4, because carbon would be required to diffuse from the ferrite to the cementite interface *against* the concentration gradient. It may be stated with equal certainty that the metastable equilibrium concentrations C_s and F_s are likewise impossible; for, if ferrite cannot grow, there is no supply of carbon to satisfy the demands of the concentration difference (F_s — C_s). However, for some intermediate crystallization velocity, for example v_3, the interface concentrations are F''' and C''', and the condition is satisfied that carbon is transferred by the kinetic process at the interfaces at exactly

the rate at which it may diffuse to or away from the interfaces under the existing concentration gradients. The interface concentrations

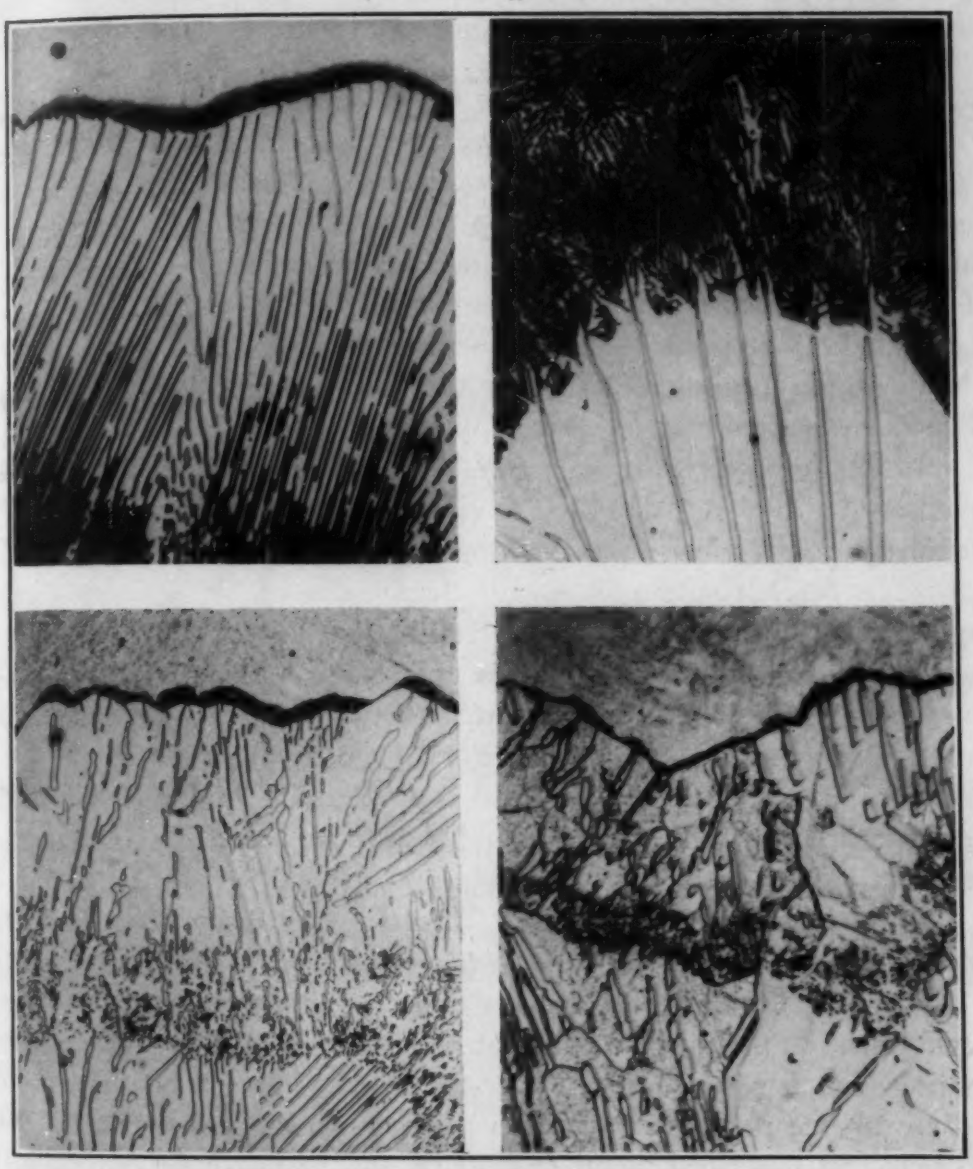

Fig. 14—Mixed Temperatures of Isothermal Transformation. Upper Left—Steel B Austenitized ½ Hour at 875 Degrees Cent. Fine Pearlite Formed at 680 Degrees Cent., Coarse Pearlite During 93 Minutes at 710 Degrees Cent. × 2500. Upper Right—Steel L Austenitized ½ Hour at 875 Degrees Cent.; Reacted 35 Minutes at 720 Degrees Cent. and 5 Seconds at 690 Degrees Cent. × 2500. Lower Right and Left—Steel L Austenitized ½ Hour at 875 Degrees Cent.; Reacted 35 Minutes at 720 Degrees Cent., 2 seconds at 690 Degrees Cent., and 10 Minutes at 720 Degrees Cent. × 1000. All Specimens Electrolytically Polished. Top Two and Lower Left—Etched in 4 Per Cent Picral. Lower Right—Etched with Vilella's Martensite Reagent. (Reduced 50 Per Cent in Reproduction.)

which will enable growth to proceed at a constant velocity are determined by a process of natural selection. As the transformation

temperature is lowered, C''' and F''', as well as C_s and F_s, are spread farther apart, furnishing one reason for the increase in the rate of growth of pearlite at lower temperatures.

Mixed Temperatures of Transformation

Isothermal transformations were carried out at mixed high and low temperatures in order to determine the effect of a given interlamellar spacing upon the structural characteristics of pearlite formed at a different temperature. An annealed commercial eutectoid steel (Steel B) was austenitized ½ hour at 875 degrees Cent. (1605 degrees Fahr.) and partially transformed at 680 degrees Cent. (1255 degrees Fahr.); the specimen was then transferred to a lead bath at 710 degrees Cent. (1310 degrees Fahr.) and reaction continued 93 minutes before quenching in water. Transformation at the high temperature proceeded around the finer pearlite formed during the low-temperature reaction (Fig. 14, upper left).

The pearlite spacing does not change abruptly at a point corresponding to the location of the interface at the time the temperature was changed, for the boundary is not sharp. On the contrary, the minimum spacing is occasionally maintained for a considerable time, and the spacing characteristic of the high temperature is established only gradually.[12] It is to be noted that cementite plates of the high temperature pearlite are parallel and pseudomorphic with the cementite of the finer pearlite.

A high purity eutectoid steel (Steel L) was austenitized ½ hour at 875 degrees Cent. (1605 degrees Fahr.) and partially reacted at 720 degrees Cent. (1330 degrees Fahr.); the specimen was then transferred to another lead bath at 690 degrees Cent. (1275 degrees Fahr.) for 5 seconds and water-quenched. The transition from coarse to fine pearlite is very sharp. Following a treatment similar to that just described, another sojourn at 720 degrees Cent. (1330 degrees Fahr.) for 10 minutes was added. During this time the fine pearlite was practically completely spheroidized as may be seen in Fig. 14 (lower pictures). The high purity steel was etched with picral (Fig. 14, lower left) and Vilella's martensite reagent (Fig. 14, lower right). The structure shows that the ferrite orientation

---

[12]Because of the tendency for pearlite spacing to be maintained, the rate of growth of pearlite at a temperature T_1 during heating or cooling, respectively, must be greater than or less than the rate of growth of pearlite formed isothermally at T_1. There is, therefore, some effect of heredity, contrary to what Jolivet (24) has assumed.

remained constant throughout the whole temperature cycle. This evidence, in conjunction with the continuity of the cementite lamellae, indicates that temperature fluctuations need not interrupt the growth of a given colony of pearlite, though the pearlite spacing may vary

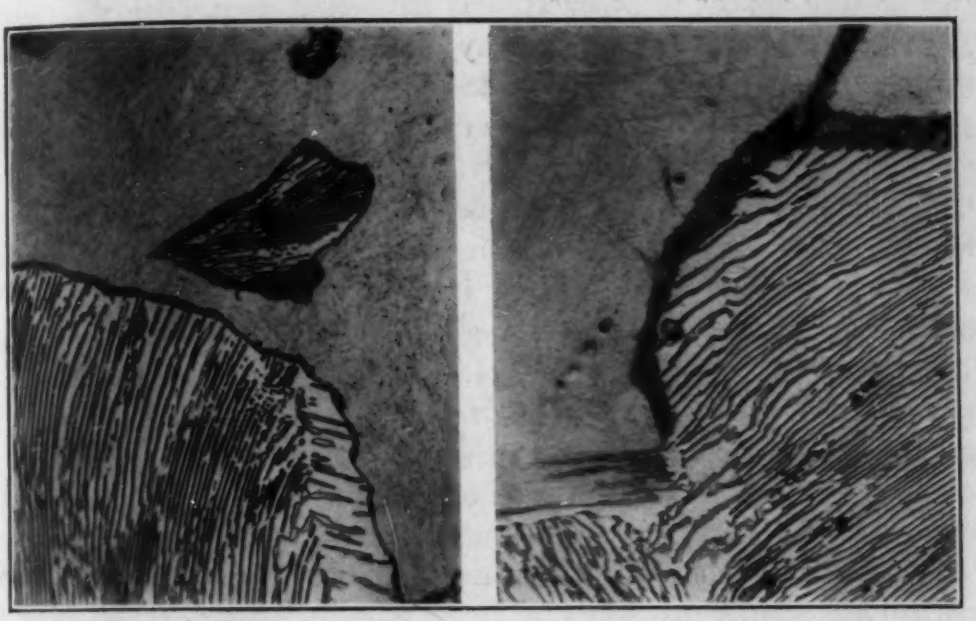

Fig. 15—Pearlite Colonies Crossing Austenite Grain Boundaries. Left—Steel L Austenitized ½ Hour at 875 Degrees Cent. and Partially Transformed at 716 Degrees Cent. × 1000. Right—Steel A Austenitized 10 Minutes at 1200 Degrees Cent., Partially Transformed at 700 Degrees Cent. and Gradient Quenched. × 1500. Picral Etched. (Reduced 50 Per Cent in Reproduction.)

according to the imposed conditions. The uniform width of the bands of fine and coarse pearlite in Fig. 14 (lower left) is evidence for the point of view that pearlite advances into austenite at a constant rate, and that whole colonies do not suddenly appear by a "pulsating process" as described by Belaiew (1).

Growth of Pearlite Across Grain Boundaries

Jolivet (24) has stated that "the case is never met with where any one zone of parallel lamellae is not entirely localized in a single grain of austenite and is not arrested in its growth by the boundaries of this grain." This statement is in accord with what one would expect on theoretical grounds; it is assumed with much justification that the orientation of the cementite of pearlite is directly related to the orientation of the austenite from which it is derived, and that ferrite takes its orientation from the cementite (26), (28). When a pearlite colony reaches a grain boundary, one would pre-

dict that since the orientation relationships with the austenite grain established in this colony are no longer satisfied in the new austenite grain, the growth of the original colony must cease.

This behavior seems to be customary, but a number of structures which appear to be exceptions have been seen. Fig. 15 (left) is a photomicrograph of high purity eutectoid Steel L reacted 35 minutes at 716 degrees Cent. (1320 degrees Fahr.). Running across the print about 5/8 of an inch from the right edge may be seen the trace of a former austenite grain boundary. The same spot on the specimen was found after etching with Vilella's martensite reagent, and the location of the boundary in the martensite passing through the two colonies was confirmed. Another instance of the same phenomenon is seen in Fig. 15 (right). A commercial steel (Steel A) was heated 10 minutes at 1200 degrees Cent. (2190 degrees Fahr.), partially transformed at 700 degrees Cent. (1290 degrees Fahr.), and then gradient quenched. The latter outlined the grain boundary at the top of the print, and the extrapolation of this line meets the small amount of free ferrite that appeared at the grain boundary at the lower left. The majority of the cementite plates are continuous across the place where the former boundary appears to have been located, though they all show a slight distortion and change of spacing.[13] It may be that the orientations of the adjoining austenite grains were nearly enough alike to allow the colony to trespass the boundary, though the explanation is probably not as simple as this in view of the fact that twins in austenite have no visible effect on the structure of pearlite. The latter statement is based on the fact that during a period of several years, in which hundreds of samples of pearlite were subjected to careful examination, no structure was observed showing changes in lamellar directions at an interface and reversal of this change to the original direction such as might arise in growth across twins, and as is observed in the trespassing of slip lines across twins. The ineffectiveness of twins might lie in the weakness of the Widmanstätten tendency and the preponderant influence of established carbon concentration gradients which would not vary with orientation.

Mechanism of Formation of Pearlite Versus Temperature

The statement is usually made that as the reaction temperature

[13]The evidence in Fig. 15 is not wholly unmistakable, for it relies upon the assumption of the continuity of the austenite grain boundary in the extrapolated direction.

is lowered, the pearlite tends to grow radially to a greater extent.[14] Radiating edgewise growth is often considered as characteristic of the mechanism of formation of troostite (fine pearlite) only, but Fig. 16A shows that it may occur equally well in steel J at high tem-

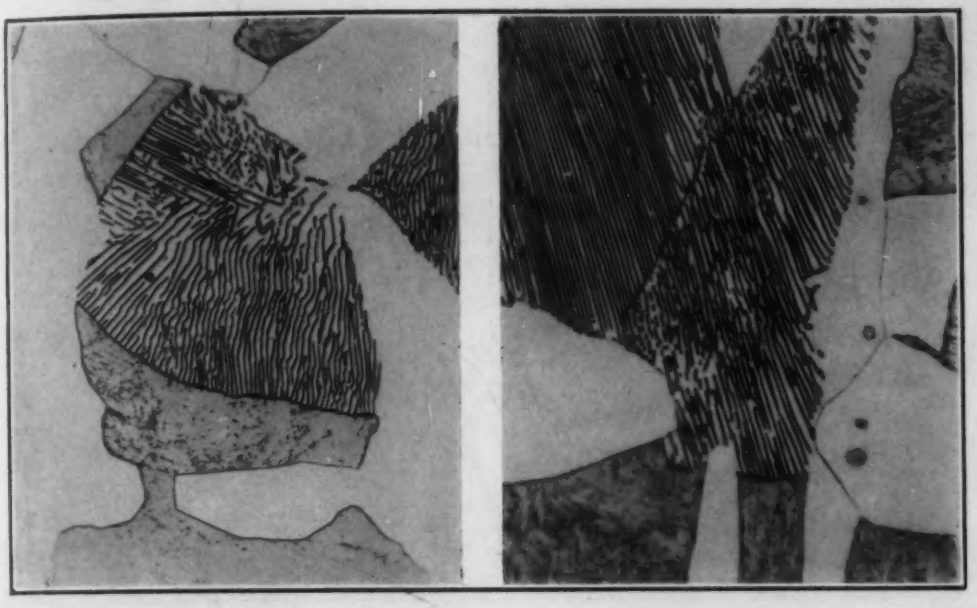

Fig. 16A Fig. 16B

Fig. 16—Steel J Austenitized ½ Hour at 915 Degrees Cent. and Partially Transformed at 703 Degrees Cent. Electrolytic Polish, Picral Etch. × 1500. (Reduced 50 Per Cent in Reproduction.)

peratures (703 degrees Cent.). Another photomicrograph of the same sample of 0.57 per cent carbon steels shows, on the other hand, a colony made up entirely of parallel plates (Fig. 16B).

It has sometimes been claimed that the lamellae of fine pearlite are curved more than those of coarse pearlite. The evidence on which this statement is based may be more apparent than real. The cementite lamellae of pearlite are not all perfectly plane, as may be seen in sections normal to the plates which show their true spacing. In more oblique sections, these same lamellae are spaced farther apart and appear to be markedly curved, for the obliquity of the cutting exaggerates the curvature. In a fine pearlite, however, only those areas are resolved in which the apparent spacing is great, and since it is these areas that show exaggerated curvature, the false impression may be obtained that all fine pearlite is curved while all but a fraction of coarse pearlite is straight. There is nothing in the present theory of formation of pearlite that calls for a change in the mech-

[14]See for example Carpenter and Robertson, Reference 21, and Jolivet, Reference 23.

anism of formation of the pearlite colony with temperature, though the spacing and colony size do decrease with undercooling, so that the outlines of pearlite nodules at a given magnification appear more regular at low than at high transformation temperatures.

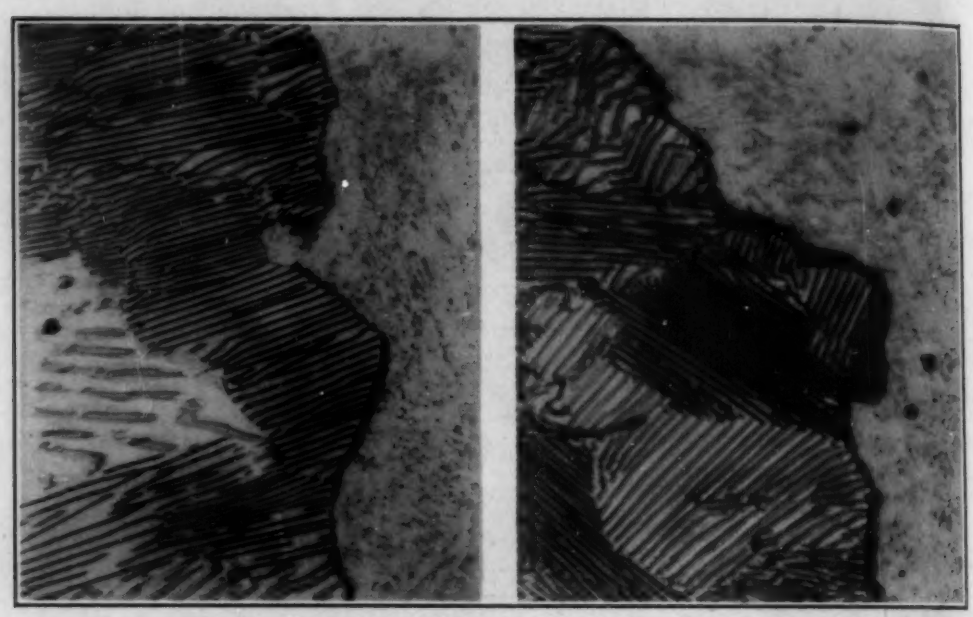

Fig. 17A Fig. 17B

Fig. 17—Growth of a Pearlite Nodule in Steel A. Austenitized 10 Minutes at 1200 Degrees Cent.; Transformed 45 minutes at 700 Degrees Cent. × 2500. (Reduced 50 Per Cent in Reproduction.)

The Pearlite Nodule

Pearlite colonies are the units of which larger pearlite masses originating from a single nucleus—nodules—are composed; the growth of a pearlite nodule is made up of the sum of the growths of these individual colonies. The growth of colonies is terminated by impingement with other nodules or by the appearance of new colonies for any of several reasons. (a) A new colony may be nucleated by cementite at the ferrite: austenite interface, during either sidewise or edgewise growth, providing the cementite precipitates upon a different plane of the family $\{hkl\}_\gamma$. (b) If cementite is nucleated because of strains, or inclusions, or concentration gradients at a distance from the growing interface, a new colony results unless the same plane of the family is used. (c) Colonies do not ordinarily cross grain boundaries, so that growth of a given colony ceases at the boundary, even though transformation stresses frequently initiate nucleation of a new colony in the next grain. Figs.

17A and B illustrate the appearance of pearlite colonies at the pearlite: austenite interface of a large nodule in Steel A which was austenitized 10 minutes at 1200 degrees Cent. (2190 degrees Fahr.) and transformed 45 minutes at 700 degrees Cent. (1290 degrees Fahr.).

Pearlite Nodules Formed at Temperatures Near the Knee of the S-Curve

Nodular troostite is the term that was originally applied to the rounded areas of dark-etching and not wholly resolved material that appears in partially hardened steel. These nodules, which are generally accepted to be fine pearlite, serve to outline the former grain boundaries of austenite. This phenomenon may be attributed to the fact that the rate of nucleation of pearlite at a grain boundary is much higher than the rate within the grains.

Pearlite nucleated at a grain boundary may grow into only one grain in the form of a hemisphere, though frequently a colony in the adjoining grain is nucleated, presumably because of the stresses, thus producing a spherical nodule. This volume of pearlite might more precisely be referred to as a "bi-grained nodule," since the pearlite is derived from two austenite grains. Similarly, if the original nucleus appears at a grain edge or corner, a nodule may result which involves several grains, as Jolivet (24) has pointed out.

During transformation of pearlite at the knee of the S-curve a great many nodules are formed at the grain boundaries which are completely outlined early in the reaction. Subsequent transformation results from the inward growth of these nodules until impingement occurs at the center of the grains. Johnson and Mehl (39) have calculated master reaction curves for various combinations of the physical quantities which determine the rate of transformation —the rate of nucleation, N; the rate of growth, G; and the radius of the grains, a.

Even though the rate of nucleation within austenite grains is much less than at the grain boundaries, there is nothing that prevents nuclei from forming randomly; and, indeed, occasionally nodules are nucleated within the grains. Profuse general nucleation may occur in aluminum-killed steels, whose grain sizes have been coarsened by prolonged heating at elevated temperatures; the partially hardened zone of a quenched bar exhibits a structure in which the grain boundaries are clearly outlined and numerous spherical nod-

ules are found within the grains (40). The increase in the rate of general nucleation is attributed to the effect of randomly distributed

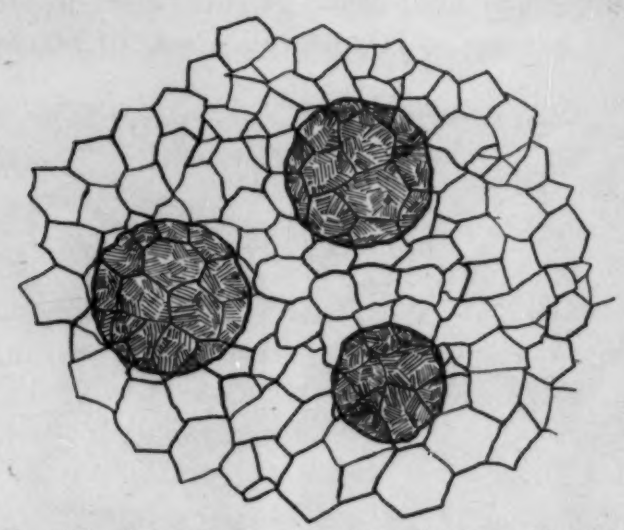

Fig. 18A—Schematic Drawing of Pearlite Group Nodules.

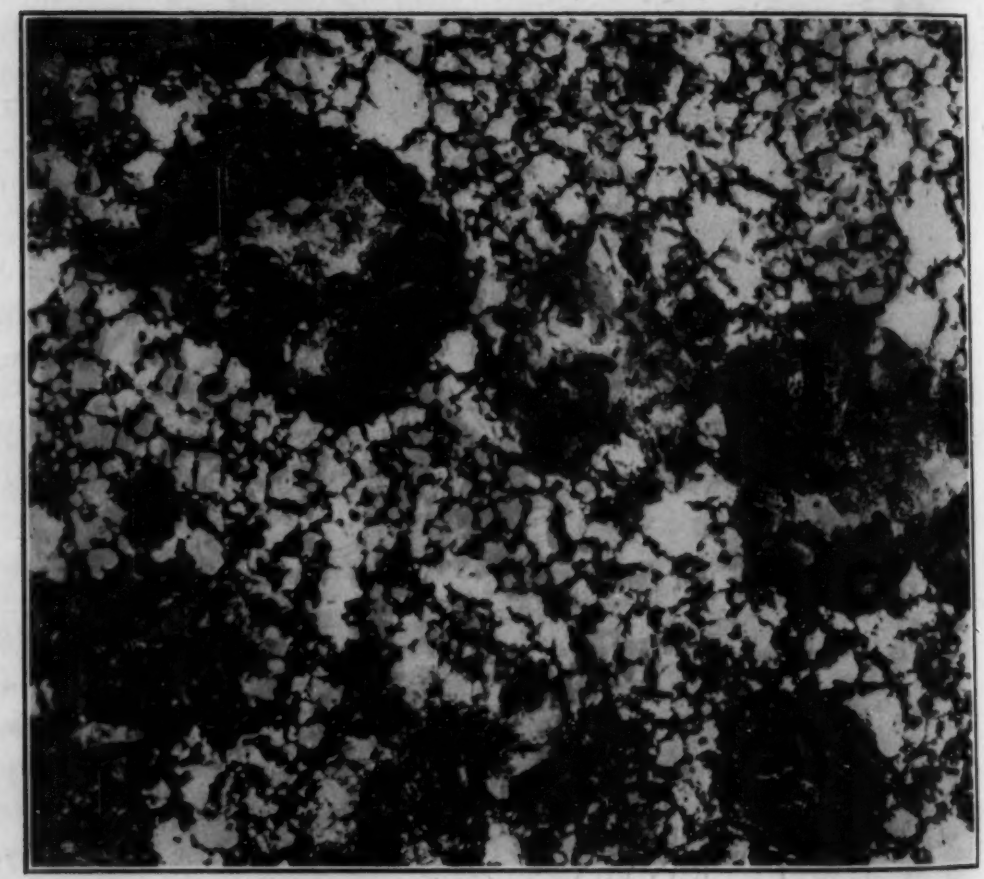

Fig. 18B—Group Nodules in Steel A Whose Grain Size is Revealed by a Gradient Quench. Austenitized ½ Hour at 875 Degrees Cent.; Transformed 5½ Minutes at 690 Degrees Cent. × 100.

alumina inclusions, though undissolved carbides and undissipated concentration gradients may operate in a similar manner.

Formation of Pearlite Nodules Near Ae_1

As the transformation temperature is raised, the rate of nucleation and the rate of growth both decrease, but the decrease in N is greater than that of G with the result that the number of nodules per unit volume of completely reacted samples is less and, hence, also the number of nodules per austenite grain. In fact, as we shall now show, N may become so small that the pearlite nodules grow many times larger than the austenite grains before impingement renders further growth impossible.

Fig. 18A is a diagrammatic representation of partial transformation in a eutectoid steel reacted near Ae_1. The pearlite nodules, derived from single original nuclei, grow larger than the austenite grains. For clarity, volumes of pearlite which form entirely within one grain, either as spheres or hemispheres, might be referred to as uni-grained nodules while those that encompass more than one grain might be called multi-grained nodules or austenite grain group nodules. The latter name has been tentatively adopted, though it has been shortened for convenience to simply "group nodule."[15]

The fact that group nodules do grow larger than the austenite grains is convincingly demonstrated by the following experiment: A sample of eutectoid steel (Steel A) was heated ½ hour at 875 degrees Cent. (1605 degrees Fahr.) and oil-quenched, then austenitized ½ hour at 875 degrees Cent. and quenched into a lead bath at 690 degrees Cent. (1275 degrees Fahr.). After 5½ minutes at 690 degrees Cent. (1275 degrees Fahr.) the specimen was gradient quenched. Along one portion of the bar, the rate of cooling had been just lower than the critical quenching velocity and the austenite grain size was revealed by the deposition of fine pearlite along the grain boundaries. As illustrated in Fig. 18B, the group nodules have diameters about eight times as large as the austenite grains.

The nodules in steel A, as well as those in all the other steels examined, were approximately spherical in both longitudinal and cross sections; the possibility is thus eliminated that segregation is

[15] A bi-grained nodule is distinguished from a group nodule by the fact that, though it may be growing into two grains, it does not completely contain at least one austenite grain.

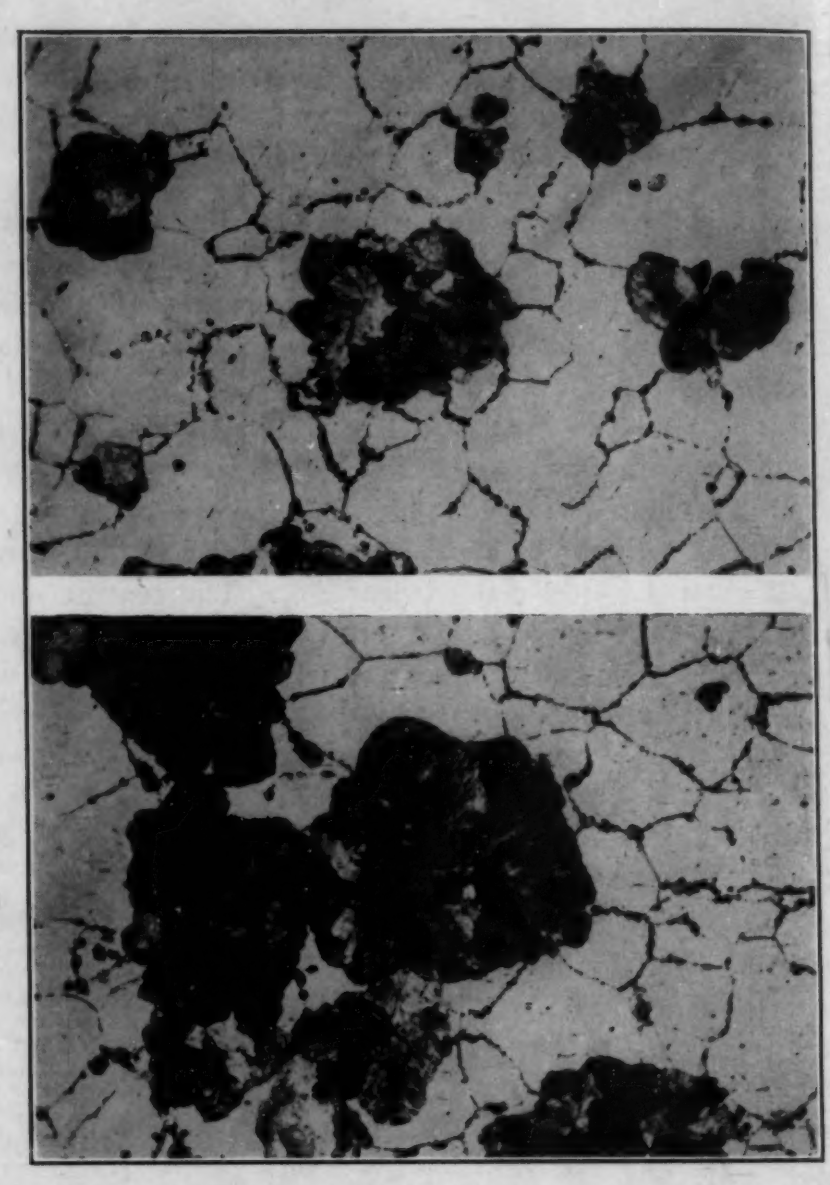

Fig. 19—Grain Boundary Nucleation of Group Nodules in Steel A. Austenitized 10 Minutes at 1200 Degrees Cent.; Transformed 8 Minutes at 690 Degrees Cent. and Gradient Quenched. × 100. Longitudinal Section of Bar. (Reduced 50 Per Cent in Reproduction.)

in any way responsible for the occurrence of group nodules, nor could any other heterogeneity cause them, for they occur in steel A, for example, after an austenitizing treatment at 1200 degrees Cent. (Fig. 19).

It is known that pearlite is nucleated preferentially at austenite grain boundaries at reaction temperatures around the knee of the S-curve. At temperatures near Ae_1, where the rate of nucleation is much lower, it seems logical to assume that the same or even a

greater percentage of nuclei should appear at grain boundaries—sites for which the energy requirements for nucleation are least. Some indication that this is the case is given by the photomicrographs of steel A presented in Figs. 19A and B. Specimens were pretreated as described above, austenitized 10 minutes at 1200 degrees Cent. (2190 degrees Fahr.), reacted 8 minutes at 690 degrees Cent. (1275 degrees Fahr.), and gradient quenched. As far as may be judged, even at the relatively high reaction temperature of 690 degrees Cent., the nodules originated at grain boundaries.

Growth of Group Nodules

The growth of a group nodule proceeds in the same manner as the growth of uni-grained nodules or bi-grained nodules, except for the complication introduced by the crossing of grain boundaries. A grain boundary may serve as a site of easy nucleation for colonies slightly in advance of the approaching interface, it may act as an obstacle to continued growth, or the strains accompanying the volume change of the austenite to pearlite transformation may promote nucleation of a new colony in the next grain at the instant the grain boundary is reached. In the first case, the radial rate of increase of the nodule is greater than the rate of growth of pearlite[16] within a single austenite grain. In the second instance the growth is retarded, and in the last it is unaffected. The growth of group nodules appears to involve an undetermined amount of all three of these processes, though the observation that the rate of growth of nodules is independent of grain size points to the third possibility, unless the first and second compensate for one another.

Transformation of austenite to pearlite near Ae_1 takes place by a process of nucleation and growth, as at lower temperature; and though nodules appear to be nucleated at grain boundaries, their growth is not arrested at the grain boundary when transformation of one grain is completed, as Mehl (1) assumed for the formation of pearlite. The whole course of the reaction of steel A at 690 degrees Cent. (1275 degrees Fahr.), after an austenitizing treatment of ½ hour at 875 degrees (1605 degrees Fahr.), may be seen in Fig. 20.

The structures observed in these photomicrographs suggest that

[16]The rate of growth of a nodule in a single austenite grain depends upon the rates of both sidewise and edgewise growth of pearlite.

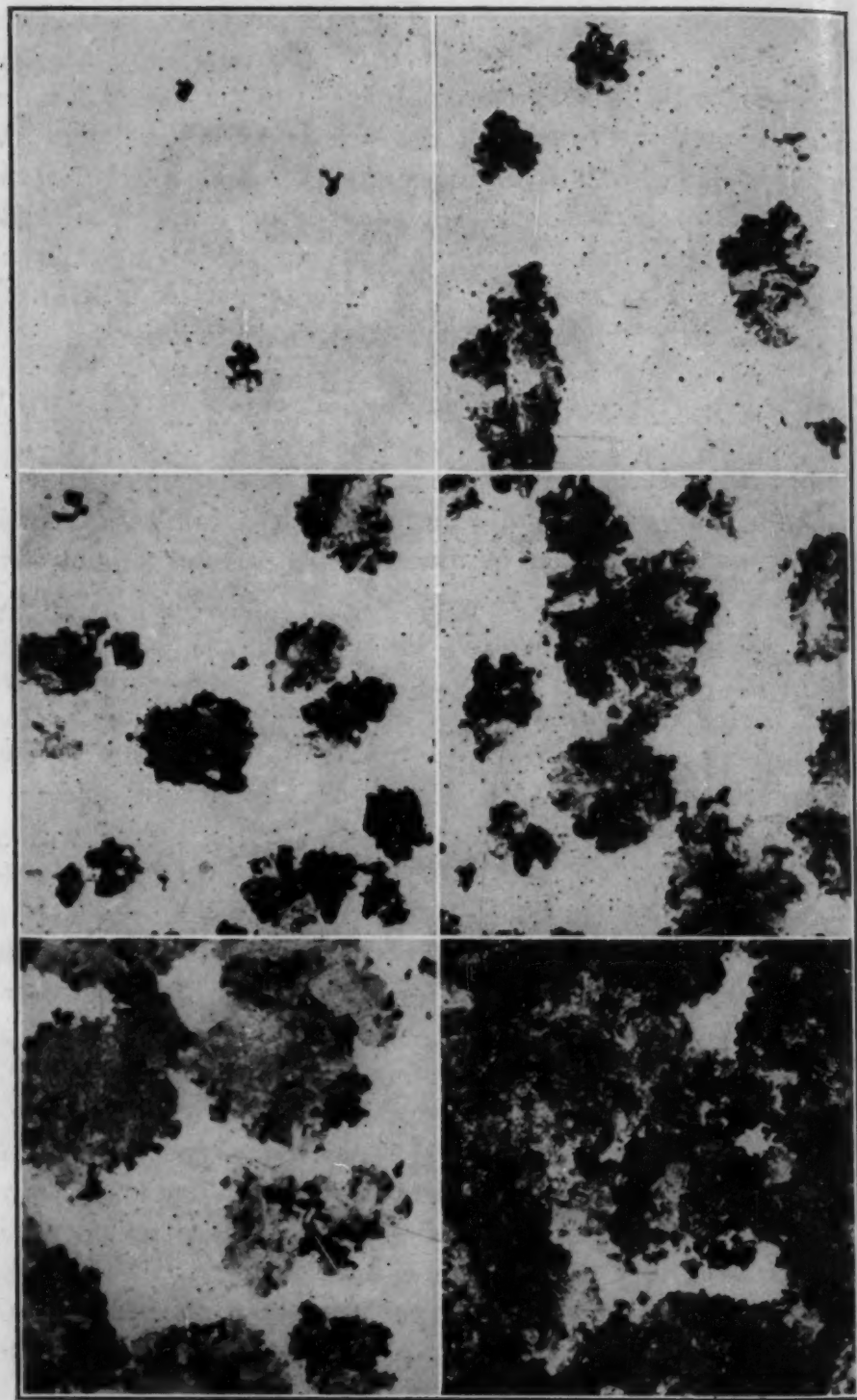

Fig. 20—Group Nodule Transformation of Steel A. Pre-Treated by Heating to 875 Degrees Cent. for ½ Hour and Oil Quenching. Austenitized ½ Hour at 875 Degrees Cent. and Transformed at 690 Degrees Cent. × 100. Austenite Grain Size No. 5. Reaction Times at 690 Degrees Cent.: Top Left—3 Minutes; Top Right—5½ Minutes; Middle Left—6 Minutes; Middle Right—6½ Minutes; Bottom Left—8 Minutes; Bottom Right—9 Minutes. (Reduced 50 Per Cent in Reproduction.)

Johnson and Mehl's (39) mathematical analysis of rates of transformation for general nucleation might be applicable. The formation of nuclei at grain boundaries imposes certain restrictions upon impingement, however, so that in the range of more than one nodule

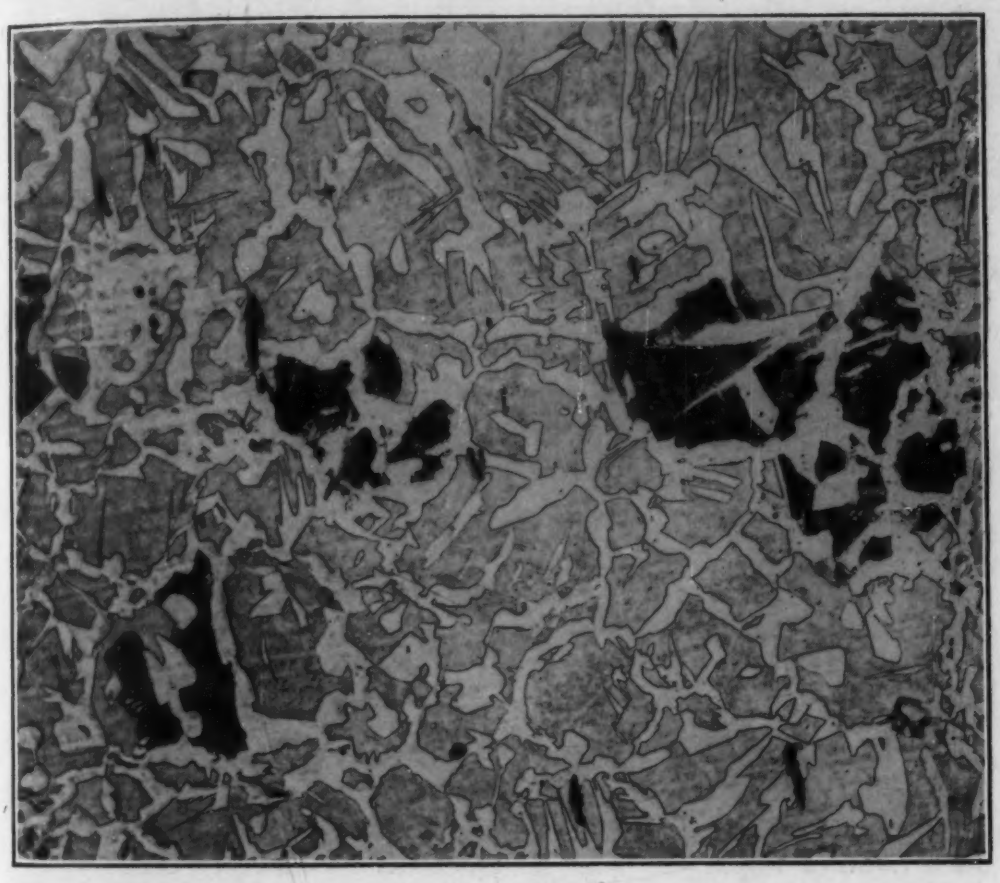

Fig. 21—Quasi-Group Nodules in Steel J (0.57 Per Cent Carbon). Austenitized ½ Hour at 915 Degrees Cent.; Transformed 41 Minutes at 703 Degrees Cent. Longitudinal Section of Bar. × 100.

per grain, the application of the analysis yields results of doubtful significance. When the group nodules are several times larger than the austenite grains, there is sufficient randomness in the location of nuclei to satisfy the conditions under which the equations for general nucleation were derived. Transformation of austenite to pearlite, involving the formation of group nodules, thus constitutes a case of quasi-general nucleation, as pointed out by Hull (41). While the general nucleation equations may be applied, austenite grain size still enters as a variable in determining the area available for nucleation.

Steels in Which Group Nodules Have Been Observed

Group nodules have been found in a variety of steels reacted at temperatures near Ae_1, and without exception as long as the carbon content is close to the eutectoid composition. These steels include three commercial heats of eutectoid steel that were silicon killed (A, B, and C), an ingot of heat C that was killed with aluminum (D), three 1 per cent carbon tool steels (E, F, and G), a tool steel containing 0.22 per cent vanadium (H), and samples of high purity eutectoid steel prepared in the manner described by Mehl and Wells (42). The chemical compositions of these steels are listed in Table I. Quasi-group nodules were seen in a 0.57 per cent carbon steel (J) and a hypoeutectoid manganese steel (K). Adjoining austenite grains in the hypoeutectoid steel of Fig. 21 appear to be separated by a continuous envelope of ferrite. In order for transformation to proceed as it does, it must be that transformation strains are transmitted through the ferrite envelope and induce nucleation in neighboring grains.

Modes of Transformation of Austenite to Pearlite versus Temperature

No reason exists for expecting an abrupt transition from grain boundary to group nodule transformation as the reaction temperature is raised. Nuclei form at grain boundaries in both cases, and growth proceeds uniformly in all directions irrespective of grain boundaries until nodules impinge. The differentiation is merely based on the disposition of pearlite volumes. In distinct grain boundary transformation, a large number of nodules are formed at the boundary of each grain, and reaction proceeds by the growth of these nodules into the centers of the grains (1). Typical group nodule transformation consists of the formation of a smaller number of nodules which grow radially, in all directions, and which eventually encompass a number of former austenite grains. Between these easily distinguished modes of transformation lie a continuous series of intermediate types. One basis for classifying modes of transformation might be the number of nodules per austenite grain in the completely reacted sample, or the reciprocal of this number.

The average number of austenite grains per nodule, for group nodule transformation, may be shown to be a function of Johnson

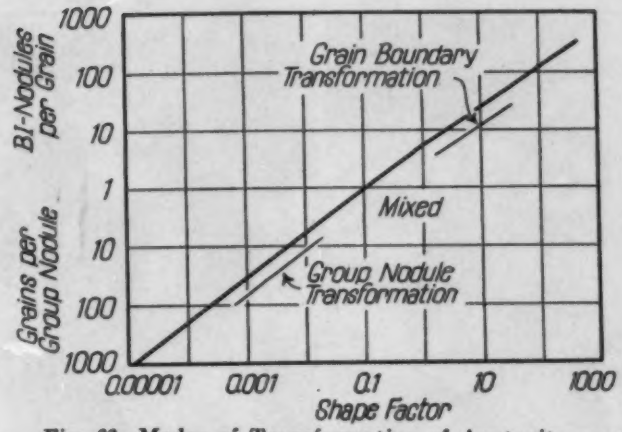

Fig. 22—Modes of Transformation of Austenite as a Function of the Shape Factor,

$$\lambda = \frac{a^3 N_B}{G}$$

and Mehl's (39) shape factor—$\lambda = \frac{a^3 N_B}{G}$, where a is the radius of the grain, N_B is the rate of nucleation per unit of grain boundary area, and G is the rate of growth. Johnson and Mehl (39) determined that the total number of nodules per unit volume of completely reacted sample, n_e, for general nucleation, was given by the expression:

$$n_e = 0.896\ (N_v/G)^{3/4}$$

From the relationship that N_v (rate of nucleation per unit volume) equals 3 N_B/a, and the volume of a grain $(4/3\pi a^3)$, it may be shown that the number of austenite grains per group nodule, n, is given by

$$n = 0.196\left(\frac{a^3 N_B}{G}\right)^{-3/4} = 0.196\ (\lambda)^{-3/4}$$

The above relationship, together with Johnson and Mehl's results corrected for the formation of bi-grained nodules in steel are plotted in Fig. 22. An arbitrary value of one nodule per grain is the logical one to choose to limit the domains of grain boundary and group nodule transformation. This classification is based on an average of one nodule per grain; but since nodules and grains have a distribution of sizes within a given sample, it may easily be seen that a range of λ values will exist in which a mixed mode of transformation may be employed.

The variation in the mode of transformation of austenite to pearlite with temperature is illustrated in Fig. 23 for a commercial

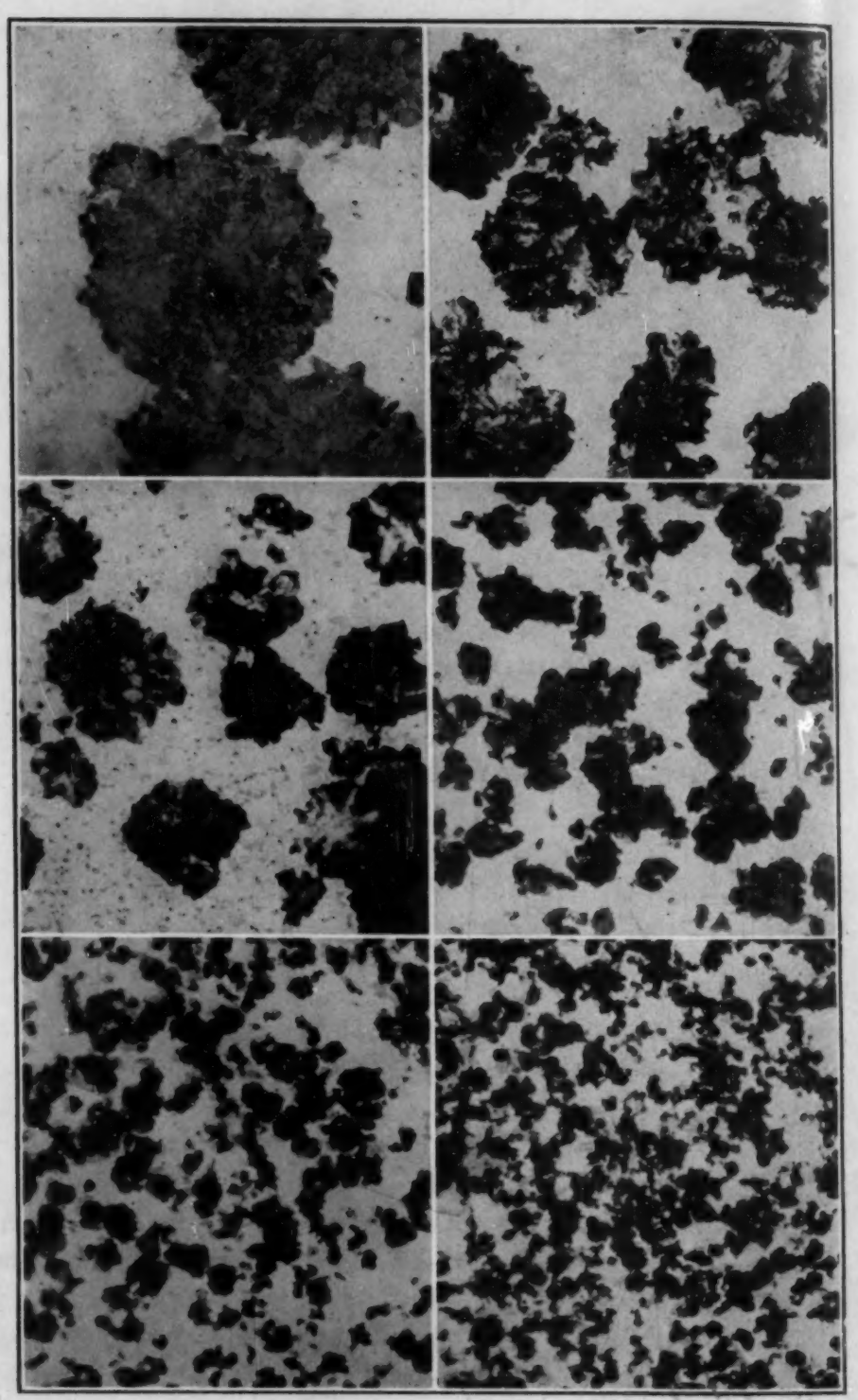

Fig. 23—Modes of Transformation of Steel B as a Function of the Reaction Temperature. Austenitized ½ Hour at 875 Degrees Cent. Austenite Grain Size 4¼. × 100. Transformed as Follows: Top Left—20 Minutes at 689 Degrees Cent.; Top Right—9 Minutes at 680 Degrees Cent.; Middle Left—120 Seconds at 670 Degrees Cent.; Middle Right—24 Seconds at 650 Degrees Cent.; Bottom Left—9 Seconds at 629 Degrees Cent.; Bottom Right—5 Seconds at 600 Degrees Cent. (Reduced 50 Per Cent in Reproduction.)

eutectoid steel (steel B). Samples were annealed, austenitized ½ hour at 875 degrees Cent. (1605 degrees Fahr.) and isothermally transformed about 50 per cent at 689, 680, 670, 650, 629, and 600 degrees Cent. (1270, 1255, 1240, 1200, 1165, 1110 degrees Fahr.). The rapid increase, with lowering temperature, of the number of nodules per unit volume or per austenite grain is apparent, as well as the gradual transition from the group nodule to the grain boundary mode of transformation.

Summary

1. Vilella's martensite reagent was used to develop etch pits in the ferrite of pearlite in electrolytically polished, high purity eutectoid steel. In this manner it was demonstrated that the ferrite lamellae of a pearlite colony have a single orientation.
2. The orientation relationships cited and the micrographic evidence presented indicate that cementite serves as the active nucleus in the formation of pearlite.
3. The alternate parallel lamellae of ferrite and cementite in a pearlite colony are produced by a process of sidewise nucleation and growth and are subsequently developed by edgewise growth, the latter mode of growth accounting for by far the larger fraction of transformation on the basis of the volume of pearlite produced.
4. The factors determining the carbon concentration gradients in austenite during sidewise and edgewise growth are discussed.
5. The pearlite spacing established by sidewise nucleation and growth decreases as the transformation temperature is lowered, because the rates of nucleation of ferrite and cementite increase more rapidly with supersaturation than do the rates of growth.
6. The factors determining the pearlite spacing established during edgewise growth are the same as those which determine spacing during sidewise nucleation and growth. The two spacings are not necessarily identical, but there is experimental evidence to show that the difference is not great.
7. Pearlite is nucleated almost exclusively at grain boundaries at all reaction temperatures, unless non-metallic inclusions or undissolved carbides promote general nucleation.
8. The transformation of austenite to pearlite, at temperatures near Ae_1, involves the nucleation and growth of approximately spherical nodules—"group nodules"—to a size which may be many

times larger than that of the austenite grains. Group nodule transformation was found to occur in a variety of steels, and even to a certain extent in distinctly hypoeutectoid steels.

9. The average number of austenite grains per group nodule (n) in a completely reacted steel bears a simple relation to the rates of nucleation and growth and the grain size:

$$n = 0.196 \left(\frac{a^3 N_B}{G}\right)^{-3/4}$$

Bibliography

1. R. F. Mehl, "The Physics of Hardenability," Hardenability of Alloy Steels, American Society for Metals Symposium, 1938.
2. R. F. Mehl, "Pearlite," Campbell Memorial Lecture, Fall Meeting of the American Society for Metals, 1941.
3. M. Gensamer, E. B. Pearsall, and G. V. Smith, "Mechanical Properties of the Isothermal Decomposition Products of Austenite," TRANSACTIONS, American Society for Metals, Vol. 28, 1940, p. 380.
   M. Gensamer, E. B. Pearsall, W. S. Pellini, and J. R. Low, "The Tensile Properties of Pearlite, Bainite, and Spheroidite," American Society for Metals Preprint, 1941.
4. H. C. Sorby, *Journal,* Iron and Steel Institute, 1886, No. 1, p. 140.
5. F. Abel and Deering, Institution of Mechanical Engineers Proceedings, 1885, p. 30.
6. Müller, *Stahl und Eisen,* Vol. 8, p. 291.
7. H. M. Howe and A. Sauveur, *Journal,* Iron and Steel Institute, 1896, No. 1, p. 170.
8. H. M. Howe, *Journal,* Iron and Steel Institute, 1895, No. 2, p. 258.
9. F. Osmond, "Methode Generale pour l'Analyse Microscopique des Aciers au Carbone," 1895, p. 18.
10. F. Osmond, Bulletin de la Societe d'Encouragement pour l'Industrie Nationale, May, 1895.
11. F. Osmond, Discussion to reference 7.
12. C. Benedicks, *Journal,* Iron and Steel Institute, 1905, No. 2, p. 352.
13. Heyn, *Journal,* Iron and Steel Institute, 1902, No. 1, p. 160.
14. Kourbatoff, *Revue de Metallurgie,* Feb., 1905, p. 169.
15. H. M. Howe and A. G. Levy, *Journal,* Iron and Steel Institute, 1916, No. 2, p. 210.
16. R. Vogel, *Zeit. anorg. Chemie,* Vol. 76, 1912, p. 425.
17. A. Portevin, *Journal,* Institute of Metals, 1923, No. 1, p. 239.
18. F. L. Brady, *Journal,* Institute of Metals, 1922, No. 2, p. 369.
19. A. F. Hallimond, *Journal,* Iron and Steel Institute, 1922, No. 1, p. 359.
20. N. T. Belaiew, *Journal,* Iron and Steel Institute, 1922, No. 1, p. 201.
21. N. T. Belaiew, *Revue de Métallurgie,* April, 1935, p. 145. Also discussion to reference 1.
22. H. C. H. Carpenter and J. M. Robertson, *Journal,* Iron and Steel Institute, 1932, No. 1, p. 309.
23. O. W. Ellis, TRANSACTIONS, American Society for Metals, Vol. 22, 1934, p. 139.
24. H. Jolivet, *Journal,* Iron and Steel Institute, 1939, No. 2, p. 95.
25. Discussion to reference 20.
26. R. F. Mehl and D. W. Smith, *Transactions,* American Institute of Mining and Metallurgical Engineers, Iron and Steel Division, Vol. 116, 1935, p. 330.
27. R. F. Mehl, C. S. Barrett, and D. W. Smith, *Transactions,* American

Institute of Mining and Metallurgical Engineers, Iron and Steel Division, Vol. 105, 1933, p. 215.
28. Unpublished research, Metals Research Laboratory, Carnegie Institute of Technology.
29. Unpublished research, Metals Research Laboratory, Carnegie Institute of Technology.
30. A. Portevin and P. Chevenard, *Comptes rendus,* Vol. 204, 1937, p. 772.
31. A. Portevin and H. Jolivet, Annales de l'Academie des Sciences Techniques a Varsovie, Vol. 4, 1937, p. 177.
32. A. Portevin and H. Jolivet, *Comptes rendus,* Vol. 208, 1939, p. 1404. Also references 1 and 24.
33. R. Marc, *Zeit. Electrochem.,* Vol. 15, p. 679.
34. H. Miers and F. Isaac, *Proceedings,* Royal Society, Vol. 79(A), 1907, p. 322.
35. G. E. Pellissier, M. F. Hawkes, W. A. Johnson and R. F. Mehl, "The Interlamellar Spacing of Pearlite," American Society for Metals Preprint No. 41, 1941.
36. R. F. Mehl and L. K. Jetter, "The Mechanism of Precipitation from Solid Solution," Age Hardening of Metals, American Society for Metals Symposium, 1939.
37. R. F. Mehl and O. T. Marzke, *Transactions,* American Institute of Mining and Metallurgical Engineers, Institute of Metals Division, Vol. 93, 1931, p. 123.
38. K. Honda, *Journal,* Iron and Steel Institute, 1926, No. 2, p. 417; discussion by Hultgren.
39. W. A. Johnson and R. F. Mehl, *Transactions,* American Institute of Mining and Metallurgical Engineers, Iron and Steel Division, Vol. 135, 1939, p. 416.
40. E. C. Bain, *Journal,* Iron and Steel Institute, 1938, No. 2, p. 33.
41. F. C. Hull, Discussion to Reference 39.
42. R. F. Mehl and C. Wells, *Transactions,* American Institute of Mining and Metallurgical Engineers, Iron and Steel Division, Vol. 125, 1937, p. 429.

DISCUSSION

Written Discussion: By N. A. Ziegler and W. L. Meinhart, Research Laboratories, Crane Co., Chicago.

To amplify the authors' conclusion that "cementite serves as the active nucleus in the formation of pearlite", we would like to present evidence that sometimes ferrite can also act as a nucleus. The two accompanying photomicrographs (at 500 and 1000 diameters) represent structures of a 4 to 6 per cent chromium, 0.5 per cent molybdenum steel of the following composition: 0.47 per cent silicon, 0.70 per cent manganese, 0.28 per cent carbon, 5.25 per cent chromium, 0.62 per cent molybdenum, 0.05 per cent aluminum, which is well known for its thermal sluggishness. This particular dilatometer specimen was austenitized at 1000 degrees Cent. (1830 degrees Fahr.), and after that isothermally treated for 16 hours at 780 degrees Cent. (1440 degrees Fahr.). The dilatometric curve and metallographic evidence indicate that this time period at a given temperature was too short to allow the austenite decomposition to reach completion. Consequently, when the specimen was cooled to room temperature, after the isothermal treatment, it still was partially austenite. The latter was preserved as such down to about 300 degrees Cent. (570 degrees

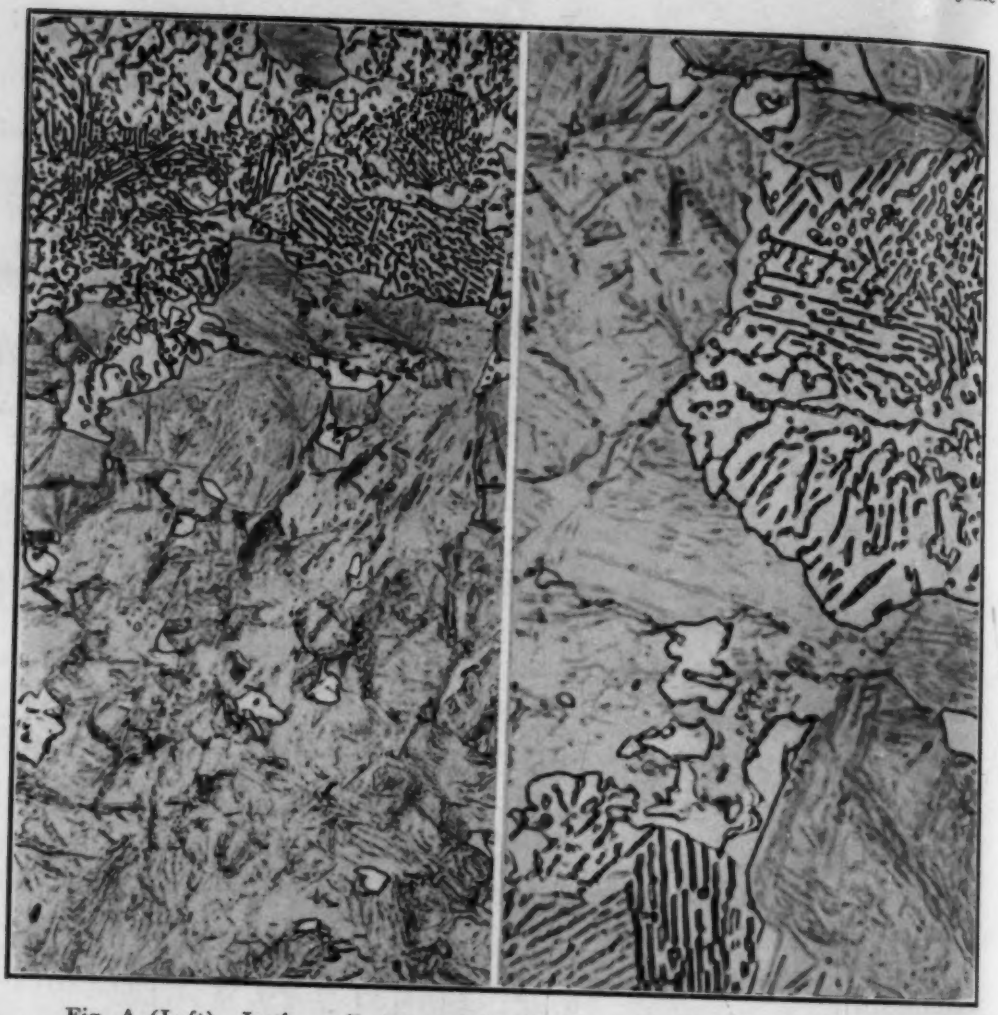

Fig. A (Left)—Isothermally Treated for 16 Hours at 780 Degrees Cent. VPN 269. Incompletely Transformed. Etched in Nital. × 500.
Fig. B (Right)—Isothermally Treated for 16 Hours at 780 Degrees Cent. VPN 269. Incompletely Transformed. Etched in Nital. × 1000.

Fahr.) when it was transferred into martensite. The resultant microstructure thus is: (1) pearlite, formed at the temperature of isothermal treatment and (2) martensite formed at the temperature of the suppressed transformation. The pearlite resembles nodular troostite by its external shape and radially arranged inner structure. Besides pearlite, this structure also contains small ferritic islands, which are "proeutectoid" ferrite, noted and described by some previous investigators.[17] Apparently, in this particular case, these ferrite particles are the first product of high temperature austenite transformation, serving as nuclei for further development of pearlitic (or troostitic) grains.

Written Discussion: By G. C. Williams, associate professor of chemical engineering, University of Louisville, Louisville, Ky.

The paper presented by Messrs. Hull and Mehl is without a doubt a

[17]R. A. Grange and J. M. Kiefer, "Transformations of Austenite on Continuous Cooling and Its Relation to Transformation at Constant Temperature," TRANSACTIONS, American Society for Metals, Vol. 29, 1941, p. 85.

timely and valuable addition to the field of ferrous physical metallurgy. It has classified the existent theories of pearlite formation both as to similar and opposing ideas and has presented numerous interesting photomicrographs. Indeed, the excellence of Hull's photomicrographs causes grave doubts as to the validity of certain implied conclusions.

I refer specifically to the concept of sidewise nucleation and growth as being important in comparison to edgewise expansion. Edgewise growth could explain any angular interception of lamellar plates with an initiating grain boundary but a sidewise parallel plate extension of a field would present lamellae parallel to the initiating area. By this reasoning, lamellae would be expected to parallel grain boundaries, but this phenomenon is not found in any photomicrograph. Parallel lamellae in the interior of a grain could be an end projection of the growing cementite plates.

Authors' Reply

Messrs. Ziegler and Meinhart correctly point out that proeutectoid ferrite may act as a center for the nucleation of pearlite. Austenite grain boundaries, nonmetallic inclusions, and undissolved carbides also serve as centers for the nucleation of pearlite. However, we consider the "active" nucleus in the formation of pearlite to be the phrase, either ferrite or cementite, that first occurs with the orientation that it is known to have in the final product—pearlite. The available data indicate that this "active" nucleus is cementite.

Mr. Williams assumes that sidewise growth of pearlite should result in lamellae parallel to the initiating area, and, since pearlite lamellae are not found parallel to the grain boundary, he concludes that sidewise nucleation and growth cannot be important in comparison to edgewise expansion.

It is unfortunate that Mr. Williams did not offer an explanation for the assumption by which he disposes of the concept of sidewise nucleation and growth. Crystallographic orientation relationships are known to exist between austenite and the ferrite and cementite of pearlite. The original cementite nucleus, though formed at or near the grain boundary, is precipitated upon a crystallographic plane which would rarely coincide with the grain surface. It is not to be expected, therefore, that the lamellae should be parallel to the initiating grain boundary. (See Fig. 24).

We have attempted to demonstrate that the genesis of a pearlite colony requires simultaneous sidewise nucleation and growth and edgewise growth; all colonies are formed by a combination of both processes, not some colonies by the former and others by the latter. This principle is illustrated in Fig. 5. When pearlite is nucleated at the grain boundary, as is usually the case, the mechanism of formation is not changed. The original cementite nucleus (Fig. 24a) extends in the plane of the plate and thickens in the perpendicular direction until ferrite is nucleated on the side surfaces. The ferrite in turn grows in a direction parallel to the plane of the original nucleus and also in the perpendicular direction (Fig. 24b). We have chosen to designate the growth in these directions as edgewise and sidewise growth, respectively. Although edgewise and sidewise growth are similar in some respects, it is profitable to

distinguish between them in order to clarify our understanding of the mechanism of formation of pearlite.

During the edgewise growth of pearlite the carbon concentration gradients in austenite become nearly independent of time (see Fig. 12); ferrite and cementite extend simultaneously into austenite. During sidewise growth, how-

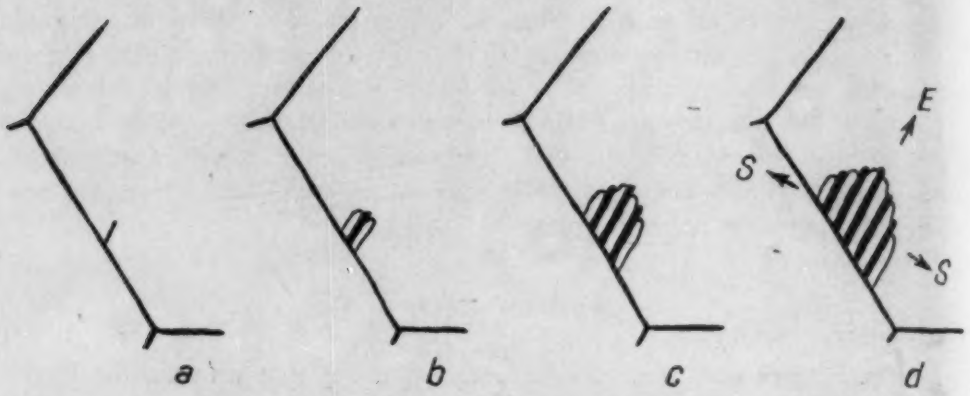

Fig. 24—Formation of Pearlite at the Grain Boundary in a Eutectoid Steel by Simultaneous Edgewise Growth and Sidewise Nucleation and Growth.

ever, marked concentration fluctuation at and near the austenite interface result in alternate nucleation and growth of ferrite and cementite.[18] (See Fig. 6). The lamellae produced in this manner grow sidewise a distance equal to the thickness of the ferrite or cementite plates, whereas by edgewise growth the same lamellae may be extended fifty or more interlamellar spacings. How is one to decide which is more important—the creation or the growth of the lamellae? Are not both processes essential?

[18]Sidewise nucleation and growth of pearlite is actually a misnomer, for ferrite or cementite lamellae are nucleated and grow sidewise alternately and not simultaneously as in the case of edgewise growth.

EFFECTS OF SMALL AMOUNTS OF ALLOYING ELEMENTS ON GRAPHITIZATION OF PURE HYPEREUTECTOID STEELS

By Charles R. Austin and B. S. Norris

Abstract

The paper deals with the subcritical graphitizing characteristics of 1.1 per cent carbon steels made from electrolytic iron melted and cast under hydrogen in an induction furnace, and containing ½ per cent or less of one of the following third elements: manganese, silicon, nickel, chromium, copper, aluminum, sulphur, phosphorus, or tin. The experimental investigation relates to the role played by carbide size and residual strain in the several alloys, resulting from some treatment prior to subcritical tempering, and to the effect of environment during heat treatment, on carbide stability.

Under certain conditions the steels containing aluminum, manganese and silicon may completely graphitize on tempering. The amount or rate of graphitization may be increased by a prior treatment, which results in a high degree of dispersion of the carbide or produces a critical amount of strain in the alloy. Similarly the diffusion of oxygen into the steel during any high temperature pretreatment or during tempering promotes graphitization. This phenomenon appears to be dependent on a nucleating effect of aluminum, manganese or silicon oxides when present in suitable form or degree of dispersion.

The steels containing the elements, nickel, chromium, copper, sulphur (free from manganese) or tin exhibit resistance to graphitization independent of strain, carbide size, or oxygen penetration.

IN previously published researches (1)[1] attention has been directed to studies on the factors which tended to promote marked graphitization of commercial plain carbon hypereutectoid steels when tempered for long periods at subcritical temperatures. In an attempt to

[1]The figures appearing in parentheses refer to the bibliography appended to this paper.

A paper presented before the Twenty-third Annual Convention of the Society held in Philadelphia, October 20 to 24, 1941. Of the authors, Charles R. Austin is professor of metallurgy, The Pennsylvania State College, State College, Pa., and B. S. Norris is metallurgist, U. S. Pipe and Foundry Co., Burlington, N. J. Manuscript received June 28, 1941.

throw further light on factors influencing graphitization a series of pure iron-carbon alloys were prepared containing small amounts of one added element.

A recent paper (2) by the authors dealt with the effects of these small amounts of alloying elements on the resistance to softening by tempering, and the present paper will provide a discussion on the susceptibility of the pure alloys to subcritical graphitization. The details of melting, casting and fabrication of the steels have been given in the paper cited and only the data on chemical composition are herein reproduced (see Table I).

Details of the studies on the factors affecting graphitization will be discussed under the following sections:

1. The effect of temperature and of time on the qualitative and quantitative graphitization of the steels as a function of the added element.
2. The effect of pretreatment and carbide size on the tendency to graphitize during tempering.
3. Studies on the effect of strain on graphitization.
4. Observations on the profound effect of vacuum homogenization on graphitizing characteristics of the steels.

Graphitization as a Function of the Added Element

All the alloys were in the form of ⅜-inch diameter rolled bar stock, and contained up to a maximum of ½ per cent of one of the elements commonly found in steels, and shown in the tabulated data. Prior to tempering, the samples were homogenized in vacuum at 1000 degrees Cent. (1830 degrees Fahr.) for 1 hour and quenched in water. The tempering treatments were conducted in a lead bath covered with charcoal or "lead-pot" carbon to prevent oxidation or at least to reduce oxidizing effects to a minimum. The progress of tempering up to 125 hours maximum was followed by means of Rockwell B hardness values, and the semilogarithmic relation between hardness and tempering time for some of the steels is well shown in Fig. 1. However linearity holds only when the carbides are stable. As soon as carbide dissociation or graphitization occurs it is accompanied by a marked drop in hardness as shown for the aluminum steels (Fig. 1).

The two higher aluminum alloys (0.07 and 0.37 per cent) exhibited an obvious tendency to soften by graphitization at 550 and

590 degrees Cent. (1020 and 1095 degrees Fahr.). At 550 degrees Cent. (1020 degrees Fahr.) both steels exhibited this characteristic after 25 hours tempering. At 590 degrees Cent. (1095 degrees Fahr.) the 0.37 aluminum alloy begins to graphitize rapidly after only 5

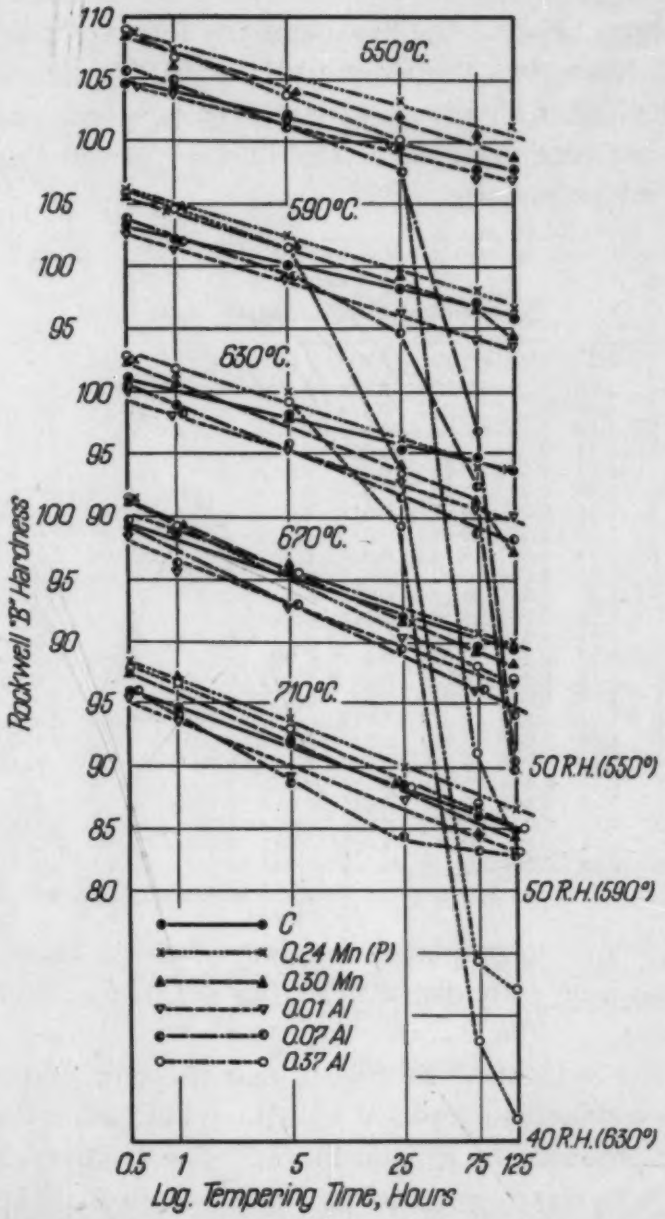

Fig. 1—Semi-Logarithmic Plot Showing Relation Between Hardness and Tempering Time at 550, 590, 630, 670 and 710 Degrees Cent. For Carbon, Manganese and Aluminum Steels.

hours. Tempering at 630 degrees Cent. (1165 degrees Fahr.), the high aluminum steel alone showed evidence of carbide instability,

while at 670 and 710 degrees Cent. (1235 and 1310 degrees Fahr.) all steels exhibit the hardness-tempering time linearity and hence resistance to graphitization, up to 125 hours.

Of the two manganese steels, only the one containing 0.30 per cent shows any discontinuity. At 590 and 630 degrees Cent. (1095 and 1165 degrees Fahr.) the departure from linearity occurs between 75 and 125 hours but the magnitude is small compared with that noted for the higher aluminum alloys. The apparent carbide stability in the 0.24 per cent manganese steel may be due to the presence of 0.031 per cent phosphorus.

Table I

Chemical Composition Per Cent

Steel	Alloy	C	Mn	Si	Ni	Cr	Cu	Al	S	P	Sn
87	None	1.08	0.006	0.021	0.017	0.002	0.008	<0.005	0.015	0.012	<0.003
89	None	1.09	0.005	0.023	0.018	0.003	0.006	<0.005	0.016	0.012	<0.003
26	Al	1.12	0.005	0.03	0.015	0.003	0.009	0.012	0.015	0.014	<0.003
27	Al	1.15	0.006	0.01	0.018	0.002	0.008	0.073	0.015	0.014	<0.003
28	Al	1.14	0.006	0.015	0.015	0.002	0.011	0.37	0.014	0.014	<0.003
72	Mn	1.14	0.04	0.01	0.014	0.003	0.013	0.006	0.015	0.014	<0.003
73	Mn	1.11	0.08	0.01	0.018	0.003	0.009	0.006	0.014	0.014	<0.003
76	Mn (P)	1.10	0.24	0.015	0.013	0.002	0.004	0.007	0.017	0.031	<0.003
83	Mn	1.14	0.30	0.042	0.015	0.003	0.006	0.003	0.019	0.014	<0.003
77	Si	1.08	0.006	0.08	0.014	0.003	0.006	0.006	0.016	0.012	<0.003
29	Si	1.20	0.005	0.12	0.015	0.003	0.007	0.007	0.015	0.012	<0.003
78	Si	1.08	0.006	0.14	0.012	0.003	0.005	0.008	0.017	0.012	<0.003
79	Si	1.15	0.006	0.48	0.010	0.002	0.004	0.006	0.015	0.014	<0.003
66	Ni	1.10	0.009	0.028	0.08	0.002	0.007	<0.005	0.014	0.012	<0.003
67	Ni	1.14	0.005	0.022	0.13	0.003	0.006	0.007	0.014	0.012	<0.003
74	Ni	1.04	0.007	0.024	0.53	0.003	0.008	0.006	0.017	0.012	<0.003
82	Cr	1.07	0.004	0.033	0.015	0.07	0.004	0.003	0.018	0.014	<0.003
84	Cr	1.14	0.004	0.030	0.017	0.13	0.004	0.003	0.016	0.014	<0.003
85	Cr	1.16	0.006	0.024	0.018	0.46	0.007	<0.005	0.015	0.012	<0.003
69	Cu	1.11	0.006	0.01	0.018	0.003	0.068	<0.005	0.014	0.015	<0.003
70	Cu	1.10	0.005	0.01	0.015	0.002	0.104	<0.005	0.015	0.014	<0.003
71	Cu	1.16	0.005	0.01	0.015	0.002	0.35	0.007	0.014	0.014	<0.003
80	S	1.15	0.006	0.01	0.017	0.003	0.005	0.007	0.048	0.012	<0.003
81	Sn	1.08	0.004	0.024	0.016	0.003	0.007	0.003	0.018	0.012	0.05

The resistance to graphite formation of all the other steels listed in Table I has been fully demonstrated in the former publication (2) on these alloys.

It is quite evident from Fig. 1 that the temperature at which tempering is conducted may have a profound effect on the magnitude of softening produced by graphitization. The relative effect of temperature is more clearly revealed in Fig. 2 where Rockwell B values, after tempering 125 hours, are plotted against the tempering temperature.

The hardness data for the 0.48 per cent silicon steel, which is essentially free from graphitization, are included to illustrate the normal spheroidization softening as a function of temperature. The

behavior of the plain carbon and the 0.01 aluminum steels similarly demonstrate carbide stability.

With the 0.07 per cent aluminum alloy maximum graphitization occurs at 550 degrees Cent. (1020 degrees Fahr.) but with 0.37 per cent aluminum the steels are completely graphitized after 125 hours at any temperature within the limits 550 to 630 degrees Cent. (1020 to 1165 degrees Fahr.). The partial graphitization of the 0.3 per cent manganese alloy at 630 degrees Cent. (1165 degrees Fahr.) should also be noted.

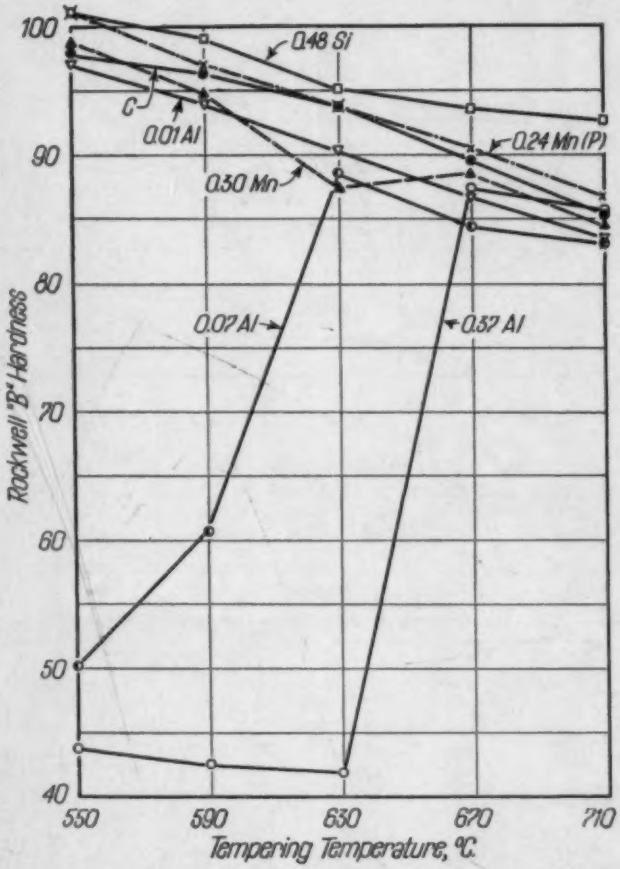

Fig. 2—Relation Between Tempering Temperature and Hardness For Carbon, Manganese, Silicon and Aluminum Steels Tempered For 125 Hours.

In order to determine quantitatively the relative amount of graphite present in the various alloy steels after tempering for 125 hours at temperatures ranging from 510 to 710 degrees Cent. (950 to 1310 degrees Fahr.), a set of large specimens was quenched from 1000 degrees Cent. (1830 degrees Fahr.), tempered and analyzed chemically for graphite. On account of the relatively rapid rate of

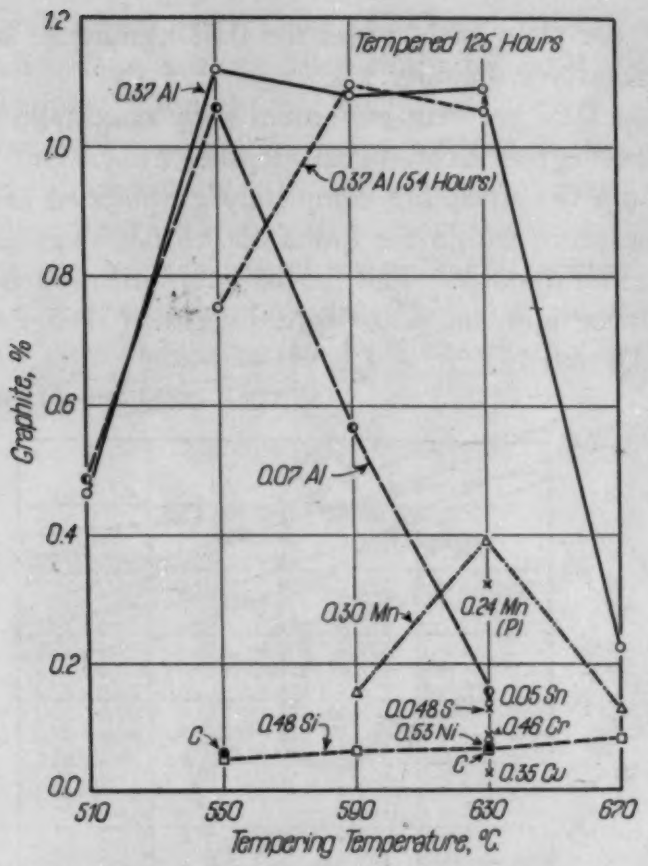

Fig. 3—Relation Between Tempering Temperatures and Quantity of Graphite Formed in Carbon and the High Alloy Steels Containing Approximately ½ Per Cent Added Element.

Table II
Chemical Analyses for Graphite

Steel	Per Cent Alloy	Tempering Temp., °C.	Time at Temp., Hrs.	Per Cent Graphite	Steel	Per Cent Alloy	Tempering Temp., °C.	Time at Temp., Hrs.	Per Cent Graphite
87	None	550	125	0.06	76	0.24 Mn (P)	630	125	0.32
87	None	630	125	0.07	83	0.30 Mn	590	125	0.16
27	0.07 Al	510	125	0.49	83	0.30 Mn	630	125	0.39
27	0.07 Al	550	125	1.06	83	0.30 Mn	670	125	0.13
27	0.07 Al	590	125	0.57	79	0.48 Si	550	125	0.05
27	0.07 Al	630	125	0.14	79	0.48 Si	590	125	0.07
28	0.37 Al	550	54	0.75	79	0.48 Si	630	125	0.07
28	0.37 Al	590	54	1.10	79	0.48 Si	670	125	0.09
28	0.37 Al	630	54	1.06	79	0.48 Si	710	125	0.09
28	0.37 Al	510	125	0.47	74	0.53 Ni	630	125	0.07
28	0.37 Al	550	125	1.12	85	0.46 Cr	630	125	0.09
28	0.37 Al	590	125	1.08	71	0.35 Cu	630	125	0.03
28	0.37 Al	630	125	1.09	80	0.048 S	630	125	0.13
28	0.37 Al	670	125	0.23	81	0.05 Sn	630	125	0.15

graphitization in the 0.37 aluminum alloy, similar data were also obtained for 54 hours temper. The analytical results are listed in Table II and plotted in Fig. 3.

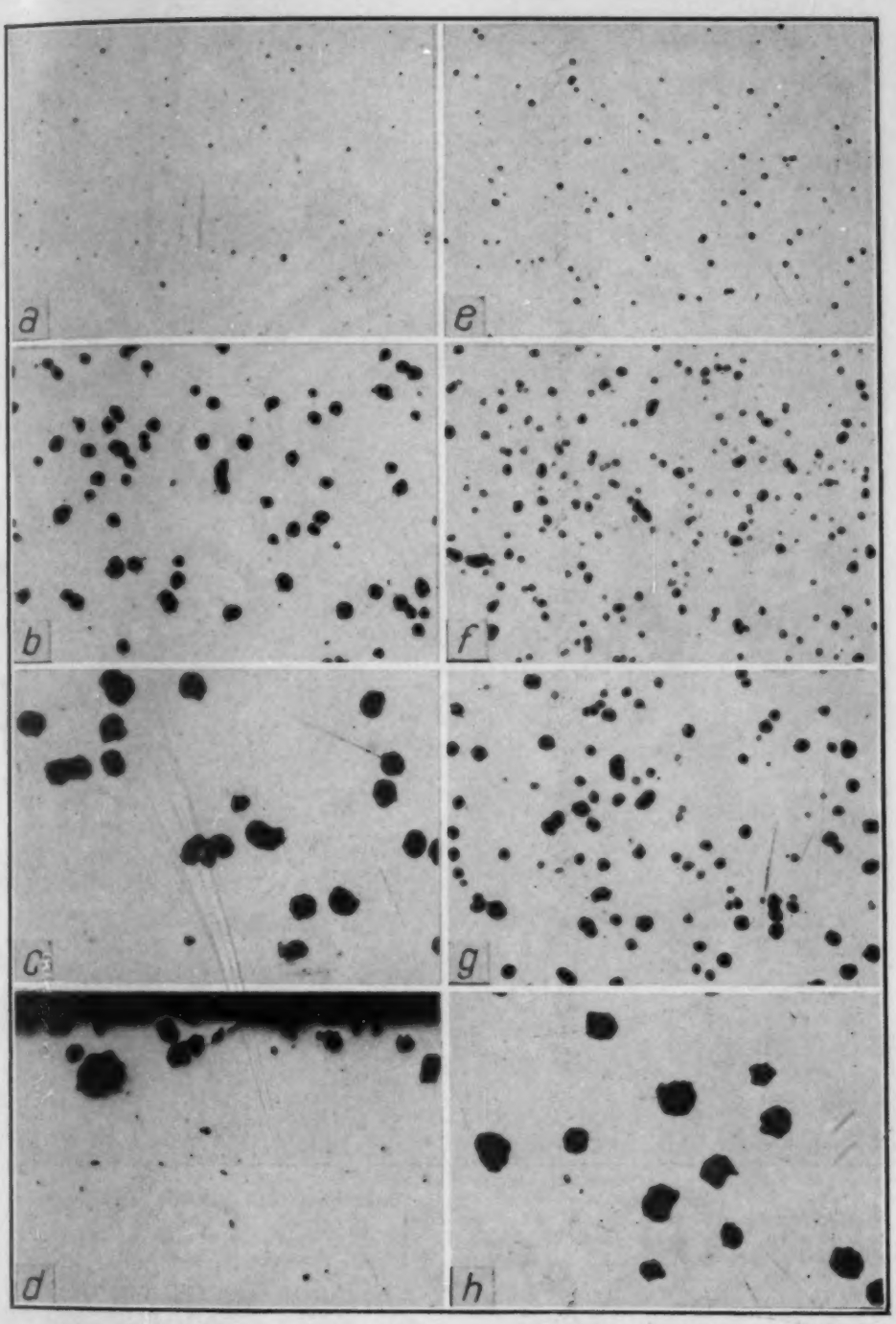

Fig. 4—Unetched Sections of Carbon, Aluminum, and Silicon Steels Tempered 125 Hours at Temperature Indicated. × 100.
At 550 Degrees Cent., a—Carbon; b—0.07 Aluminum; e—0.48 Silicon; f—0.37 Aluminum. At 590 Degrees Cent., c—0.07 Aluminum; g—0.37 Aluminum. At 630 Degrees Cent., d—0.07 Aluminum (Edge); h—0.37 Aluminum.

The results confirm consistently the observations made from interpretations of the hardness curves. Thus the aluminum steels alone completely graphitize and the high manganese steel (0.30 per cent)

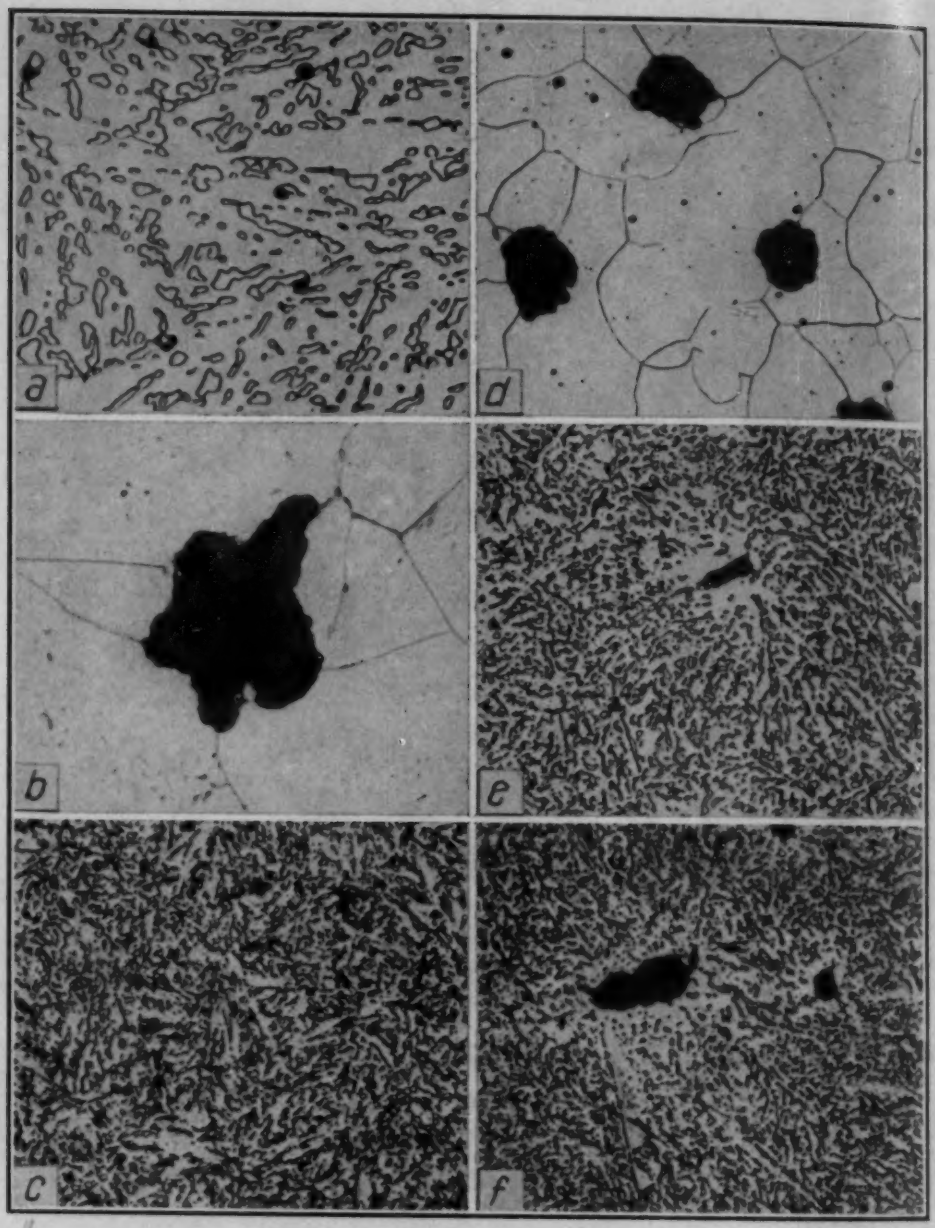

Fig. 5—Etched Sections of Carbon, Aluminum, Silicon and Manganese Steels Tempered 125 Hours at 630 Degrees Cent.
a—0.48 Silicon; b—0.37 Aluminum. × 1000; c—0.48 Silicon; d—0.37 Aluminum. × 250; e—0.08 Manganese; f—0.30 Manganese. × 250.

shows about ⅓ graphitization after 125 hours at 630 degrees Cent. (1165 degrees Fahr.). The plain carbon and the steels containing approximately ½ per cent of silicon, nickel, chromium, or copper are essentially stable after prolonged annealing at subcritical temperatures.

Tests on the 0.37 aluminum steel show that graphitization is practically complete in 54 hours or less at 590 and 630 degrees Cent.

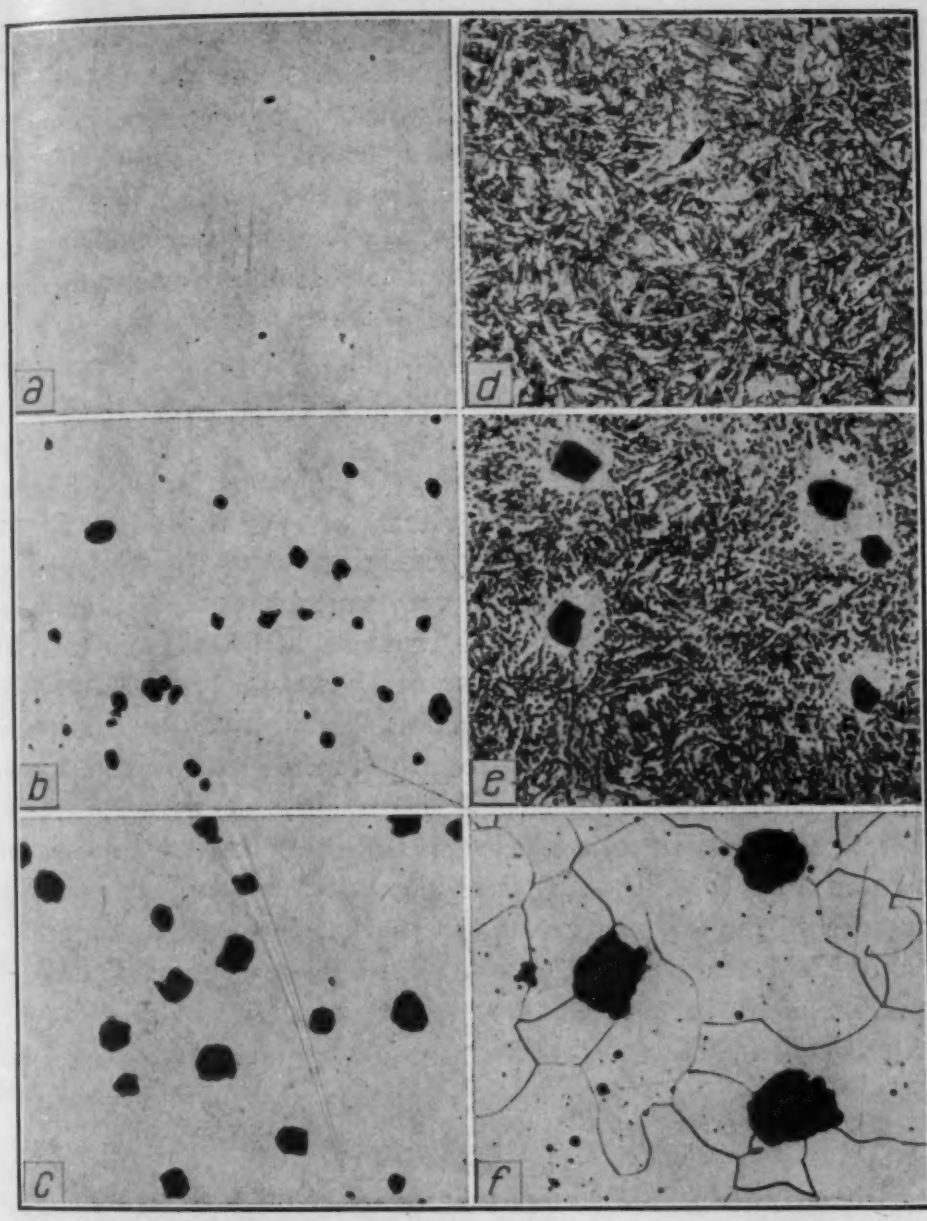

Fig. 6—Microsections of the 0.37 Aluminum Steel Tempered at 630 Degrees Cent. For 5, 25, and 125 Hours.
Unetched, a—5 Hours; b—25 Hours; c—125 Hours. × 100. Etched, d—5 Hours; e—25 Hours; f—125 Hours. × 250.

All the specimens treated for observations on graphitization after tempering 125 hours were studied under the microscope, and some of the unetched structures at 100 diameters are reproduced in Fig. 4. The pronounced graphitization of the 0.07 aluminum steel at 550 and 590 degrees Cent. (1020 and 1095 degrees Fahr.) is evident from Figs. 4B and 4C. At 630 degrees Cent. (1165 degrees Fahr.) graphitization is limited to the edge of the specimen. Furthermore, as the

tempering temperature is raised the graphite particles became larger and less numerous. This is equally true for the steel containing 0.37 aluminum as the temperature of treatment is raised from 550 to 630 degrees Cent. (1020 to 1165 degrees Fahr.) (Figs. 4F, 4G and 4H).

Whenever graphite was present in a steel after tempering in a lead bath, the graphite particles were always smaller at the edge than in the interior. Since this behavior prevailed on the transverse edge, cut prior to heat treatment, as well as on the peripheral edge of a specimen, the difference in size of graphite particles is the result of heat treatment rather than of a condition inherited from the fabrication processes.

Some etched structures resulting from tempering 125 hours at 630 degrees Cent. (1165 degrees Fahr.) are shown in Fig. 5. The essentially complete resistance to graphitization of the 0.48 per cent silicon steel, as compared with the very unstable 0.37 aluminum steel may be noted by comparing Figs. 5A and 5B at 1000 diameters. The same steels at 250 magnifications are shown in Figs. 5C and 5D. The structures for the alloys containing 0.08 and 0.30 per cent manganese (Figs. 5E and 5F) illustrate the fact that a graphite nucleus grows at the expense of the carbide immediately surrounding it.

The progress of graphitization as a function of time is well shown in Fig. 6 which illustrates the unetched and etched microstructures of the 0.37 per cent aluminum steel when tempered for 5, 25 and 125 hours at 630 degrees Cent. (1165 degrees Fahr.). It should be noted that a higher magnification has been used to provide greater detail in the etched sections.

Pretreatment and Carbide Size on Graphitization

Schwartz (3) has stated that graphitization is markedly accelerated during the malleableizing anneal of white iron by a rapid cool from a high temperature prior to anneal. One of the present authors has also brought attention to the effect of quenching on tendency to graphitization of commercial hypereutectoid steels (1).

In order to obtain definite information on the effect of quenching *per se*, or of the fine carbide size resulting from this treatment, the steels containing 0.07 and 0.37 per cent aluminum, 0.30 per cent manganese and 0.48 per cent silicon were heated for 125 hours at 630 degrees Cent. (1165 degrees Fahr.) in the lead bath without any previous hardening treatment. In this "as received" condition the

carbides were spheroidized as a result of the commercial anneal that had been given to the steels subsequent to rolling.

All the steels were strongly resistant to graphitization indicating that carbide had little tendency to dissociate unless finely dispersed or under strain as a result of prior quenching. The microstructures for the 0.37 aluminum and 0.30 manganese steels are shown at 250 and 1000 diameters in Figs. 7A, B and E, F. These structures should be compared with those obtained by a similar 630 degrees Cent. (1165 degrees Fahr.) temper after quenching from 1000 degrees Cent. (1830 degrees Fahr.) (Fig. 5). The aluminum alloy completely graphitized (Fig. 5B and D) and the manganese steel exhibited limited but definite carbide instability (Fig. 5F).

An effort was also directed to a study of the effect of carbide particle size as distinct from any quenching strain effect that might modify carbide behavior. Accordingly, two specimens of the most unstable (0.37 aluminum) steel were first quenched after vacuum annealing for 1 hour at 1000 degrees Cent. (1830 degrees Fahr.). One specimen was annealed ½ hour and the other for 125 hours at 710 degrees Cent. (1310 degrees Fahr.), a temperature where the carbides were previously found to be stable and where a marked difference in carbide size could be obtained as a result of varying the time at temperature.

The samples were then treated for graphitization by tempering for 125 hours at 630 degrees Cent. (1165 degrees Fahr.) in the lead bath. The very small amount of graphite formed is readily noted from the microstructures (Figs. 7C, G and D, H). However with the omission of the 710 degrees Cent. (1310 degrees Fahr.) treatment complete graphitization would have occurred, as shown in Figs. 5B or 5D.

The results indicated that particle size was not important. However, it was considered that even ½ hour at 710 degrees Cent. (1310 degrees Fahr.) might render the carbides sufficiently large so as to have a stabilizing effect. Hence the study was extended to 1000 degrees Cent. (1830 degrees Fahr.) water quenched samples of 0.07 and 0.37 aluminum and 0.30 manganese steels tempered for ½ hour at 710 degrees Cent. (1310 degrees Fahr.) and 5 hours at 400 degrees Cent. (750 degrees Fahr.). It was assumed that stress relief would probably be complete in both cases but that the specimens pretempered at 400 degrees Cent. (750 degrees Fahr.) would insure

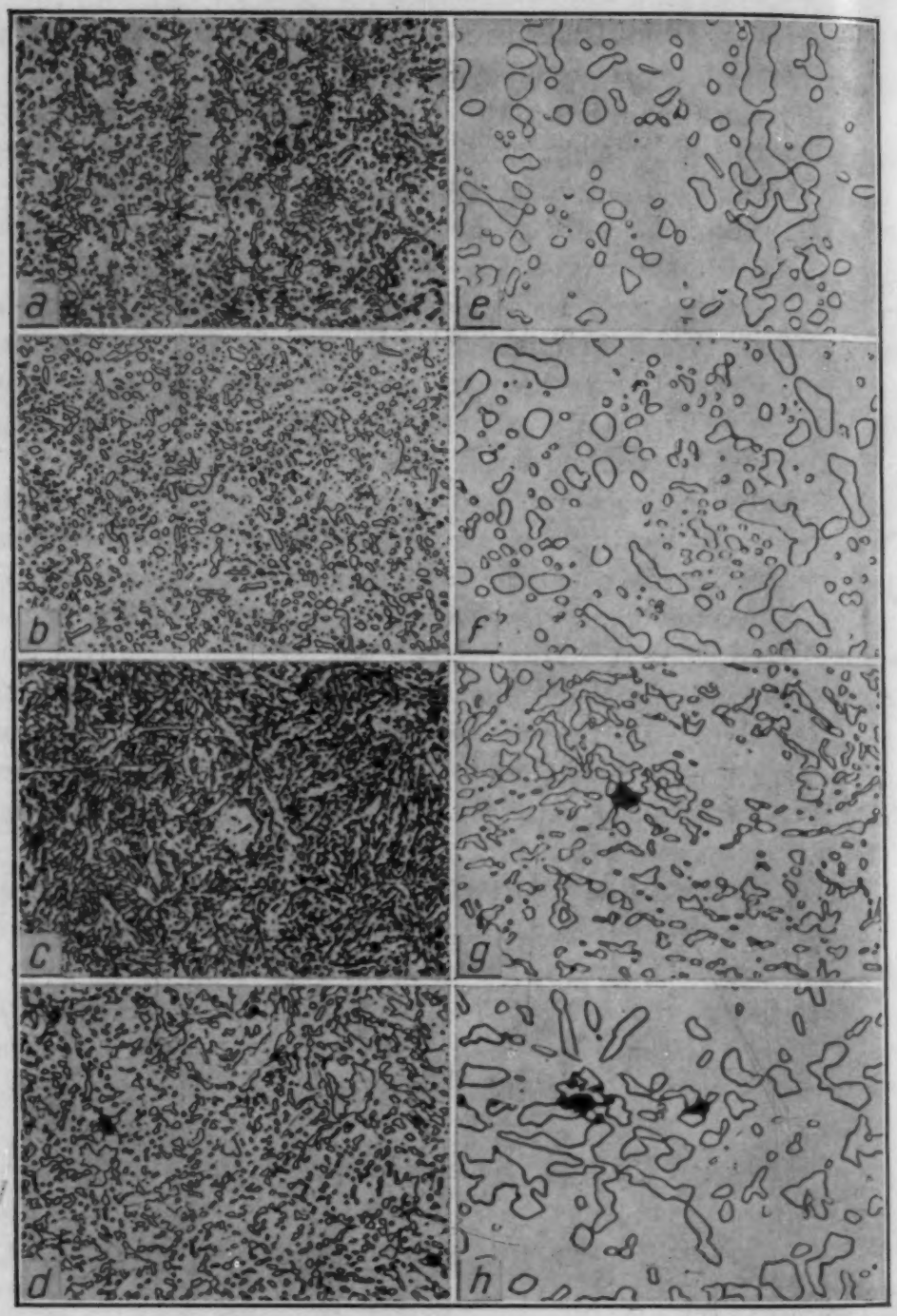

Fig. 7—Microsections of High Aluminum and Manganese Steels All Tempered at 630 Degrees Cent. For 125 Hours, After Pretreatment Indicated.

Tempered in As Received or Spheroidized Condition—0.37 Aluminum: a—× 250; e—× 1000. 0.30 Manganese: b—× 250; e—× 1000. Quenched After 1 Hour at 1000 Degrees Cent. and Pretempered ½ Hour at 710 Degrees Cent. 0.37 Aluminum: c—× 250; g—× 1000. Quenched After 1 Hour at 1000 Degrees Cent. and Pretempered 125 Hours at 710 Degrees Cent. 0.37 Aluminum; d—× 250; h—× 1000.

very fine carbide size at a nongraphitizing temperature, and at a nongraphite nucleating temperature.

The samples were then further tempered at a temperature where previous studies had indicated maximum carbide instability. In the 0.07 aluminum sample 125 hours at 550 degrees Cent. (1020 degrees Fahr.) was used and for the 0.37 aluminum and 0.30 manganese

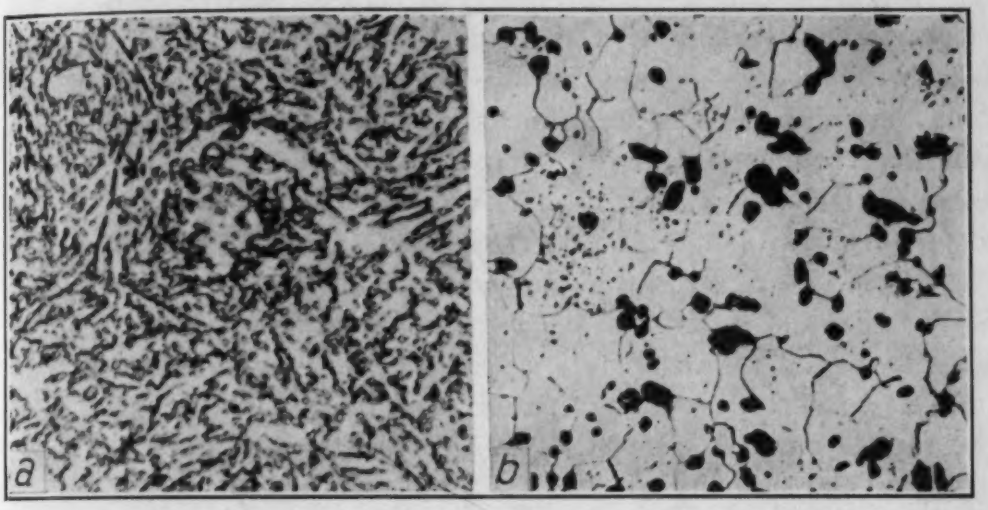

Fig. 8—Microsections of the 0.07 Per Cent Aluminum Steel Quenched From 1 Hour at 1000 Degrees Cent and Then Tempered as Indicated.
a—Pretempered ½ Hour at 710 Degrees Cent and Then 125 Hours at 550 Degrees Cent. × 500. b—Pretempered 5 Hours at 400 Degrees Cent. Then 125 Hours at 550 Degrees Cent. × 250.

steels 630 degrees Cent. (1165 degrees Fahr.) was selected.

With the high aluminum alloy the 710 degrees Cent. (1310 degrees Fahr.) pretreatment apparently again tended to stabilize the carbide although the amount of graphitization was greater than that observed in Fig. 7C. With the 400 degrees Cent. (750 degrees Fahr.) pretreatment the alloy exhibited practically complete graphitization after 125 hours at 630 degrees Cent. (1165 degrees Fahr.). The same general characteristics were observed in the 0.07 per cent aluminum steel which was tempered for 125 hours at 550 degrees Cent. (1020 degrees Fahr.). With a pretreatment at 710 degrees Cent. (1310 degrees Fahr.) the cementite was stabilized (Fig. 8A), but with the 400 degrees Cent. (750 degrees Fahr.) pretreatment almost complete graphitization resulted (Fig. 8B). Graphitization occurred in both samples of the 0.30 per cent manganese steel but the amount of carbide decomposition was markedly greater in the 400 degrees Cent. (750 degrees Fahr.) pretreated sample.

Thus the results obtained would seem to indicate that steels possessing an extremely small carbide particle size are much less stable and hence prone to graphitization at subcritical temperatures than those more coarsely spheroidized.

Effect of Strain on Graphitization

Since graphitization was found to be associated with quenched steels, some observations were made on the effect of strain on carbide stability during tempering. A small cylinder of the 0.37 per cent aluminum steel in the commercially annealed spheroidized state was deformed on the round surface and on one end by a Brinell hardness penetrator. The sample was then annealed for 125 hours at 630 degrees Cent. (1165 degrees Fahr.).

Prior to heat treatment the structure was similar to that shown in Figs. 7A and E, whereas after the anneal it appeared as shown in Fig. 9. Fig. 9A illustrates the appearance of an unetched longitudinal section which bisects the two Brinell impressions. The half of the sample omitted from Fig. 9A was practically free of graphite. The size and quantity of graphite formed appear to depend on the degree of cold working. These characteristics are well illustrated by Figs. 9C, D, and E. Immediately under the impression the unchanged carbides are followed by very coarse graphitization (Fig. 9C), then by complete graphitization (Fig. 9D), and finally by an unchanged structure (Fig. 9E) at a location where the strain ceased to be effective, or possibly where strain was absent. These observations suggest a critical strain for maximum graphitization.

It is of interest to record that when manganese, silicon, copper, nickel, and chromium steels, containing approximately ½ per cent of alloy, were cold worked and annealed similarly to the high aluminum steel, graphite formed only in the manganese steels. Graphite was also absent from the plain carbon steel. It appears that strain alone will not cause the cementite to decompose. However, when strain occurs in the presence of moderate amounts of aluminum or manganese, cementite becomes unstable.

Thus it is evident that a stressed condition may have a profound accelerating effect on graphitization. Further evidence illustrating this fact is shown in Fig. 9B at 7 diameters magnification in a sample of the 0.07 per cent aluminum steel. When this specimen was heated for 125 hours at 630 degrees Cent. (1165 degrees Fahr.)

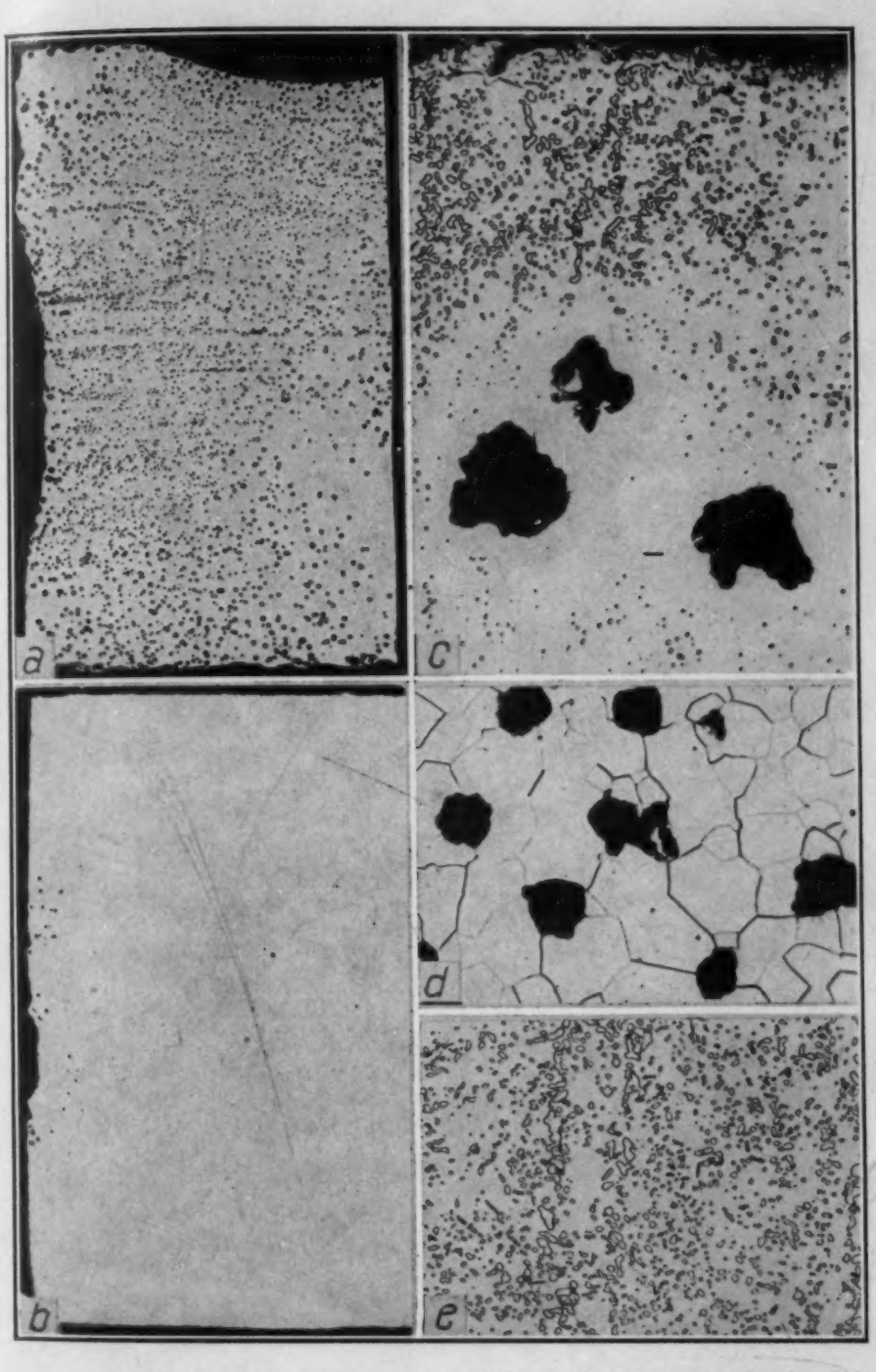

Fig. 9—Longitudinal Sections of 0.37 Also 0.07 Aluminum Steels, Deformed With Brinell Impression in the As Received Spheroidized Condition, and Then Tempered 125 Hours at 630 Degrees Cent.

0.37—Aluminum: a—One-Half Sample Showing Graphite Unetched and Two Brinell Impressions. × 7; c—Etched Edge Near Impression. × 250; d—Some Distance From Edge. × 250; e—Much Further From Impression—Unstressed. × 250. 0.07 Aluminum: b—Unetched Section Showing Graphitization Near Stencil Mark. × 7.

in a lead bath, without any previous hardening treatment graphite formed near two stencil marks.

In order to confirm and extend these observations, studies were also made on cold deformed bars of the 0.37 aluminum and 0.30 manganese steels. Pieces of the ⅜-inch diameter bars in the as received spheroidized condition, were bent cold into circles around a 2-inch diameter mandril. An arc was cut from each of the two steel

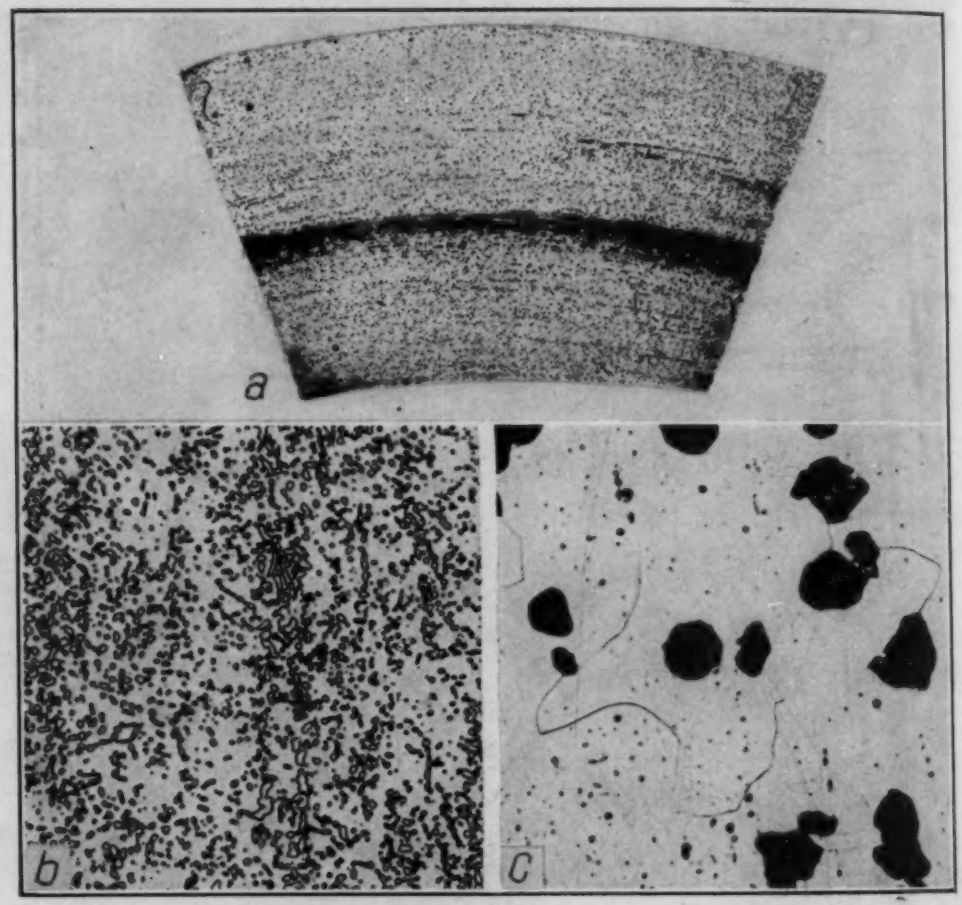

Fig. 10—Sections Showing Effect of Strain on Graphitization on the 0.37 Aluminum Steel Tempered in As Received, Spheroidized, But Strained Condition For 125 Hours at 630 Degrees Cent.
a—Etched Macrosection. × 5. Showing Stable Neutral Axis; b—Etched Section on Neutral Axis. × 250; c—Etched Section in Strained Area. × 250.

samples and tempered for 125 hours at 630 degrees Cent. (1165 degrees Fahr.) in covered lead. Unstressed samples were included as check tests. Longitudinal sections were cut and examined for macro- and microstructure.

A light picral etch clearly defined the neutral axis of the aluminum bar on account of the staining of the cementite and freedom

from graphitization. (Fig. 10A at 5 diameters). A fine line defining the neutral axis could also be observed in the manganese steel but it was not possible to reproduce the appearance in macro form. The limited amount of graphitization in the centre zone could be noted however at 50 diameters. The microstructures of the aluminum steel at the unstressed neutral axis (Fig. 10B) and the stressed area (Fig. 10C) clearly confirm the unstabilizing effect of strain on the carbides.

Vacuum Homogenization and Graphitization

Boyles (4) and Boegehold (5) have shown that the presence of hydrogen in the furnace atmosphere during the melting of cast iron may retard the formation of graphite during solidification, and also during the malleableizing anneal. Since the steels studied in the present investigation were melted and solidified in a hydrogen atmosphere, it was thought that sufficient hydrogen might have been retained during the fabrication process to prevent some of the alloying elements such as silicon, nickel, and copper from promoting graphitization during the tempering treatment. These elements are known to promote graphitization in malleable iron.

In an attempt to evaluate the possible effect of hydrogen on graphitization, samples of the various steels were subjected to one or other of the following combined heat treatments.

1. Hardening the as received steel after 1 hour in vacuum at 1000 degrees Cent. (1830 degrees Fahr.), and tempering in carbon covered lead bath.
2. High temperature homogenization in vacuum, followed by hardening after 1 hour in vacuum at 1000 degrees Cent. (1830 degrees Fahr.) and tempering in a carbon covered lead bath.
3. High temperature homogenization in vacuum, followed by hardening after 1 hour in vacuum at 1000 degrees Cent. (1830 degrees Fahr.), and tempering in vacuum.
4. Hardening the as-received steel after 1 hour in vacuum at 1000 degrees Cent. and tempering in vacuum.

The high temperature homogenization consisted of heating the specimens for 20 hours at 1025 degrees Cent. (1875 degrees Fahr.) followed by 12 hours at 1125 degrees Cent. (2055 degrees Fahr.), and then oil quenching the samples after furnace cooling to 1025 degrees Cent. (1875 degrees Fahr.). The "vacuum" pressure dur-

ing treatment was approximately 0.1 millimeters mercury.

Vacuum tempering was conducted at a mercury pressure of about 0.05 millimeters. Specimens were water quenched after all tempering treatments.

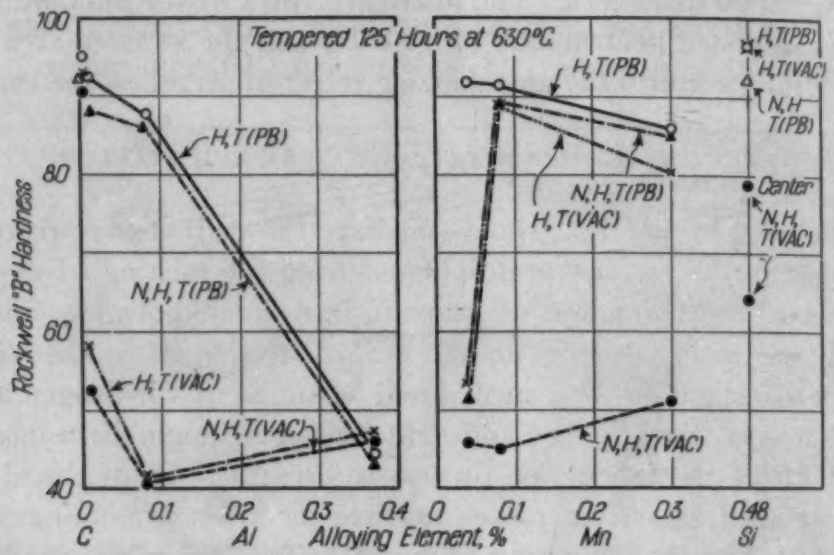

Fig. 11—Relation Between Alloy Content and Hardness of Carbon, Aluminum, Manganese and Silicon Steels, After the Four Different Combinations of Heat Treatment Listed on Page 14.
N—Normalized or Homogenized in Vacuum at 1025 and 1125 Degrees Cent. H—Water Quench After 1 Hour in Vacuum at 1000 Degrees Cent. T (Pb)—Tempered 125 Hours in Covered Lead. T (Vac.)—Tempered 125 Hours in Vacuum.

The eight steels initially selected for the various treatments were as follows:

Plain Carbon 0.48 per cent Silicon
0.01, 0.07 and 0.37 per cent aluminum
0.04, 0.08 and 0.30 per cent manganese

The results of the listed treatments on the hardness after tempering for 125 hours at 630 degrees Cent. (1165 degrees Fahr.) are shown plotted in Fig. 11. The letter "N" signifies high temperature homogenization or "normalizing", "H" indicates the hardening quench after 1 hour at 1000 degrees Cent. (1830 degrees Fahr.) and the (Pb) or (Vac.) following "T" for tempering designates whether tempering was conducted in lead or in vacuum. Examination of these data permit the following conclusions:

a. The hardness of the plain carbon steel was approximately 90 Rockwell B after all treatments, indicating complete carbide stability.
b. The hardness of the high (0.37 per cent) aluminum steel

was about 45 Rockwell B after all treatments, indicating complete carbide instability, or graphitization.

c. The low aluminum steels (0.01 and 0.07) showed carbide stability on tempering in lead and either marked or complete graphitization on tempering in vacuum. The vacuum homogenization at high temperature appears to have little effect on subsequent carbide stability on tempering.

d. With the silicon steel the only treatment favorable to graphitization consisted of the triple vacuum treatment No. 3.

e. The triple vacuum treatment No. 3 caused almost complete graphitization in each of the three manganese steels whereas if the high temperature vacuum treatment was omitted the carbides were fairly stable, whether the tempering was conducted in lead or vacuum. The low 0.04 manganese steel however did not follow this generalization.

The possibility that these so-called vacuum treatments listed under Nos. 2 and 3, as well as under No. 4 caused the introduction of oxygen into the alloys will be discussed later.

In order to ascertain if the high temperature vacuum homogenization, or the vacuum tempering, would similarly profoundly affect the carbide stability of the steels containing nickel, copper, chromium, sulphur, tin, and small amounts of silicon, samples of these specimens were subjected to treatment No. 3 which has been recorded as follows: High temperature homogenization or normalizing in vacuum followed by hardening after 1 hour in vacuum at 1000 degrees Cent. (1830 degrees Fahr.), and tempering in vacuum.

Specimens of plain carbon high aluminum and high silicon steels were also included to check the results already described. However, in addition to the series of tests tempered for 125 hours at 630 degrees Cent. (1165 degrees Fahr.), an additional series was treated for 125 hours at 710 degrees Cent. (1310 degrees Fahr.), a temperature just under the critical where all previous studies had demonstrated carbide stability for all steels.

The hardness data from the 630 degrees Cent. (1165 degrees Fahr.) tests have been plotted in the upper half of Fig. 12 and those for 710 degrees Cent. (1310 degrees Fahr.) in the lower half of the same chart. At 630 degrees Cent. (1165 degrees Fahr.) the check specimens of carbon, high aluminum, and high silicon may be noted to react in essentially the same manner as depicted in Fig. 11. However, a more uniform hardness was obtained in the silicon steel

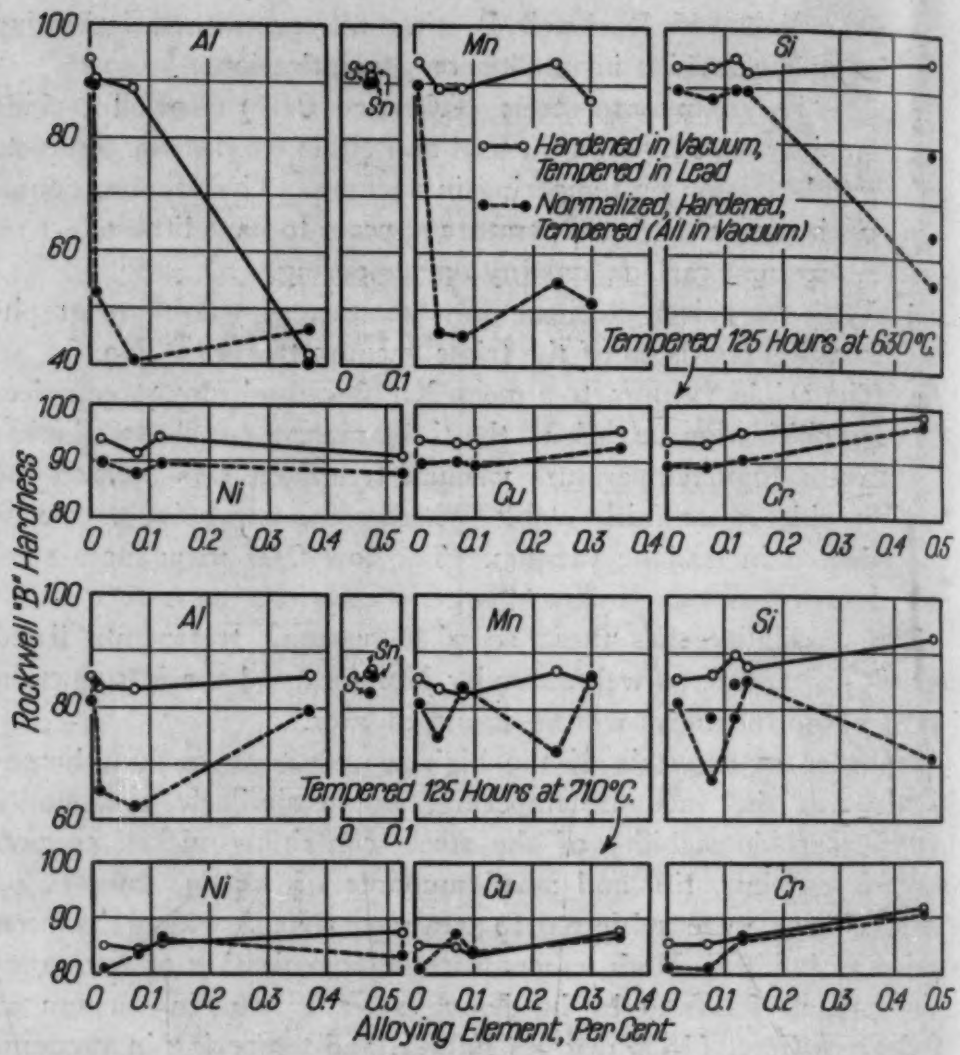

Fig. 12—Relation Between Alloy Content and Hardness of All the Steels After Tempering.

Series 1—(o———o) Hardened From 1 Hour in Vacuum at 1000 Degrees Cent and Tempered in Covered Lead at 630 or 710 Degrees Cent. Series 2—(o - - - - o) Normalized or Homogenized in Vacuum at 1025 and 1125 Degrees Cent., Then Hardened From 1 Hour in Vacuum at 1000 Degrees Cent. and Tempered in Vacuum at 630 or 710 Degrees Cent.

after the "check" heat treatment since no hard spot was present in the center of the sample. The "check" sample had a lower average hardness because of the absence of hard spots.

For purposes of comparison, the data obtained by hardening from 1 hour in vacuum at 1000 degrees Cent. (1830 degrees Fahr.) and subsequently tempering in covered lead, and published previously, have also been included in the charts for both the 630 and the 710 degrees Cent. (1165 and 1310 degrees Fahr.) temper.

It is quite evident from the 630 degrees Cent. (1165 degrees

Fahr.) curves that the triple all vacuum treatment produces a marked softening in all the aluminum manganese and silicon alloys, but that the difference is only slight with the nickel copper and chromium steels and for the sulphur and tin steels.

One other point should also be emphasized. The substitution of vacuum tempering (T. Vac.) for the oxygen free lead bath (T. Pb) has a profound effect on acceleration of graphitization of the low aluminum alloys (see Fig. 11).

In the previous publication on these steels attention was directed to the stability of the carbides on tempering at 710 degrees Cent. (1310 degrees Fahr.), including even the 0.37 aluminum alloy. However, with the triple vacuum treatment the aluminum manganese and silicon alloys all exhibit definite softening as a result of graphitization. Little or no effect can be seen in the nickel, copper or chromium steels (Fig. 12).

All treated alloys were examined under the microscope. Consider first the alloys tempered for 125 hours at 630 degrees Cent. (1165 degrees Fahr.). When hardened from 1000 degrees Cent. (1830 degrees Fahr.) and tempered in a lead bath the 0.37 aluminum alloy alone showed complete absence of carbide. The other aluminum and the manganese steels showed only small amounts of graphite, with the 0.30 per cent manganese alloy being least stable. These metallographic observations correlate with the hardness data in Fig. 11.

On triple vacuum treating, the steels containing 0.07 and 0.37 aluminum, 0.04 and 0.08 manganese were completely graphitized, while the 0.01 aluminum, 0.24 and 0.30 manganese and 0.48 silicon steels contained only a small amount of carbide. Typical examples of these structures can be noted in Fig. 13 where the degree of graphitization is best gaged by the relative absence of carbide in the etched sections.

The nickel, copper and chromium alloys were practically free from graphite after either of the above treatments.

Consider now the alloys tempered for 125 hours at 710 degrees Cent. (1310 degrees Fahr.). All the alloys hardened from 1000 degrees Cent. (1830 degrees Fahr.) and tempered in lead were free from graphite. On subjecting to the triple vacuum treatment, the aluminum, manganese and silicon steels undergo some softening beyond that resulting from carbide spheroidization but the apparent amount of graphite formed is much less than that obtaining at 630

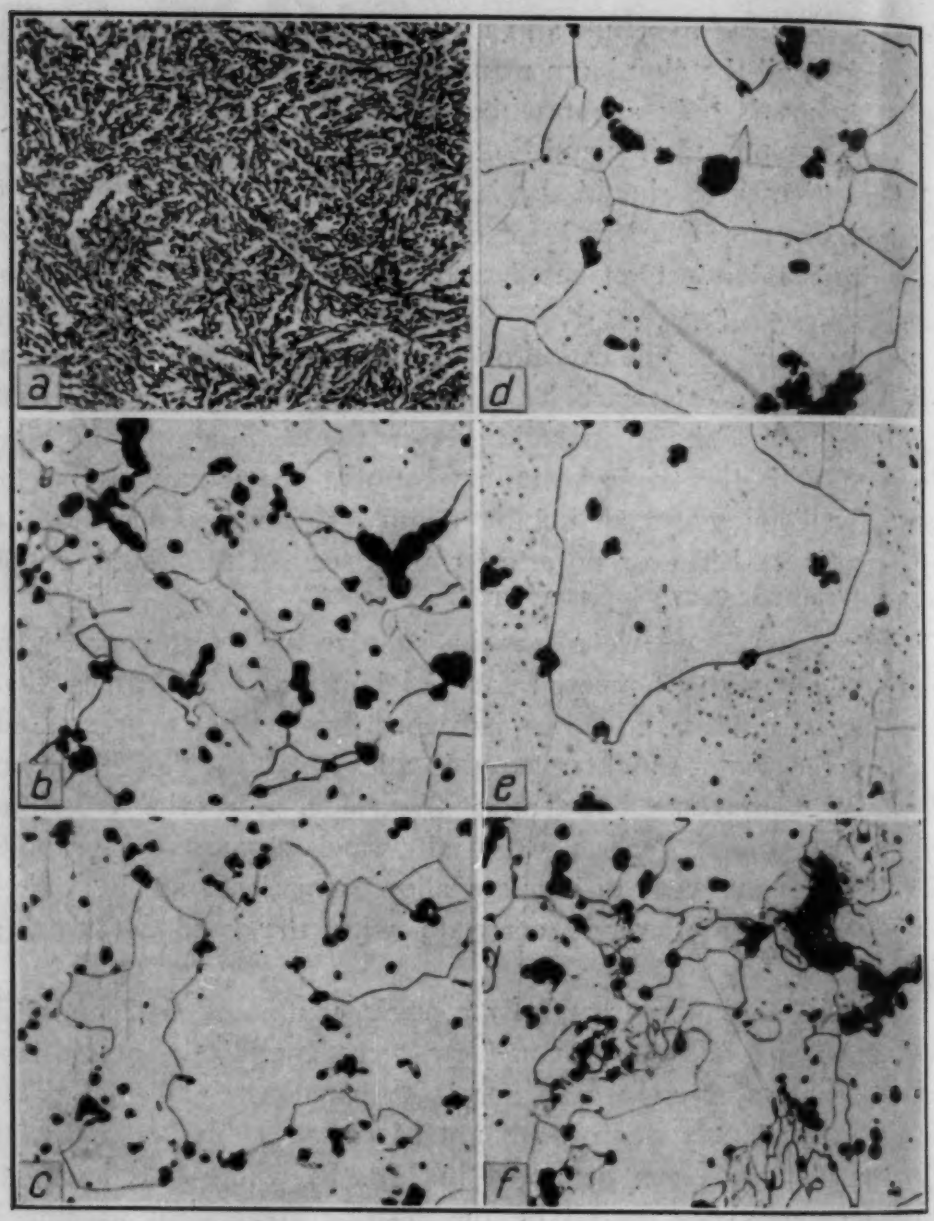

Fig. 13—Microsections of Carbon, Aluminum, Manganese and Silicon Steels After a Triple Vacuum Treatment. Homogenized at 1025 and 1125 Degrees Cent., Water Quenched From 1000 Degrees Cent. and Vacuum Tempered 125 Hours at 630 Degrees Cent. × 250.

a—Carbon; b—0.07 Aluminum; c—0.37 Aluminum; d—0.08 Manganese; e—0.30 Manganese; f—0.48 Silicon.

degrees Cent. (1165 degrees Fahr.). With copper, nickel and chromium the vacuum treatments again appear to have little effect on unstabilizing the carbides.

An interesting point was observed in this last series of tests at 710 degrees Cent. (1310 degrees Fahr.), when the triple vacuum

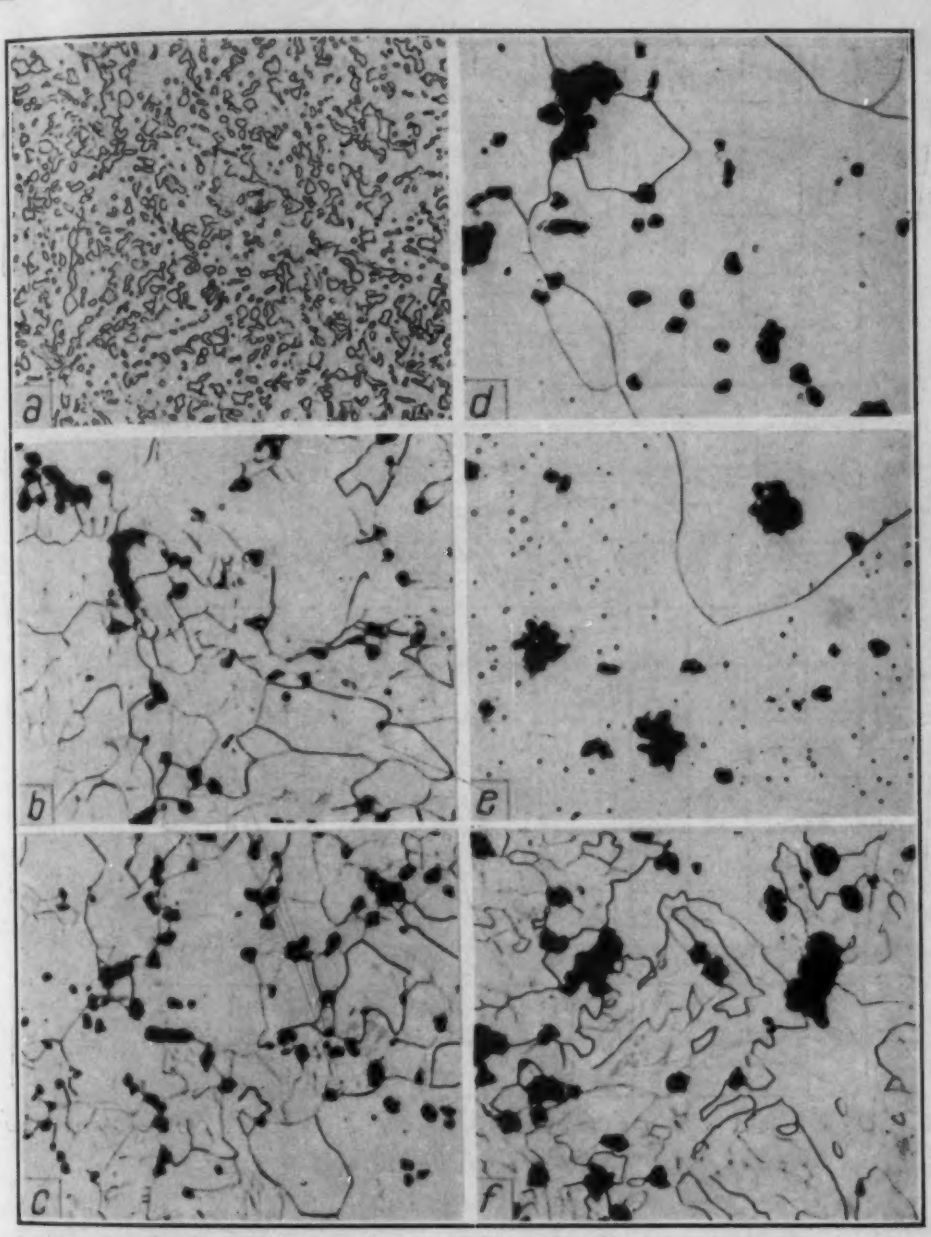

Fig. 14—Microsections of Carbon, Aluminum, Manganese and Silicon Steels After a Triple Vacuum Treatment. Homogenized at 1025 and 1125 Degrees Cent., Hardened From 1 Hour in Vacuum at 1000 Degrees Cent. and Vacuum Tempered 125 Hours at 710 Degrees Cent. × 250.
a—Carbon; b—0.07 Aluminum; c—0.37 Aluminum; d—0.08 Manganese; e—0.30 Manganese; f—0.48 Silicon.

treated alloys were examined under the microscope. The hardness data (Fig. 12 lower half) suggest only partial or limited graphitization of the aluminum, manganese and silicon steels whereas metallographic examination showed that all the aluminum alloys, the 0.04 and 0.08 manganese and the 0.48 silicon steels were completely graphitized, while a large amount of graphite and little free cementite

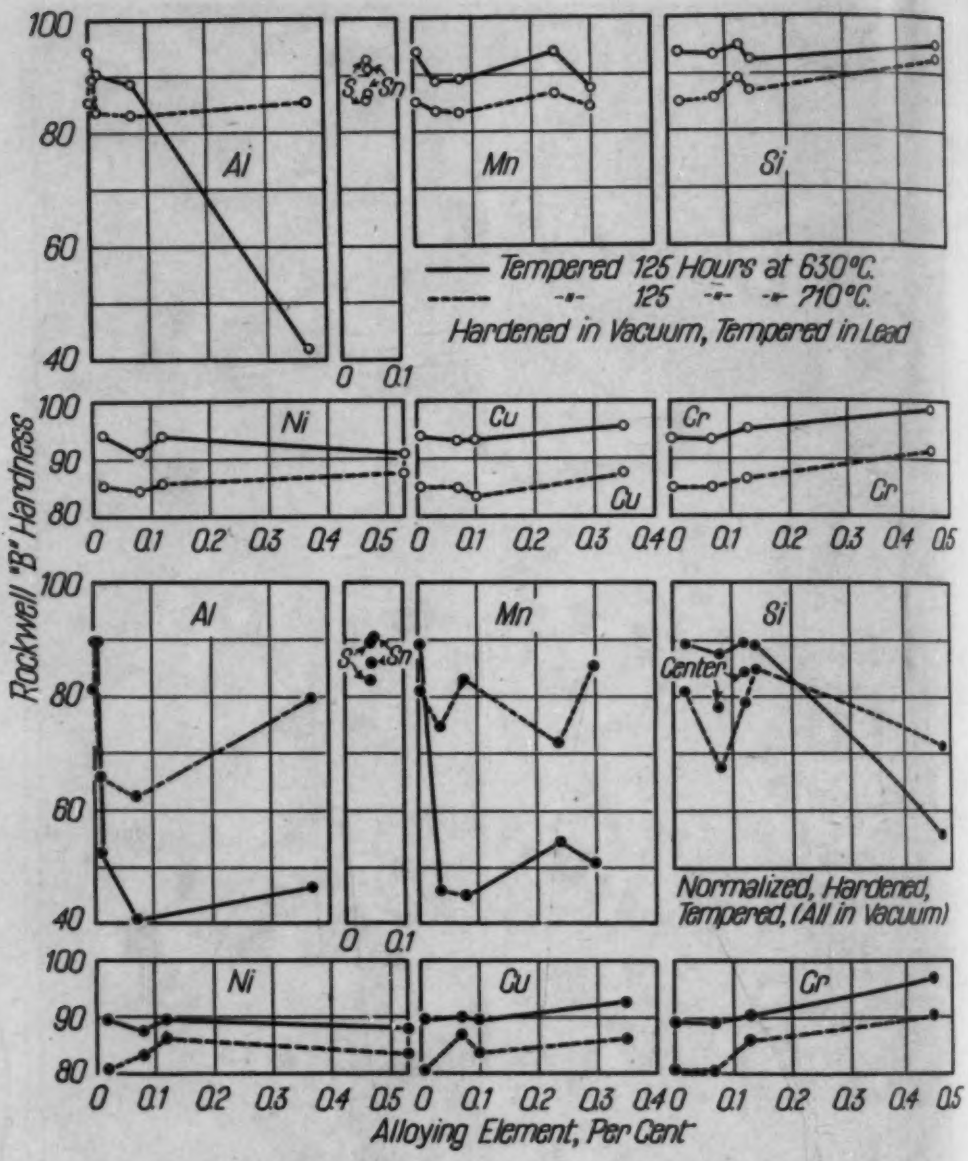

Fig. 15—Relation Between Alloy Content and Hardness of All the Steels After Tempering.

Series 1—Hardened in Vacuum and Tempered in Lead. Series 2—Normalized or Homogenized in Vacuum at 1025 and 1125 Degrees Cent. Then Hardened From 1 Hour in Vacuum at 1000 Degrees Cent. and Tempered in Vacuum. o——o Tempered 125 Hours at 630 Degrees Cent. o- - - -o Tempered 125 Hours at 710 Degrees Cent.

were present in 0.24 and 0.30 manganese and the 0.08 silicon steels. The structures of some of the alloys are shown in Fig. 14.

It has not been established why such high hardness values persist in the steels after complete graphitization even though all specimens were quenched from the tempering graphitizing temperature.

In order to depict more clearly the relative effect of tempering at 710 degrees Cent. (1310 degrees Fahr.) as compared with 630

degrees Cent. (1165 degrees Fahr.) the hardness data have been assembled in Fig. 15, for both the normal harden and temper in covered lead and for the triple vacuum treatment. The figures are self explanatory but the marked effect of tempering temperature on the hardness of the aluminum, manganese, and silicon steels, when given the vacuum treatment, is very clearly shown.

General Comments

The present investigation has supplied additional information to demonstrate that factors which promote carbide decomposition at subcritical temperatures may be quite different from those that are known to act at temperatures lying in the critical range. Chemical elements such as nickel and copper, known to make cementite unstable at temperatures above the lower critical, have little effect on graphitization at temperatures below the critical. The strongly graphitizing element, silicon, exhibits similar characteristics.

Manganese which is usually regarded as a carbide stabilizer appears to accelerate carbide decomposition on prolonged tempering below the critical range.

Attention has also been directed to the effect of the amount of alloying element on the temperature where graphitization takes place most readily. Thus the temperature of maximum graphitization of the 0.07 aluminum steel is about 550 degrees Cent. (1020 degrees Fahr.) whereas with 0.37 per cent aluminum complete breakdown of the carbide is obtained within the temperature range of 590 and 630 degrees Cent. (1095 and 1165 degrees Fahr.) after 55 hours. For the steel of manganese content most prone to graphite formation, (0.30 per cent), tempering at 630 degrees Cent. (1165 degrees Fahr.) has been established as the optimum temperature.

Despite these comments it must be emphasized that the nature and amount of alloying element provide only the basic steel in which it may be possible to develop graphitization by tempering. Carbide size and strain must also be considered. Thus none of the alloys herein discussed will graphitize appreciably even after 125 hours at subcritical temperatures if the steel is free from strain and if the carbide particle size is similar to that observed after a commercial spheroidizing treatment. However, even under these conditions it has been shown that the 0.37 aluminum alloy may be graphitized

when tempering is conducted in an environment different from that obtaining in an oxygen-free lead bath.

Although an attempt has been made to separate the effects dependent on carbide size from those produced by strain, it is difficult

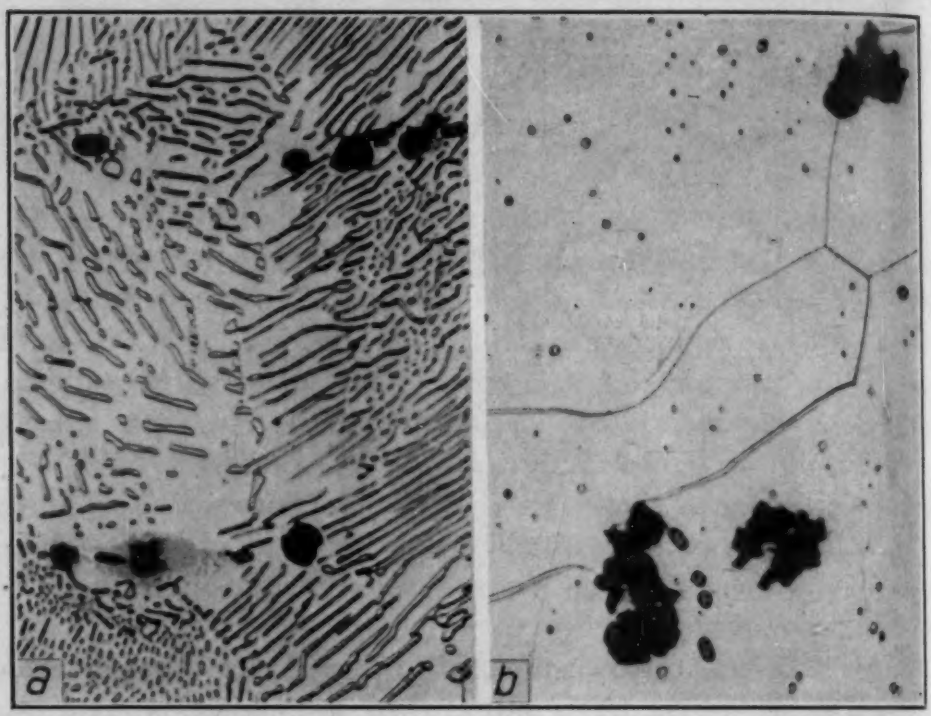

Fig. 16—Microsections of 0.37 Manganese Steel Illustrating Location of Graphite With Reference to Manganese Sulphide. × 1000.
a—Slowly Cooled From 1125 Degrees Cent. Vacuum Treatment. b—Tempered 125 Hours at 630 Degrees Cent. After Hardening.

to entirely insure isolation of one factor from the other. Furthermore, when a piece of steel is quenched, submicroscopic cracks may be formed which present locations favorable for the formation of graphite. This feature will be discussed more fully in a subsequent research on the graphitizing behavior of commercial steels.

One further point, regarding the unanticipated effect of manganese on tending to render the carbides unstable, may be noted. Etched microsections reproduced in Fig. 16 illustrate the fact that graphite formation appears to be associated with manganese sulphide inclusions. Fig. 16a shows this characteristic in the 0.30 manganese steel, containing 0.019 per cent sulphur, when slowly cooled from above the critical range, while Fig. 16b exhibits the close association between manganese sulphide inclusion and graphite location in the same steel when hardened and then tempered at 630 degrees Cent.

It is interesting to note that sulphur, *per se,* does not promote graphitization, for the sulphur steel, containing 0.048 of that element, or two to three times the amount present in the manganese alloy, did not graphitize. This appears to differentiate between the effect of manganese sulphide as compared with iron sulphide.

One of the most striking results obtained in these studies on graphitization developed from the substitution of so-called vacuum tempering for treatment in oxygen-free covered lead, and the addition of the prolonged high temperature vacuum anneal prior to hardening. It has been pointed out that the authors considered that residual hydrogen might have stabilized the carbides since the high aluminum alloy alone exhibited graphitizing behavior (2) comparable with that found in many commercial hypereutectoid steels (1).

According to Zapffe and Sims (6) and Schwartz and Guiler (7) hydrogen diffused out of steel very readily when the steel was heated at elevated temperatures. Thus it may be assumed that most of the hydrogen in the present alloys was lost during fabricating. Furthermore, since graphitization was accelerated in certain instances by the vacuum treatment below the eutectoid temperature, independent of whether the prior vacuum treatment at 1025 and 1125 degrees Cent. (1875 and 2055 degrees Fahr.) had been used, it cannot be deemed logical to ascribe this marked increase in carbide instability to dehydrogenation.

One of the authors has recently indicated (1) that when an element, aluminum in particular, is present in the steel, the amount of graphitization can be increased by annealing under oxidizing conditions. Thus while modified treatments herein reported are described as "vacuum" treatment, it must be realized that the steels are subjected for long periods to low oxygen pressures. Unpublished data obtained in the laboratory with commercial steels have also shown that intermediate amounts of graphitization occur as a result of "vacuum" treatment compared with the use of oxygen free covered lead and an oxidized lead bath. The latter treatment yields maximum carbide dissociation.

Considering first the data obtained from tempering at 630 degrees Cent. (1165 degrees Fahr.) it may be recalled that the published paper dealing with these pure alloys demonstrated that the high aluminum steel was the only alloy in the series to show much graphitization. By substituting a vacuum temper for oxygen-free lead the lower aluminum and the low manganese alloys are rendered readily

graphitizable. The carbides in all the other alloys are essentially unaffected by the modification of treatment. Thus it would seem that the solution of oxygen under suitable conditions may serve as a potent graphitizing agent.

With the triple vacuum treatment, which merely adds a prior vacuum anneal at 1025 and 1125 degrees Cent. (1875 and 2055 degrees Fahr.) all the manganese and the high silicon steels show practically complete graphitization. Again the other alloys are unaffected.

After tempering at 710 degrees Cent. (1310 degrees Fahr.) the published data (2) have clearly shown that the carbides are stable in all the alloys. By substituting the triple vacuum treatment the picture is entirely changed. While the hardness data (Fig. 12) suggests only moderate graphitization in aluminum manganese and silicon steels. Metallographic examination (see Fig. 14) reveals the following information. Complete graphitization had occurred in all the aluminum steels, in the lower manganese and in the high silicon alloys, while considerable carbide dissociation was also found in the higher manganese and 0.08 silicon steels.

This change in reaction to tempering as a result of change in environment clearly demonstrates that the factors controlling carbide dissociation cannot be limited to alloying element, strain and carbide size. The results of the effect of oxygen penetration can be expected to be revealed to a greater degree when the low temperature vacuum tempering is preceeded by what has been termed the homogenizing anneal above 1000 degrees Cent. (1830 degrees Fahr.) in vacuum. That such is the case is clear from the results of the various experimental procedures outlined.

It may be noted that such oxygen penetration is effective only when the strong deoxidizing elements aluminum, silicon and manganese are present in the steel. Although chromium similarly possesses strong reducing power the high stability of chromium bearing carbides is well known.

As regards the high hardness values noted in some of the graphitized steels Davenport and Bain (8) have demonstrated that a relatively high hardness may result when a low carbon steel is quenched from a temperature close to the A_1 critical point, and aged at room temperature for several days. It is possible that the high hardness value obtained after complete graphitization at 710 degrees

Cent. (1310 degrees Fahr.) followed by water quench may be ascribed to precipitation hardening since several days elapsed between the time of heat treatment and hardness determinations.

Summary

1. Studies on the tendency for graphitization on tempering for prolonged periods at subcritical temperatures have been made on hypereutectoid alloys containing up to about ½ per cent manganese, silicon, nickel, chromium, copper or aluminum and on alloys containing about 0.05 per cent sulphur or tin.

2. When the alloys were quenched to the martensitic structural condition and tempered in an oxygen-free environment, as represented by covered lead, the high aluminum (0.37 per cent) alloy alone showed marked graphitization. It was almost completely graphitized after 75 hours annealing within the temperature range 550 to 630 degrees Cent. (1020 to 1165 degrees Fahr.

3. Experimental investigation of the role played by carbide size and by strain indicates that a fine degree of carbide dispersion or the presence of some critical strain may be required to promote carbide dissociation. Thus the most unstable steel (0.37 per cent aluminum) fails to graphitize on tempering in covered lead when the steel is free from strain and when the carbide size is comparable to that found in a commercially spheroidized high carbon steel.

4. Similarly the diffusion of oxygen into the steel during homogenization or during tempering in an environment of low oxygen pressure may promote graphitization. This phenomenon appears to be dependent on a nucleating effect of certain oxides such as alumina, when present in suitable form or degree of dispersion.

5. The effectiveness of fine carbide size, strain, or oxygen diffusion however, is dependent on the presence of certain elements in the steel. Thus high carbon steels containing aluminum, manganese and silicon may be rendered freely graphitizing. The steels containing the elements, nickel, chromium, copper, sulphur (free from manganese), or tin exhibit resistance to graphitization independent of strain, carbide size, or oxygen penetration.

6. The temperature of maximum graphitization depends on the nature and amount of the alloying element present in the steel.

7. In general, the degree of graphitization is clearly indicated by the hardness of the alloy after tempering even though the sub-

critical heat treatment be followed by a water quench. However, aluminum manganese and silicon alloys may be almost completely graphitized after treatment at 710 degrees Cent. (1310 degrees Fahr.) even though the decrease in hardness is small. This has been ascribed to age-hardening.

ACKNOWLEDGMENT

The authors wish to acknowledge the assistance of J. H. Steeves and L. C. Cavalier who confirmed the effects of strain on graphitization in their senior thesis as students in the Department of Metallurgy.

Bibliography

1. C. R. Austin and B. S. Norris, "Effect of Tempering Quenched Hypereutectoid Steels on the Physical Properties and Microstructure". TRANSACTIONS, American Society for Metals, Vol. 26, 1938, p. 788-845. "Temperature Gradient Studies on Tempering Reactions of Quenched Hypereutectoid Steels", *Transactions*, American Institute of Mining and Metallurgical Engineers, Vol. 131, 1938, p. 349-71.

   C. R. Austin and M. C. Fetzer, "Effect of Composition and Steel Making Practice on Graphitization Below the A^1 of Eighteen 1 Per Cent Carbon Steels", *Transactions*, American Institute of Mining and Metallurgical Engineers, *Metals Technology*, September 1940. "Cementite Stability and its Relation to Grain Size, Abnormality and Hardenability", TRANSACTIONS, American Society for Metals, Vol. 29, 1941, p. 339-354.
2. C. R. Austin and B. S. Norris, "Effects of Small Amounts of Alloying Elements on the Tempering of Pure Hypereutectoid Steels". TRANSACTIONS, American Society for Metals, Vol. 29, 1941, p. 244-68.
3. H. A. Schwartz, "The Conversion of Solid Cementite into Iron and Graphite", *Journal*, Iron and Steel Institute, Vol. 11, 1938, p. 205.
4. A. Boyles, "Freezing of Cast Iron". *Transactions*, American Institute of Mining and Metallurgical Engineers, Vol. 125, 1937, p. 141.
5. A. L. Boegehold, "Some Unusual Aspects of Malleable Iron Melting". TRANSACTIONS, American Society for Metals, Vol. 26, 1938, p. 1084.
6. C. A. Zapffe and C. E. Sims, "Hydrogen, Flakes and Shatter Cracks", *Metals and Alloys*, Vol. 11, Junue 1940, p. 177.
7. H. A. Schwartz and G. M. Guiler, "Hydrogen in Solid White Cast Iron", *Transactions*, American Foundrymen's Association, Vol. XLVII, March 1940, p. 742.
8. E. S. Davenport and E. C. Bain, "The Aging of Steel", TRANSACTIONS, American Society for Metals, Vol. 23, 1935, p. 1047.

DISCUSSION

Written Discussion: By H. A. Schwartz, manager of research, National Malleable and Steel Castings Co., Cleveland.

The authors have adopted a field so far somewhat neglected by the students

of graphitization. No doubt influenced by questions of commercial application, previous investigators have usually dealt with cast irons rather than steels and have frequently given more attention to "first stage graphitization" above the critical temperature. The present publication is particularly timely in view of the developing interest in the graphitizable steels which in principle at least fall within the general carbon concentration range investigated by Austin and Norris.

The reader cannot but be impressed when reading the present paper with the complexity of conditions which determine the graphitizing rate. Many of these factors touched upon by the authors have been given more or less attention by earlier investigators but they have added to the possible effective causes, the question of strain and the question of the size distribution of cementite nuclei. The difficulties underlying a separation of these individual causes and their detailed isolated study is made plain in the paper.

This commentator is particularly pleased to see that attention has been given to the possible effects of hydrogen and oxygen which are fields which his own organization has found worthy of much attention. The observation that temper carbon nodules are sometimes smaller and more numerous near the surface than well within is an observation which has been made previously in connection with the white cast irons; it has not, however, occurred to us before to investigate an area near a cut surface as distinguished from near a cast surface, since we accepted, apparently erroneously, and without sufficient confirmation, the probable explanation that the fineness of grain was related to some condition set up during freezing. Austin and Norris' correlation of this phenomenon with a surface not related to the fabrication of the original material, and hence with the heat treating phenomenon, is of great interest. The observation that graphitizing rate does not always increase with temperature is decidedly surprising and points to a combination of acceleration and retardation causes, all of which are increased with rising temperature, but perhaps in such a manner that retardation is stimulated more than acceleration under particular temperature conditions. With less experienced observers one would be tempted to believe that their temperature recorded as 710 degrees Cent. (1310 degrees Fahr.) was actually above A_1 for at least part of the time and so at a point where graphitization could not go beyond approximately the eutectoid concentration. Had this occurred the microscopic evidence would have been so plain, however, that we are no doubt safe in assuming that investigators familiar in the field would have detected the occurrence immediately.

It is perhaps worth while to refer to the fact that a specimen quickly quenched should be under triaxial tensile stress in the interior. This stress distribution tends to increase the volume of the interior and should therefore favor the graphitizing reaction which is accompanied by an increase in volume. The present commentator is inclined to regard lead baths with some suspicion, being uncertain to what extent they can be kept free from oxides by a carbon covering on their surfaces. Before a difference in behavior between vacuum heat treatments and heat treatments in lead is ascribed to the presence of oxygen in the incomplete vacuum and its absence in the lead bath, perhaps some demonstration should be furnished as to the activity of oxygen in the particular lead bath employed. The authors are wise in recording their facts

and leaving the explanations in a somewhat tentative state. The paper will certainly form a useful contribution to the literature on graphitization.

Authors' Reply

B. S. NORRIS: I should like to make a few comments concerning several of the points that Dr. Schwartz mentioned.

Previous work conducted by the authors on commercial carbon tool steels has shown that a heating at 710 degrees Cent. (1310 degrees Fahr.) does not raise the temperature above the A_1 critical. Steel bars, 12 inches long and ⅜ inch in diameter, were completely hardened and then tempered in a furnace with a temperature gradient ranging from 500 to 800 degrees Cent. (930 to 1470 degrees Fahr.). After soaking for 75 hours, the bars were furnace cooled and then sectioned longitudinally. Hardness and microscopic surveys revealed that minimum hardness and maximum graphitization occurred in the vicinity of 670 degrees Cent. (1240 degrees Fahr.), the hardness became greater and the amount of graphitization smaller with increase in temperature. Pearlite did not appear in the microstructure until the temperature reached approximately 730 degrees Cent. (1345 degrees Fahr.). These results clearly illustrated that graphitization was a maximum at a temperature appreciably below the critical range.

Although some oxygen may be present in the lead bath when it is covered with either charcoal or "lead pot" carbon, it is believed that the quantity of oxygen is too small to exert a noticeable effect on graphitization.

C. R. AUSTIN: As one of the authors of this paper, I should like to say that we are pleased to have the comments of Dr. Schwartz, who is, of course, an authority in this field.

I have not had an opportunity to read his comments and maybe I did not understand all of them in detail, but in one portion, I believe, he refers to the effect of strain on the graphitization. I don't recall just how that was phrased, but I think he refers to the section subject to tensile stress where graphitization may occur more readily.

This effect of strain, as well as the effect of softness of ferrite, we have attempted to study in connection with graphitization of commercial steel. We have this very simple theory. Since graphitization occurs with increase in volume, possibly the observed tendency for graphite formation was some function of the softness of the ferrite matrix. Thus a steel with a rigid or hard ferrite might be expected to exhibit high carbide stability or strong resistance to graphitization.

The results of creep test studies made on commercial steels which were first spheroidized and then subjected to the conventional creep test at 670 degrees Cent. (1240 degrees Fahr.), did not lend confirmation to this hypothesis. No simple correlation could be obtained between creep rate as a measure of resistance to deformation of the ferrite matrix and carbide stability.

The high temperature homogenization tests were considered more from the point of removal of hydrogen. We also considered the fact that perhaps during fabrication there was ample time for hydrogen removal. Of course,

these specimens after casting are heated up for a time and forged and heat treated in various ways, and to some of us there seemed little reason to believe that hydrogen would not be removed. At first we called this a high temperature vacuum treatment. By that I refer to the triple vacuum treatment where the specimen was heated up to about 1160 degrees Cent. (2120 degrees Fahr.) for several hours and then cooled down to 1000 degrees Cent. (1830 degrees Fahr.), quenched, and subsequently graphitized below the eutectoid. But probably it is some homogenization effect, rather than the removal of the hydrogen, that has a role in the effect on graphitization.

Of course, graphitization seems to be accelerated by the presence of aluminum oxide, and there might be some diffusion effects, some state of aggregation, some change in the state of aggregation of the aluminum oxide at those high temperatures which might tend to put the alumina in a form which would favor the graphitization. For instance, in other studies we found that if alumina was added to the ladle, those steels did not graphitize; if alumina was added to the mold, then that same steel apparently graphitized very readily. Consequently, we seem to have fairly good evidence that not only the presence of aluminum oxide but the state of aggregation of this oxide has an important bearing on the subsequent graphitization.

EFFECTS OF INITIAL STRUCTURE ON AUSTENITE GRAIN FORMATION AND COARSENING

By M. Baeyertz

Abstract

Evidence is presented on how and where austenite grains grow as a piece of steel is heated. In 0.45 to 1.00 per cent carbon steels, the formation of austenite grains was found to be influenced by the form of the carbide (lamellar versus spheroidal), while the dendritic pattern of the steel was decisive as to the position where the formation of austenite began. In the pearlitic (lamellar) structures, austenite grain formation was seen to proceed along the direction of the lamellae, so that individual pearlite colonies often resulted in the formation of elongated austenite grains; from spheroidal structures, the austenite grains were equi-axed. In the dendritic pattern, grain formation began in the regions between branches of the dendrites (interbrachial regions), and also in those regions between dendrites (interdendritic regions) that were low in sulphide inclusions. On heating to higher temperatures the grains thus formed were the first to show noticeable coarsening. On the other hand, those interdendritic regions which contained appreciable groups of sulphide inclusions were the last to form austenite and were also the last to coarsen. This relationship to sulphide inclusions indicated a possible connection with an observed behavior in steels higher in sulphur, where it was found that (especially in the cast state) steels treated with aluminum plus sulphur had higher coarsening temperatures than steels treated with aluminum without the added sulphur.

The Beginnings of Austenite Grain Formation

THE structure from which austenite forms is an important factor in determining the manner in which that austenite will coarsen on further heating. This relation was indicated by Grossmann (1)[1] when he showed that prior heat treatment influences the coarsening

[1]The figures appearing in parentheses refer to the bibliography appended to this paper.

A paper presented before the Twenty-third Annual Convention of the Society held in Philadelphia, October 20 to 24, 1941. The author, M. Baeyertz, is associated with the metallurgical division, South Works, Carnegie-Illinois Steel Corp., Chicago. Manuscript received June 14, 1941.

behavior of austenite. Except for the inhibiting action of undissolved particles (oxides, carbides, etc.) which remain in the austenite after its formation, the effect of prior structure would appear to be limited to determining the grain size and shape at the time of formation. It is with these latter aspects of the effect of prior structure that we shall concern ourselves.

Suppose, for example, that we heat a piece of steel composed ferrite-plus-pearlite. The pearlite areas are the first to become austenite, and only when nearly all the pearlite is consumed does the transformation spread to the free ferrite. This phenomenon has been adequately described by Grossmann. (2), (3). Similarly, and probably more commonly recognized, in a hypereutecoid steel with a pearlite-plus-cementite structure, the pearlite becomes austenite first and the solution of the carbide is complete only on reaching the A_{cm} temperature. It, therefore, seems pertinent to examine exactly how austenite grains grow from pearlite, and what are the characteristics of the austenite grain structure so formed. This may be readily done by heating bars of steel in such a way that one end of the bar reaches a temperature above the Ac_3 or the A_{cm} and the other end remains below the Ac_1. In our studies ½ by ½ by 12-inch bars were put in a furnace at 1100 degrees Fahr. (595 degrees Cent.) so that one end protruded about an inch beyond the furnace door. The temperature of the furnace was raised at a rate of approximately 100 degrees Fahr. (40 degrees Cent.) per hour to the desired temperature. The bars were then quenched in water so that any austenite formed on heating would be transformed to martensite or dark etching decomposition products, and could readily be distinguished from the untransformed portions of the structure. Such a specimen affords a continuous series of the structures obtained on heating to the various temperatures along the length of the bar.

Steels with carbon contents of 0.45 to 1.00 per cent were used. The heats had been made with little or no aluminum in the ladle. One or more ingots in each heat were treated with aluminum. Four by 4 or 5 by 5-inch billets from the aluminum treated ingots and from one untreated ingot of each heat were studied. The analyses are given in Table I. The mechanism of the austenite formation was similar regardless of the carbon content or the amount of the aluminum addition, provided that the prior structures were of the same general character. For this reason the following discussion applies to 0.45 to 1.00 per cent carbon steels in general.

Before discussing the formation of austenite from pearlite it seems well to give brief consideration to the structure of pearlite. Pearlite which has formed from a single austenite grain is known to be composed of ferrite grains having a limited number of mutually related orientations, as shown by Mehl and Smith (4). Each pearlite colony as it is sometimes called, that is, the pearlite which has formed from a single nucleus, includes ferrite of a single orientation. Such

Table 1

Steel S.A.E.	Ingot	Pounds Aluminum Added in Ladle	Pounds Aluminum Added in Mold Per Ton	Carbon	Manganese	Phosphorus	Sulphur	Silicon
1045	Untreated	30	None	0.44	0.72	0.031	0.034	0.19
	Al treated	30	1½	0.44	0.72	0.033	0.034	0.19
1055	Untreated	30	None	0.56	0.76	0.020	0.035	0.18
	Al treated	30	1	0.55	0.76	0.020	0.035	0.18
1075	Untreated	None	None	0.76	0.64	0.015	0.024	0.23
	Al treated	None	1½	0.75	0.64	0.015	0.024	0.21
1095	Untreated	25	None	1.01	0.36	0.021	0.031	0.35
	Al treated	25	¾	1.00	0.36	0.020	0.030	0.34
1060	No. 15	None	None	0.58	0.86	0.014	0.024	0.14
	16	None	¼	....	....	.....	.....	....
	17	None	½	....	....	.....	.....	....
	18	None	1	....	....	.....	.....	....
	19	None	2	....	....	.....	.....	....

a division of the pearlite into colonies, as evidenced by the direction and continuity of the lamellae, is a matter of common observation and may be seen by way of example in Figs. 1 and 2. In relatively coarse pearlites, with suitable magnification after etching in 2 per cent nital, it is possible to distinguish the ferrite grain boundaries which separate the pearlite colonies. An example is shown in Fig. 3. That these ferrite grain boundaries are indeed the boundaries between ferrite of different orientations is indicated by the roughening of the ferrite on etching, as illustrated by Fig. 4. In the pearlite colony on the right of the photomicrograph the ferrite has roughened more than that of the colony at the left in which the cementite lamellae emerge at very wide angle. A further proof of the identity of orientation of the ferrite lamellae in each pearlite colony is obtained on heating pearlite to a temperature sufficiently high to spheroidize the cementite without the formation of austenite. The pearlite colony then becomes a single ferrite grain in which the cementite spheroids are embedded. This may be seen in the spheroidized portion of Fig. 5.

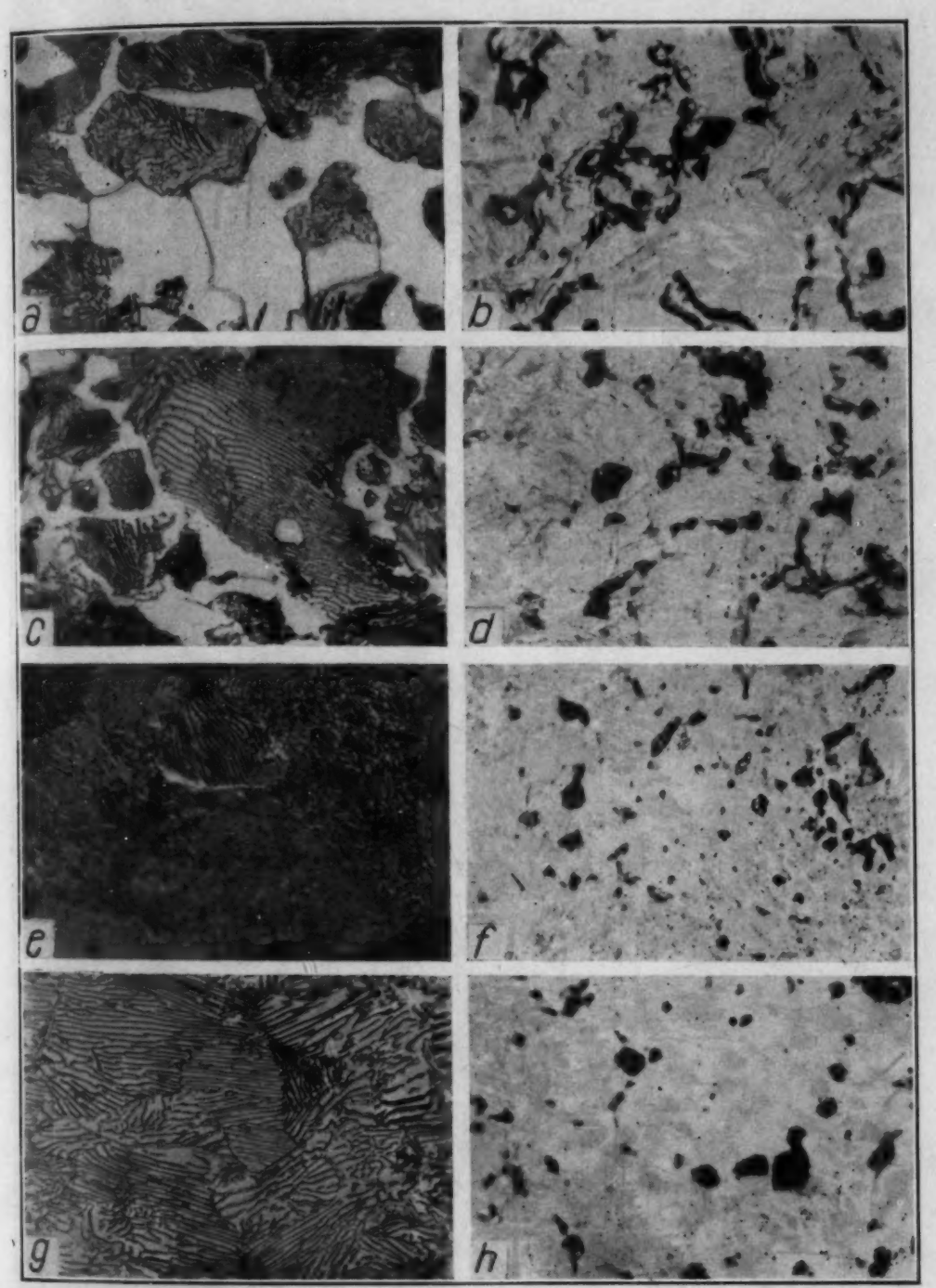

Fig. 1—Comparison of Pearlite Colony Size and Uncoarsened Austenite Grain Size Formed on Heating Pearlite. Austenite Grains in Photomicrographs at Right Outlined by Ferrite and Fine Pearlite or by Fine Pearlite. × 500. a and b, S.A.E. 1045; c and d, S.A.E. 1055; e and f, S.A.E. 1075; g and h, S.A.E. 1095.

Even in quite fine pearlites it is possible to discern the ferrite grain boundaries between colonies by selecting areas at which the lamellae

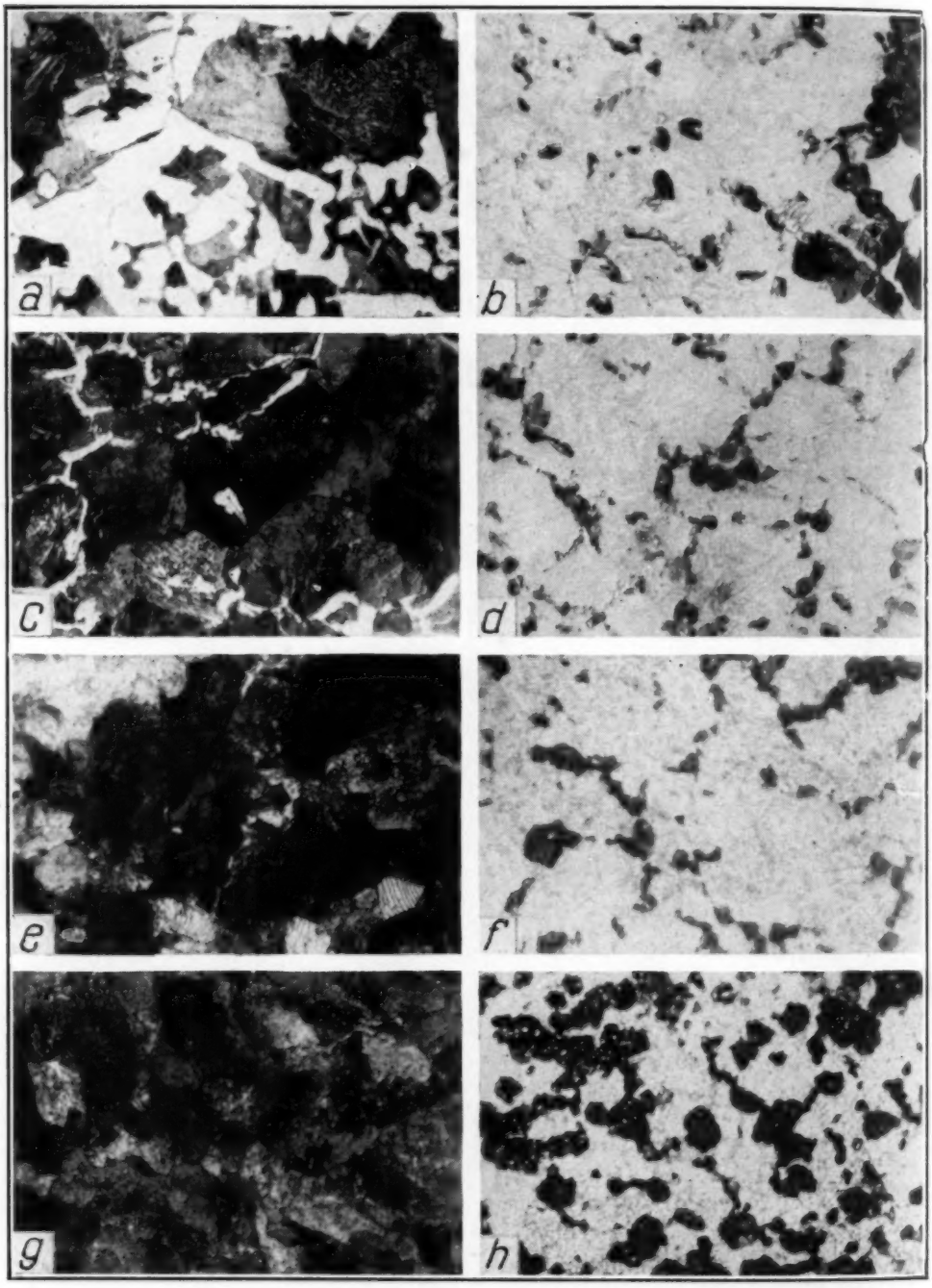

Fig. 2—Comparison of Pearlite Colony Size and Uncoarsened Austenite Grain Size Formed on Heating Pearlite. Austenite Grains in Photomicrographs at Right Outlined by Ferrite and Fine Pearlite or by Fine Pearlite. × 500. a and b, S.A.E. 1045; c and d, S.A.E. 1055; e and f, S.A.E. 1075; g and h, S.A.E. 1095.

emerge at a wide angle, as for example in the center of Fig. 6.

Turning now to the formation of austenite from pearlite, it

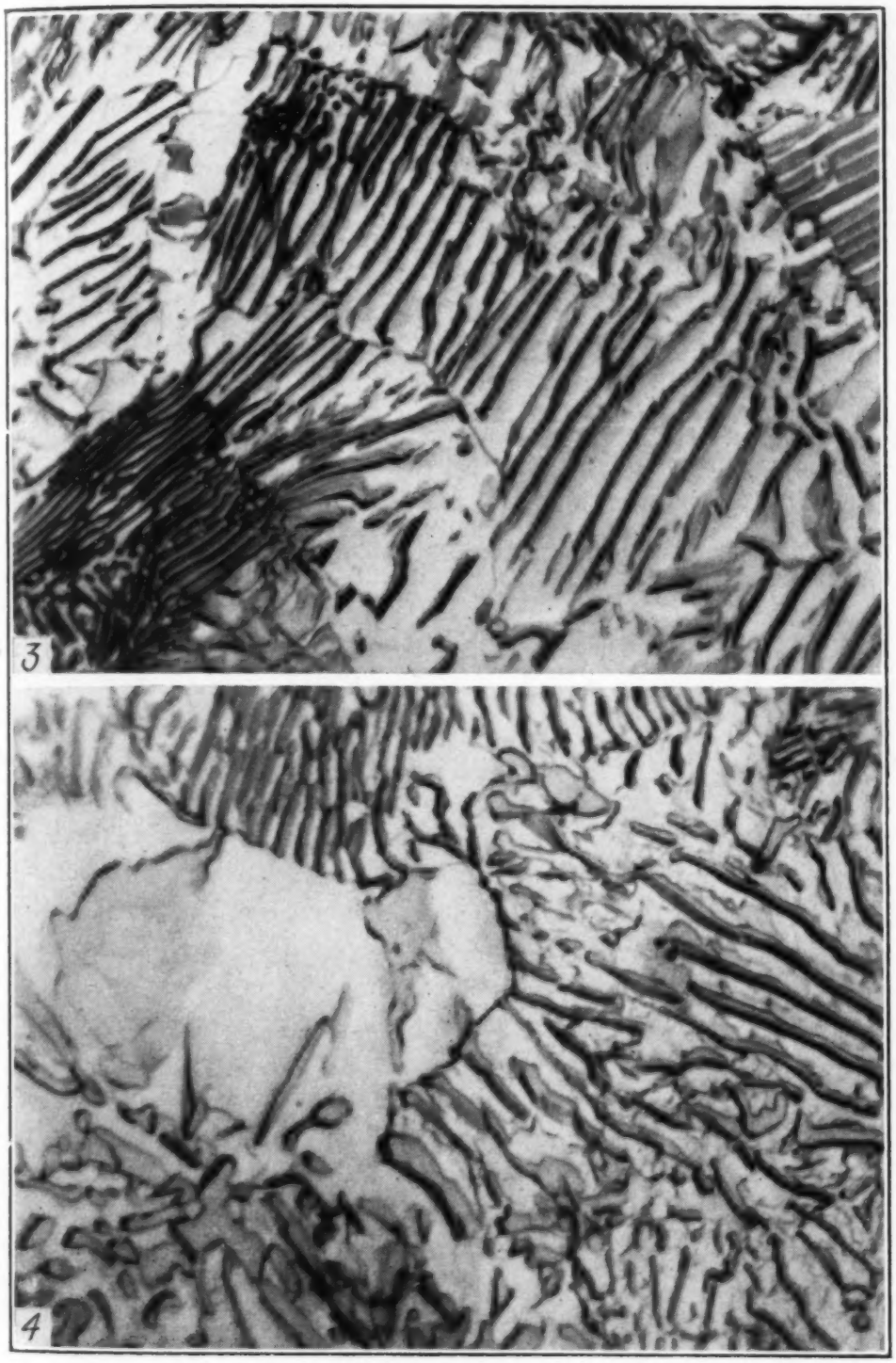

Fig. 3—Ferrite Grain Boundaries Between Pearlite Colonies. × 2000.
Fig. 4—Difference in Orientation of Ferrite of Adjacent Colonies as Shown by Roughening on Etching in 2 Per Cent Nital. × 2000.

seems necessary to assume that austenite which forms at the Ac_1 must be of eutectoid carbon content. Nucleation of austenite grains would therefore be expected to occur at the phase boundaries between ferrite and cementite, and indeed this appears to be the case. Ferrite grain boundaries were not observed to play any part in the nucleation of austenite grains in pearlite.

The initial stages of the formation of austenite from pearlite are illustrated by Fig. 7. In the pearlite colony at the left of the photomicrograph, numerous small austenite grains (which have transformed on quenching to dark etching decomposition products) replace small portions of the cementite lamellae and the ferrite between two cementite lamellae. This pearlite colony also contains one austenite grain which replaces five or six cementite lamellae and intervening ferrite, and has transformed to dark etching products on quenching, and other large austenite grains which have transformed to martensite with a fringe of dark etching products. The formation of austenite begins in exactly the same way in finer pearlites, as may be seen in Fig. 8 which shows the steel in Fig. 6 after reheating just above the temperature required to initiate the transformation.

The nature of the nucleation of austenite is perhaps more clearly shown in Figs. 9 and 10. Diffusion of the carbon (carbide) has not occurred immediately after transformation so that, on quenching, the austenite which was formed by transformation decomposed into dark etching products in the areas high in carbon (locations of cementite lamellae) and to ferrite in the low carbon areas (locations of ferrite lamellae). This may be seen in the two small transformed areas in the upper left and upper center portions of Fig. 9. In the lower right portion of Fig. 9 four dark specks are indicated by an arrow. These are quite surely dark etching decomposition products of austenite which formed at the ferrite-cementite phase boundary, with untransformed ferrite below and cementite above, and thus represent the very beginnings of austenite formation. A similar condition is shown in Fig. 10. Small dark specks occur on the cementite lamellae which emerge at a wide angle in the right and lower portion of the photograph, definitely ahead of the advancing front of austenite formation. The small specks or groups of specks are dark etching transformation products which represent tiny austenite grains that have grown from nuclei at the cementite-ferrite phase boundaries.

As tiny austenite grains (such as the smallest in Figs. 7, 9 and

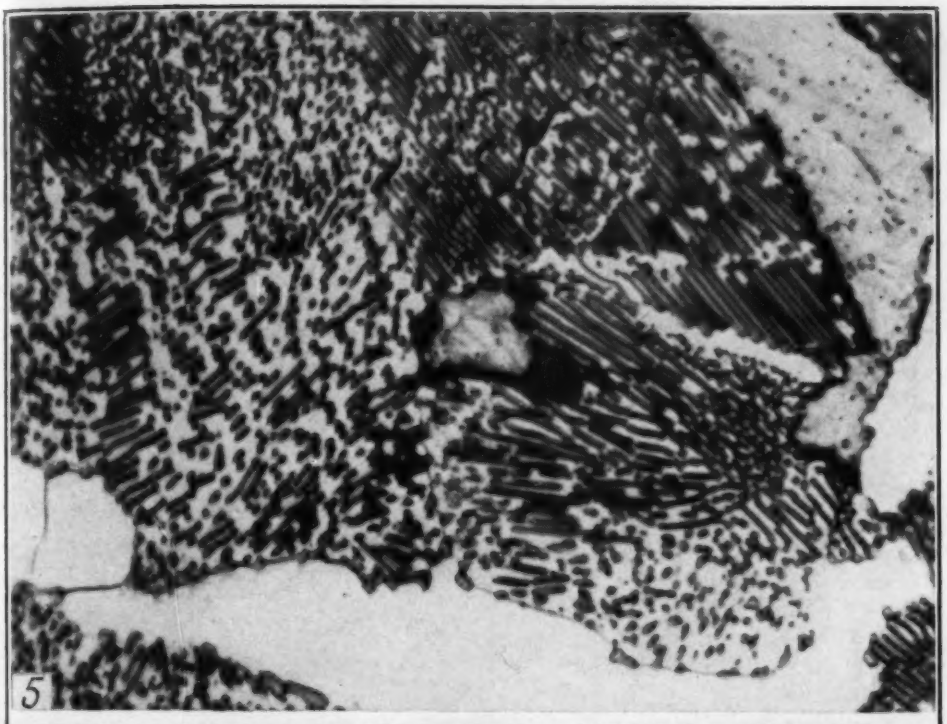

Fig. 5—On Spheroidizing Pearlite Colony Becomes Single Grain in Which Cementite Spheroids Are Dispersed. Limitation of Austenite Grain Growth by Ferrite Grain Boundaries in Pearlite. × 2000.

Fig. 6—Ferrite Grain Boundaries Between Colonies in Relatively Fine Pearlite. × 2000.

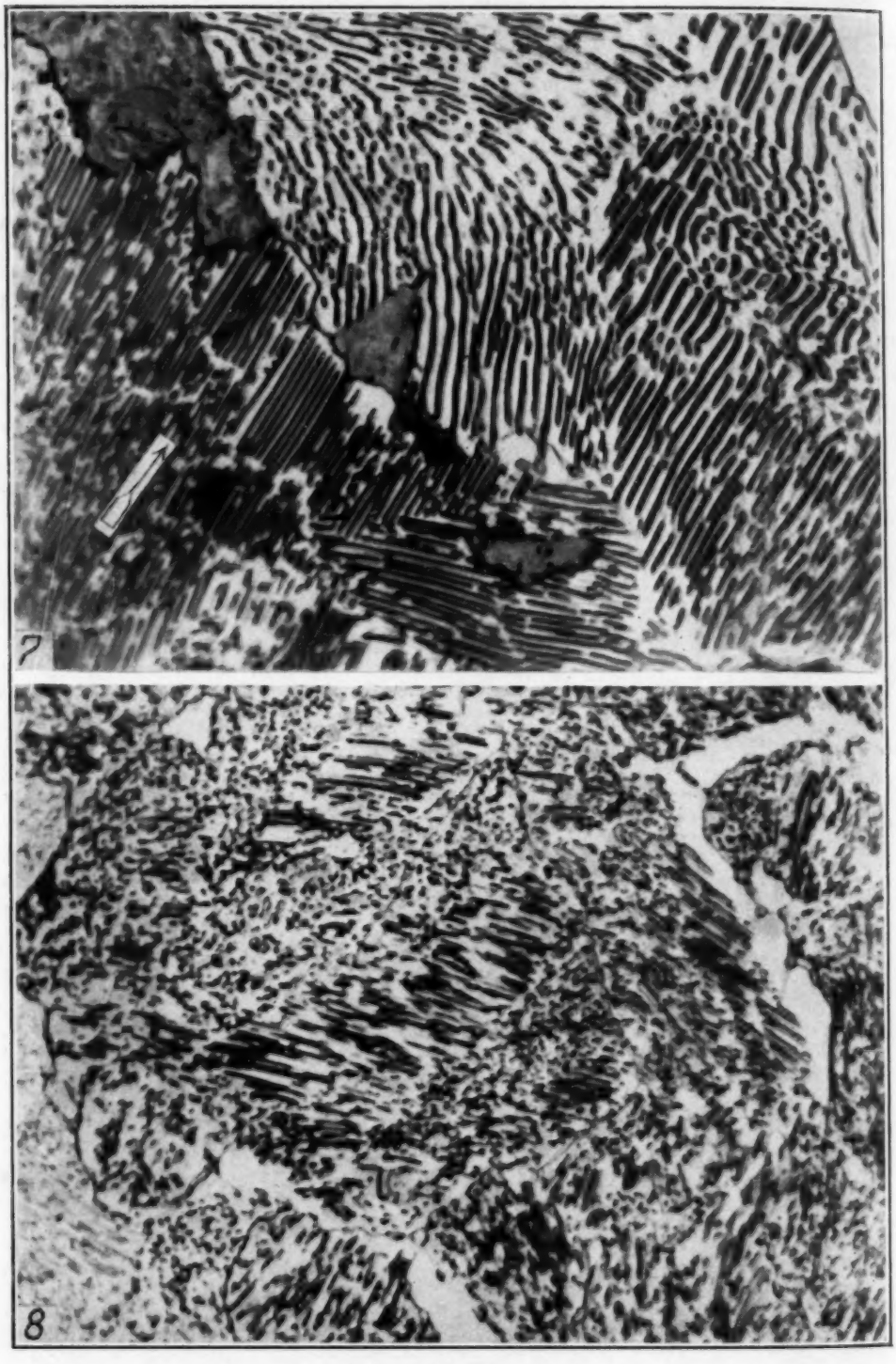

Fig. 7—Beginning of Austenite Transformation in Pearlite. Limitation of Austenite Grain Growth by Ferrite Grain Boundaries Between Pearlite Colonies. × 2000.

Fig. 8—Beginning of Austenite Grain Formation in Relatively Fine Pearlite, Same Structure as Shown in Fig. 6 After Reheating. × 2000.

10) grow into contact with each other, the one possessing the advantage in size at the time of contact probably survives at the expense of smaller grains. After an austenite grain is well established (as for example the grains which have transformed to martensite in Fig. 7) it possesses such a distinct advantage in size over any small grains that may form from nuclei in neighboring ferrite-cementite phase boundaries, that it readily grows at their expense. Thus, as the temperature is raised, the surviving austenite grains apparently grow both by transformation of contiguous ferrite and cementite and by atomic rearrangement of any tiny austenite grains with which they come in contact.

Two limitations of austenite grain growth have been observed. First, in steels in which the austenite contains sufficient undissolved particles of oxides, carbides, etc., to inhibit coarsening, a considerable discrepancy in the size of contiguous grains can exist without appreciable grain growth. This apparently holds only after the austenite grains have attained some minimum size since, even in inhibited steels, very tiny austenite grains grow both at the expense of adjacent ferrite and cementite and of smaller austenite grains with which they come into contact. This is in accord with accepted laws of crystal growth, whereby the smaller the grain size in any crystal aggregate, the greater is its tendency to coarsen. Secondly, austenite grains do not grow readily across the ferrite grain boundaries between pearlite colonies. This restriction of growth may be seen in Figs. 5 and 7. These two limitations insure that, with steels in which coarsening is effectively inhibited, the austenite produced by heating pearlite will have a grain size equal to or less than the colony size of the pearlite from which it formed, provided of course that the austenite was not subsequently heated above its coarsening temperature. Figs. 1 and 2 illustrate the relation between pearlite colony size and the austenite grain size obtained on heating that structure, in steels of various carbon contents to which sufficient aluminum has been added to inhibit coarsening. The austenite grain size in Figs. 1-b, d, f, h and 2-b, d, f, h is indicated by fine pearlite (dark) which outlines the grains, the centers of which have transformed to martensite (light). Fig. 1 shows structures with relatively large pearlite colonies, Fig. 2 the same steels so treated that the pearlite colonies are smaller. In each steel reduction of the pearlite colony size has comparably reduced the austenite grain size.

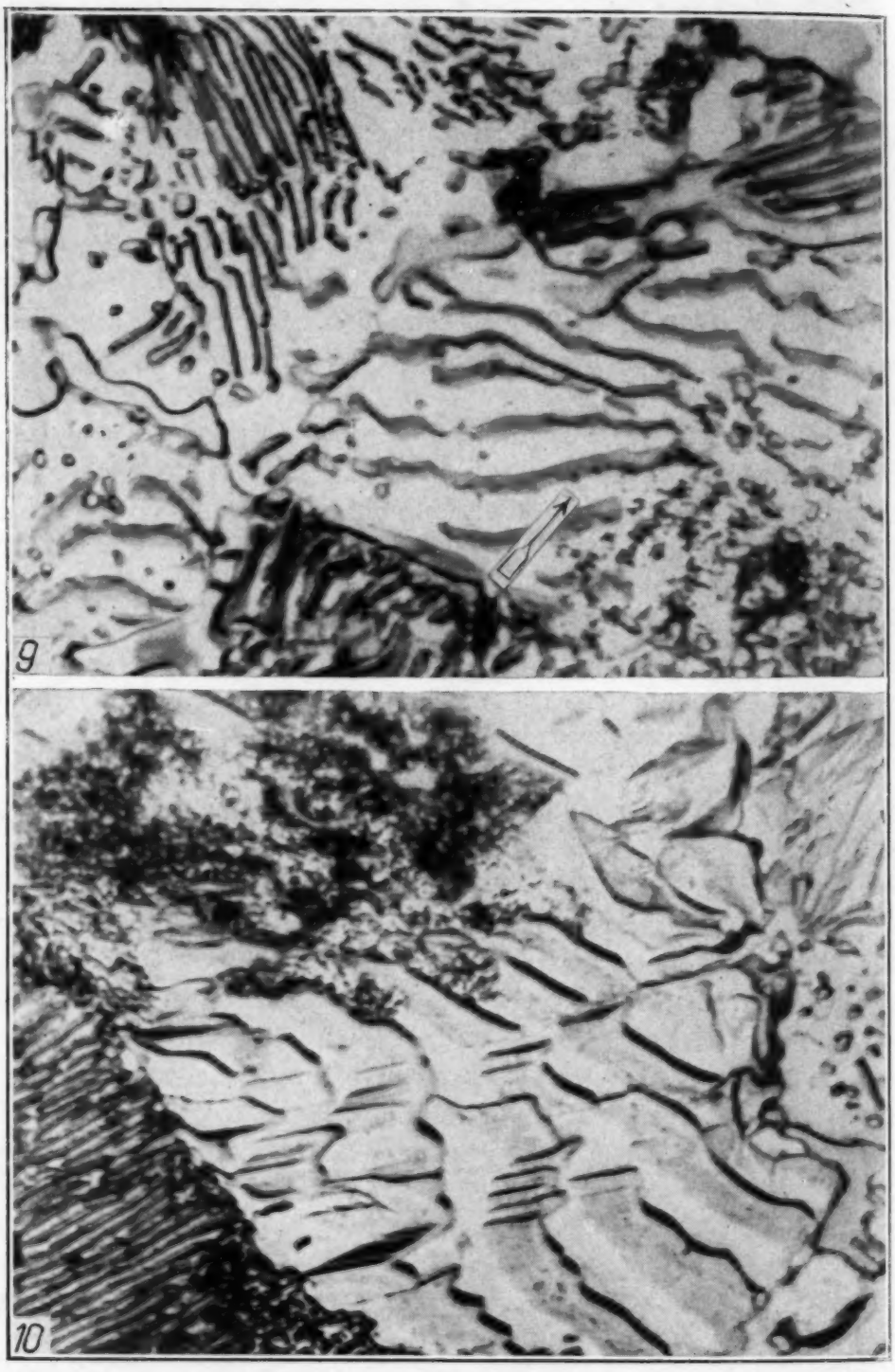

Figs. 9 and 10—Tiny Austenite Grains Formed at Ferrite-Cementite Phase Boundaries Ahead of Advancing Front of Transformation. × 2000.

Shape of Austenite Grains Influenced by Carbide Form

The nucleation of austenite at the ferrite-cementite phase boundaries evidently imparts a peculiar grain structure to austenite produced from pearlite, provided that coarsening during the formation of austenite is inhibited. Austenite grain growth follows along the pearlite lamellae, as may be seen in Fig. 11. The martensite (medium gray) and the fine pearlite (dark) are transformation products of the austenite present at the time of quenching. The sample was etched electrolytically in 10 per cent aqueous solution of chromic acid. In martensite and fine pearlite this method of etching reveals carbon (cementite) concentration and rarefaction corresponding to prior pearlite lamellae when diffusion is incomplete. The "pearlite ghosts" are continuous with the lamellae of the untransformed pearlite. This is shown in greater detail in a small area in Fig. 12. Thus, on completion of the transformation, the austenite grains are often elongated and irregular in shape, taking their conformation from the lamellae of the pearlite. Such a grain structure is illustrated by Fig. 13, where many of the grains are seen to be elongated rather than equi-axed.

The formation of austenite from martensite and spheroidized structures obtained from martensite proceeds in an entirely different manner. With martensite spheroidization occurs very readily below the Ac_1. Thus, the austenite produced above the Ac_1 is formed not from martensite proper but from a spheroidized structure. It therefore seems important to examine the structure produced by tempering martensite, and also by tempering fine pearlite, since fine pearlite is frequently associated with martensite in quenched steels. The characteristic plate structure of martensite and the growth of cementite spheroids on tempering are too well known to need description, but the ferrite grain structure of tempered martensite has received less attention. Fig. 14 illustrates the microscopic appearance of medium carbon martensite, in which the size and shape of the ferrite grains are not evident except by inference. If martensite is tempered sufficiently the surviving cementite particles are readily seen and, with suitable etching in 2 per cent nital, the ferrite grain structure is also revealed, as may be seen in Fig. 15. After a spheroidizing treatment of 12 hours at 1300 degrees Fahr. (705 degrees Cent.), the ferrite grain structure is even more clearly evident, as in Fig. 16. A comparison of the as-quenched martensite with the

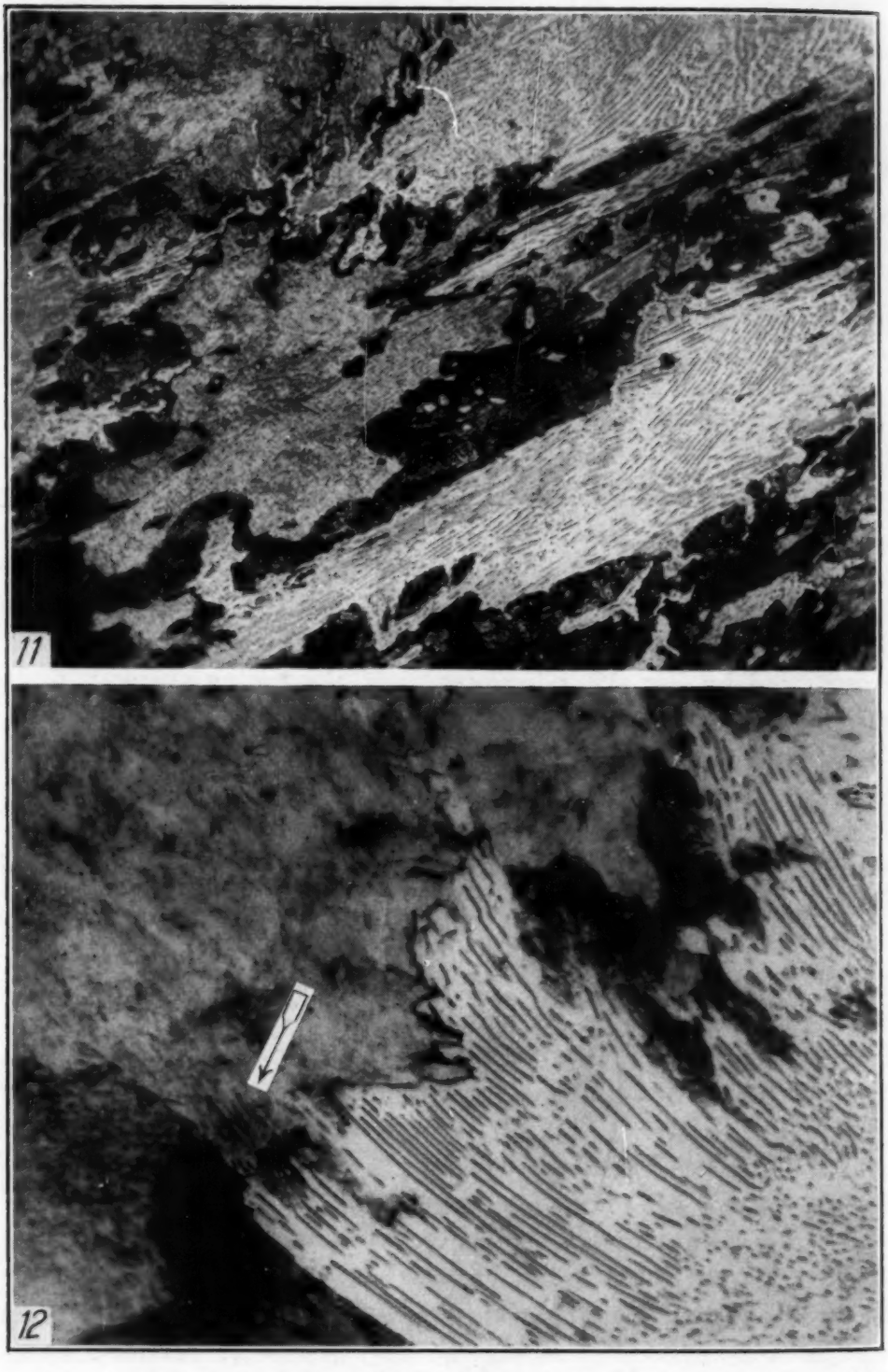

Fig. 11—Austenite Transformation Following Along Pearlite Lamellae. Etched Electrolytically in 10 Per Cent Aqueous Chromic Acid to Show "Pearlite Ghosts" in Martensite and Fine Pearlite Formed on Quenching. × 500.

Fig. 12—Same as Fig. 11. × 2000.

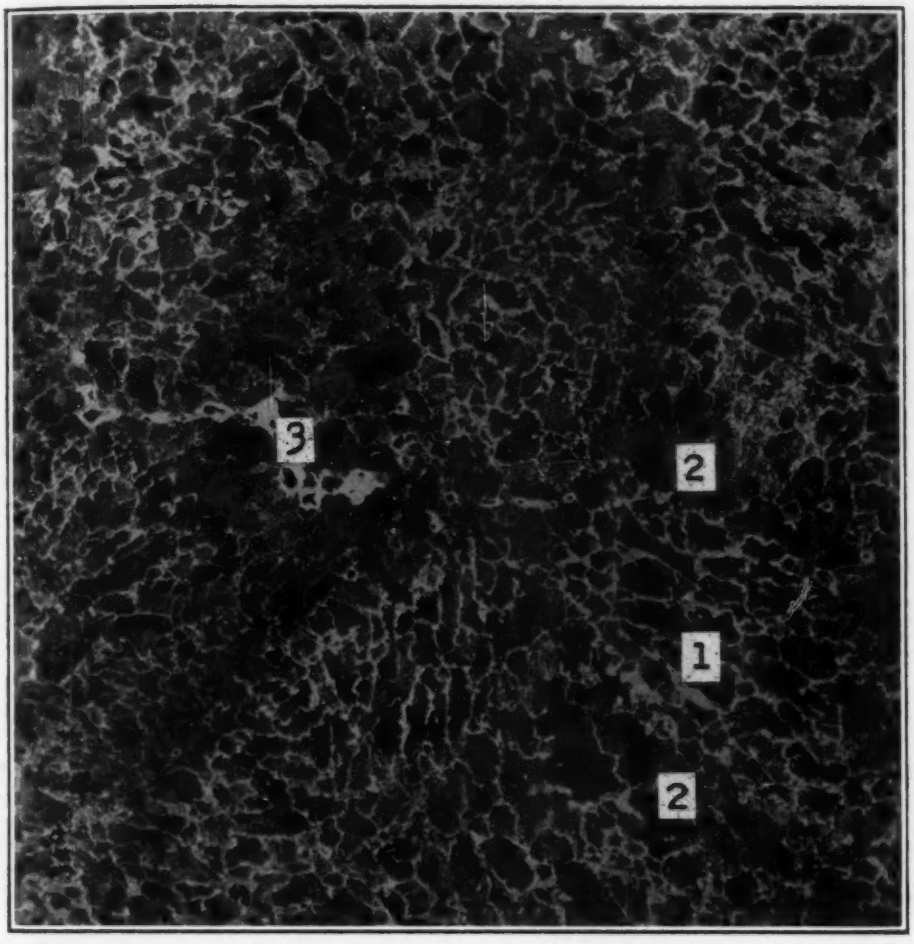

Fig. 13—Elongated and Irregularly Shaped Grains Formed From Pearlite. (Austenite Cooled at Rate to Allow Separation of Ferrite in Austenite Grain Boundaries.) × 100.

structure after tempering indicates that the ferrite grains of the tempered structure coincide with the martensite plates; that is, each martensite plate is a single ferrite grain or becomes one on tempering. After the spheroidizing treatment, the ferrite grain structure is essentially the same as in tempered martensite, except for a small amount of grain growth. Since the extent of each martensite plate is limited by the grain size of the austenite from which the martensite is formed on quenching, the ferrite grain structure of martensite depends on the immediately preceding austenite grain size, as well as on the characteristic mode of decomposition of austenite to form martensite. The more stable cementite particles which survive on tempering (grow by precipitation of cementite or carbon dissolved from neighboring less stable particles) occur preferentially in the fer-

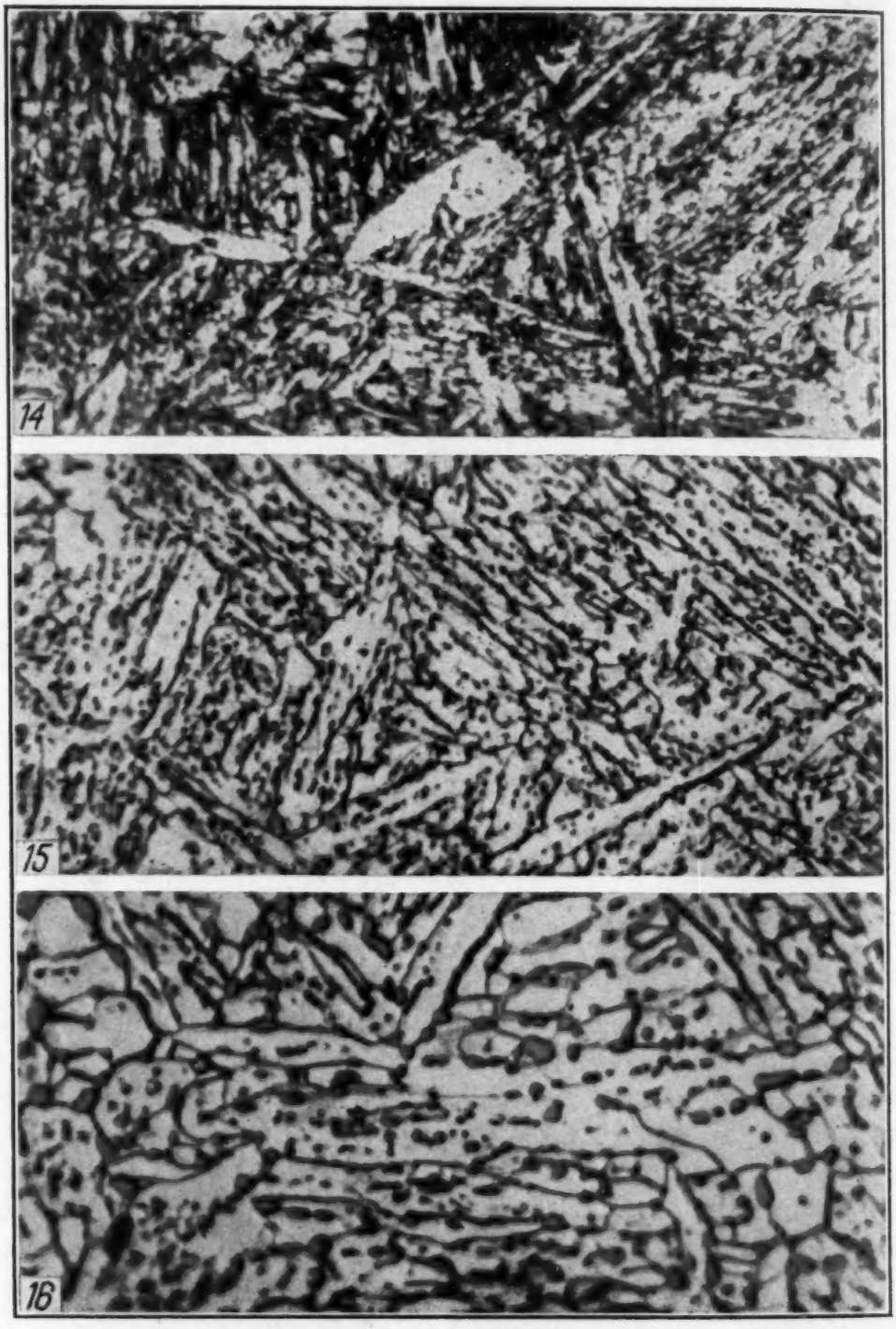

Fig. 14—Medium Carbon Martensite. × 2000.
Fig. 15—Same as Fig. 14 After Tempering. × 2000.
Fig. 16—Same as Fig. 14 After Spheroidizing. × 2000.

rite grain boundaries or in the position which corresponds to the so-called "midrib" of the martensite plates, as in Figs. 15 and 16. No dif-

ference was observed in the tempered and spheroidized structure of steels with various carbon contents (0.45 to 1.00 per cent), except an increase in the number of cementite particles with the larger carbon contents.

On tempering or spheroidizing structures which contain both martensite and fine pearlite, the characteristic ferrite grain structure of each is retained. Each nodule (colony) of fine pearlite becomes a single ferrite grain in which spheroids of cementite are dispersed. Tempered and spheroidized structures of a hypoeutectoid steel which originally had a martensite-plus-fine pearlite structure are shown in Figs. 17 and 18 respectively; and of a hypereutectoid steel in Figs. 19 and 20, respectively. The hypereutectoid steels contained undissolved proeutectoid cementite in the as-quenched martensite-plus-fine pearlite structures, and it was the proeutectoid carbide particles which appear to be the most stable, probably because of their larger size in the as-quenched structure. Figs. 21 and 22 illustrate the ferrite grain structure resulting from fine pearlite-plus-proeutectoid cementite on tempering and spheroidizing, respectively. The ferrite grains are identical with the pearlite colonies from which they form, just as in the coarser pearlites. The only difference is that the pearlite colonies, and the resulting ferrite grains, become smaller the finer the pearlite.

Turning to the formation of austenite on heating martensite or martensite-plus-fine pearlite, the transformation occurs in a structure which is more or less spheroidized, depending on the rate of heating. The mechanism of austenite formation appears to be essentially the same irrespective of the degree of spheroidization. For example, Fig. 23 shows as-quenched martensite, Fig. 24 the beginning of austenite formation on reheating this martensite, and Fig. 25 on reheating martensite which has received a spheroidizing treatment of 12 hours at 1300 degrees Fahr. (705 degrees Cent.). After both treatments the transformation has begun in the grain boundaries of the prior austenite. This was first observed by Robertson on reheating martensite of 0.43 per cent and less of carbon (5). If the quenched structure consists of martensite-plus-fine pearlite, the fine pearlite occurs preferentially at the grain boundaries of the prior austenite, as is well known. On reheating austenite forms first in the ferrite grains derived from the fine pearlite. The nucleation of austenite, however, apparently occurs as with coarser pearlites; that is, within the ferrite grain. This is seen in the partially transformed ferrite grain derived from fine pearlite (upper right portion of Fig. 26).

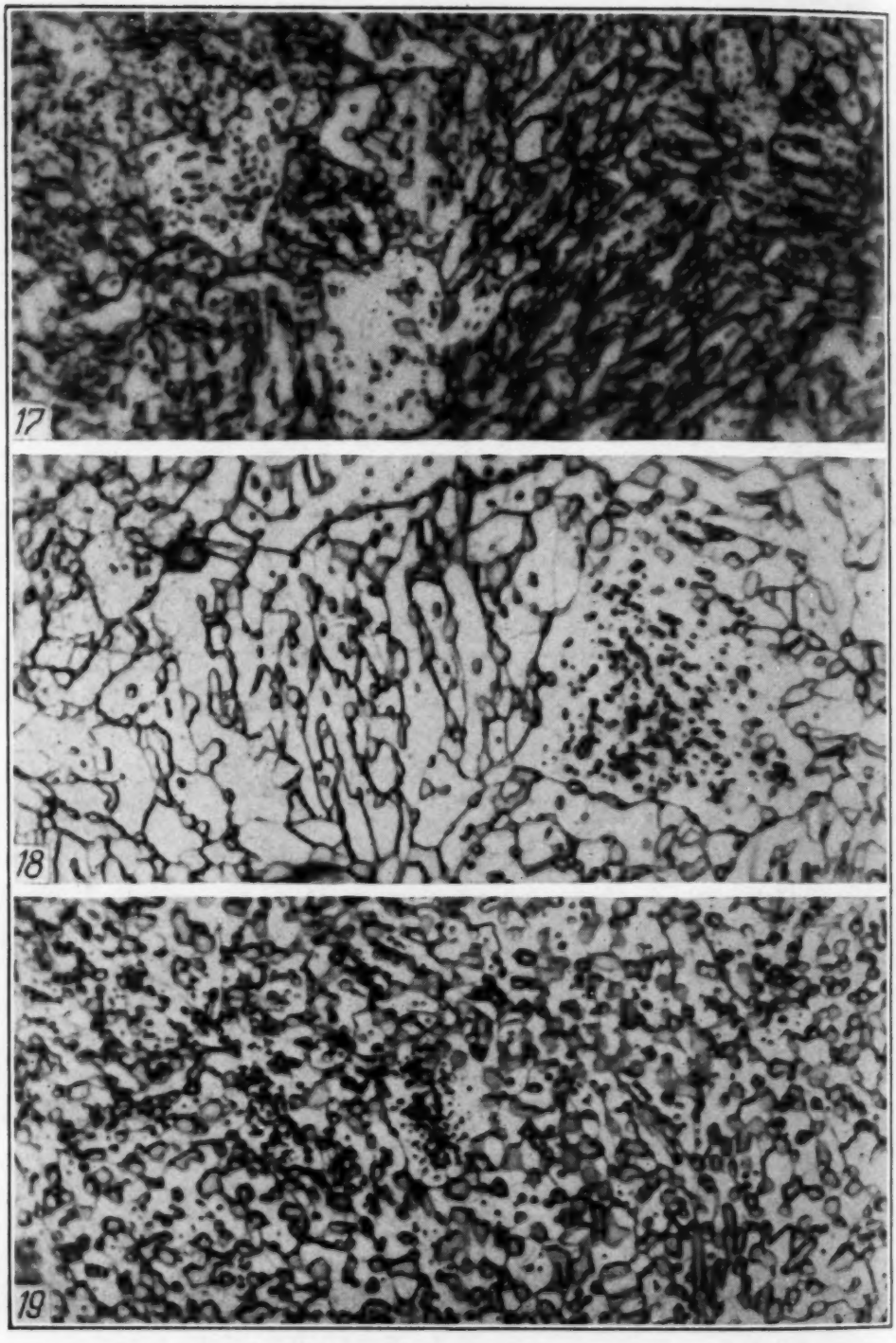

Fig. 17—Hypoeutectoid Steel, Martensite-Plus-Fine Pearlite After Tempering.
Fig. 18—Same as Fig. 17 After Spheroidizing.
Fig. 19—Hypereutectoid Steel, Martensite-Plus-Fine Pearlite-Plus-Proeutectoid Cementite After Tempering. All Photomicrographs. × 2000.

The formation of austenite from a spheroidized structure obtained from martensite is illustrated by Figs. 27 to 30. The sphe-

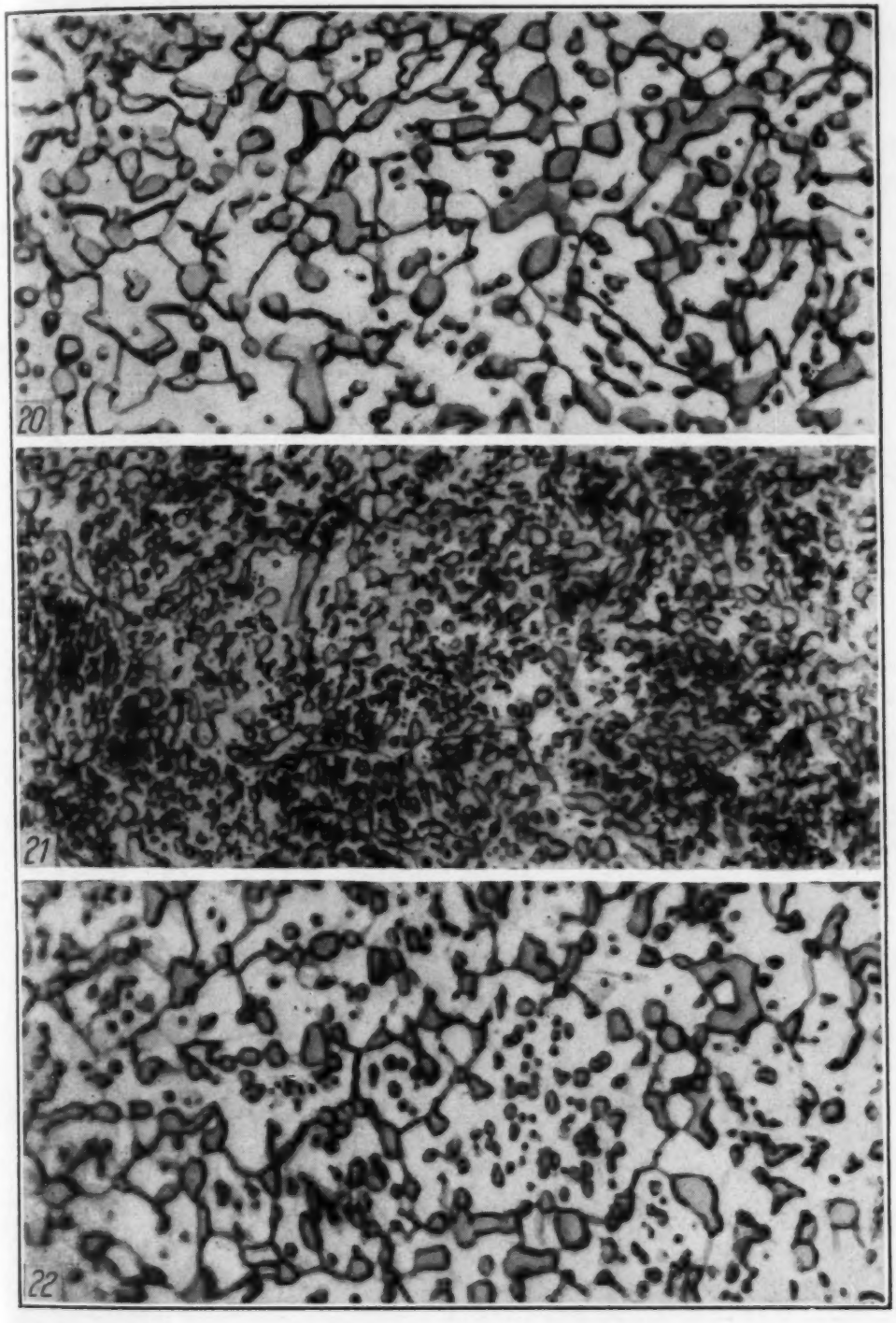

Fig. 20—Same as Fig. 19 After Spheroidizing. × 2000.
Fig. 21—Hypereutectoid Steel, Fine Pearlite-Plus-Proeutectoid Cementite After Tempering. × 2000. Fig. 22—Same as Fig. 21 After Spheroidizing. × 2000.

roidized 0.45 per cent carbon steel is used as an illustration because the cementite particles are less numerous and hence the ferrite grain

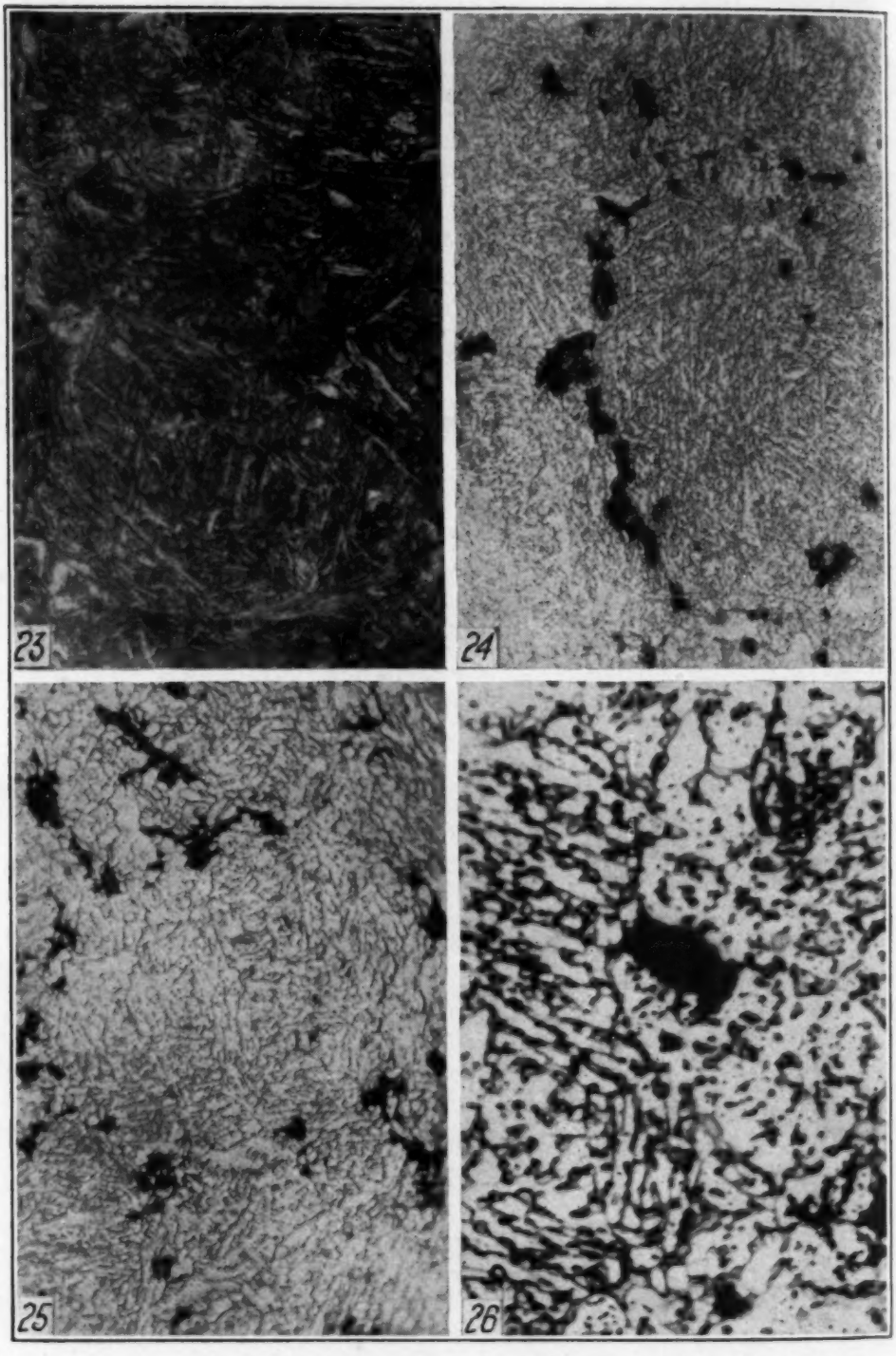

Fig. 23—As-Quenched Martensite, Etched with Vilella's Grain Size Reagent.
Fig. 24—Same Steel as Fig. 23, Beginning of Transformation in Tempered Martensite. Transformation Begins in Grain Boundaries of Prior Austenite.
Fig. 25—Same Steel as Fig. 23, Beginning of Transformation in Spheroidized Martensite. Transformation Begins in Grain Boundaries of Prior Austenite.
Fig. 26—Beginning of Transformation in Tempered Martensite-Plus-Fine Pearlite. Nucleation of Austenite at Cementite-Ferrite Phase Boundaries Within Ferrite Grains Derived by Tempering Pearlite Colonies. × 2000. Figs. 23, 24, 25. × 500.

boundaries are plainly evident. Insofar as could be judged, however, formation of austenite takes place in the same way irrespective of carbon content or the degree of spheroidization. As mentioned before, the transformation begins in the grain boundary regions of the prior austenite. There austenite nuclei form at the ferrite-cementite phase boundaries around those cementite particles which lie in the ferrite grain boundaries. Several such tiny austenite grains may be seen in Fig. 27. Fig. 28 shows the structure after heating to a somewhat higher temperature. The austenite grains which have formed in the grain boundaries of the prior austenite have grown larger, and new austenite grains have begun to form along the rows of cementite particles in the ferrite grain boundaries within the prior austenite grains. As the temperature is raised the formation of austenite grains continues until the remaining ferrite grains are each separated from the next by austenite, as in Fig. 29. As the heating is continued, the austenite grains which initiated the transformation (in the prior austenite grain boundaries) attain a considerable advantage in size over the austenite grains which formed later (within the prior austenite grains). One of these larger grains may be seen in Fig. 30. That it was a single austenite grain is evident from the martensitic markings, since one martensite plate crosses the entire grain. These larger austenite grains continue to grow by transformation of contiguous ferrite and rearrangement of smaller austenite grains with which they come into contact until the structure becomes completely austenitic or austenite-plus-undissolved cementite. With this mechanism of austenite grain formation it is evident that the austenite grain size, on completion of the transformation, will be equal or less than that of the prior austenite, provided that coarsening has not occurred. In contrast to the elongated and irregular grain shapes in austenite formed from pearlite, the grain structure produced from tempered or spheroidized martensite is equiaxed.

The Influence of the Dendritic Pattern

In austenite formed on heating pearlitic structures, and tempered and spheroidized martensite as well, the transformation progresses according to the dendritic pattern of the steel. Since it is not easy to follow the dendritic pattern in rolled steel, sections from five ingots of the S.A.E. 1060 steel were studied. In this heat only manganese and silicon had been added in the ladle but amounts of

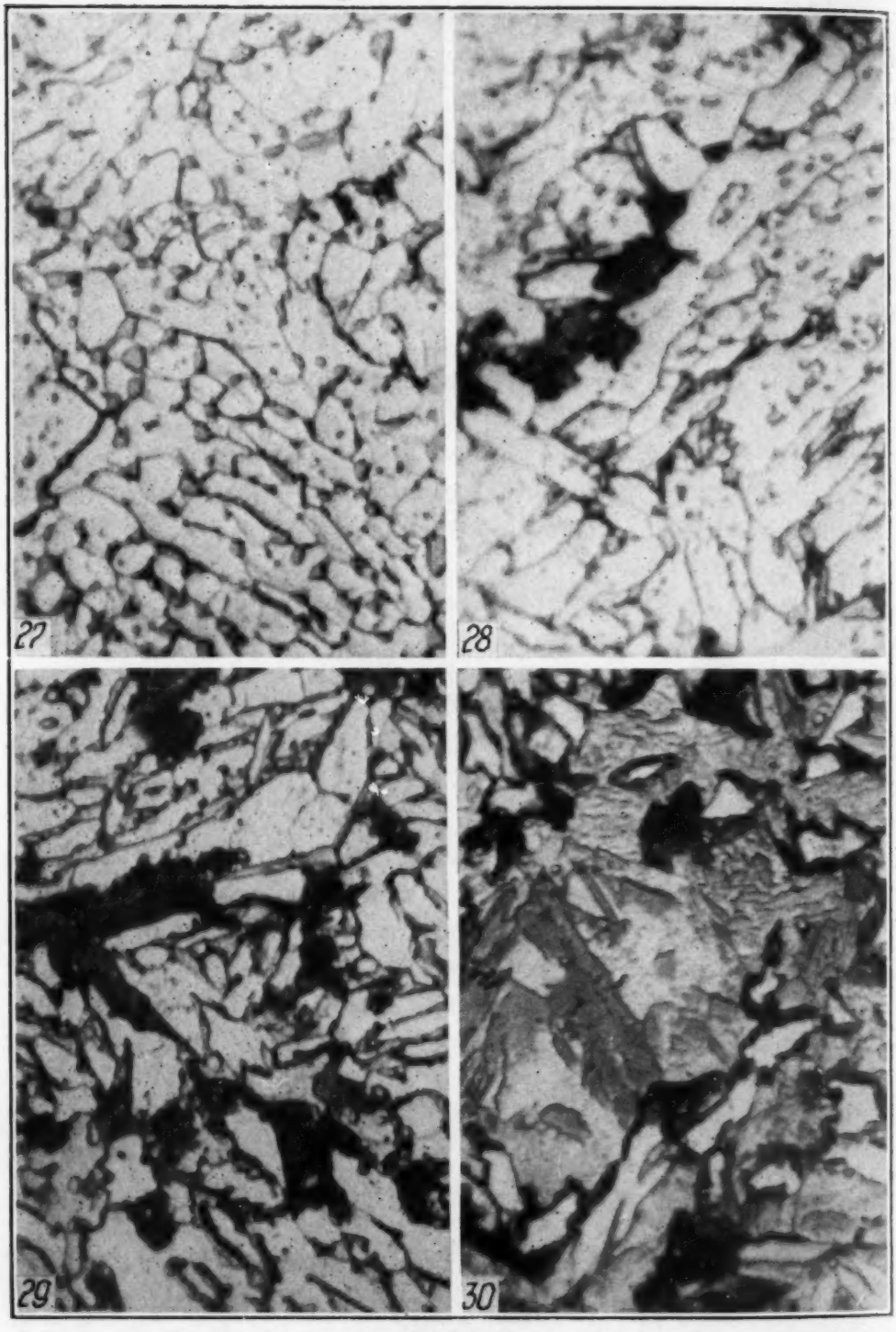

Fig. 27—Beginning of Transformation in Spheroidized Martensite. Tiny Austenite Grains (Dark) at Ferrite-Cementite Phase Boundaries in Region of Prior Austenite Grain Boundaries. × 2000.

Fig. 28—Same as Fig. 27 Heated to Higher Temperature. Growth of Austenite Grains (Dark) in Prior Austenite Grain Boundaries, Formation of New Austenite Grains Within the Prior Austenite Grains. × 2000.

Fig. 29—Same as Fig. 24 Heated to Higher Temperature. Nearly Every Ferrite Grain Within the Prior Austenite Grains is Now Separated by Austenite (Martensite After Quenching). × 2000.

Fig. 30—Same as Fig. 25 Heated to Higher Temperature. Surviving Austenite Grain, One of Those Which Started in Prior Austenite Grain Boundaries.

aluminum varying from 0 to 2 pounds per ton had been added in the molds. Full slices had been taken from the lower part of each ingot in the as-cast condition.

The dendritic pattern of cast steel may be divided into three general regions: (a) The axes of the dendrites (these are the primary axis and the axes of the subsidiary branches), (b) the interbrachial areas (these are the regions within a single dendrite which lie between the axes), and (c) the interdendritic areas. This is in the order in which solidification proceeds, and the distribution of the sulphide inclusions follows this pattern. In addition to the sulphides, ingot 15 (no aluminum) contained inclusions of glass and of glass-plus-a crystalline silicate. The aluminum treated ingots contained corundum, and ingot 16 (¼ pound aluminum per ton) some glass-plus-corundum inclusions. Of all of these inclusions, only the sulphides were observed to bear any relation to the as-formed austenite grain structure or the initiation and progress of the grain coarsening. Ingot 15 (no aluminum) contained (manganese-iron) sulphide-plus-glass inclusions as well as (manganese-iron) sulphide inclusions. The former evidently separated from the liquid steel as droplets of a liquid solution containing both sulphide and silica. On cooling these droplets separated into two immiscible liquid phases, namely, a solution containing the major portion of the sulphide and a solution containing the major portion of the silica. This phenomenon has been described by Benedicks and Löfquist (6). The sulphide-plus-glass inclusions did not always occur in the interbrachial or interdendritic areas. The (manganese-iron) sulphide inclusions, however, were invariably interbrachial or interdendritic. The addition of ¼ pound of aluminum per ton in the mold had a pronounced effect on the (manganese-iron) sulphide inclusions, as may be seen by comparing Figs. 31A and B. With still larger aluminum additions the (manganese-iron) sulphide inclusions had the appearance illustrated by Fig. 31C. In the aluminum treated ingots all of the sulphide inclusions occurred in the interbrachial or interdendritic regions. Such observations on the effect of aluminum in causing all of the sulphide inclusions to occur between the dendrites or dendrite axes were first reported by Sims and Lillieqvist (7).

Whether the austenite is formed from pearlite or from tempered or spheroidized martensite, the transformation begins in the regions having the lowest Ac_1 temperature. These areas are related to the dendritic pattern of the steel, and thereby to the distribution

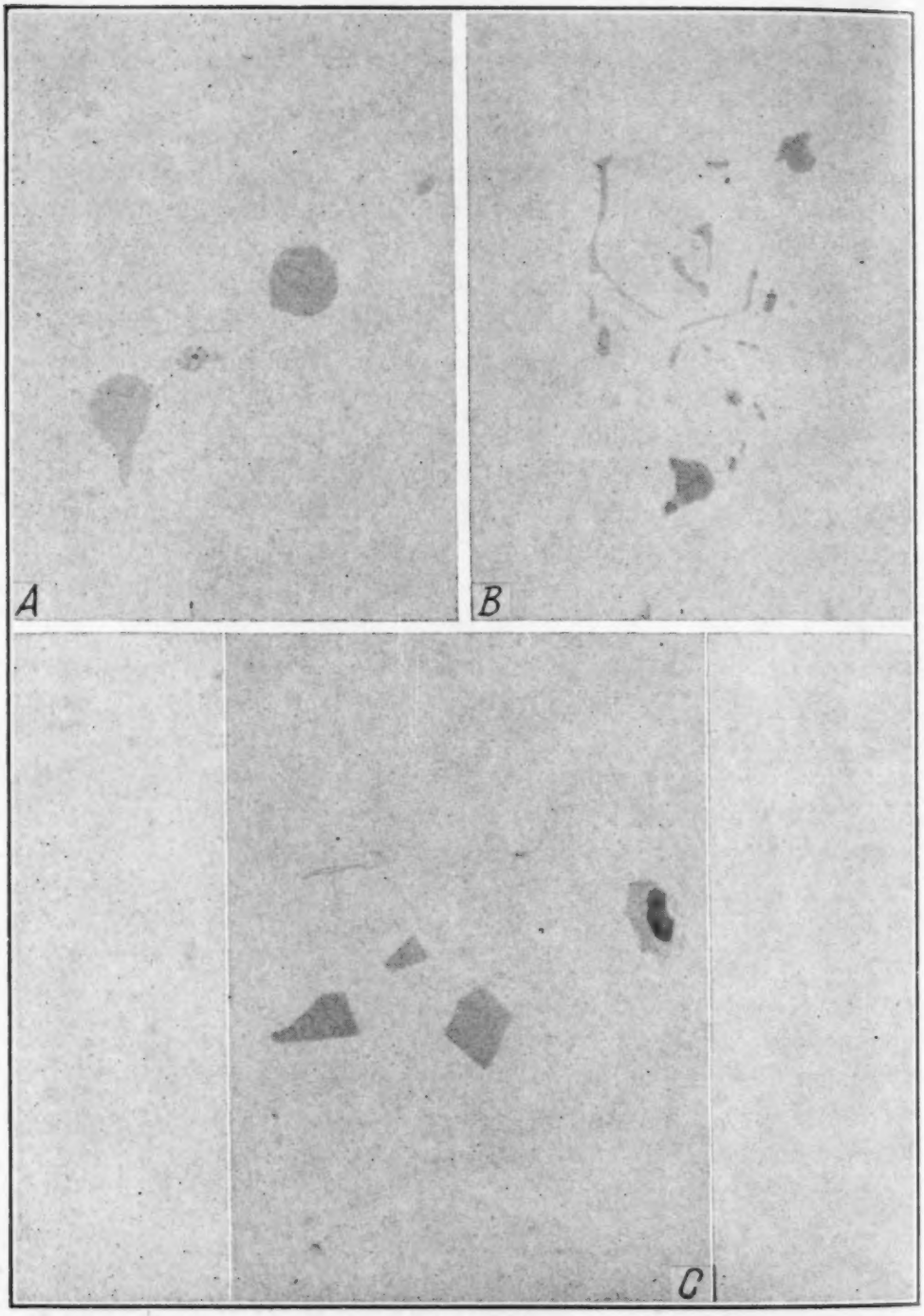

Fig. 31—Typical Sulphide Inclusions in Ingots of S.A.E. 1060 Steel. × 500. A, Ingot With No Aluminum Whatever. B, Ingot With ¼ Pound Aluminum Per Ton in Mold. C, Ingots With ⅛, 1 and 2 Pounds Aluminum Per Ton in Molds.

of sulphide inclusions. In the S.A.E. 1060 steel ingots austenite formation on heating began in the interbrachial areas or interdendritic

regions with few sulphide inclusions and passed next to the axes of the dendrites, while the interdendritic regions around groups of sulphide inclusions were the last to transform. This is illustrated by Figs. 32 and 33, which show specimens heated to temperatures between the Ac_1 and the Ac_3 and then quenched in water. In each photograph the dendrite axes have been indicated by the numeral "1", the interbrachial areas or interdendritic regions with few sulphide inclusions by "2", and the interdendritic regions around groups of sulphide inclusions by "3". In Fig. 32 formation of austenite has just begun in the "2" areas as shown by the patches of martensite there. In Fig. 33 the transformation is nearly complete in the "2" areas where the structure is almost entirely martensite (gray), is partial in the "1" areas which are composed of martensite (gray)-plus-ferrite (white), and has only just begun in the "3" areas. As austenite forms in each respective area of the dendritic pattern, the nucleation of austenite and the progress of the transformation follows the pattern determined by the prior martensitic or pearlitic structure, as related above.

The effect of the dendritic pattern on the initiation and progress of austenite formation influences the grain size distribution in the resulting austenite. In the ingots with a sufficient aluminum addition to inhibit coarsening during the transformation, the larger grains occurred in the interbrachial and those interdendritic areas which contained few sulphide inclusions. This may be seen in Fig. 13, in which the dendrite axes have been designated by the numeral "1", the interbrachial areas and the interdendritic regions with few sulphide inclusions by "2", and the interdendritic regions around groups of sulphide inclusions by "3". The sulphide inclusions in the "3" area are black since this specimen was etched electrolytically with chromic acid which attacks (manganese-iron) sulphide.

On continuing the heating to the coarsening temperature of the steel, coarsening begins with the larger grains in the interbrachial and the interdendritic areas with few sulphide inclusions, as may be seen in Figs. 34 and 35. In the S.A.E. 1060 ingots this was the case whether the coarsening temperature was high, intermediate or low, provided it was above the Ac_3. It would thus seem that the dendritic pattern determines in this way the pattern of the so-called "duplex" structure, which is obtained in partially coarsened pieces of steel. The last regions to coarsen are the interdendritic areas which contain numerous sulphide inclusions. Coarsening in 4 by 4-inch bil-

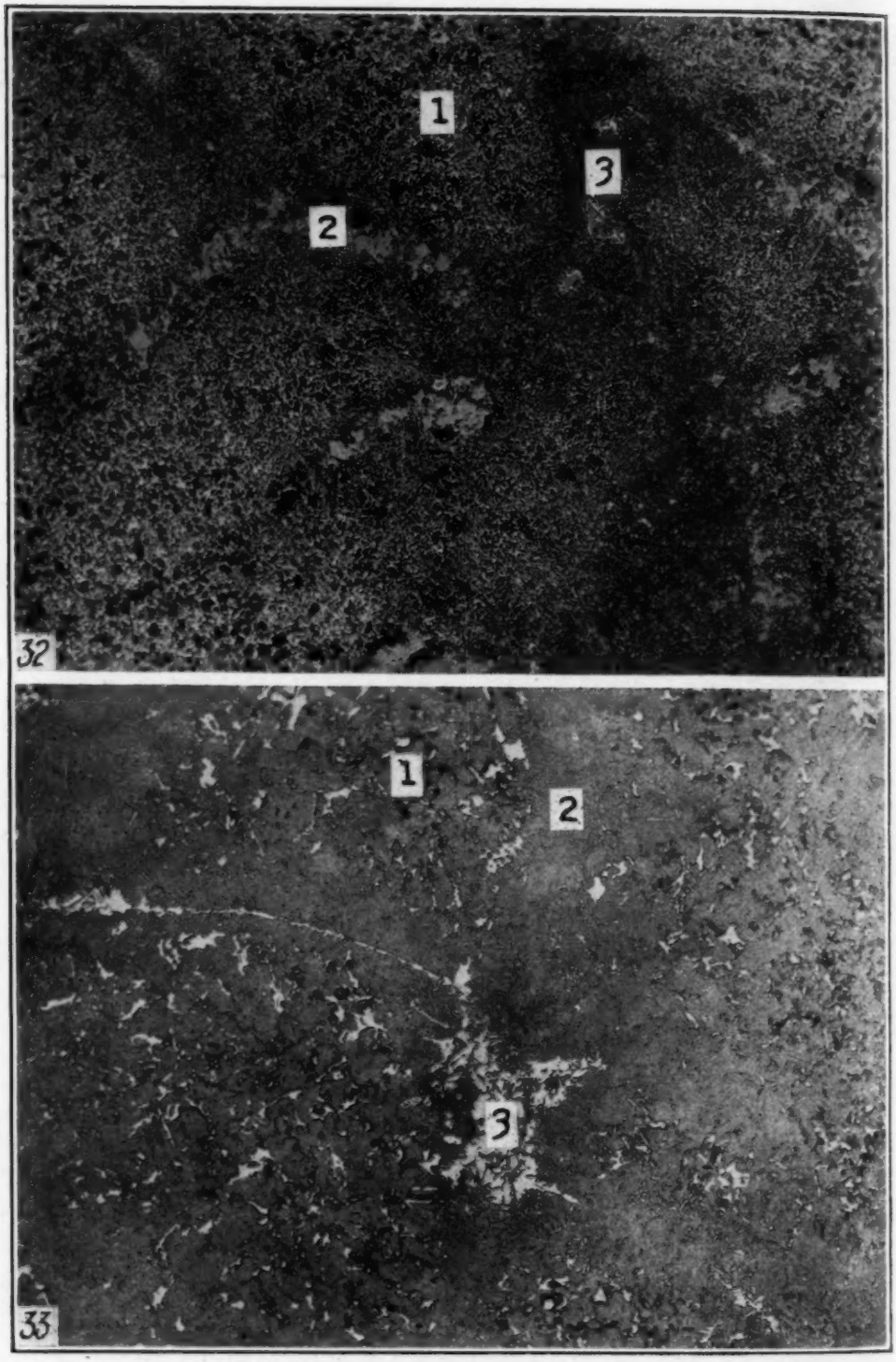

Fig. 32—Beginning of Austenite Transformation in Ingot Structure. Specimen Quenched in Water After Heating Slightly Above the Ac_1. × 100.

Fig. 33—Partial Austenite Transformation in Ingot Structure. Specimen Quenched in Water After Heating to a Temperature Between the Ac_1 and the Ac_3. × 100.

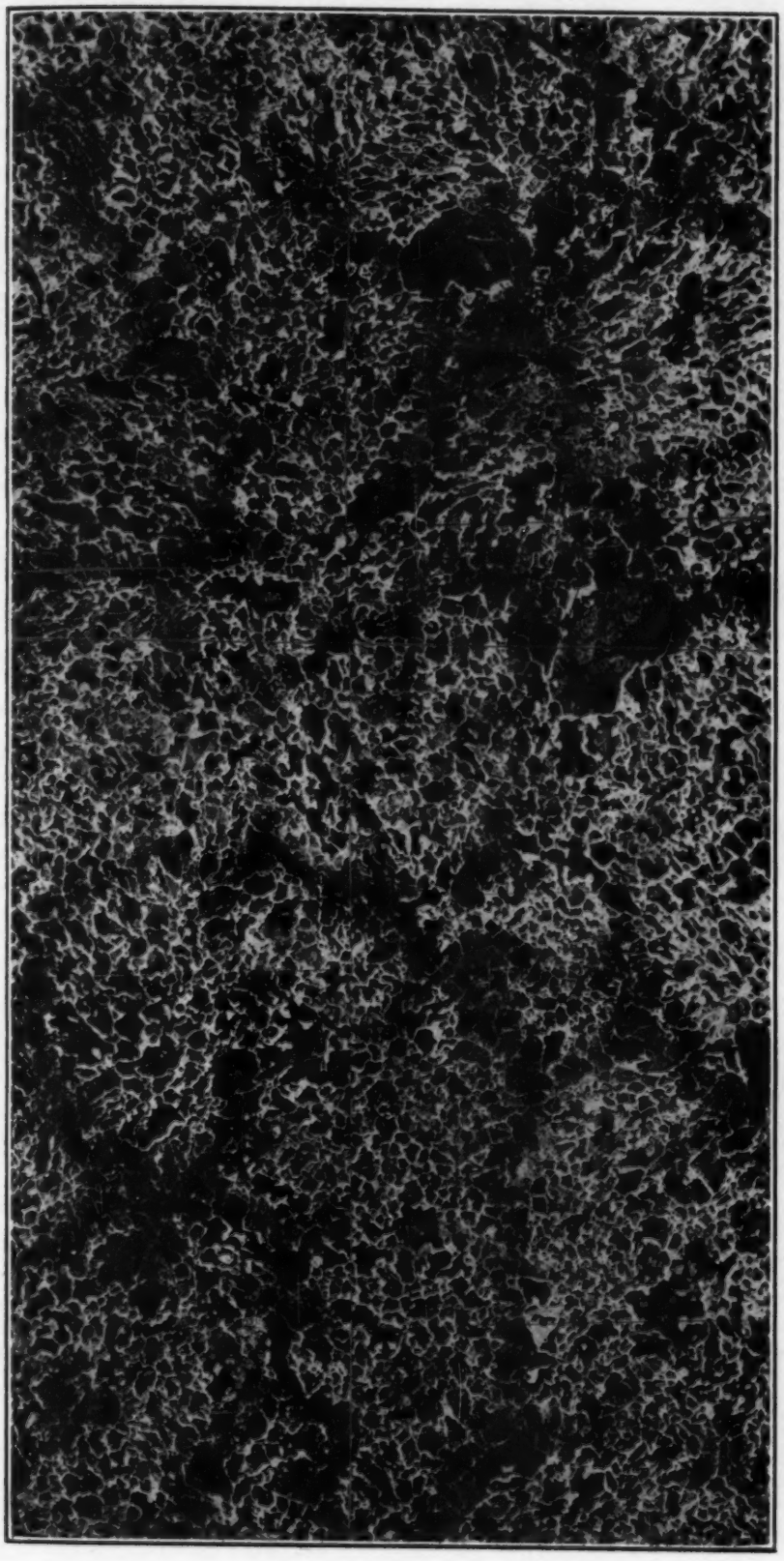

Fig. 34—Beginning of Coarsening on Reheating Ingot Structure of Pearlite-Plus-Ferrite. (Subsequently Cooled at Rate to Allow Separation of Ferrite in Austenite Grain Boundaries.) Note Numerous Somewhat Elongated Grains. × 50.

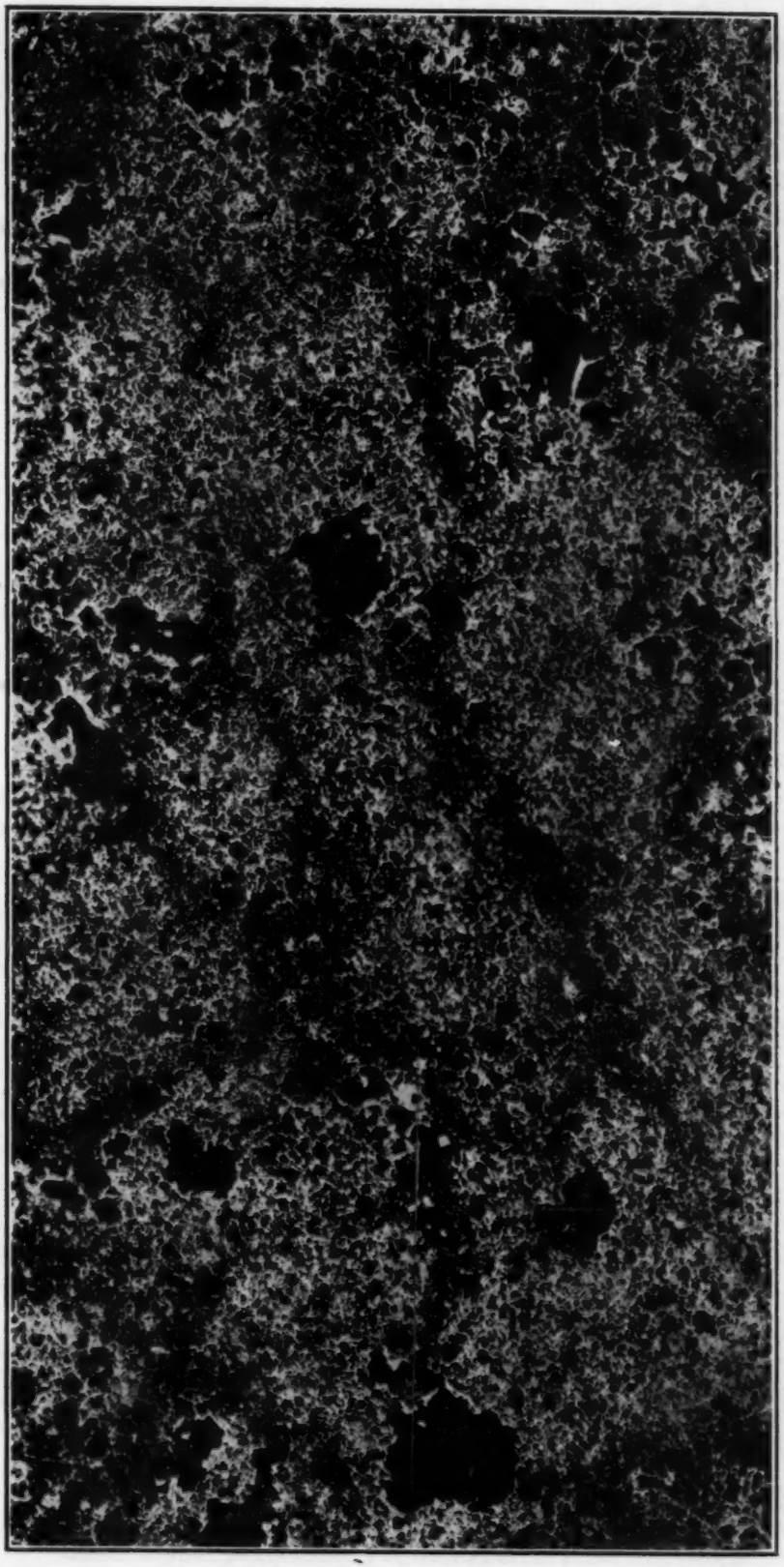

Fig. 35—Beginning of Coarsening on Reheating Ingot Structure Which Has Been Quenched to Form Martensite. (Subsequently Cooled at Rate to Allow Separation of Ferrite in Austenite Grain Boundaries.) Note That Grains Are Mainly Equi-Axed, and Compare with Fig. 34. × 50.

lets and in 1⅛-inch rounds rolled from the S.A.E. 1060 ingots was studied and, insofar as we have been able to determine, the dendritic pattern in the rolled product controls the coarsening in the same way as in the ingots. Without the evidence on the coarsening of ingot structures, however, the observations on the rolled structure would not be convincing because the bands representing the dendritic pattern are too close together. For this reason it is difficult to ascertain the original position of a grain after it has grown enough to be known to have coarsened.

Effect of Sulphur on Grain Coarsening

The idea that sulphur influences austenite grain coarsening is not new, but the fact that the interdendritic areas which contained groups of sulphide inclusions were the last to coarsen made it seem of interest to make a rather complete survey on the effect of sulphur on the austenite grain coarsening. Thirty 20-pound induction furnace heats were made and poured in a 3 by 3-inch mold. The group included two ranges of carbon (0.14 to 0.18 and 0.55 to 0.64 per cent), three ranges of sulphur (0.013 to 0.018, 0.042 to 0.048 and 0.092 to 0.116 per cent), and five aluminum additions (0, ¼, ½, 1, and 2 pounds per ton). The low carbon group contained 0.40 to 0.49 per cent of manganese and 0.13 to 0.22 per cent of silicon; the high carbon group, 0.65 to 0.73 per cent of manganese and 0.22 to 0.32 per cent of silicon. Phosphorus was in the neighborhood of 0.006 in both groups. The coarsening characteristics were determined on ¾ by ¾ by 1¼-inch pieces cut from the ingots. The grain size was obtained from the cores of the specimens after heating (in carburizing compound in 6-inch square boxes) for 8 hours at temperature, as indicated by a thermocouple placed at the center of the box. The weighted average A.S.T.M. austenite grain size after 8 hours at temperature is plotted against the testing temperature in Figs. 36 and 37. In the absence of any aluminum whatever, increasing sulphur causes restriction of austenite grain coarsening in both the 0.15 and the 0.60 carbon groups. In the aluminum treated steels there is the customary rise in the coarsening temperature as the amount of the aluminum addition is increased. In each group with the same carbon and aluminum addition, sulphur in general raises the coarsening temperature above that obtained with the aluminum addition alone. Exceptions appear with approximately 0.045 per cent of sul-

phur; in the 0.15 per cent group with ½ pound of aluminum per ton, and in the 0.60 per cent carbon group with ½, 1 and 2 pounds of aluminum per ton. In the 0.15 per cent carbon group approximately 0.1 per cent of sulphur, without any aluminum whatever,

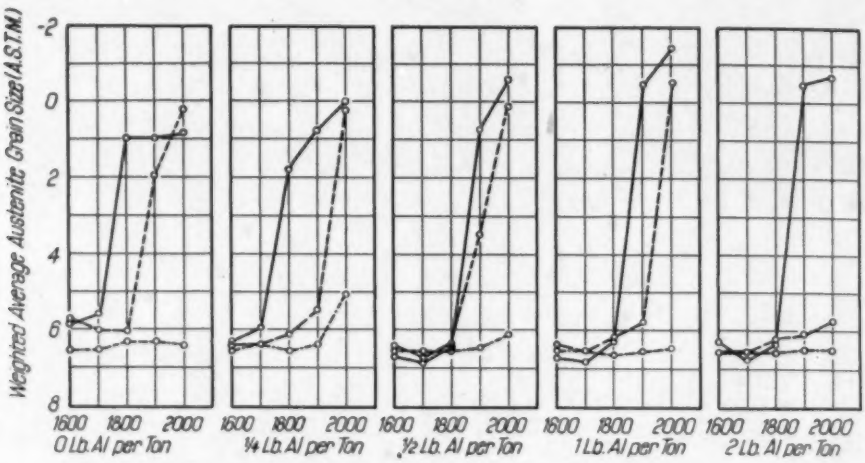

Fig. 36—Austenite Grain Coarsening of Steels With 0.14 to 0.18 Per Cent Carbon, and Various Sulphur and Aluminum Additions. Legend: Solid Lines 0.013-0.018 Per Cent Sulphur; Dash Lines 0.043-0.048 Per Cent Sulphur; Dotted Lines 0.092-0.116 Per Cent Sulphur.

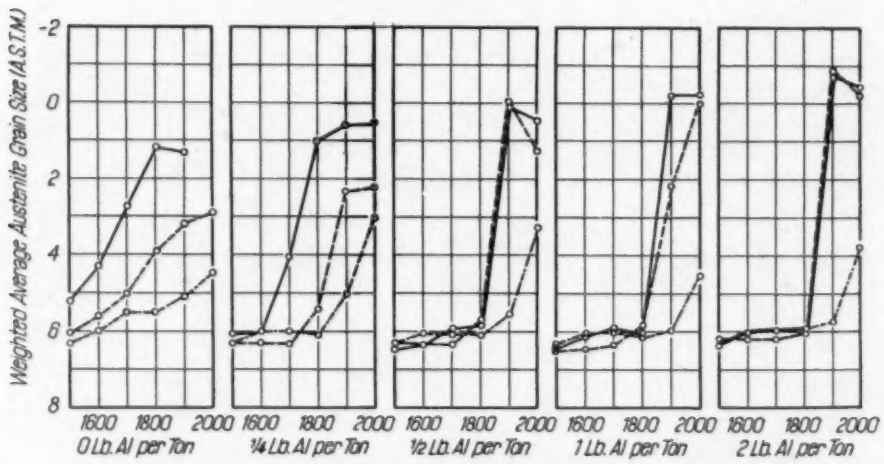

Fig. 37—Austenite Grain Coarsening of Steels With 0.55 to 0.64 Per Cent Carbon, and Various Sulphur and Aluminum Additions. Legend: Solid Lines 0.016-0.018 Per Cent Sulphur; Dash Lines 0.042-0.044 Per Cent Sulphur; Dotted Lines 0.093-0.100 Per Cent Sulphur.

raised the coarsening temperature higher than did 2 pounds of aluminum per ton with approximately 0.015 per cent of sulphur. In the 0.60 per cent carbon group, approximately 0.1 per cent of sulphur with ¼ pound of aluminum per ton raised the coarsening temperature as high as did ½, 1 and 2-pound additions of aluminum with approximately 0.017 per cent of sulphur. It should be borne in mind

that these results are, therefore, not directly applicable to steel mill production where the dendritic pattern is more pronounced in the ingots but is distorted in rolling, and other factors as well are known to influence austenite grain coarsening. It was to avoid confusion by these other factors that the specimens were tested in the cast state. The effect of sulphur was found to be much less marked in rolled commercial billets, though only one series was tested, so that further comparison would be desirable between cast and rolled products.

Summary

Austenite grain formation in 0.45 to 1.00 per cent carbon steel takes place in entirely different ways in the same steel depending on whether the prior structure is pearlitic or martensitic.

In pearlite, nucleation of austenite grains occurs at the ferrite-cementite lamella boundaries within the pearlite colonies. They grow along the pearlite lamellae so that, in the absence of coarsening, the structure contains elongated and irregularly shaped grains which take their conformation from the pearlite lamellae from which they form. Austenite grains do not readily grow across the ferrite grain boundaries which separate the pearlite colonies, so that, in the absence of coarsening, the austenite grain size at the end of the transformation is equal to or less than that of the prior pearlite colony size.

In both pearlitic and martensitic structures the formation of austenite begins in the regions which have the lowest Ac_1, and these are determined by the dendritic pattern of the steel. In S.A.E. 1060 ingots, the lowest Ac_1 was observed in the interbrachial areas (between the branches) of the dendrites or in the interdendritic areas which contain few sulphide inclusions. Larger grains are formed in these areas than in the other parts of the dendritic pattern. It is these larger grains which coarsen first on heating.

When sulphur in amounts up to 0.1 per cent was added to steel of 0.15 and 0.60 per cent of carbon with aluminum additions of 0 to 2 pounds per ton, the general effect of the additional sulphur was to restrict coarsening or raise the coarsening temperature in excess of any inhibiting action due to the aluminum additions.

The author gratefully acknowledges the many suggestions and helpful criticism of Dr. M. A. Grossmann who initiated this study, and the assistance of many members of the South Works staff.

Bibliography

1. M. A. Grossmann, "Grain Size in Metals, with Special Reference to Grain Growth in Austenite," TRANSACTIONS, American Society for Metals, Vol. 22, 1934, p. 861-877.
2. M. A. Grossmann, "On Grain Size and Grain Growth," TRANSACTIONS, American Society for Steel Treating, Vol. 21, 1933, p. 1079-1104.
3. M. A. Grossmann, "On Grain Size and Grain Growth", "Principles of Heat Treatment," American Society for Metals, 1934.
4. R. F. Mehl and D. W. Smith, *Metals Technology*, American Institute of Mining and Metallurgical Engineers, T. P. 566, Sept. 1934.
5. J. M. Robertson, Iron and Steel Institute, *Carnegie Scholarship Memoirs*, 1931, p. 48.
6. C. Benedicks and H. Löfquist, "Non-Metallic Inclusions in Iron and Steel," 1931, p. 120.
7. C. E. Sims and G. A. Lillieqvist, American Institute of Mining and Metallurgical Engineers, Iron and Steel Division, Vol. 100, 1932, p. 154-175.

DISCUSSION

Written Discussion: By Frederick C. Hull, research laboratories, Westinghouse Electric & Manufacturing Co., East Pittsburgh, Pa.

With a suitable 2 per cent nital etch, M. Baeyertz has been able to develop ferrite grain boundaries between pearlite colonies (Fig. 3) and a uniform roughening of the ferrite throughout a given colony (Fig. 4). The latter result is in conformity with the earlier observations of Belaiew and Rosenhain that pearlite colonies may be distinguished by a uniformity in the orientation of etch pits in the ferrite. The photomicrographs intended to support this statement have, in general, been most disappointing.

A technique has now been developed that yields satisfactory photomicrographic evidence on the point. A specimen of high purity steel containing 0.90 per cent carbon and prepared in the manner described by Mehl and Wells[1] was austenitized one-half hour at 1605 degrees Fahr. (875 degrees Cent.) and transformed to coarse pearlite at 1330 degrees Fahr. (722 degrees Cent.). After electrolytic polishing, the sample was etched about fifteen seconds in Vilella's Martensite Reagent (1 gram picric acid, 5 cubic centimeters concentrated hydrochloric acid, 95 cubic centimeters ethyl alcohol). The ferrite of pearlite was attacked differentially in the several colonies, as may be seen in Fig. A. A number of attempts were made to duplicate these results with a commercial steel, but they proved to be unsuccessful. Additional photomicrographs of differential ferrite etching are to be found in the paper by Hull and Mehl[2] that is printed in this issue of TRANSACTIONS, page 381.

---

[1]R. F. Mehl and C. Wells, *Transactions* American Institute of Mining and Metallurgical Engineers, Iron and Steel Division, Vol. 125, 1937, p. 429.

[2]F. C. Hull and R. F. Mehl, "The Structure of Pearlite", published in this issue of TRANSACTIONS, p. 381.

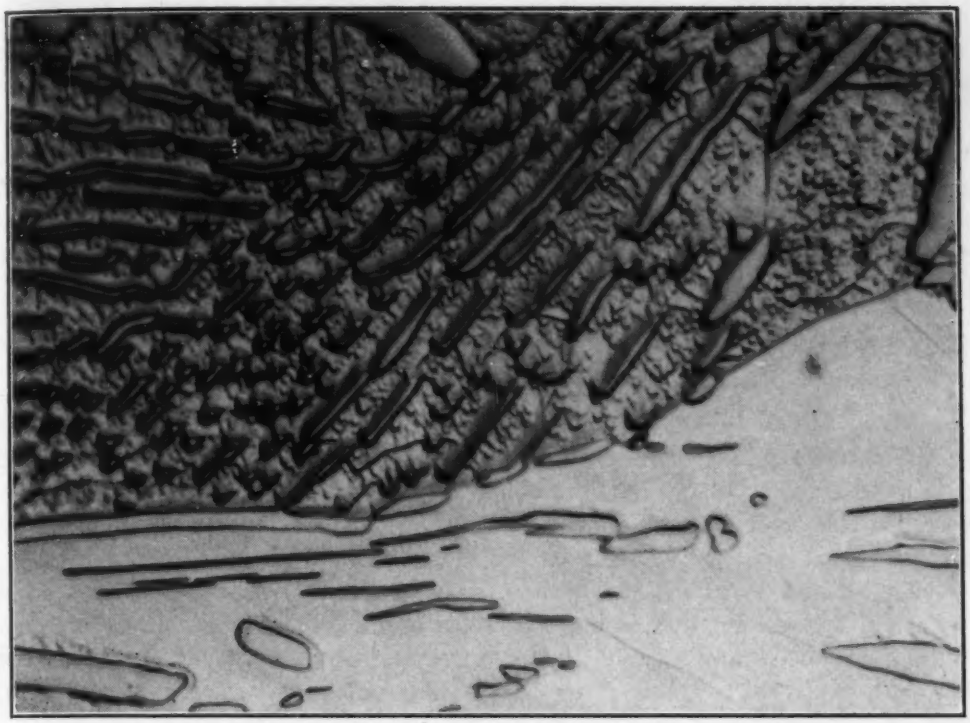

Fig A—Differential Etching of the Ferrite of Pearlite. High Purity Steel. Electrolytically Polished and Etched with Vilella's Martensite Reagent. Austenitized ½ Hour at 1605 Degrees Fahr. (875 Degrees Cent.) and Transformed at 1330 Degrees Fahr. (722 Degrees Cent.). ×1500.

Oral Discussion

G. A. ROBERTS:[3] I would like to ask the author two questions, which concern some of the experiments that I have made on this subject.

The author has stated that austenite grains formed from pearlite are elongated, while those forming from spheroidized structures are equiaxed. If the steels are sufficiently annealed so that there is absolutely no banding present or *no evidence of dendritic structure,* does this condition still prevail? It has been my experience that any steel which is sufficiently banded so that under suitable cooling conditions the ferrite and pearlite separate in longitudinal strips will produce these elongated austenitic grains. This is to be associated with growth in one direction only along lines conforming to segregated regions producing the lowest A_1 temperature. However, if this banding and dendritic segregation is largely eliminated, I find that the usual equiaxed austenitic grains are formed.

In the second place, the remarks concerning the effect of pearlite colony size on the austenite grain size need to be considered. It is well known that a very large range of pearlite colony sizes can be produced by altering the temperature of their formation from the knee to just below the Ae_1. It seems that this range for pearlite colony sizes is all out of proportion to the small change in grain size that accompanies austenitizing from these various struc-

[3]Vanadium-Alloys Steel Company Fellow, Carnegie Institute of Technology, Pittsburgh.

tures. If the pearlite colony size does control the austenite grain size in accordance with the author's views, there should be no limit to the grain refinement possible in *any* steel, for on cooling each austenite grain forms numerous pearlite colonies, which would thus lead to numerous austenite grains in place of each former one on reheating just above A_1. The possibilities of this are startling when we consider the next cooling and reheating on the same specimen. Producing fine-grained steels from coarse-grained steels would be an extremely simple process. I should like to hear the author elaborate on her findings in this respect.

Author's Reply

First, I would like to thank the discussers of this paper. With regard to the ferrite etching, I think I would like particularly to thank Mr. Hull for his excellent photograph of something which I have tried to show and was not half as successful in doing. The grains are apparently much better shown by his etching technique in the alloy which he had to work with.

To answer some of Mr. Roberts' questions, I have never seen a steel in which the banding was entirely removed, although I would like to say that I think the banding probably has an effect on the growth of the elongated grains, because these grains grow over a range of temperature and, of course, they start in the areas having the lowest Ac_1 and continue to the areas having the highest Ac_1. It stands to reason that that must be the mechanism that produces an elongated grain, and that banding must come into this picture.

With regard to the pearlite colonies and their effect on austenitic grains, the statement in the paper is that the colony size determines the austenitic grain size only in that it determines the maximum size; that is, the austenitic grain size is equal or less than that of the colony size, and I think it is that thing which allows the evening-out of grain sizes which Mr. Roberts talked about. When you have a large pearlite colony size, you may have several austenitic grains growing from the same colony. When you have a smaller pearlite colony size, you may have more nuclei than one, which grows into that pearlite colony, but by and large, the number of nuclei which survive in the transformation are a smaller number than in the case of the larger pearlite colonies.

With regard to the production of fine-grained steel from coarse-grained steel, that is exactly what we may do, *but only at the time of transformation.* As soon as two or more austenite grains grow into contact with each other in a so-called coarse-grained steel (one without coarsening inhibitors), the austenite grains begin to coarsen (favored austenite grains survive at the expense of less favored austenite grains), and austenite grain growth continues steadily throughout the transformation period and during any heating which the steel undergoes above the critical range. There is no stabilization of the austenite grain size over a temperature range above the critical as in the fine-grained steels. As indicated on page 467, in order to observe the effect of the limitation of the austenite grain size by the pearlite colony size, the coarsening temperature must not have been exceeded.

THE EFFECT OF NORMAL ELEMENTS AND ALLOY ELEMENTS ON THE RATE OF AUSTENITE TRANSFORMATION IN CAST IRON AT CONSTANT TEMPERATURE

By Charles Nagler and William P. Wood

Abstract

This paper presents a study of the effect of normal elements (carbon, silicon, phosphorus, sulphur, and manganese) and alloy elements (chromium, nickel, and molybdenum) on the rate of austenite transformation in cast iron at 1200 degrees Fahr. (650 degrees Cent.). The data was determined on a specially designed magnetic transformation furnace which can operate from room temperature up to 1300 degrees Fahr. (705 degrees Cent.). The rate of austenite transformation was followed by taking ammeter readings every 2.5 seconds until the reaction was completed. Quantitative data for the incubation period and transformation time was determined for each sample studied. This method appears to have a major advantage over the tedious metallographic determination in that sufficient quantitative data can be determined for the construction of a complete isothermal transformation curve of cast iron in a relatively short time. Transformation data was determined on synthetic induction furnace heats of cast iron that were made from Armco iron, graphite, phosphide and sulphide or iron, ferro alloys of silicon and manganese, and nickel, chromium, and molybdenum of commercial purity. Irons were poured into dry sand molds, and specimens for study were machined from the centers of the transverse bars.

IN order to avoid the use of metallography in the determination of austenite transformation rates, a method has been devised, based on the magnetic changes which accompany the transformation. This method makes it possible to determine a transformation curve in a much shorter time and with greater accuracy than is possible with the metallographic method which was developed by Davenport and Bain.

Of the authors, Charles Nagler is instructor of metallography, University of Minnesota, Minneapolis, and William P. Wood is professor, Department of Chemical and Metallurgical Engineering, University of Michigan, Ann Arbor, Mich. Manuscript received August 17, 1940.

Their procedure was to heat a sample above the critical range for 1 hour, rapidly quench the sample in a lead bath maintained at a predetermined subcritical temperature for a definite length of time, and rapidly quench in water. These steps were repeated with different samples from the same source, the length of time in the lead bath being increased by a short interval for each successive sample. The samples were polished, etched, and examined microscopically. The amount of austenite was then estimated by observing the amount of martensite present in the sample. Because of the large number of samples required and the necessity for polishing the samples and estimating the degree of transformation, this method becomes a long and tedious process.

The purpose of this paper is to explain the apparatus, procedure, and calculations involved in determining transformation rates by the magnetic method and to show the results obtained with the present equipment. These points will be discussed in the order mentioned after a brief review of the preliminary work.

Preliminary Work

In order to observe the progress of austenite transformation, it is necessary to cool the properly heated specimen rapidly to a subcritical temperature of study and to maintain it at that temperature within narrow limits. The quenching to this subcritical temperature must be rapid enough to preserve the austenite essentially unchanged down to the observation temperature, and to prevent transformation from occurring at any temperature above or below the one chosen for study.

Theoretical Basis—When steel or cast iron transform from the austenitic to the pearlitic, acicular or martensitic state, one of the important properties that is radically changed is the magnetic permeability. Although the permeability is somewhat different among the products of the austenitic transformation, the order of magnitude of the permeability of austenite is entirely different from that of its decomposition products. This change in permeability is, in reality, a measure of the degree of transformation.

Development of the Transformer Apparatus—With this phenomenon as a basis, the authors devised an apparatus in which the sample, after being quenched for a few seconds in the lead bath, was placed between the poles of a specially designed alternating cur-

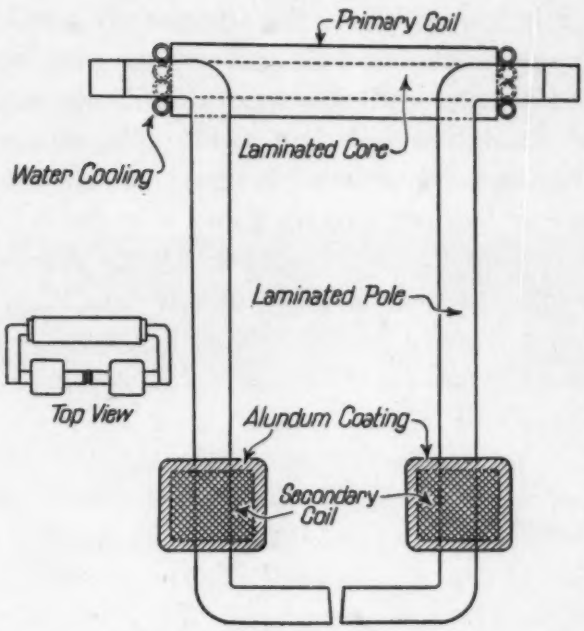

Fig. 1—Detail of Transformer.

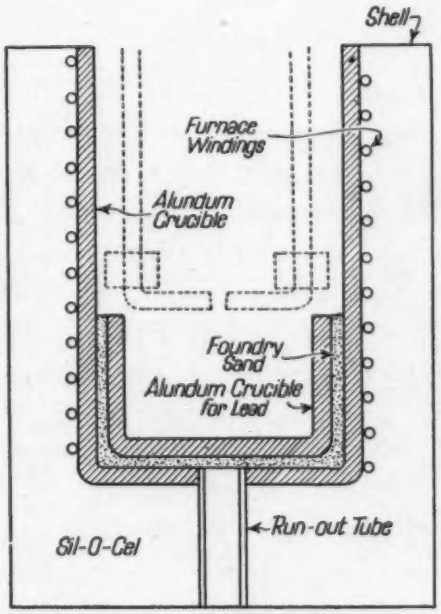

Fig. 2—Lead Pot Furnace.

rent transformer. As the transformation took place, the permeability of the sample increased, causing an increase in the e.m.f. generated in the secondary coil. The changes in the secondary current were read on an ammeter, and the results were plotted as ammeter readings against time. On the basis of the assumption that the sec-

ondary current is a measure of the amount of austenite in the sample, this plot was the same as a plot of per cent austenite against time.

The chief difficulty with the apparatus illustrated in Figs. 1 and 2 was that the secondary coils had to be replaced after about forty-eight hours of use, since it was necessary to keep them either submerged in the lead bath or directly above it in the hottest part of the furnace. The insulation on the copper wire windings did not stand up under the intense heat in the furnace, and the secondary coil would be short circuited. A thin sheet of mica was placed between each set of windings, and a thick coating of alundum cement around the outside of the coil.

The next step in the development of the apparatus was to devise a means of keeping the coils outside the furnace. It was found that if the magnetic circuit was not completed, a larger current was induced in the secondary, and accordingly the idea of using a solenoid in place of the transformer seemed logical. The construction of such a unit was completed, and the results of the tests made with it have been quite satisfactory.

Apparatus

The Transformation Furnace—In this apparatus the coils are placed outside the furnace tube and are water cooled with the result that, at the time of this writing, they have been in use for over five months, and are still in excellent condition.

A photograph is shown of the furnace in Fig. 3, and a detailed drawing of the unit in Fig. 4. The transformation furnace is mounted on a piece of transite board having the dimensions 18 by 24 by 0.5 inches. The board rests on the furnace containing the lead bath, and serves both as the bottom of the upper furnace, and as a platform for supporting the coils. It was found that the coils could not be placed outside the furnace shell, as was desired, because the current induced in the secondary coil was then too small to be measured with any degree of accuracy. Consequently, they are placed in openings cut from the furnace shell and separated from the Sil-O-Cel packing by helical water cooling coils, one of copper tubing between the cores and the windings, and the other of lead tubing around the outside of the coils. Copper tubing is wound into a spiral water wall between the furnace tube and the primary coil. The primary coil is wound with about 1500 turns of number 22 enameled copper, cotton covered magnet wire, and the secondary with about 250 turns of

number 18 enameled copper magnet wire. The reason for using the different sizes of wire is that it is desirable to have a small current in the primary in order to avoid excessive heating, and a large current in the secondary to obtain more accurate readings. Having 1500 turns on the primary gives a current of 1.5 amperes in the coil.

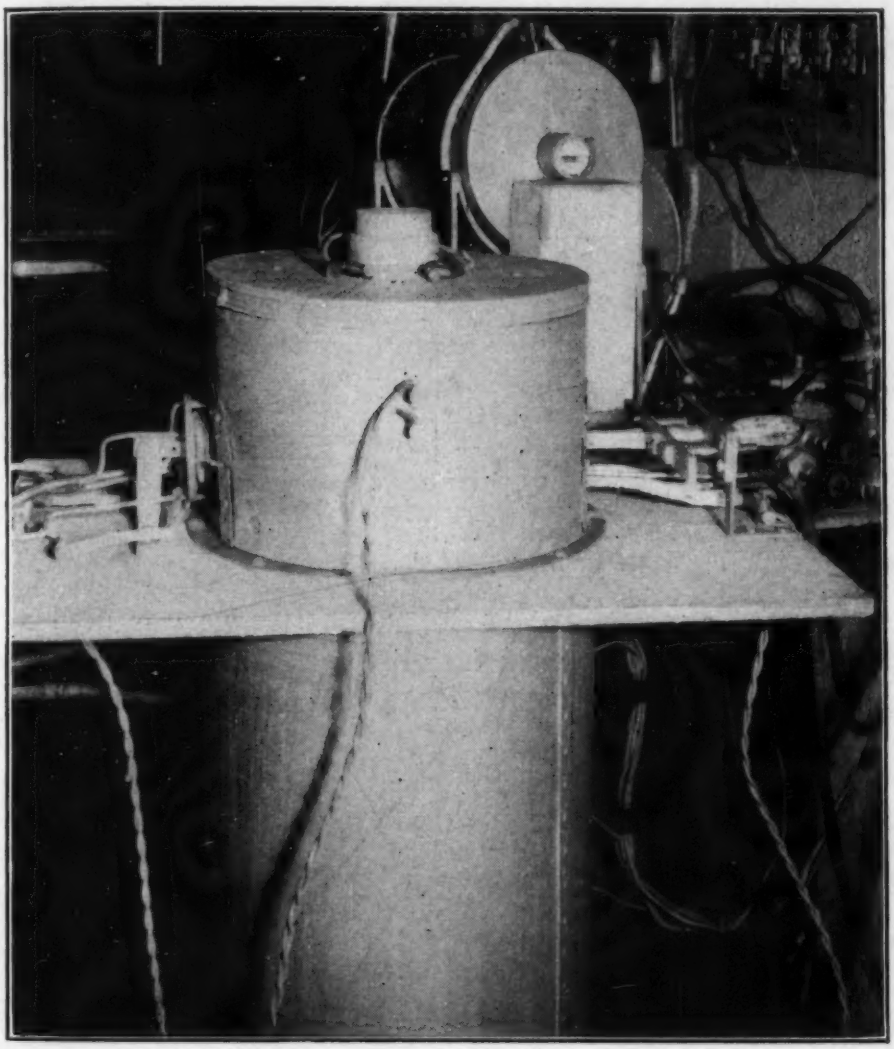

Fig. 3—Transformation Furnace.

In the secondary coil there was induced a current of 0.40 of an ampere with ⅛-inch air gap between the poles, and 1.00 ampere with the poles together, or with a magnetic material in the air gap. This is only true when the poles are at room temperature.

The cores, which are of laminated low carbon iron 0.5 inch square by 8 inches long, pass through openings in the furnace tube

and are supported on transite boards both inside and outside the furnace shell. Small transite blocks are cemented in the furnace tube openings to prevent short circuiting of the cores against the heating element. The primary core is stationary, and the secondary core is movable to permit placing of the sample between the poles.

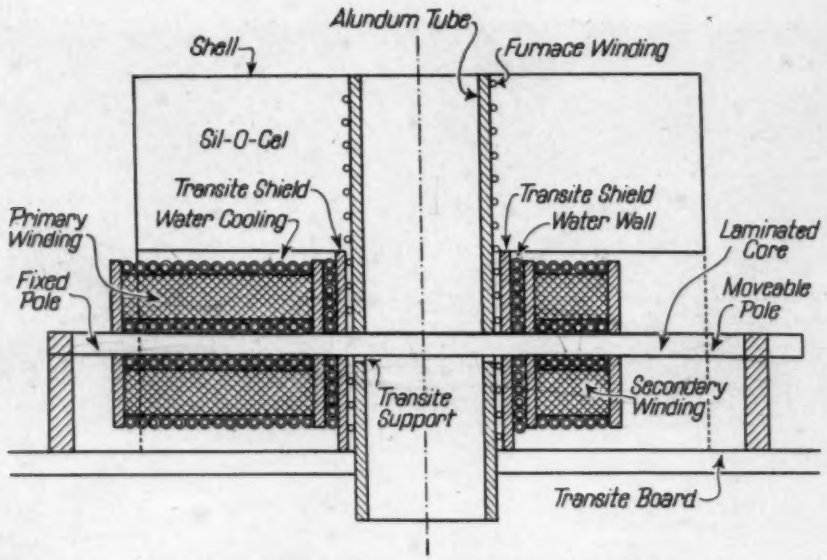

Fig. 4—Detail Drawing of Transformation Furnace.

Nitrogen gas preheated in a separate furnace was used as an atmosphere in the transformation and sample preheat furnace to prevent oxidation of the poles and decarburization of the samples. When decarburization takes place, there is found a layer of ferrite on the surface of the sample. The presence of this ferrite layer tends to give erratic results. By varying the time of solution, it was found that it greatly influenced the rate of transformation. The temperature of solution also greatly influences the transformation rate. To eliminate these variables, it was decided that the temperature of solution should be 1600 degrees Fahr. (870 degrees Cent.), and the time of solution 1 hour. These conclusions were drawn after a series of preliminary investigations.

Two thermocouples are mounted in the furnace, one passing down through the packing along the outside of the heating unit and into the lead bath, and the other passing horizontally through the center of the furnace, with the hot junction inside a small hole in the primary core ⅛ of an inch away from the pole face.

The sample used was 0.5 inch square by ⅛ inch thick and was attached to chromal wires about 18 inches long. It was assumed

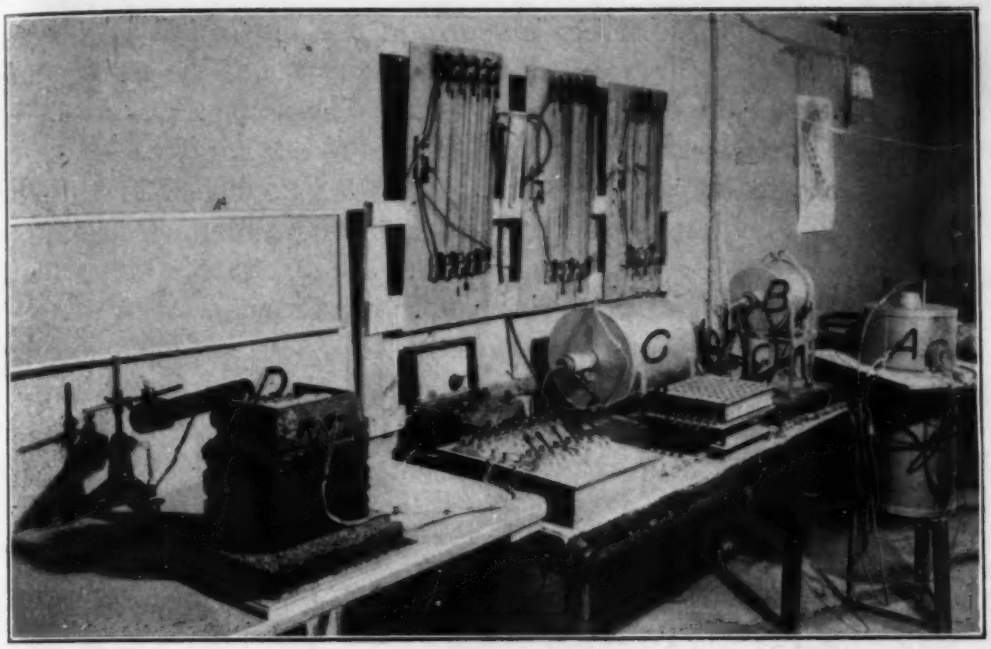

Fig. 5—Arrangement of Equipment.

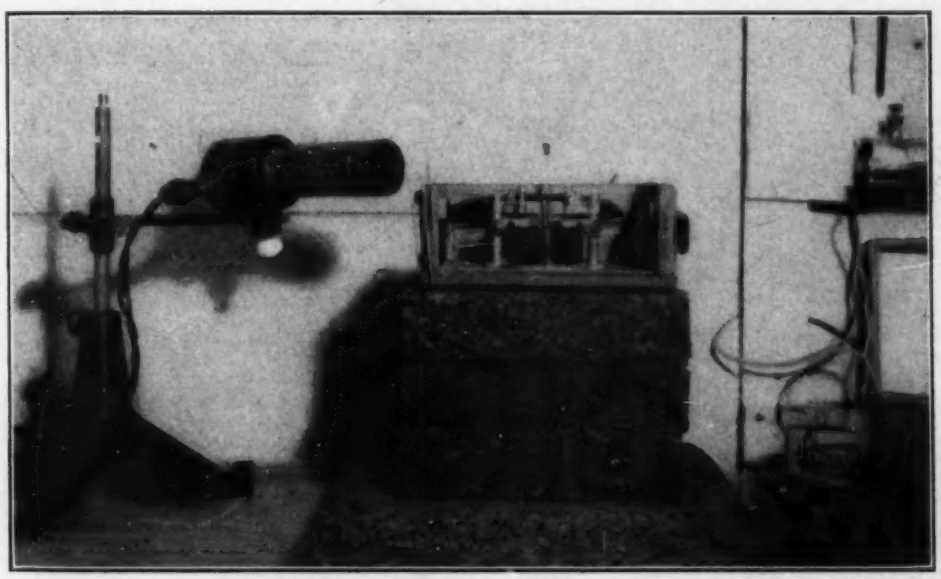

Fig. 6—Arrangement of Mirror and Light-Beam on Secondary Ammeter.

that a sample of this size would come to the temperature of the lead bath after about three seconds of quenching, which is before any transformation might take place.

Auxiliary Equipment—The auxiliary equipment includes the preheating furnace for the nitrogen, sample preheating furnace, and the necessary resistance boards, ammeters, potentiometer, and switch-

boards. The complete set-up is shown in Fig. 5. In this Fig., A is the transformation furnace, B the preheat furnace, C the gas heating furnace, and D the secondary ammeter. The secondary current is read on an ammeter, having a scale of zero to one ampere.

In order to increase the accuracy of these readings, a small mirror is mounted on the ammeter needle, and a light beam, focussed on the mirror, is reflected onto a large scale mounted on the wall behind the light source. This arrangement is shown in detail in Fig. 6.

Preparation of Samples—In order to study the effect of the varying composition and alloying elements on the rate of transformation in cast iron a series of synthetic heats of iron were made in an induction furnace. The charge consisted of Armco iron and graph-

Table I

Heat No.	Carbon	Manganese	Sulphur	Phosphorus	Molybdenum	Nickel	Chromium	Silicon
1718-A	2.51	0.63	0.082	0.157	....	....	....	2.10
-B	2.80	0.63	0.082	0.157	....	....	....	2.10
-C	3.06	0.63	0.082	0.157	....	....	....	2.10
-D	3.39	0.63	0.082	0.157	....	....	....	2.10
1719-A	3.15	0.44	0.097	0.148	....	....	....	2.24
-B	3.15	0.77	0.097	0.148	....	....	....	2.24
-C	3.15	1.08	0.097	0.148	....	....	....	2.24
-D	3.15	1.39	0.097	0.148	....	....	....	2.24
1720-A	3.10	0.64	0.039	0.154	....	....	....	2.20
-B	3.10	0.64	0.087	0.154	....	....	....	2.20
-C	3.10	0.64	0.152	0.154	....	....	....	2.20
-D	3.10	0.64	.....	0.154	....	....	....	2.20
1722-A	3.07	0.63	0.098	0.058	....	....	....	2.15
-B	3.07	0.63	0.098	0.118	....	....	....	2.15
-C	3.07	0.63	0.098	0.212	....	....	....	2.15
-D	3.07	0.63	0.098	0.314	....	....	....	2.15
1723-A	3.02	0.64	0.100	0.157	0.01	....	....	2.11
-B	3.02	0.64	0.100	0.157	0.35	....	....	2.11
-C	3.02	0.64	0.100	0.157	0.71	....	....	2.11
-D	3.02	0.64	0.100	0.157	1.00	....	....	2.11
1724-A	3.19	0.63	0.089	0.159	....	None	....	2.05
-B	3.19	0.63	0.089	0.159	....	0.51	....	2.05
-C	3.19	0.63	0.089	0.159	....	1.02	....	2.05
-D	3.19	0.63	0.089	0.159	....	1.49	....	2.05
1733-A	3.36	0.67	0.095	0.155	....	....	None	2.03
-B	3.36	0.67	0.095	0.155	....	....	0.25	2.03
-C	3.36	0.67	0.095	0.155	....	....	0.50	2.03
-D	3.36	0.67	0.095	0.155	....	....	0.78	2.03
1734-A	3.24	0.66	0.094	0.155	....	....	....	1.43
-B	3.24	0.66	0.094	0.155	....	....	....	1.72
-C	3.24	0.66	0.094	0.155	....	....	....	1.92
-D	3.24	0.66	0.094	0.155	....	....	....	2.13

ite, and common foundry grades of ferro-silicon, ferro-manganese, ferro-phosphorus, ferro-chromium, ferro-molybdenum, iron sulphide, and nickel were added in order to obtain the desired compositions. The chemical composition of the irons used in this study are given in Table I.

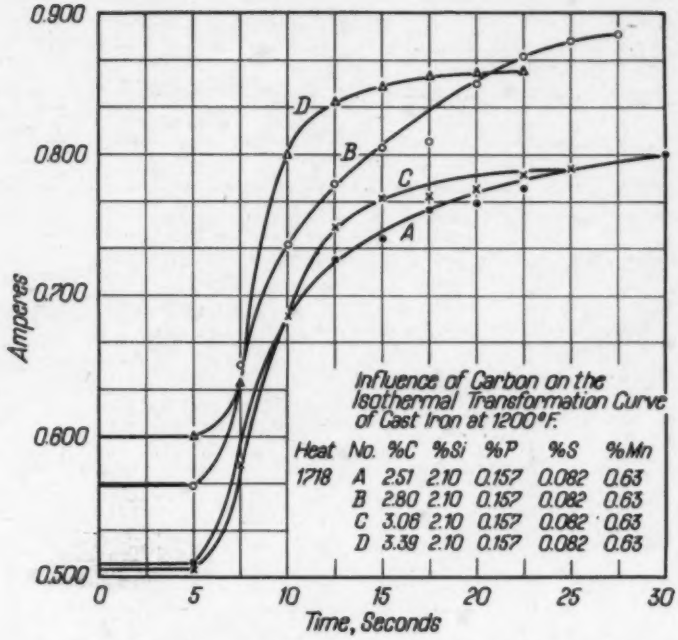

Fig. 7—Influence of Carbon on the Isothermal Transformation Curve of Cast Iron at 1200 Degrees Fahr.

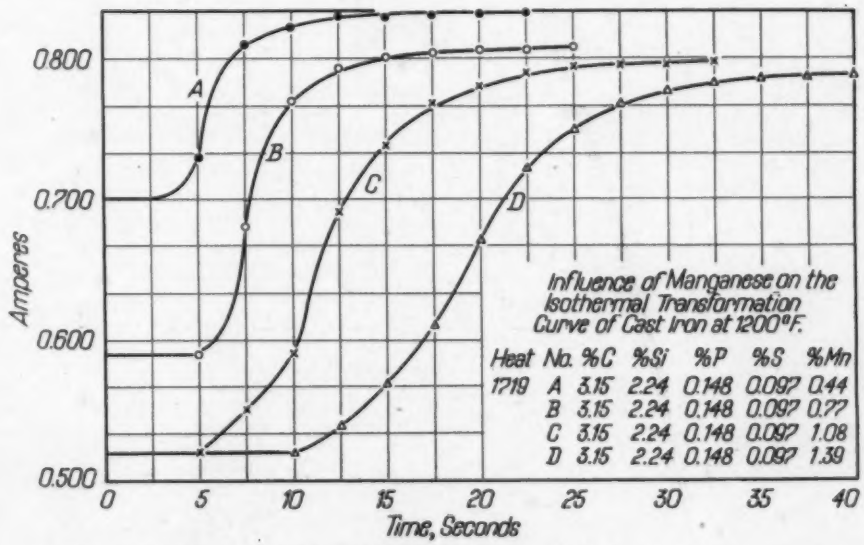

Fig. 8—Influence of Manganese on the Isothermal Transformation Curve of Cast Iron at 1200 Degrees Fahr.

The irons were poured into 1.2 inch standard arbitration transverse test bars in dry sand molds. Sample bars, 9 by 0.5 by 0.5 for use in this investigation, were machined from the centers of the transverse test bars. The melts were not deoxidized, but poured directly after melting.

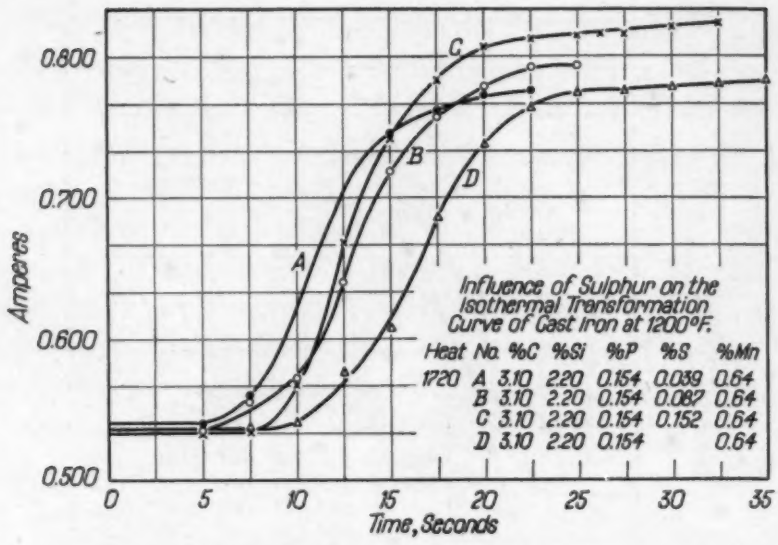

Fig. 9—Influence of Sulphur on the Isothermal Transformation Curve of Cast Iron at 1200 Degrees Fahr.

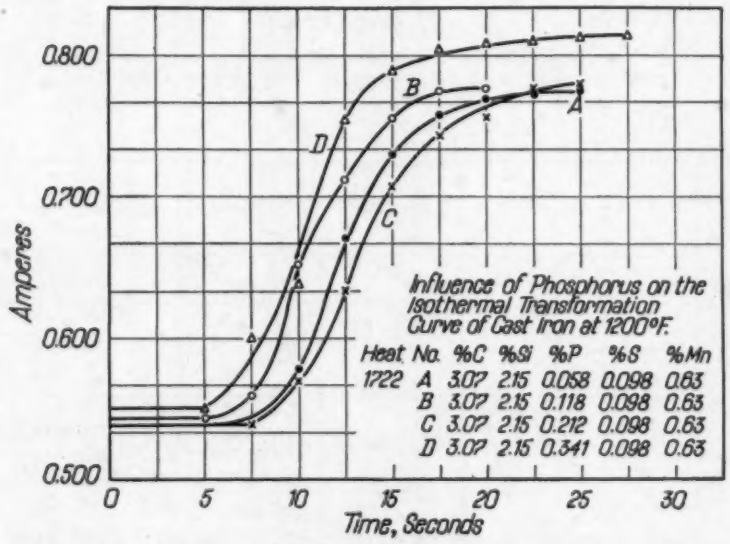

Fig. 10—Influence of Phosphorus on the Isothermal Transformation Curve of Cast Iron at 1200 Degrees Fahr.

Operation of Apparatus

The general procedure for determining a transformation curve is as follows: The lead bath and poles are heated to a desired temperature, and the sample is preheated in a nitrogen atmosphere for 1 hour. The sample is then removed, quenched rapidly in the lead bath for 3 seconds, and immediately placed between the poles. Readings of the secondary ammeter are taken at regular intervals of 2.5 seconds. The time is measured with the aid of a stopwatch.

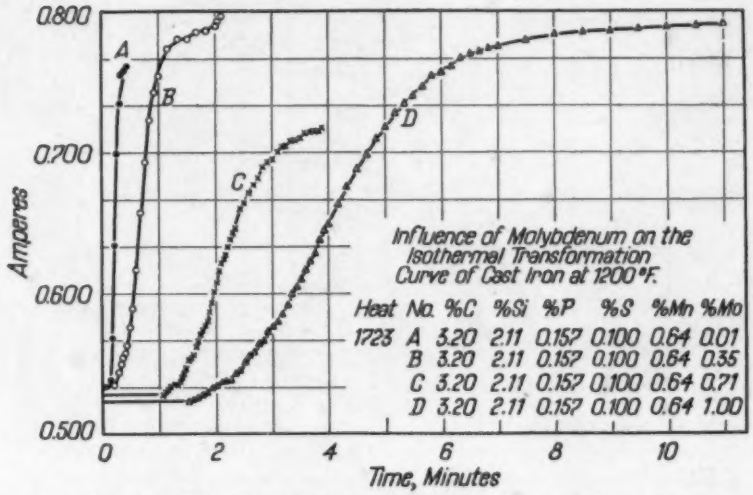

Fig. 11—Influence of Molybdenum on the Isothermal Transformation Curve of Cast Iron at 1200 Degrees Fahr.

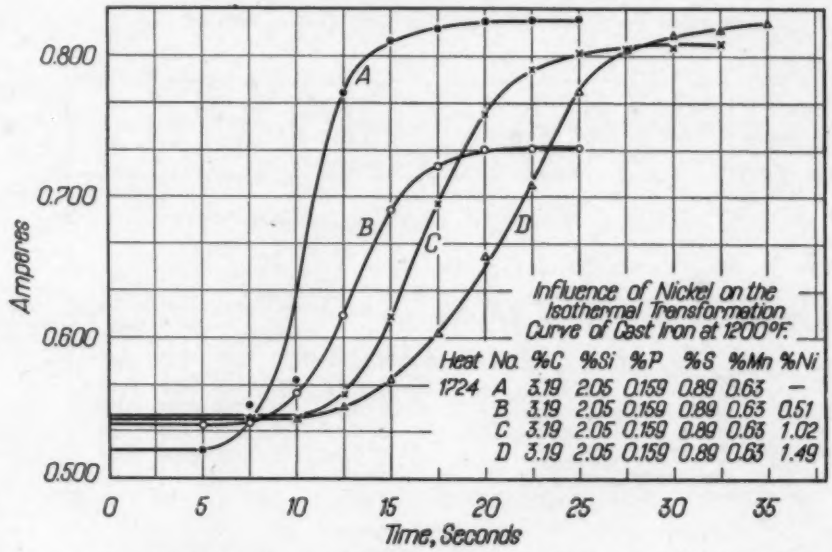

Fig. 12—Influence of Nickel on the Isothermal Transformation Curve of Cast Iron at 1200 Degrees Fahr.

Readings are started from the moment the sample is immersed into the lead bath. During the transformation the poles must be kept in firm contact with the sample. The data are plotted as ammeter readings against time.

Calculation of Data

Bain[1] concluded that the transformation of austenite followed a first order unimolecular reaction; i.e., a reaction in which only

[1]E. C. Bain, "On the Rate of Reactions in Solid Steel," *Transactions*, American Institute of Mining and Metallurgical Engineers, Iron and Steel Division, Vol. 100, 1932.

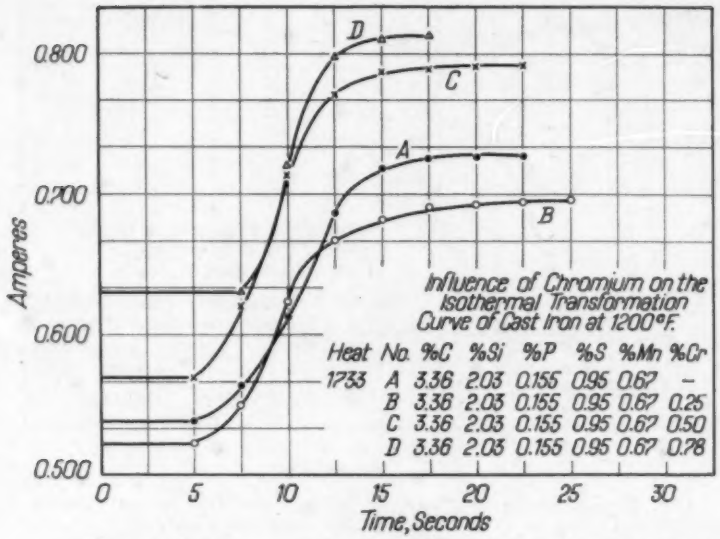

Fig. 13—Influence of Chromium on the Isothermal Transformation Curve of Cast Iron at 1200 Degrees Fahr.

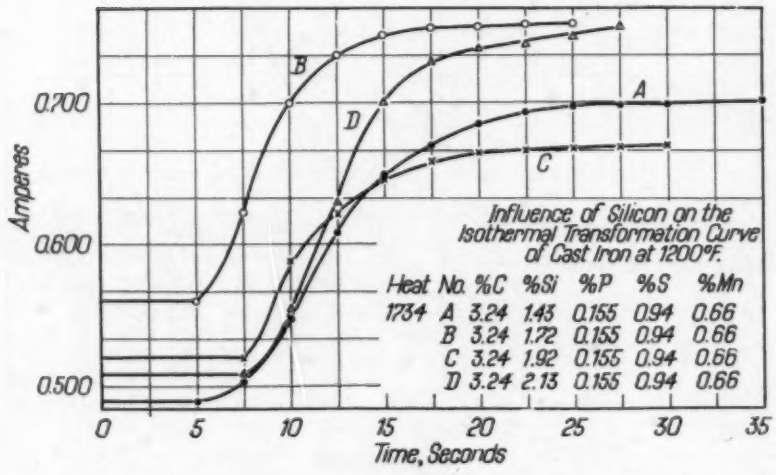

Fig. 14—Influence of Silicon on the Isothermal Transformation Curve of Cast Iron at 1200 Degrees Fahr.

one substance is involved, and the rate of decomposition of which is directly proportional to the concentration. Such a reaction can be expressed mathematically by the equation

$$-\frac{dc}{dt} = KC$$

where C is the concentration of the material, K is a proportionality factor, and $-\frac{dc}{dt}$ is the rate at which the concentration decreases.

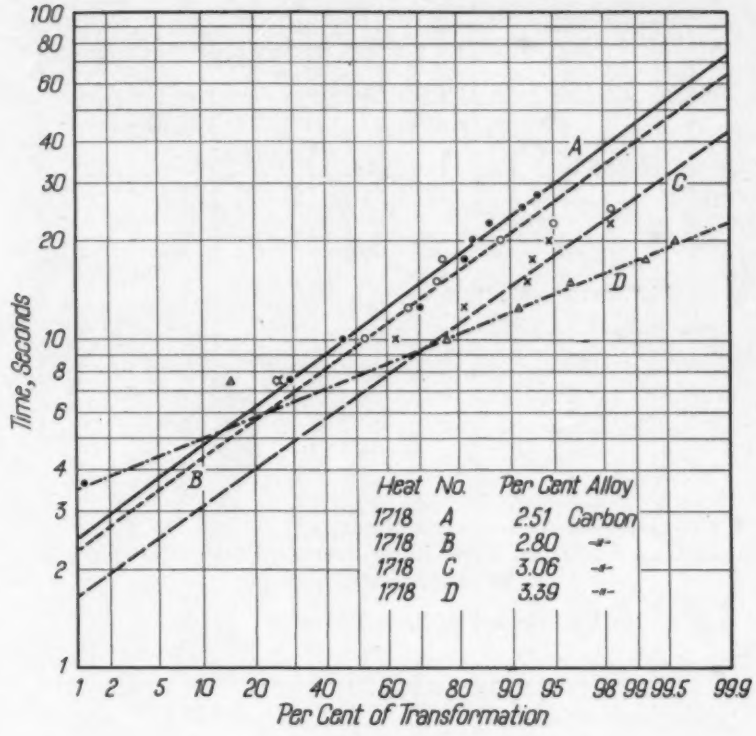

Fig. 15—Logarithmic Probability Plot.

Integrating this equation between the limits of C_1 at t_1 and C_2 at t_2 gives

$$-\int_{c_1}^{c_2} \frac{dc}{c} = K \int_{t_1}^{t_2} dt$$

and $-(\ln c_2 - \ln c_1) = K\ (t_2 - t_1)$

$$K = \frac{\text{Ln} \frac{C_1}{C_2}}{t_2 - t_1}$$

If t_1 is equal to zero, this equation may be modified to the form,

$$K = \frac{\text{Ln} \frac{C_o}{C_\theta}}{t}$$

Where c_o is the concentration at the beginning of the transformation; i.e., when $t = o$, and c_θ is the concentration at any time, t.

For the purposes of this report the equation is written in the form,

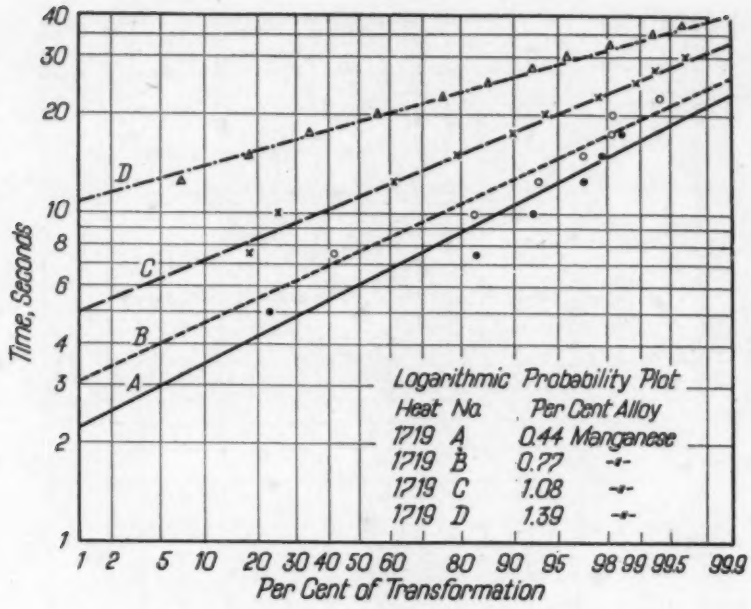

Fig. 16—Logarithmic Probability Plot.

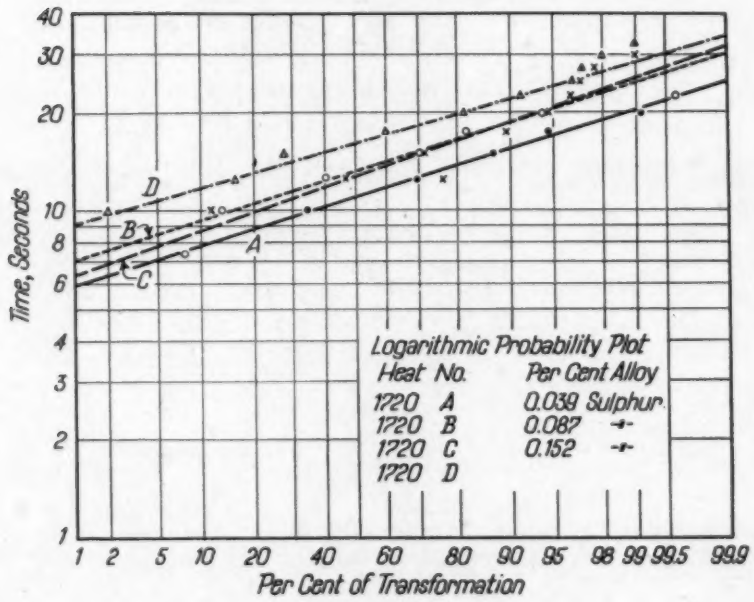

Fig. 17—Logarithmic Probability Plot.

$$Kt = \ln \frac{A_o}{A_\theta}$$

where A_o is the initial concentration of the austenite and A_θ is the concentration of the austenite at any time, t. It will be seen from this equation that a straight line should result if $\log \frac{A_o}{A_\theta}$ is plotted

against time. However, difficulty was experienced, the data did not seem to fit a straight line function. Austin and Rickett[2] suggested the use of logarithmic probability curve in plotting austenitic transformation data, and this method proved rather satisfactory.

The transformation data as determined was plotted on Cartesian co-ordinates, and are given in Figs. 7 to 14. The logarithmic probability plot as given in Figs. 15 to 22 is the method of Austin and Rickett for treatment of the transformation data. The time for

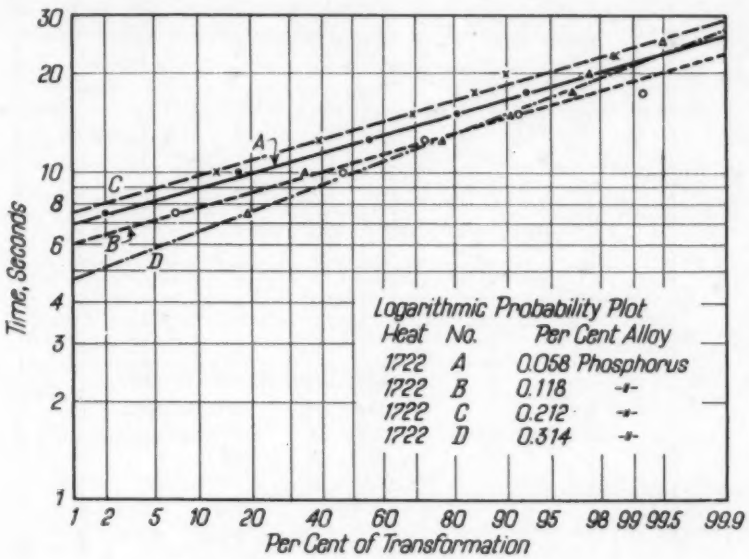

Fig. 18—Logarithmic Probability Plot.

transformation is plotted in Figs. 23 to 31, and is the time necessary to go from 1 per cent transformation to 99.5 per cent and these values are plotted against per cent of alloy element.

Discussion of Results

Examination of the plot per cent carbon vs. time for transformation on Fig. 23 indicates that as the carbon content is increased, the time for transformation is reduced. This might denote that with increasing carbon content, and fixed silicon, the carbides in solution in the austenite tend to be more unstable and appear to transform much more rapidly. The plot, Fig. 24, carbon plus ⅓ silicon vs. time for transformation is identical with the plot of Fig.

[2]J. B. Austin and R. L. Rickett, "Kinetics of the Decomposition of Austenite at Constant Temperature," *Metals Technology*, T. P. 964, September, 1939.

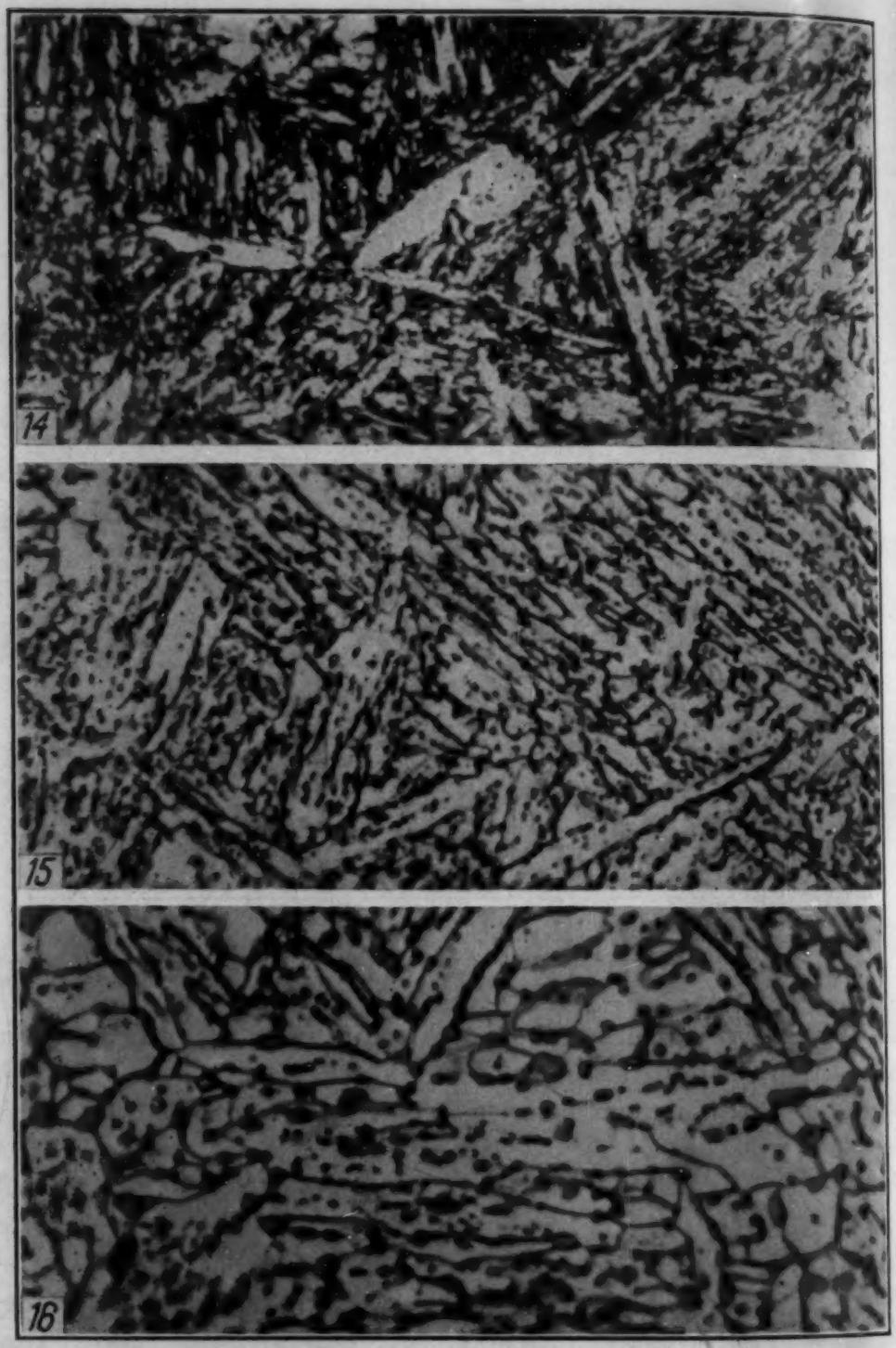

Fig. 14—Medium Carbon Martensite. × 2000.
Fig. 15—Same as Fig. 14 After Tempering. × 2000.
Fig. 16—Same as Fig. 14 After Spheroidizing. × 2000.

rite grain boundaries or in the position which corresponds to the so-called "midrib" of the martensite plates, as in Figs. 15 and 16. No dif-

against time. However, difficulty was experienced, the data did not seem to fit a straight line function. Austin and Rickett[2] suggested the use of logarithmic probability curve in plotting austenitic transformation data, and this method proved rather satisfactory.

The transformation data as determined was plotted on Cartesian co-ordinates, and are given in Figs. 7 to 14. The logarithmic probability plot as given in Figs. 15 to 22 is the method of Austin and Rickett for treatment of the transformation data. The time for

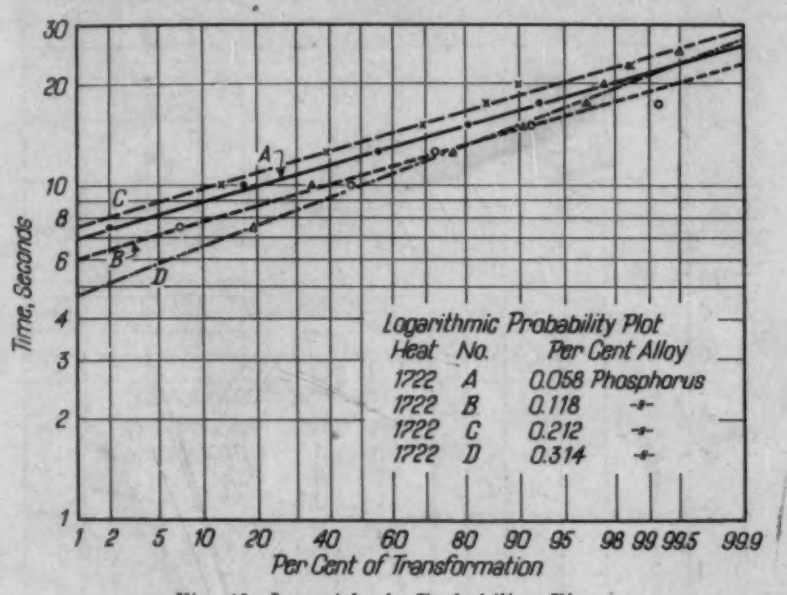

Fig. 18—Logarithmic Probability Plot.

transformation is plotted in Figs. 23 to 31, and is the time necessary to go from 1 per cent transformation to 99.5 per cent and these values are plotted against per cent of alloy element.

Discussion of Results

Examination of the plot per cent carbon vs. time for transformation on Fig. 23 indicates that as the carbon content is increased, the time for transformation is reduced. This might denote that with increasing carbon content, and fixed silicon, the carbides in solution in the austenite tend to be more unstable and appear to transform much more rapidly. The plot, Fig. 24, carbon plus ⅓ silicon vs. time for transformation is identical with the plot of Fig.

[2]J. B. Austin and R. L. Rickett, "Kinetics of the Decomposition of Austenite at Constant Temperature," *Metals Technology*, T. P. 964, September, 1939.

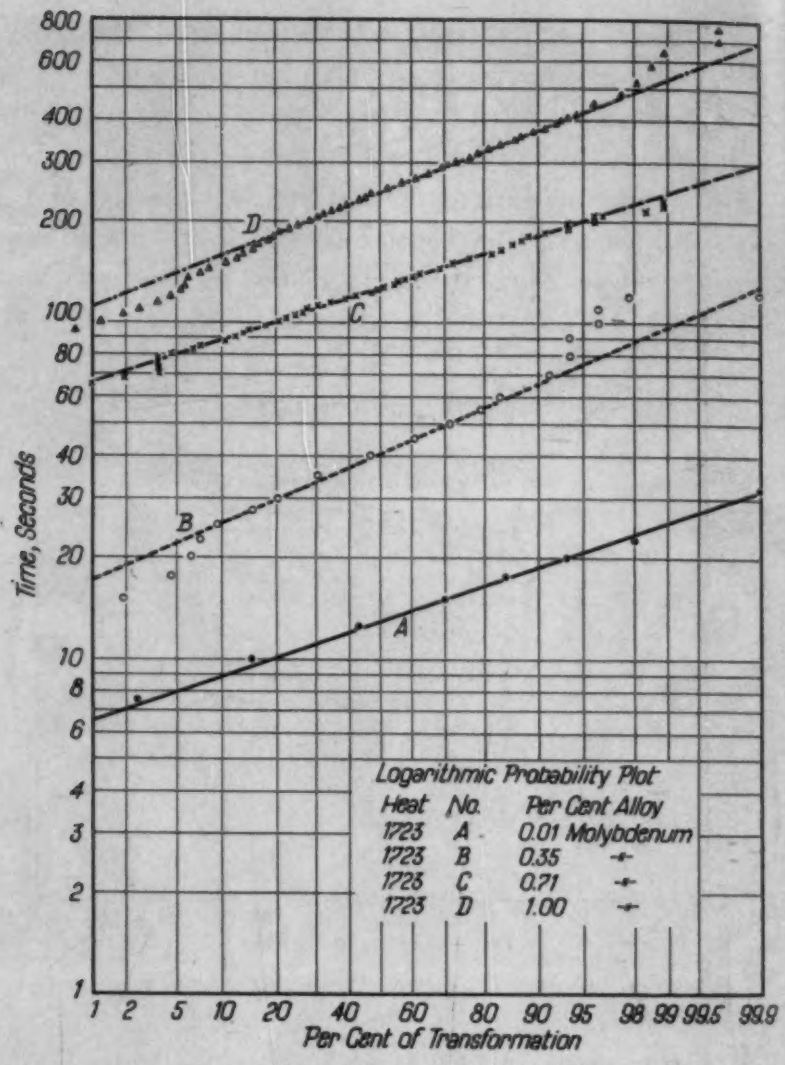

Fig. 19—Logarithmic Probability Plot.

23. The difference in position of the plot with respect to the carbon axis is due to the fact that the eutectic percentage is lowered slightly less than 30 per cent carbon for each per cent of silicon. The plot, Fig. 15, log time vs. percentage transformed (logarithmic probability) tend to show, at least in three out of the four samples studied, that as the carbon content is increased the slope of the line remains the same but there is some displacement of the plot along the time axis. The sample with the highest carbon content has a completely different slope than that of the other carbon studied, and it is impossible to explain at present this change.

Manganese and sulphur have a great affinity for each other. In the presence of a moderate excess of manganese the sulphur exists as manganese sulphide. The plot, Fig. 25, indicates that the

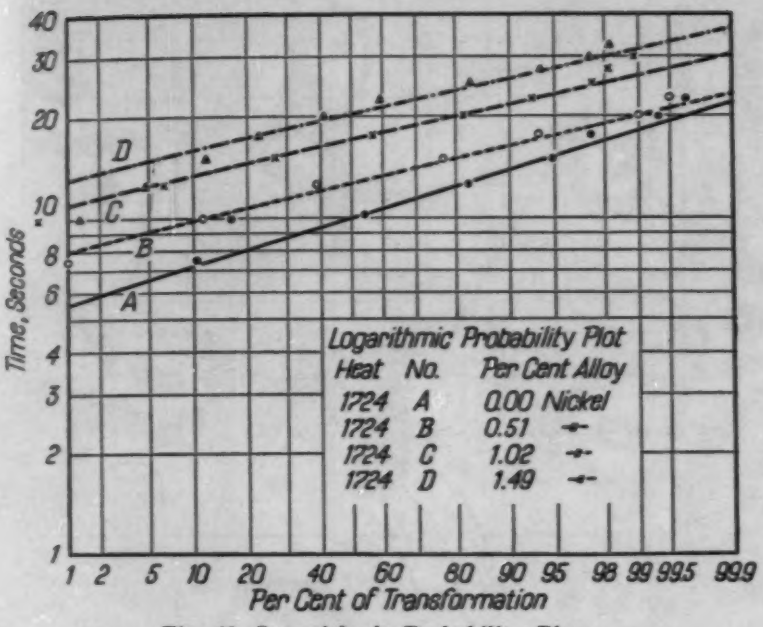

Fig. 20—Logarithmic Probability Plot.

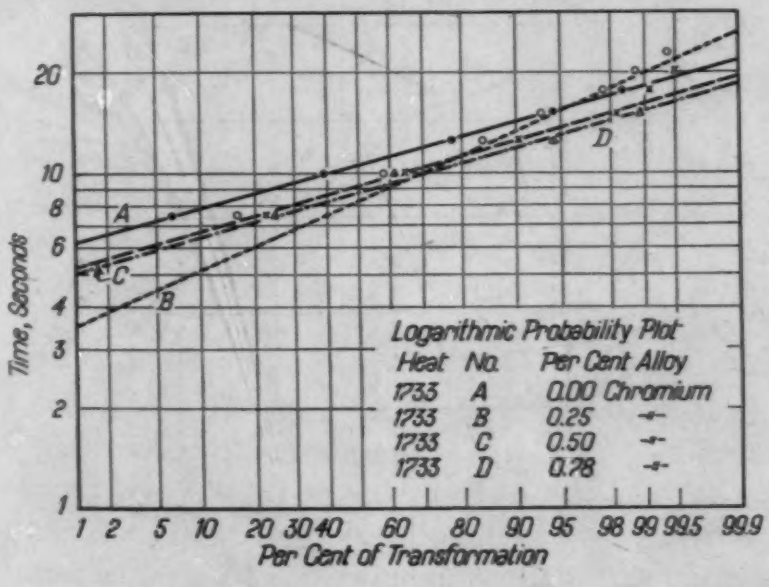

Fig. 21—Logarithmic Probability Plot.

manganese has a definite action upon the slowing down of the transformation in iron. Increasing the manganese content above 0.80 per cent causes an increase in the time for transformation.

As the sulphur content is increased, the time for transformation of the austenite is increased. The sulphur is present in the form of manganese sulphide. In cast iron an increase in the sulphur content results in an increase in the combined carbon. The

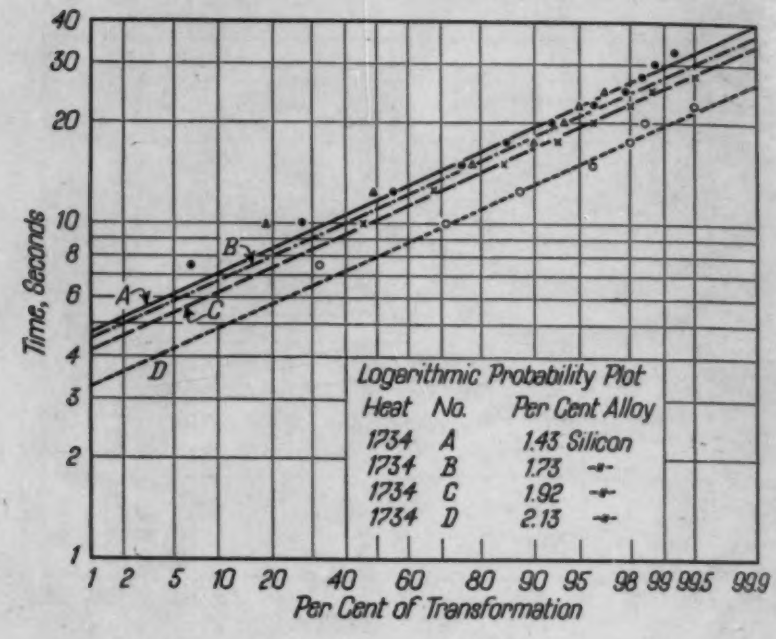

Fig. 22—Logarithmic Probability Plot.

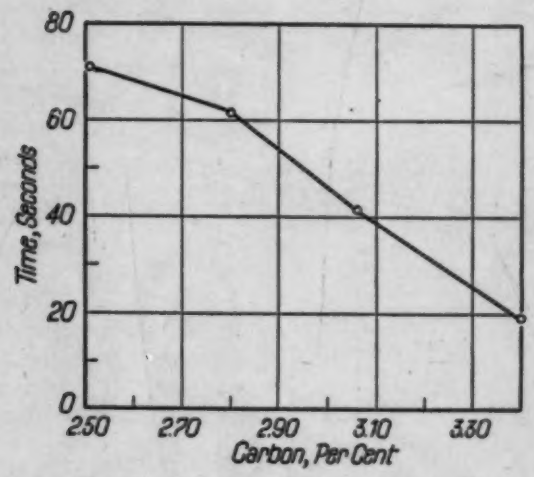

Fig. 23—Effect of Carbon on the Time for Transformation at 1200 Degrees Fahr.

plot of Fig. 26 shows the relationship between sulphur content and the time for transformation. The slope of the lines with varying per cents of sulphur remains about the same in the plot in Fig. 17. Phosphorus when added to the iron has a definite action in slowing down the transformation rate of the austenite, Fig. 27. The phosphorus is present in cast iron partially as of Fe_3P, steadite and the remainder dissolved in the ferrite. It has been generally accepted that phosphorus has no pronounced effect on the graphitization of iron. The sulphur and phosphorus above 0.10 per cent con-

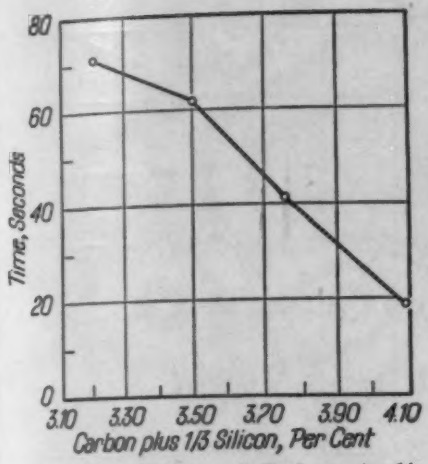

Fig. 24—Effect of Carbon + ⅓ Silicon on the Time for Transformation at 1200 Degrees Fahr.

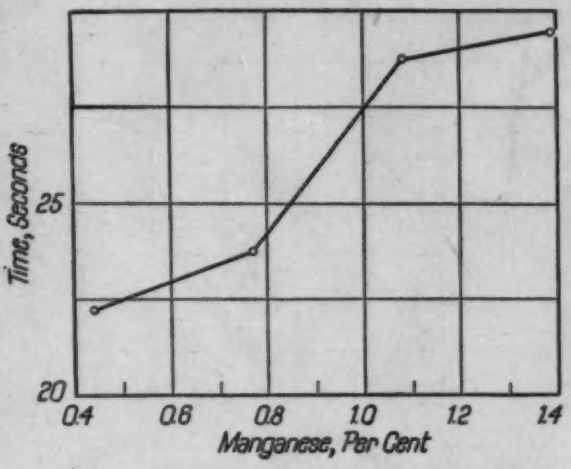

Fig. 25—Effect of Manganese on the Time for Transformation at 1200 Degrees Fahr.

tent have the same effect on the iron, as is indicated by the slopes of the lines being almost the same, Figs. 26 and 27.

Molybdenum, being a true alloying element, has a marked effect on the rate of austenite transformation. By varying the molybdenum content from 0.01 to 1.0 per cent, in the same base composition, the time for transformation can be increased about 20 times. The molybdenum slows down the time for transformation, Fig. 28, as the per cent of the alloy is increased. The plots on Fig. 19 show that with increasing molybdenum content there is little change in the slope of the lines.

The plots, Figs. 29 and 30, show the effect of nickel and chromium on the time for transformation.

Nickel speeds up the rate of austenite transformation of the iron, while in the case of chromium alloy the transformation rate is slowed down. Nickel in amounts greater than 0.50 per cent slows down the transformation reaction in cast iron. By increasing the chromium content beyond 0.25 per cent it tends to slow down the transformation rate. In most cases these two alloys are added together to iron. The nickel dissolves in the ferrite and gives fine lamella of pearlite, thereby increasing the hardness of the iron. The increase in per cent of chromium will lower the carbon content of the eutectoid. The presence of chromium is iron in the form of a complex carbide of chromium iron, and carbon tends to make it act as a stabilizer on the iron carbide.

The effect of the silicon on iron is twofold. In the case of the

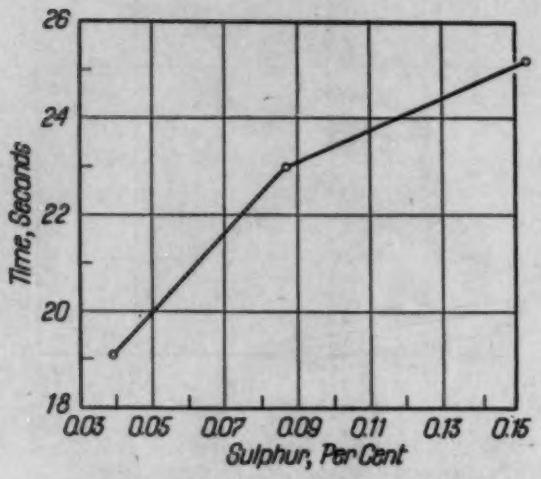

Fig. 26—Effect of Sulphur on the Time for Transformation at 1200 Degrees Fahr.

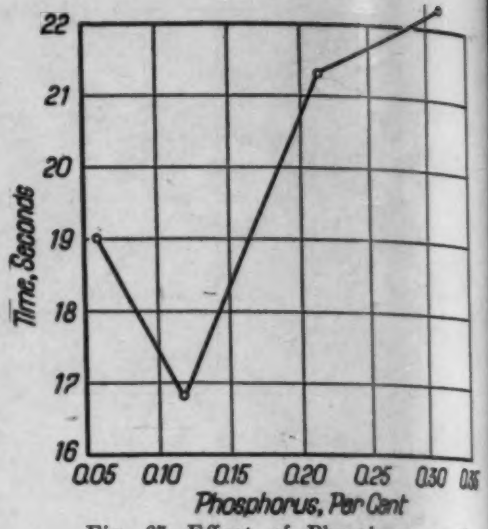

Fig. 27—Effect of Phosphorus on the Time for Transformation at 1200 Degrees Fahr.

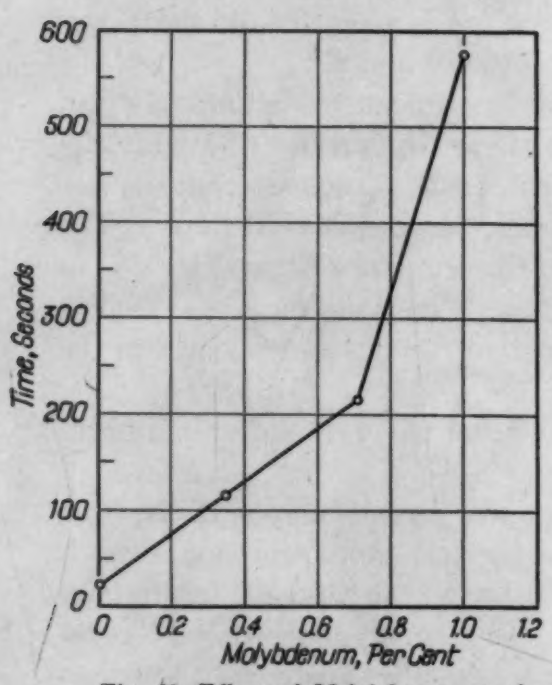

Fig. 28—Effect of Molybdenum on the Time for Transformation at 1200 Degrees Fahr.

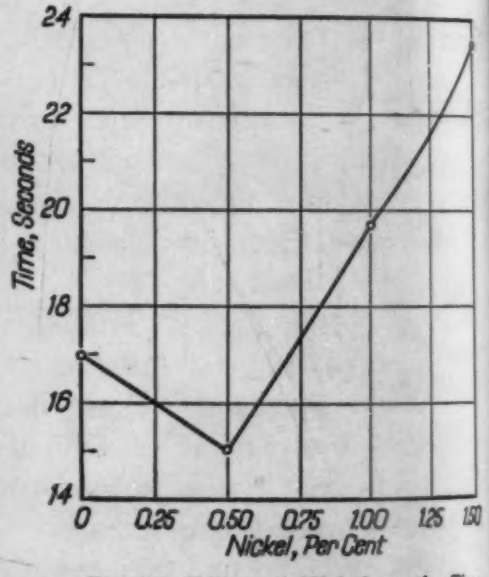

Fig. 29—Effect of Nickel on the Time for Transformation at 1200 Degrees Fahr.

iron with the silicon content of 1.72 the element has a hastening action on the transformation rate in the iron. When the amount of silicon is increased above 1.72 per cent, it has a slowing down action. These conclusions have been drawn from the plot, Fig. 31. The plot, Fig. 22, shows that there is no change in the slope of the lines with varying silicon content. Increase in the silicon will tend

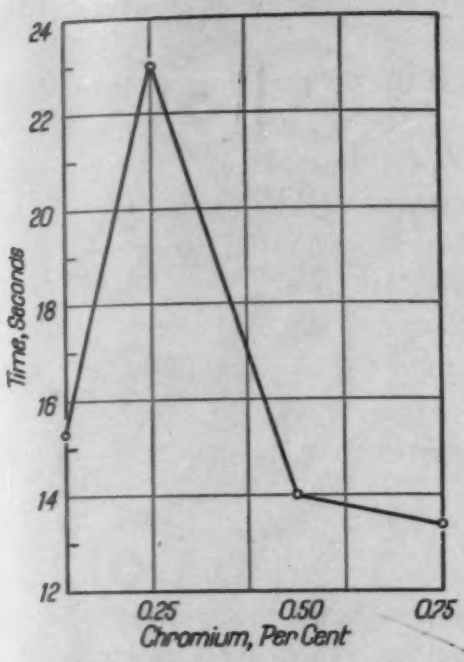

Fig. 30—Effect of Chromium on the Time for Transformation at 1200 Degrees Fahr.

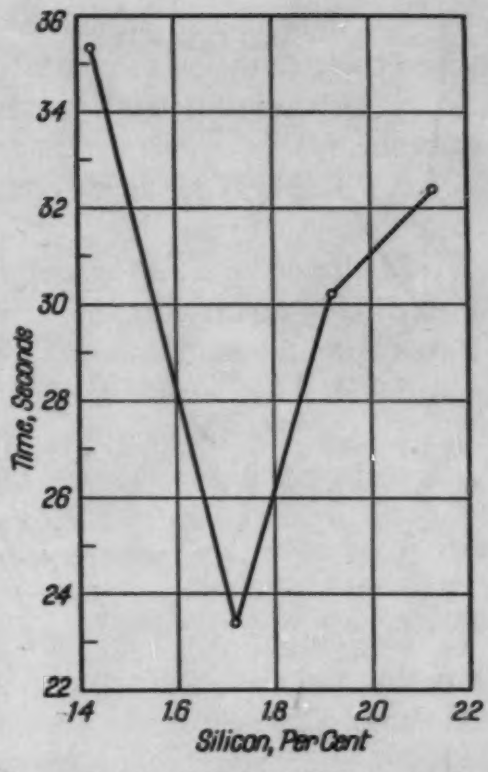

Fig. 31—Effect of Silicon on the Time for Transformation at 1200 Degrees Fahr.

to make the cementite more unstable and cause a more rapid transformation to take place.

Conclusions

The following conclusions are drawn from the study of the rate of austenite transformation at 1200 degrees Fahr. in cast irons.

1. The magnetic method of determination of the rate of transformation appears to have many advantages over the customary method of metallographic checking, because it is more accurate as well as being a faster method.

2. Decarburization, temperature of solution of the carbides, and time allowed for solution of the carbide will influence the rate at which the transformation will take place.

3. The following elements, manganese, sulphur, molybdenum, and nickel retard the rate of austenite transformation. Molybdenum retards the rate more than any other known element which is used in the metallurgical industry.

4. Carbon, and chromium carbide accelerate the rate of austenite transformation as compared with other elements.

5. Phosphorus tends to retard the transformation rate of the austenite.

6. Silicon tends to slow down the transformation rate of the austenite in cast iron.

7. Influence of alloy elements on the rate of austenite transformation in cast iron is similar to that of steel as recently shown by Davenport,[3] the only difference in effect of the alloy elements being magnitude, the direction being approximately the same.

8. Carbide formers tend to decrease the time for transformation, and graphitizers increase the time for transformation.

Acknowledgment

The authors wish to thank Dr. R. Schneidewind, Dr. D. W. Murphy, and Camillo D. Amico of the University of Michigan, and Dr. R. L. Dowdell of the University of Minnesota for their kindly criticism and suggestions. They also wish to express their appreciation to Dr. A. J. Herzig of the Climax Molybdenum Co., Detroit, for the preparation and analysis of samples used in this investigation.

DISCUSSION

Written Discussion: By Walton E. Jones, laboratory technician, Elmira Foundry Co., Inc., Elmira, N. Y.

In regard to this article on austenite transformation in cast iron, it would seem to me that under conditions given for construction and operation of magnetic transformation furnace, there would be changes in temperature gradient of the core. As any change would alter transformer losses, it would affect secondary current. Because of induction and eddy currents, the heating unit may also cause unstable operation, particularly if thermostatically controlled. Under these conditions I would be skeptical that the deviation found in the law of unimolecular reaction may not be due somewhat to transformer regulation.

I would suggest placing a shell type core with gap in center section entirely within furnace. The coils would be mounted on the outside of shell with their axis in line with center section, both to be anchored so as to always be in prox-

[3] E. S. Davenport, "Isothermal Transformation in Steels," TRANSACTIONS, American Society for Metals, Vol. 27, 1939, p. 837.

imity. The losses would be too great to read current on an ammeter but the secondary current could be regulated so as to light a small bulb. The amount of light from this bulb could be determined with a photoelectric cell, amplifier, and a microammeter.

To prevent stray induction and eddy current losses, a porcelain imbedded heating element may be used under the quench bath and separated from it by a grounded chromel plate.

I wish to commend the authors highly for their progress in this development and hope to see publication of further tests at different temperatures of carbide solution and quenching.

Written Discussion: By James R. Blanchard, research metallurgist, Climax Molybdenum Company of Michigan, Detroit.

The writer has found that there is so much information obtainable only by the metallographic method that all other methods are deemed supplementary. The metallographic method alone can distinguish the simultaneous formation of two constituents. Smith,[4] using six different methods for studying the decomposition of austenite at constant temperature, found microscopic observations to be the most reliable for determining the volume percentages of the various constituents present. For the investigation of several compositions, the metallographic technique will be found to be the most rapid.

It is thought therefore that the authors have unjustly labeled the metallographic method as tedious and inaccurate. Did the authors determine the accuracy of their method? Does the tempering of the products of formation at 1200 degrees Fahr. (650 degrees Cent.) affect the results? Would graphitization at 1200 degrees Fahr. (650 degrees Cent.) have no influence on the results?

The title and conclusion of this paper should be restricted to the decomposition of austenite at 1200 degrees Fahr. (650 degrees Cent.).

Authors' Reply

The authors are grateful for the comments of Messrs. Jones and Blanchard.

To overcome the possibility of a temperature gradient in the core the transformation furnace was at temperature for about three hours before use. With the temperature gradient from the center of the furnace to the outside being a constant, the transformer losses will be constant.

The suggestion for improvement on first reading sounds very good but the transformer must be operated over a range of temperature from 1300 to 60 degrees Fahr. (705 to 15.5 degrees Cent.). In developing the transformation furnace a set-up similar to the one suggested was used but the current induced in the second was very small so the plan was abandoned. The current amplifier idea was investigated but rejected due to the introduction of more equipment which results in greater possibility of error.

The metallographic method of isothermal transformation was labeled tedious and inaccurate on the following bases. The determination of austenite

[4]H. A. Smith, "Reactions in the Solid State. I. Initial Course of Subcritical Isothermal Diffusion Reactions in an Alloy Steel," *Transactions*, American Institute of Mining and Metallurgical Engineers, Vol. 116, 1935, p. 361.

transformation rate at any subcritical temperature necessitates the quenching of a goodly number of specimens from the solution temperature to the transformation temperature and holding for various lengths of time. In the higher temperature range where the transformation rate is rapid it takes some 20 to 25 specimens to establish the transformation rate curve. At the lower temperatures where the acicular transformation products are formed the transformation time is many hours and it takes some 40 to 50 specimens to establish the rate of austenite decomposition. There is much time consumed in preparing the specimens for metallographic study. After the specimen has been prepared the

Fig. A—Photomicrograph in Which is Shown the Product of Complete Transformation of a Cast Iron at Some Intermediate Temperature.

whole specimen is explored microscopically and the transformation rate determined by estimating the relative amounts of microconstituents present. One of the methods used is to photograph the specimen and then cut out the various areas and weigh them. The amount of transformation is then determined on the basis of weight of each microconstituent.

It is readily evident that this method has a number of disadvantages and has its inaccuracies. To better illustrate the point, Fig. A is the product of complete transformation of a cast iron at some intermediate temperature. How applicable is the method just stated for determination of the relative amount of transformation that has taken place? In this case the approximation would come just as close as the cutting out and weighing of the microconstituents.

The transformation rates were checked microscopically during the development of the method. The amount of transformation that had taken place during any time interval was checked metallographically by approximation of the relative amounts of microconstituents present. The assumption was made that any transformed austenite on quenching will appear as martensite along with the suitable transformation product of the temperature being investigated.

In regard to the tempering of the product of transformation at 1200 de-

grees Fahr. (650 degrees Cent.), it may be stated that after transformation is complete holding at temperature will cause some tempering of the transformation product. There was no apparent evidence of graphitization during transformation at 1200 degrees Fahr. (650 degrees Cent.). On holding at 1200 degrees Fahr. (650 degrees Cent.) after completion of the reaction, there apparently is nothing to prevent graphitization from taking place.

The title of the paper might have been clearer had it read "The effect of normal elements and alloy elements on the rate of transformation in cast iron at constant temperature of 1200 degrees Fahr. (650 degrees Cent.)."

METALLURGICAL CONTROL OF INDUCTION HARDENING

By F. F. Vaughn, V. R. Farlow and E. R. Meyer

Abstract

This paper has as its objective a method of metallurgical approach to control of the process of surface hardening by the use of high frequency induction equipment.

Data are presented to show the effect of the many metallurgical factors involved in this process when applied to the simple carbon steels.

For current of 3000-cycle frequency, a formula has been derived from the data whereby the required power input and time, expressed as KW/seconds, can be predetermined in order to produce results consistent with proper metallographic structure.

DURING the past few years there has been rapid development in the design and use of high frequency induction heating equipment for surface hardening. This development of equipment and its application has been much more publicized than has a consideration of the metallurgical factors involved in the process. As a matter of fact, little material dealing with this aspect of the problem has been published to date. This paper is a report of an investigation of these metallurgical factors which had as its objective a method of metallurgical approach to control of the process.

The high frequency induction heating method has been successfully used for surface hardening many types of production parts such as crankshafts, track pins, axle shafts, etc., on which a major consideration is high hardness to a specified depth for prolonging service life of the parts. Such applications require that this hardness be produced without overheating and resultant brittleness in the finished part.

Obviously some questions arise when considering the high frequency induction method for surface hardening such parts. For example:

Of the authors, F. F. Vaughn is assistant chief metallurgist, V. R. Farlow is physical testing metallurgist, and E. R. Meyer is metallurgist, Caterpillar Tractor Co., Peoria, Ill. Manuscript received September 2, 1941.

1. What maximum surface hardness can be produced, with proper metallographical structure, using the several medium carbon steels of the S.A.E. range 0.35-0.70 per cent?
2. What depth of hardness can be attained by this method?
3. What are the energy input requirements for producing a desirable hardened depth?
4. What are the effects of variations in bar sizes (diameters) in the application of this process?
5. What correlation exists between conventional hardenability measurement, e.g., "Rockwell Inches" and the response obtained in depth of hardness using this process?

Based upon the experimental data presented in this paper, the answers to the foregoing questions are as follows:

1. Maximum surface hardness is a function of carbon content, and, consistent with proper metallographic structure, increases from Rockwell C-61 for 0.35 per cent carbon steel to a maximum of Rockwell C-68 for 0.70 per cent carbon steel.
2. Optimum hardened depth, using current of 3000 cycle frequency is within the range 0.125-0.150 inch which is imposed by the metallographic limitations of (a) incomplete solution for shallow depths, and (b) grain growth and coarsening for greater depths. Both (a) and (b) are accompanied by something less than the maximum attainable surface hardness.
3. Energy input requirements are proportional to the volume of metal to be hardened to the desirable depth range. The formula $V = 0.0024\ P - 0.12$, where V is hardened volume and P is kilowatt-seconds, expresses this relation for a steel of 43.6 Rockwell Inches hardenability.
4. For hardening a unit length to the desirable depth range, energy input is a straight line function of bar size.
5. Depth of hardness is also a linear function of hardenability, e.g., "Rockwell Inches". For fixed bar size and energy input a change of one Rockwell Inch results in a corresponding change of approximately 0.0025 inch depth of hardening.

Heretofore, in seeking the answers to these questions, it has been common practice to use a trial and error process in arriving at a satisfactory procedure for hardening the parts. The experimental data in this paper were obtained for the purpose of developing a more scientific approach to the problem of fulfilling the desired engineering and metallurgical requirements with a minimum of experimental work. It is hoped that it also will provide a stimulus to further investigations of the problem.

Investigational Procedure

Hardening Equipment—A major part of our induction hardening equipment operates at 3000 cycles per second. Since this equipment was available it was decided to conduct the investigation using current of this frequency. Attention is called to this fact because data presented by Tran and Osborn[1] and by Stansel[2] show that frequency is a variable which must be considered. The electrical equipment used is all capable of precise power input setting, with 0.1 second accuracy in control of power input duration, delay time, and quenching time. Water-cooled single-turn inductor blocks of the following dimensions were used for the test bar sizes indicated:

Bar Diameter Inches	Block Length Inches	Block Bore Inches
1	1 11/32	1⅛
1½	3⅞	1⅝
2	4¼	2⅛

Hardening Cycle—The complete hardening cycle used in these tests consisted of a single impulse heating period, 0.2 seconds delay, then a quench. While the power input and duration (heating time) varied with the several experiments, the delay time and quenching time were constant throughout the investigation. All specimens were quenched through openings in the inductor block until equalized. In every case the quenching water, at a temperature of 85 to 100 degrees Fahr., was applied at 18 pounds per square inch pressure. The values given for power throughout this investigation are pre-set values and were not necessarily sustained throughout the heating period.

Metallurgical Examination—After hardening, as described subsequently, specimens were examined for surface hardness using the Rockwell C-scale. The depth of hardness penetration and the length of the hardened zone were considered as that depth below the surface, and that length on the surface, at which Rockwell C-50 was produced, because this hardness is safely above the critical hardness of the medium carbon steels generally used for induction hardened parts. Specimens for microscopic examination and for depth of hardness penetration were taken through the middle of the hardened

---

[1]A. Tran and H. B. Osborn, Jr., "Inherent Characteristics of Induction Hardening," American Society for Metals Preprint.

[2]N. R. Stansel, "Industrial Electric Heating," *General Electric Review*, Vol. 39, No. 9, 1936, p. 440.

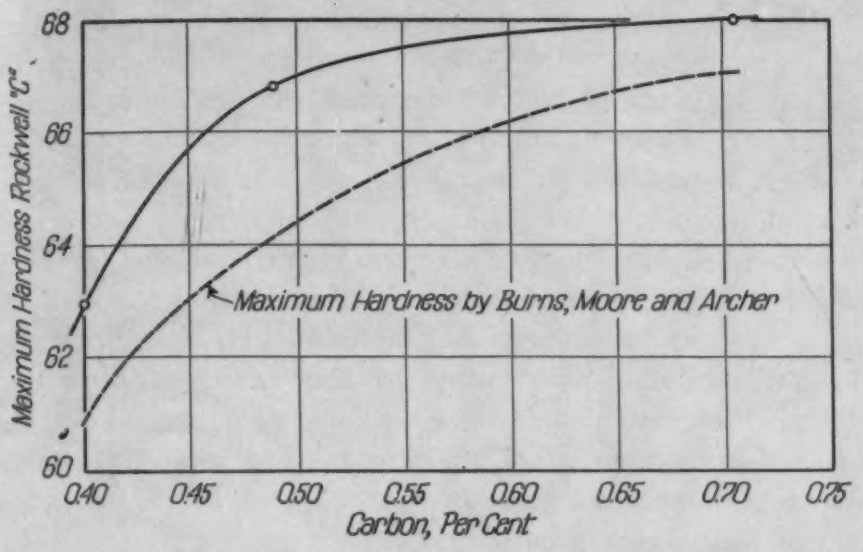

Fig. 1—Relation of Surface Hardness to Per Cent Carbon of Induction Hardened Bars. Also Maximum Hardness by Burns, Moore and Archer.

length. All photomicrographs shown were taken at 100 diameters magnification at a location 0.010 inch below the hardened surface. The specimens used for the photomicrographs were electrolytically polished and etched for 5 seconds with 1 per cent picric acid and 5 per cent hydrochloric acid in alcohol. This etchant was selected because of its characteristic of revealing martensitic grain size as well as undissolved ferrite.

Influence of Variations in Properties of the Material

Effect on Surface Hardness—There seems to have been a somewhat general misconception that it is essential to have some chromium present in the material in order to satisfactorily harden parts by the induction heating method. Several million parts made of medium carbon, fine-grained steels, containing chromium and other alloying elements only in residual quantities have been successfully surface hardened at Caterpillar Tractor Company. Hardenability is the major influencing factor which determines the application of these steels to production parts. Consequently, the material selected for use in this investigation was fine-grained, plain carbon steel within the 0.33 to 0.95 per cent carbon range. All test specimens were solid cylindrical bars turned and ground to sizes indicated in the test data.

Examination of the curves shown in Fig. 1, which substantiates evidence shown by Tran and Osborn,[1] reveals that adequate surface hardness can be obtained without the presence of alloying elements in the material. From this curve it is apparent that maximum surface hardness is purely a function of the carbon present in the material, as brought out by Burns, Moore and Archer.[3]

The term "superhardness" has been used to describe the higher hardnesses produced by the induction heating method for hardening than are obtainable by conventional methods. Hardness obtainable by induction hardening may exceed by four points Rockwell "C", the maximum obtainable by furnace heating and quenching the same material. A comparison at magnifications up to 3000 diameters, of microstructures obtained by the two methods, reveals no sound explanation of this increased hardness.

A condition present in induction hardened parts, which might be the reason for this increased resistance to penetration by the hardness indentor, is the high stress in the hardened case. This stress may be simply demonstrated by cutting longitudinally through the hardened zone of a bar which has been induction hardened to a rather shallow depth over its entire length. The hardened case will expand when it is cut through, and seize the cutting wheel.

Tempering such an induction hardened piece at 250 degrees Fahr. has been found to cause a decrease in hardness from Rockwell C-66 to C-63, whereas, a similar tempering of a 1-centimeter cube of the same material furnace heated and quenched, will only cause a decrease in hardness from Rockwell C-62 to C-61. This difference in the response to tempering might well be due to relief of quenching stresses present to a much greater degree in the induction hardened specimens.

Effect on Depth of Hardening—In order to study the influence of chemistry and hardenability on depth of hardening, an investigation was made using test pieces 2.040 inch in diameter of several S.A.E. 1035, S.A.E. 1040, S.A.E. 1045 and S.A.E. 1050 steels. Power input and duration, and quenching were constant for all specimens, namely heating at 400 kilowatts for 4 seconds (1600 kw/sec.), then quenching until equalized. This power input and time was selected as being sufficient to produce maximum surface hardness in the test bars of lowest carbon content.

[3]J. T. Burns, T. L. Moore and R. S. Archer, "Quantitative Hardenability," TRANSACTIONS, American Society for Metals, Vol. 26, 1938, p. 1.

Table I
Chemistry, Hardenability and Hardness Data

Lab. No.	Chemistry C	Chemistry Mn	Chemistry Cr	Harden-ability Rkw. Inches	Hardness (Ind. Hardened) Surface Rockwell "C"	Hardness (Ind. Hardened) Depth to Rkw. "C" 50
Q-4005	0.36	0.57	0.06	32.5	62	0.113"
Q-4101	0.40	0.85	0.03	37.9	63	0.1395
Q-4102	0.43	0.83	0.03	39.5	64	0.141
Q-4124	0.42	0.71	0.06	42.4	63.5	0.142
Q-4087	0.44	0.76	0.07	44.5	65	0.151
Q-4123	0.50	0.75	0.06	46.3	66	0.154
Q-4084	0.46	0.78	0.05	48.0	65	0.153
Q-4118	0.47	0.81	0.06	49.6	65.5	0.1705
Q-4086	0.47	0.84	0.10	52.8	65	0.1635
Q-4137	0.52	0.90	0.06	53.9	66	0.167
Q-4100	0.52	0.85	0.08	56.1	65	0.187
Q-4094	0.53	0.86	0.09	58.8	65	0.1805

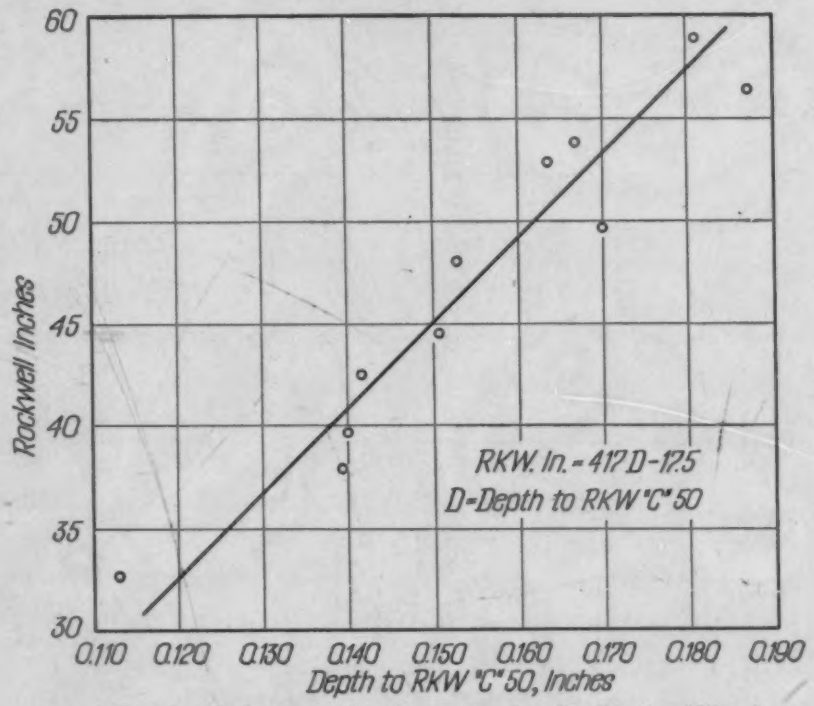

Fig. 2—Variation in Hardened Depth with Hardenability in Rockwell Inches.

Chemistry, hardenability in Rockwell Inches, and resultant hardnesses are shown in Table I. Fig. 2 shows the relation of hardenability (Rockwell Inch Value) to the depth at which Rockwell C-50 was obtained. This hardened depth may be considered to be an approximately straight line function of the Rockwell Inch Value. The equation for this line is Rkw. In. = (417 × D) — 17.5 where D is hardened depth. Stating the equation in another way,

$$D = \frac{\text{Rkw. In.} + 17.5}{417}$$

Influence of Variations in Power Input and Heating Time

In order to determine the influence of power input and duration on surface hardness, depth of hardening, and microstructure, test bars 8 inches long were turned and ground to 1.500 inch diameter. The chemistry and hardenability of the material used are shown in Table II.

Effect on Depth of Hardening—Test bars of S.A.E. 1045 steel "A" were induction hardened with varying increments of power input and duration. The curves in Fig. 3 show the relation of power input to hardened depth for several increments of heating time. These indicate a straight line relationship between power input and hardened depth for the higher heating times.

Table II

Steel	S.A.E.	C	Mn	S	P	Si	Ni	Cr	Rkw. In.
A	1045	0.49	0.79	0.028	0.019	0.23	0.20	0.07	46.3
B	1045	0.49	0.79	0.026	0.017	0.21	0.12	0.07	43.6
C	1070	0.71	0.85	0.032	0.017	0.22	0.04	0.04	58.4
D	1085	0.83	0.69	0.029	0.021	0.24	0.08	0.05	52.5
E	1095	1.01	0.43	0.035	0.030	0.38	0.03	0.05	47.6

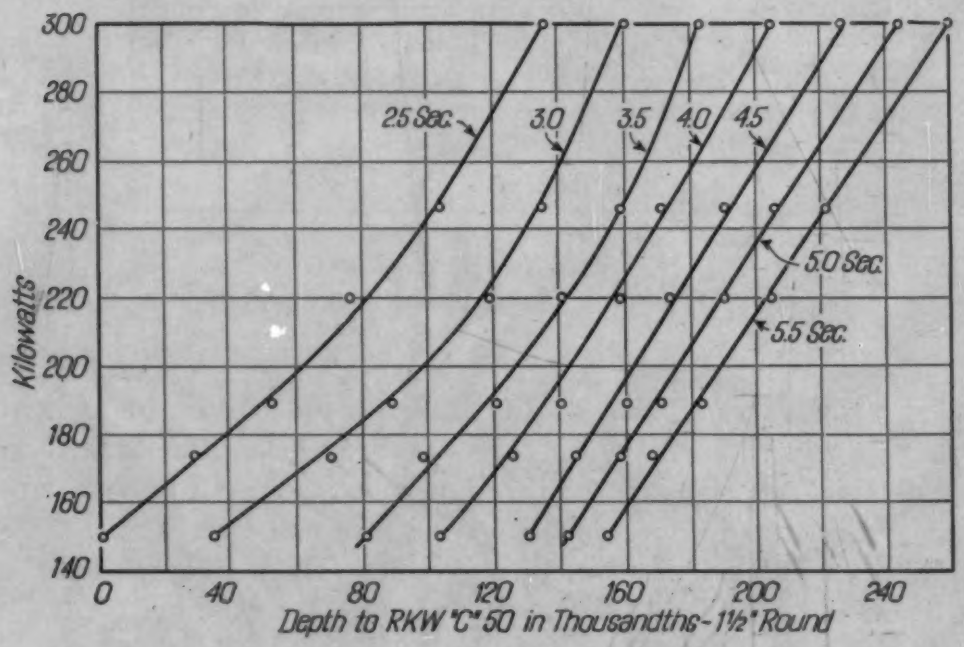

Fig. 3—Power in Kilowatts Versus Hardened Depth with Constant Heating Time.

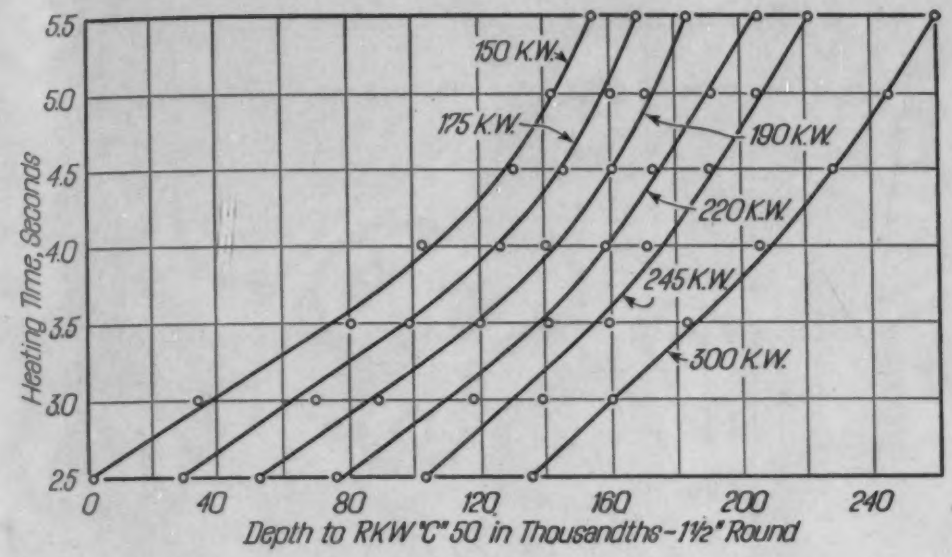

Fig. 4—Heating Time Versus Hardened Depth with Constant Power Input.

The curves in Fig. 4 show the relationship between heating time and hardened depth for several increments of power input. These curves indicate a less direct relationship between heating time and hardened depth.

Effect on Microstructure—Test bars of steels "A", "B", "C", "D", and "E" were induction hardened to produce a range from incomplete solution to overheating for each steel. The relations of energy used in kilowatt-seconds to surface hardness and hardened depth produced, as well as typical photomicrographs of the structure near the surface, are shown in Figs. 5, 6, 7, 8, and 9. The curves indicate for these materials the range of obtainable hardened depth consistent with desirable surface hardness and microstructure as well as the range of power input necessary to obtain these results. The photomicrographs show incomplete solution until maximum surface hardness is attained, then grain growth accompanies further increase in hardened depth while surface hardness decreases.

It is noteworthy for the curves on the higher carbon steels that the surface hardness curves bend sharply at the point where solution was being effected. In other words, the higher percentage of pearlite in these steels resulted in maximum surface hardness very soon after the start of solution. The S.A.E. 1070 steel combined the highest surface hardness with a wide working range. The hardened depth corresponding to a desirable microstructure was in each case 0.125-0.150 inch.

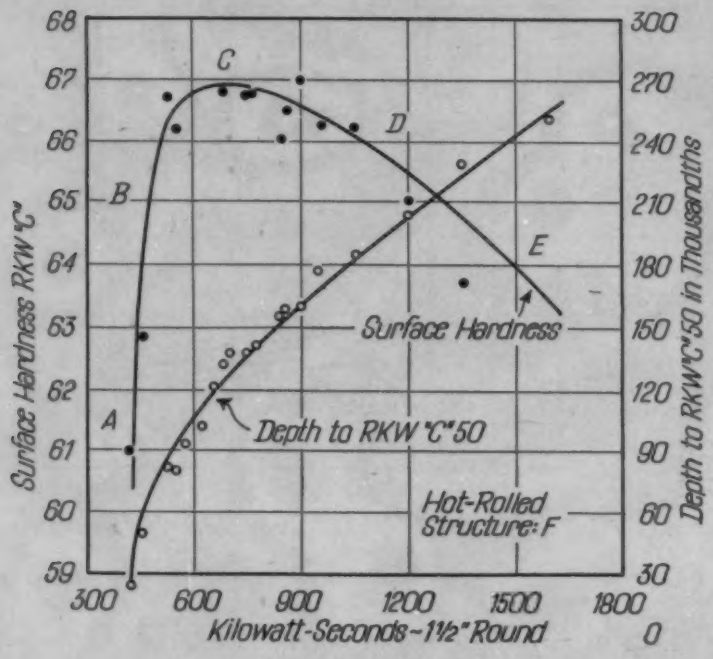

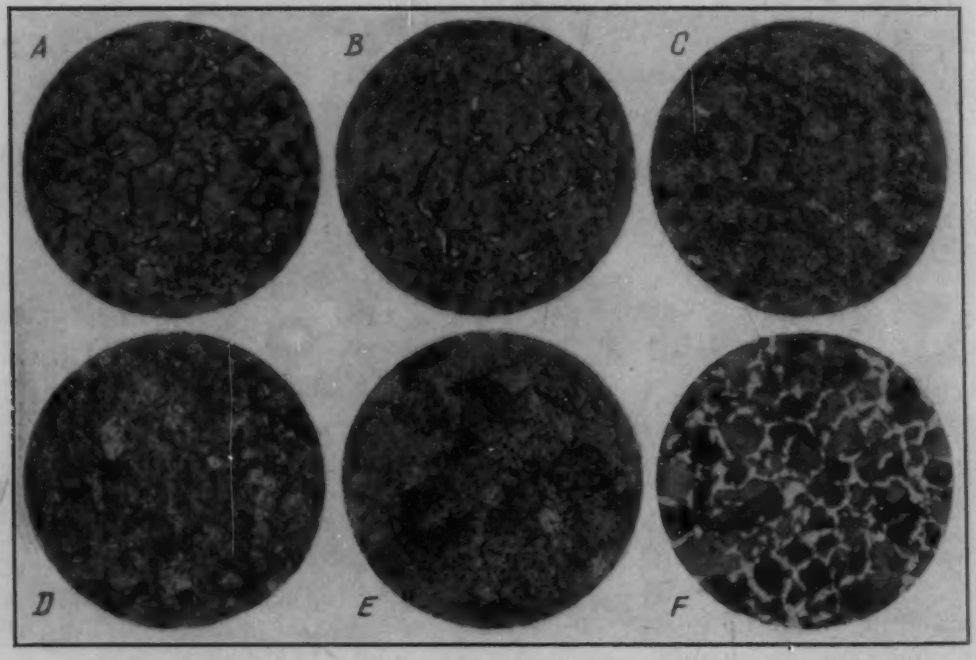

Fig. 5—S.A.E. 1045, Steel "A". 1½-Inch Round. Relation of Surface Hardness and Hardened Depth to Power in Kilowatt-Seconds; Also Microstructures Obtained. The Letters in the Diagram Show the Position of the Corresponding Photomicrograph.

Effect of Size

The effect of size on surface hardness, depth of hardening, and microstructure was investigated on test bars which were normalized,

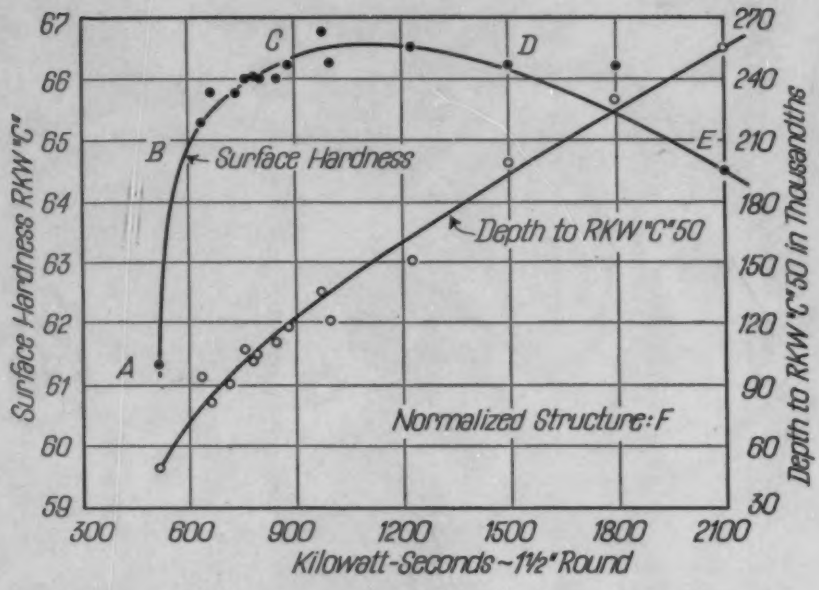

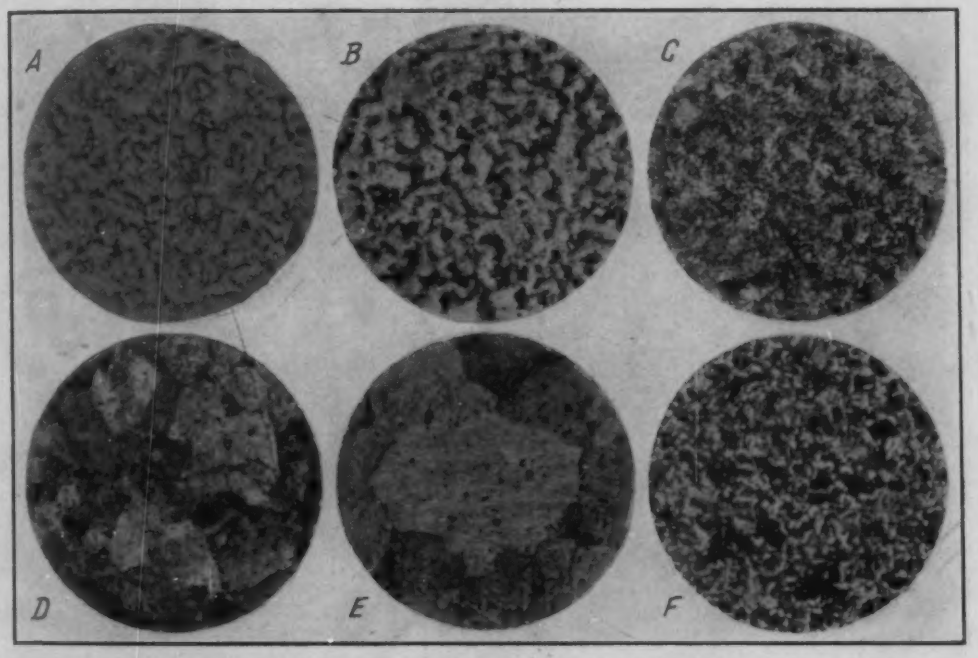

Fig. 6—S.A.E. 1045, Steel "B". Relation of Surface Hardness and Hardened Depth to Power in Kilowatt-Seconds; Also Microstructures Obtained. The Letters in the Diagram Show the Position of the Corresponding Photomicrograph.

turned, and ground to 1.000, 1.500, and 2.000 inch diameter rounds. Chemistry and hardenability of the material used was as follows:

C	Mn	S	P	Si	Ni	Cr	Rkw. In.
0.49	0.79	0.026	0.017	0.21	0.12	0.07	43.6

The test bars were induction hardened with variations of power

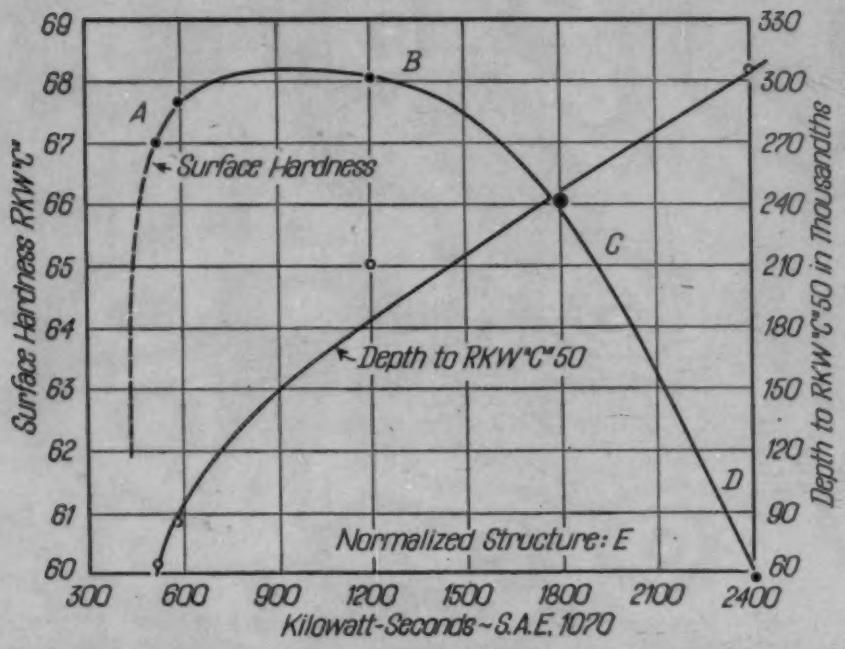

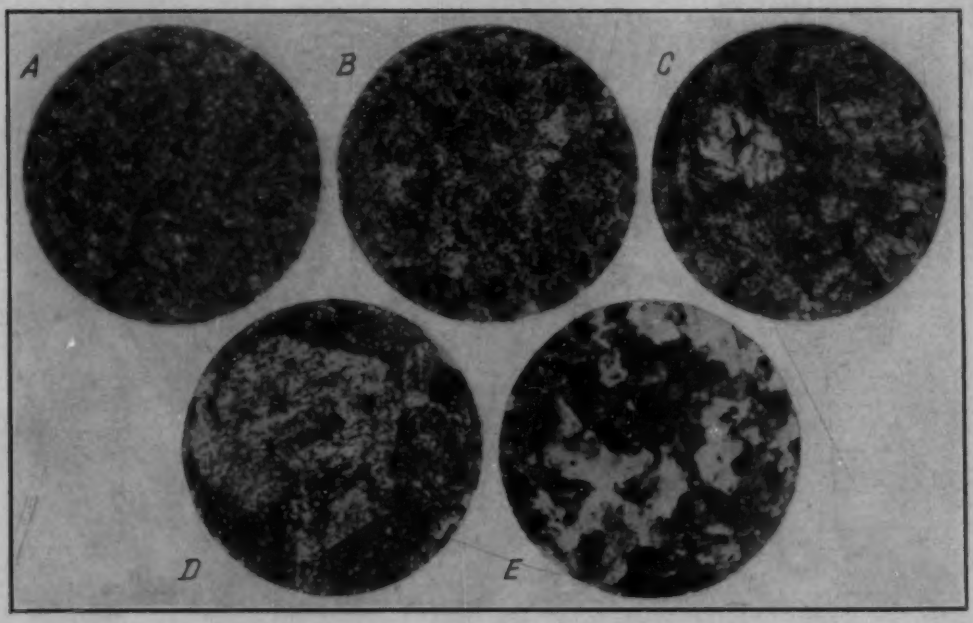

Fig. 7—S.A.E. 1070, Steel "C". Relation of Surface Hardness and Hardened Depth to Power in Kilowatt-Seconds; Also Microstructures Obtained. The Letters in the Diagram Show the Position of the Corresponding Photomicrograph.

input and time to get a range of results from underheating to overheating.

Fig. 10 shows curves for hardened depth and surface hardness versus kilowatt-seconds, together with representative microstructures for the 1.0-inch diameter bars. These curves indicate a narrow work-

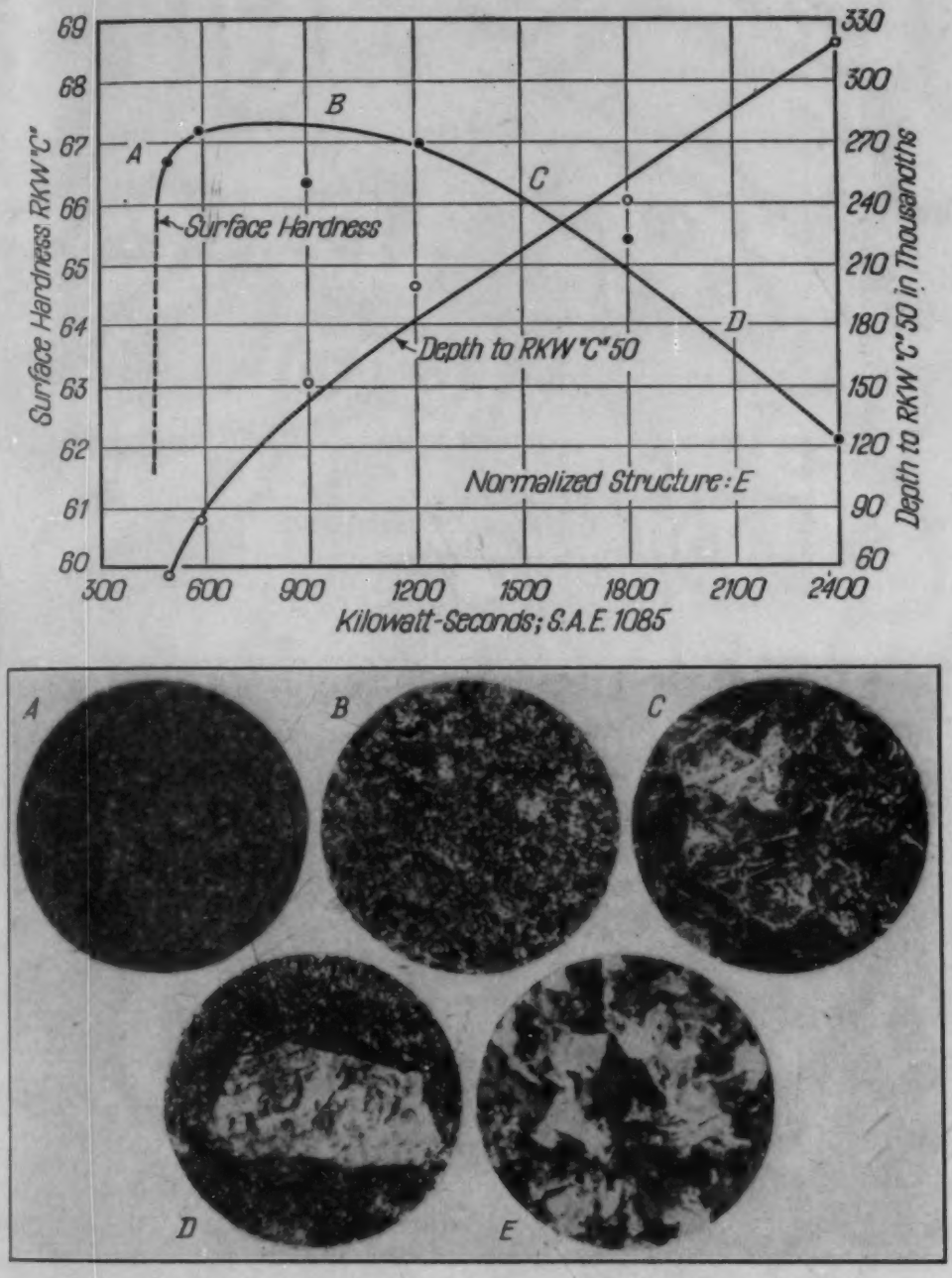

Fig. 8—S.A.E. 1085, Steel "D". Relation of Surface Hardness and Hardened Depth to Power in Kilowatt-Seconds; Also Microstructures Obtained. The Letters in the Diagram Show the Position of the Corresponding Photomicrograph.

ing range for this size bar. Fig. 6 shows curves for the same data on the 1.5-inch diameter bars. Fig. 11 shows a similar set of curves for the 2.0-inch diameter bars. These curves are not comparable without considering the difference in the lengths of the inductor blocks used.

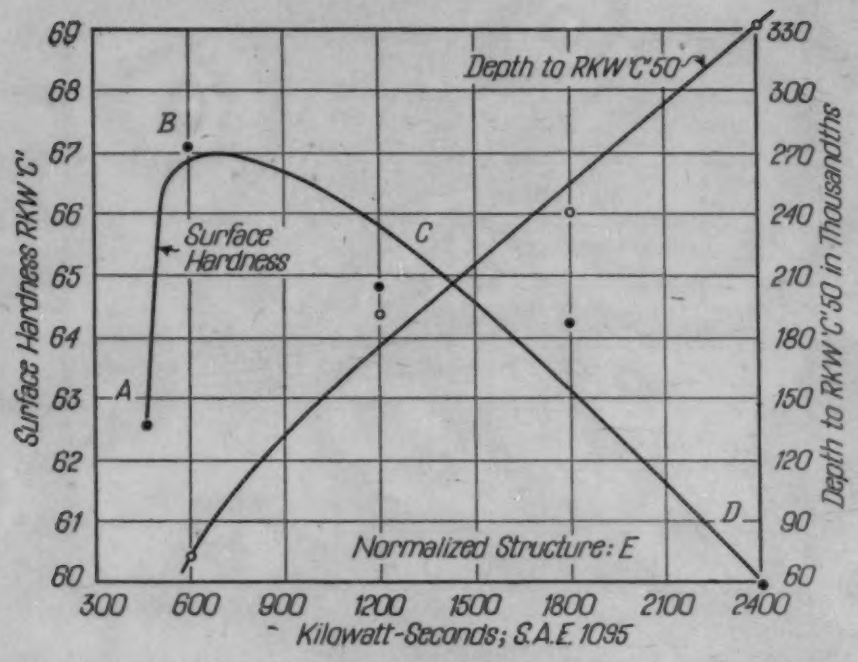

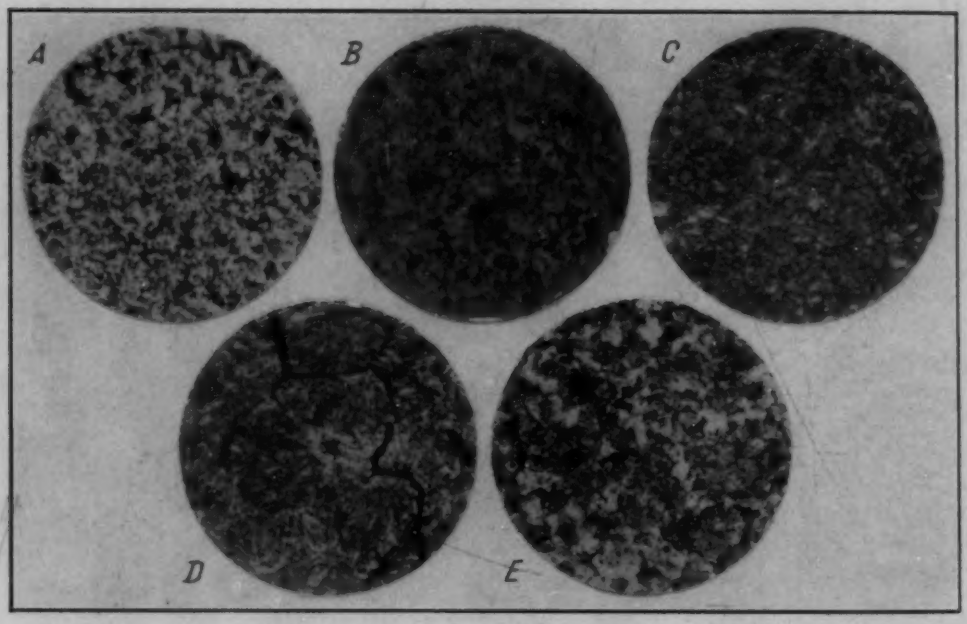

Fig. 9—S.A.E. 1095, Steel "E". Relation of Surface Hardness and Hardened Depth to Power in Kilowatt-Seconds; Also Microstructures Obtained. The Letters in the Diagram Show the Position of the Corresponding Photomicrograph.

It was determined from this same set of test specimens that with a fixed inductor block length the hardened length increases with increasing energy input. This relation for the three bar sizes, using the inductor blocks previously mentioned, is shown in Figs. 12, 13 and 14. It may be observed from these two sets of curves (Figs. 6, 10

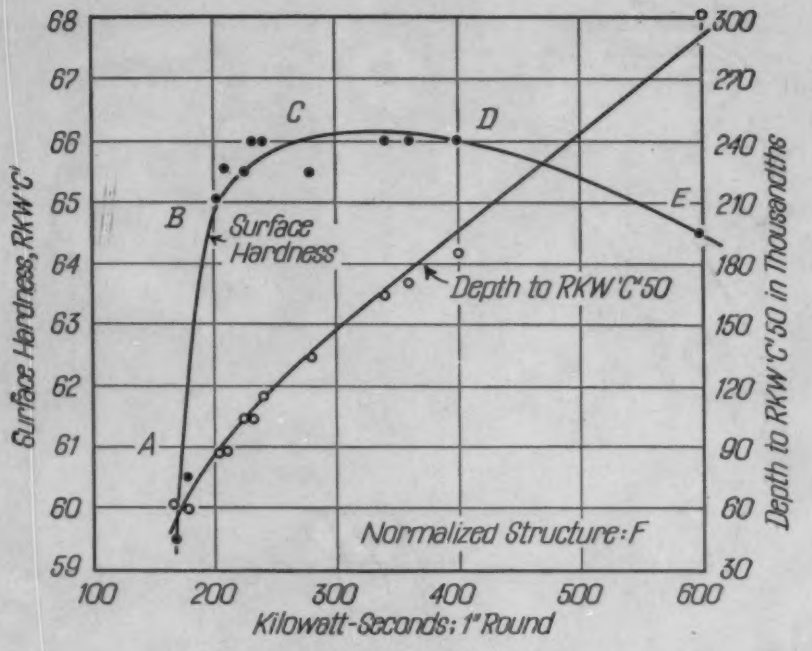

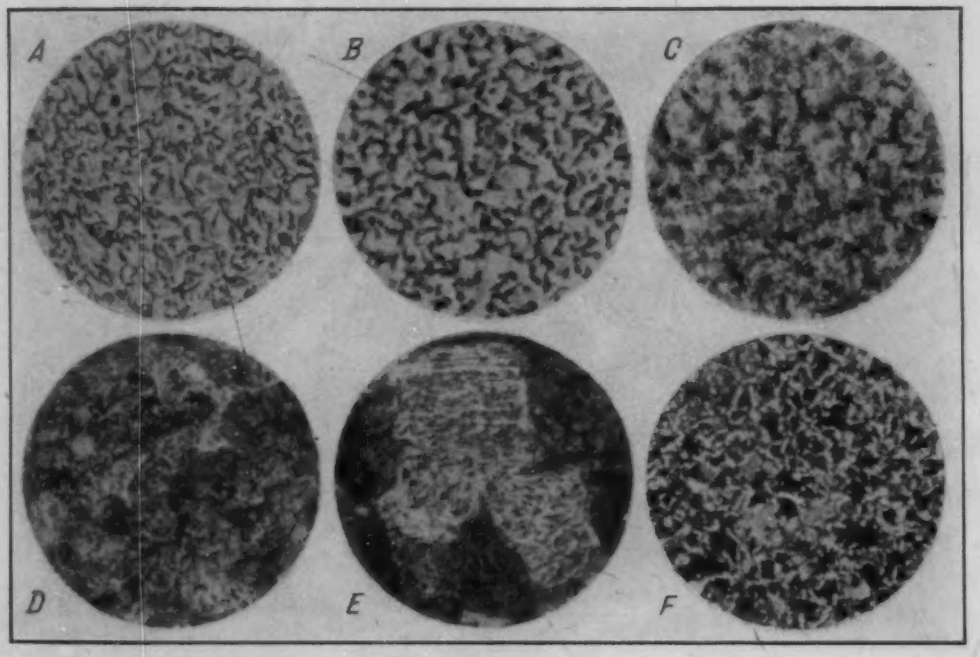

Fig. 10—S.A.E. 1045, 1-Inch Round. Relation of Surface Hardness and Hardened Depth to Power in Kilowatt-Seconds; Also Microstructures Obtained. The Letters in the Diagram Show the Position of the Corresponding Photomicrograph.

and 11, and Figs. 12, 13 and 14), that the hardened length increases with the hardened depth. Figs. 15, 16 and 17 illustrate this. Hardened length is an important factor on parts where hardening must be avoided around keyways, in fillets, or in similar locations which might

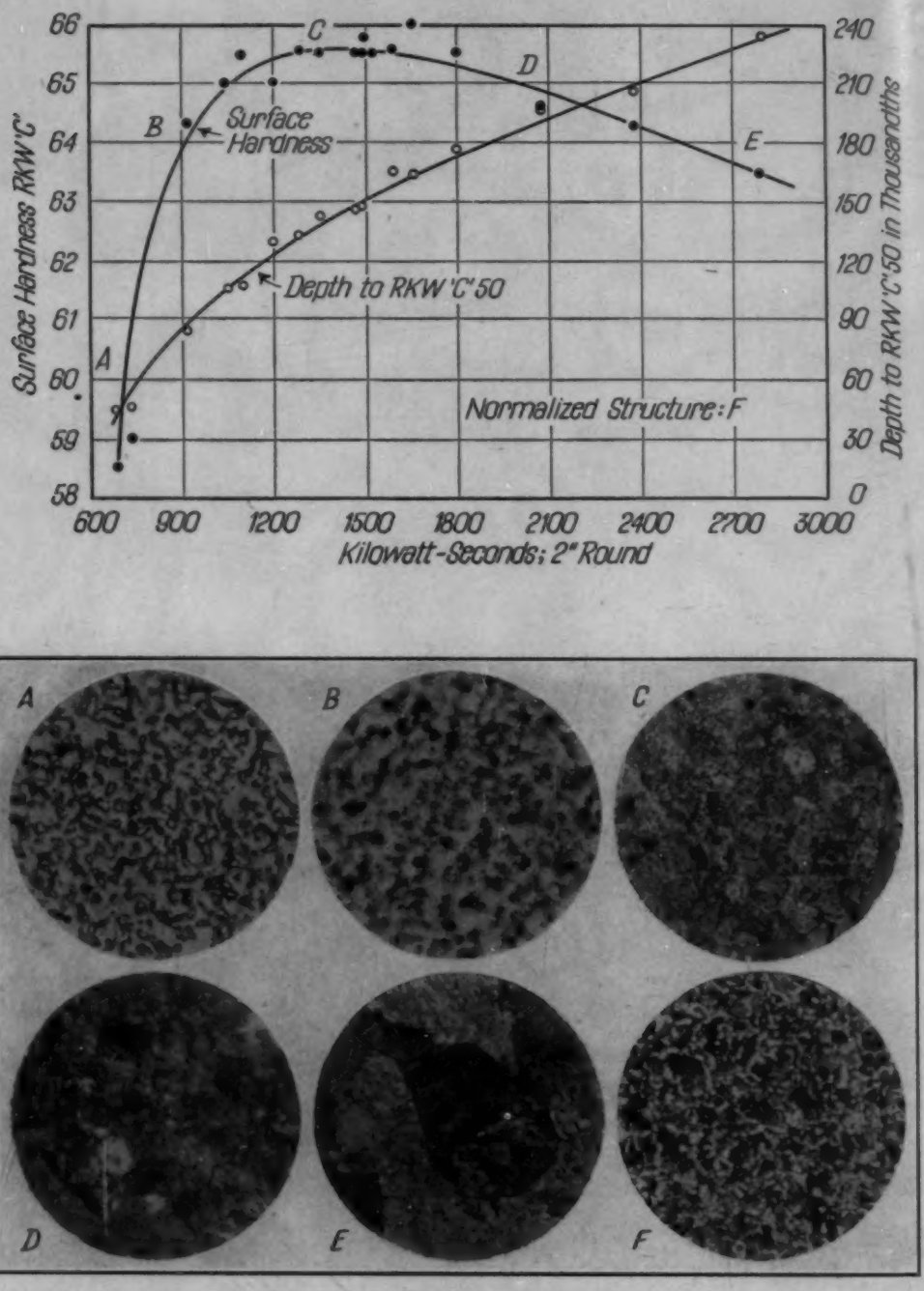

Fig. 11—S.A.E. 1045, 2-Inch Round. Relation of Surface Hardness and Hardened Depth to Power in Kilowatt-Seconds; Also Microstructures Obtained. The Letters in the Diagram Show the Position of the Corresponding Photomicrograph.

be focal points for stress concentration. There are, of course, limitations in the length of inductor blocks for a given bar size and power input but this point is not within the scope of this investigation.

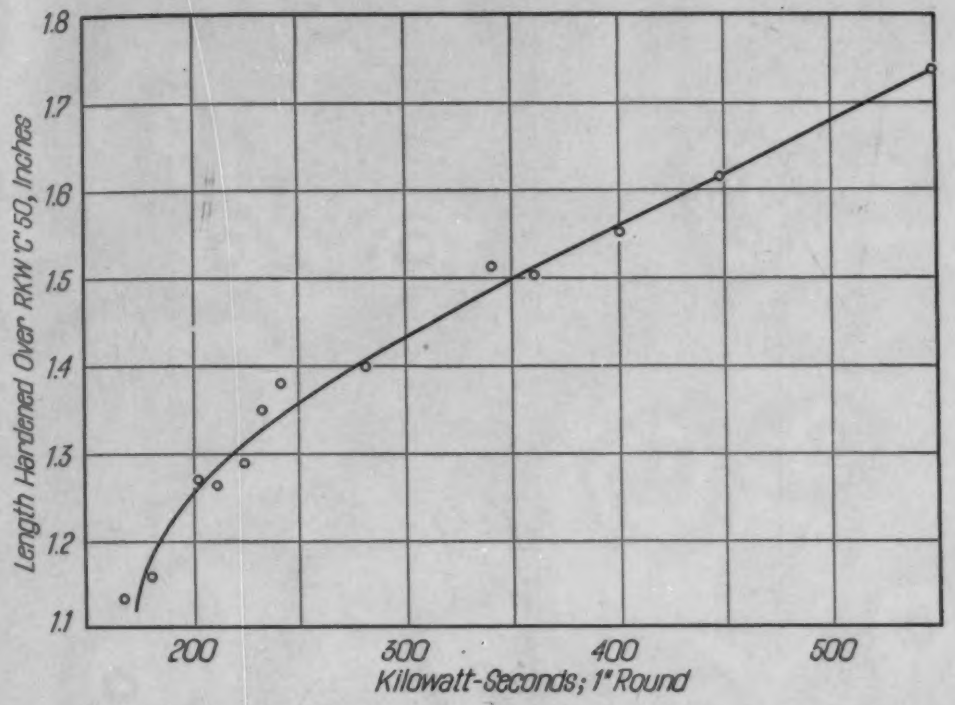

Fig. 12—S.A.E. 1045, 1-Inch Round. Relation of Hardened Length to Power in Kilowatt-Seconds.

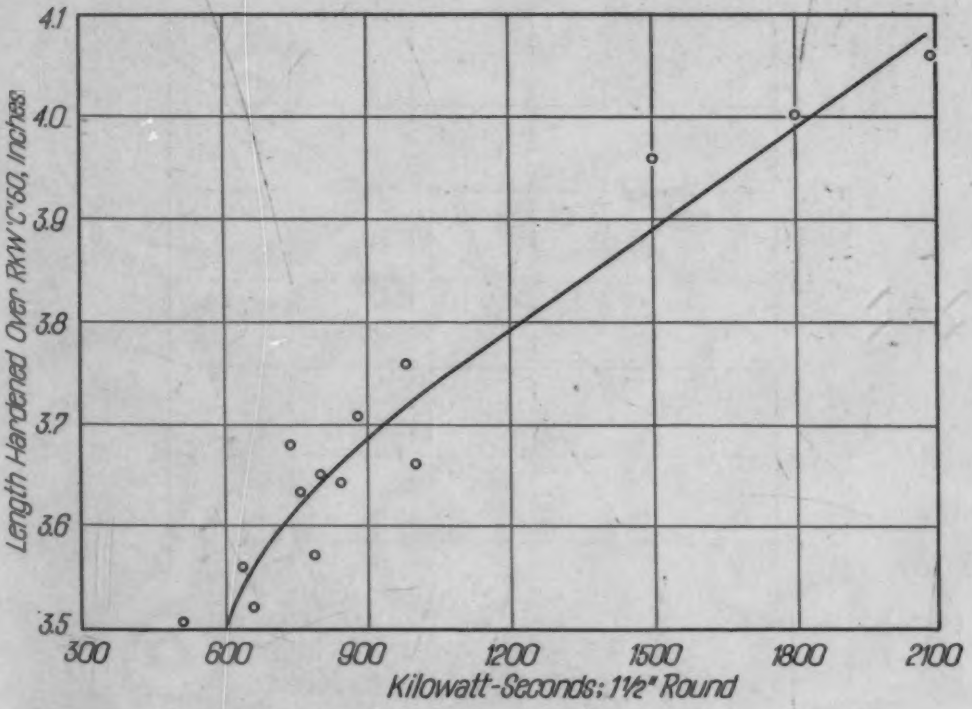

Fig. 13—S.A.E. 1045, 1½-Inch Round. Relation of Hardened Length to Power in Kilowatt-Seconds.

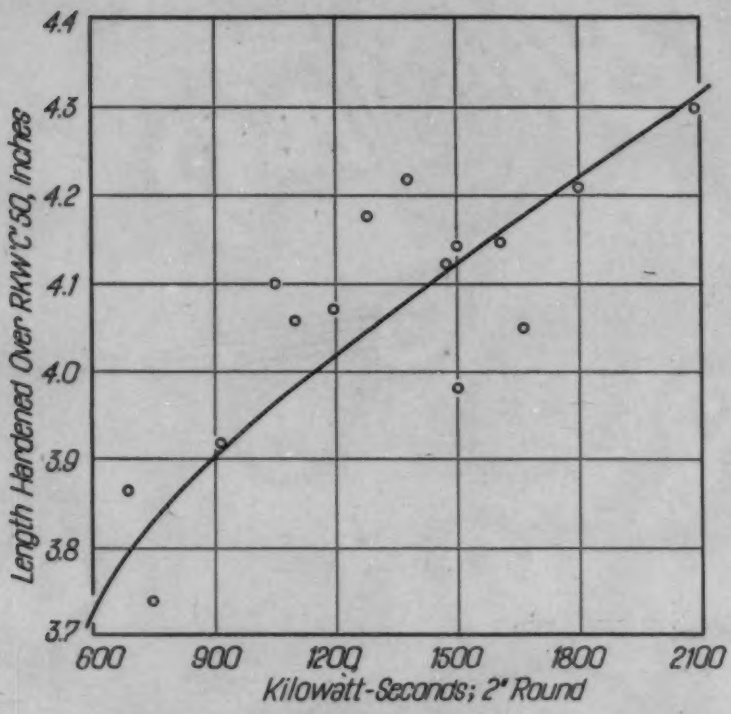

Fig. 14—S.A.E. 1045, 2-Inch Round. Relation of Hardened Length to Power in Kilowatt-Seconds.

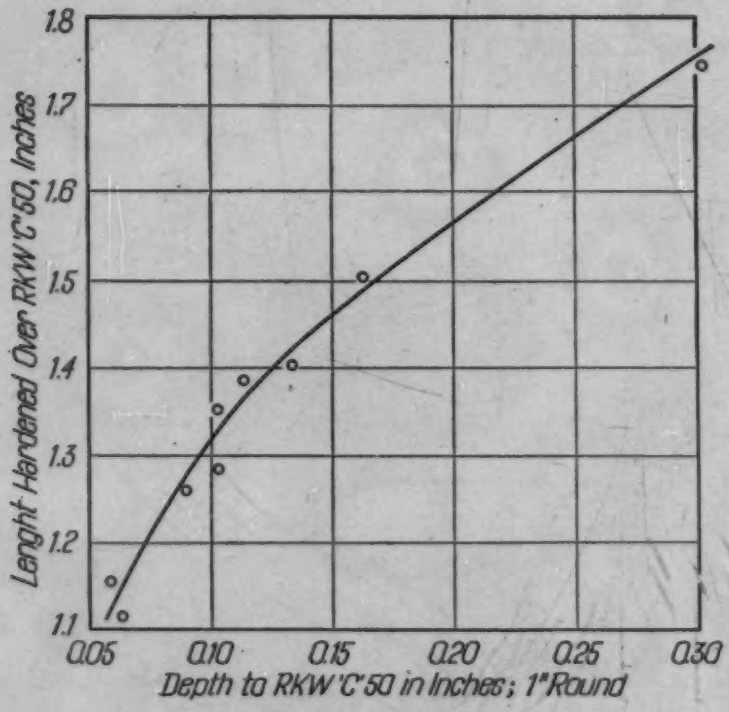

Fig. 15—S.A.E. 1045, 1-Inch Round. Relation of Hardened Length to Hardened Depth.

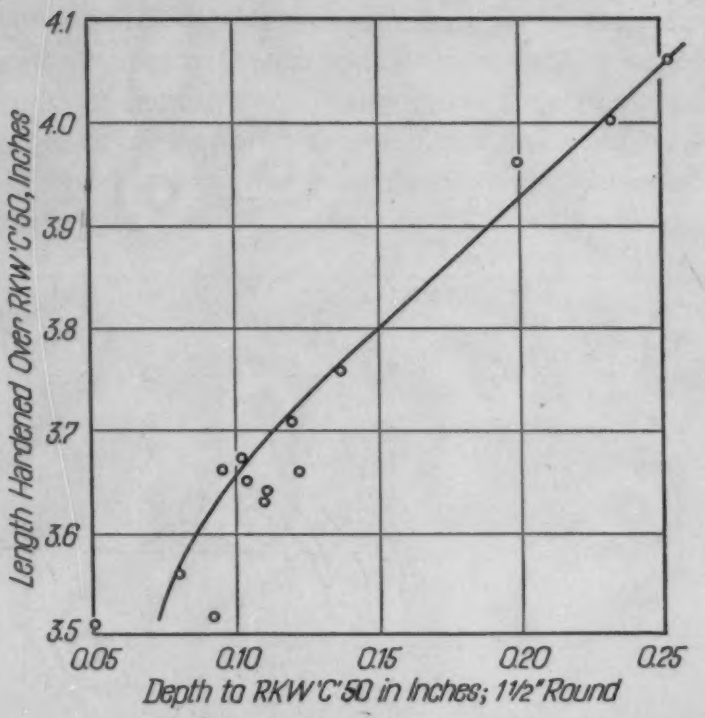

Fig. 16—S.A.E. 1045, 1½-Inch Round. Relation of Hardened Length to Hardened Depth.

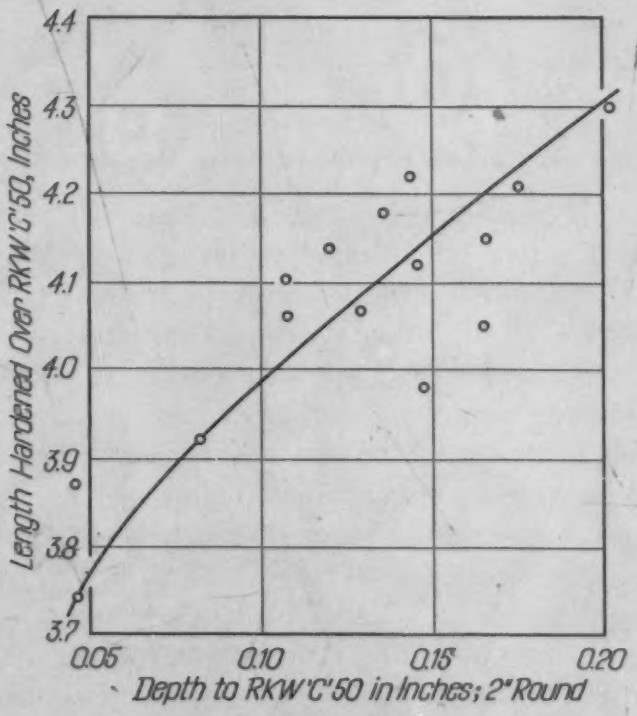

Fig. 17—S.A.E. 1045, 2-Inch Round. Relation of Hardened Length to Hardened Depth.

An examination of these results indicated the possibility of a straight line relationship between hardened volume and energy used (in kilowatt-seconds). These values were plotted for the three sizes in Fig. 18. There is a certain error involved in assuming that the relation of these two is a straight line function. However, the values near the extremes for each size which show the greatest deviation

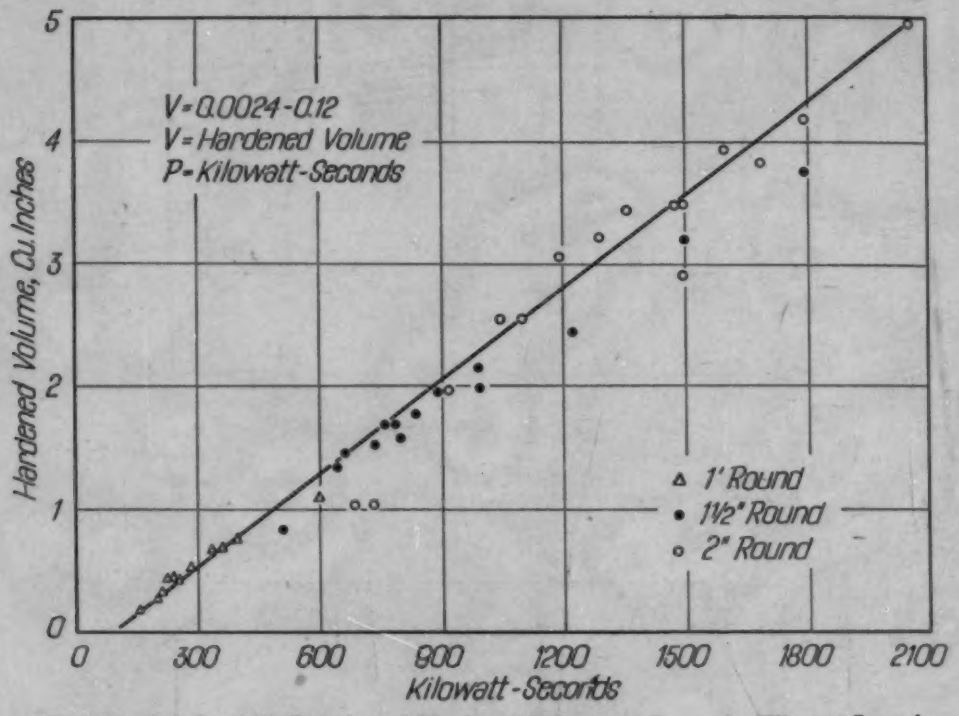

Fig. 18—S.A.E. 1045, Relation of Hardened Volume to Power in Kilowatt-Seconds.

from the straight line are also outside the range of good metallurgical practice, that is, either underheated or overheated. We may assume then that the equation for the straight line shown in Fig. 18, $V = (0.0024 \times P) - 0.12$, where V equals hardened volume in cubic inches and P equals energy in kilowatt-seconds, is correct for values within the working range conforming to best metallurgical practice.

It is thought that the hardened volume would be more closely a straight line function of energy input (kilowatt-seconds) if it were possible in every case to transform to martensite the entire volume which is heated above its critical range. This, however, becomes impossible when the ratio of volume heated above the critical range, to total volume, is large. As this ratio becomes large, the ratio of the depth which transforms to martensite to the depth heated above the critical range becomes smaller because of the diminishing quenching effect of the core as well as the larger mass of heated metal in the

case. This effect is illustrated in Fig. 19. These are specimens from the cross sections of bars which were heated with increasing amounts of energy and all were quenched in the same manner. Two distinct zones, one entirely martensitic and the other only heat affected, may be distinguished in the specimens which were given the higher power input.

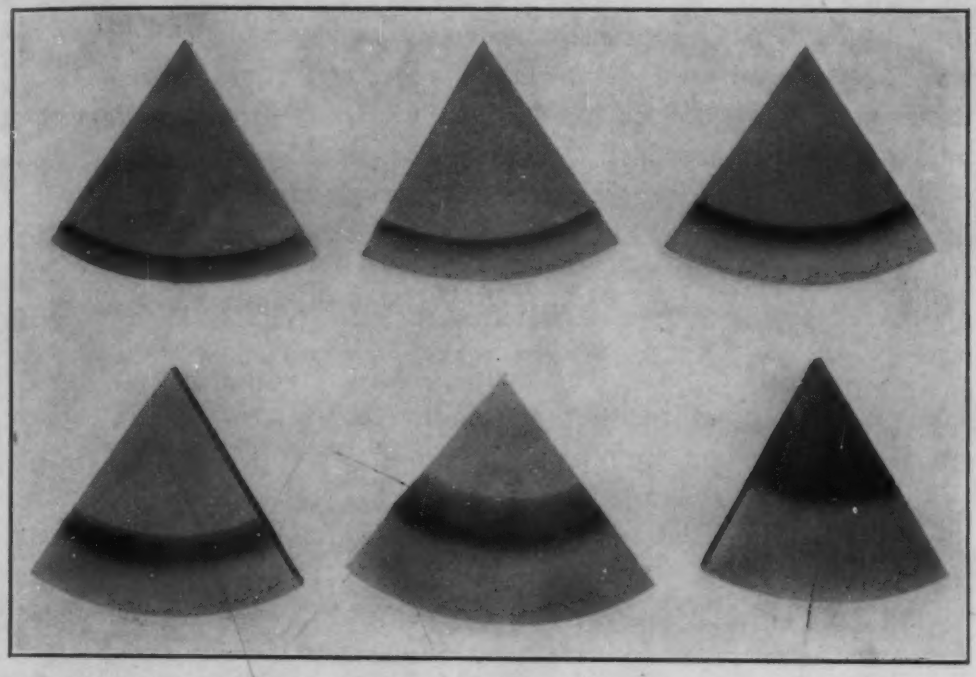

Fig. 19—Transverse Sections from S.A.E. 1045 Bars Showing Change in Relation of Hardencd Depth to Heat Affected Depth with Increase in Power Input.

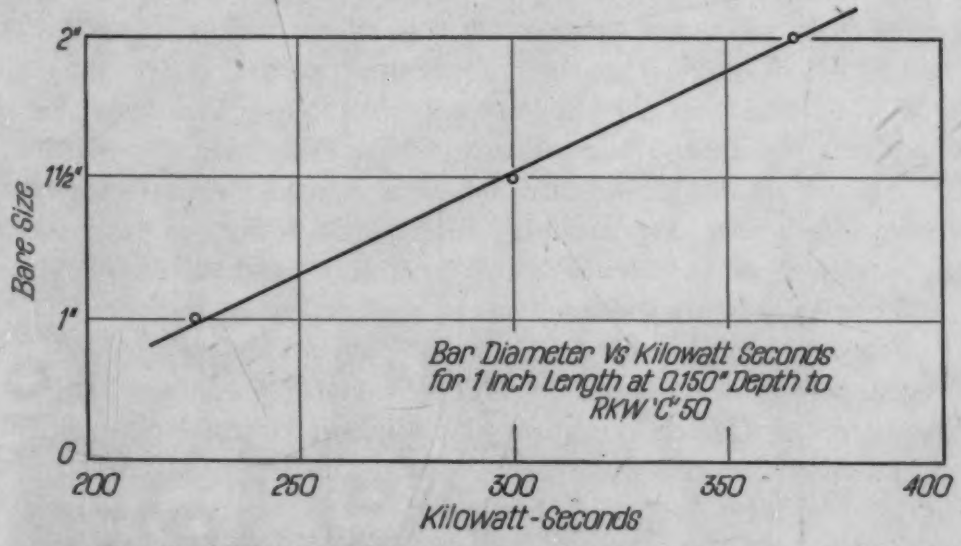

Fig. 20—S.A.E. 1045, Relation of Bar Size to Power in Kilowatt-Seconds Required for Hardening a 1-Inch Length to 0.150 Inch Deep.

An examination of Figs. 6, 10 and 11 indicates that the most desirable combination of surface hardness and microstructure is obtained in each case with a hardened depth of approximately 0.125-0.150 inch. This would seem to indicate that the attainment of the best metallurgical properties in the hardened case is dependent upon using the correct energy input necessary to produce a hardened depth of 0.125-0.150 inch and that the energy input need only be varied to compensate for different bar sizes and required hardened lengths. Fig. 20 is based on the same data, of bar diameter versus energy input in kilowatt-seconds for hardening a 1-inch length to a depth of approximately 0.150 inch. This curve would be useful only for material with a hardenability of 43.6 Rockwell Inches. An equation is developed later which takes into account hardenability variations.

Effect of Grain Growth on Notched Bar Value

A study of the effect of grain growth on Charpy impact value was made by heat treating one centimeter square keyhole Charpy specimens in the conventional manner, approaching as closely as practicable an induction hardening time cycle. The specimens were heated in lead for 60 seconds at temperatures from 1500 to 1950 degrees Fahr. (815 to 1065 degrees Cent.), then quenched into water until cold. They were drawn at 700 degrees Fahr. (370 degrees Cent.) for 1 hour in order to give higher numerical foot-pound values. Hardness values after the quench were Rockwell C-61-63 for all specimens and after the draw were Rockwell C-45-46. Impact values ranged from 12 foot-pounds for the lower hardening temperatures down to 8 foot-pounds for the higher temperatures.

An examination of the microstructures of these specimens showed complete solution in all cases and transformation to martensite. The maximum grain size was 0.007 inch. These values give a relative idea of the correlation of martensitic grain size with notch toughness although the tempering temperature used was higher than would normally be used for induction hardened parts.

For applications where a drop in notch toughness of 30 to 35 per cent would be undesirable, it is obvious that surface hardness alone is not conclusive indication of the kilowatt-second requirement for induction hardening the parts involved. In Fig. 10 the grain size produced by induction hardening with 600 kilowatt-seconds input is much too large, yet the surface hardness is Rockwell C-64-65.

A Formula for Calculating the Energy Requirement for Hardening a Given Part

The most important variables involved in hardening a part by the induction heating method are the energy required, the hardened volume, and the hardenability of the material. Equations have been developed which show the relation of hardenability to hardened depth, also the relation of energy input required, to hardened volume. The error involved in the use of this latter equation has been discussed and the error involved in the use of the former equation is considered small so long as the heat affected zone is critically cooled, as for example when the heat affected zone is comparatively shallow.

These equations may be combined to give a single equation which yields a value for the energy requirement necessary to produce a given hardened volume of material of known or stated Rockwell Inch value. These equations are combined as follows:

$$V = (0.0024 \times P) - 0.12 \text{ or } P = \frac{V + 0.12}{0.0024}$$

Where P equals energy in kilowatt-seconds and
V equals hardened volume in cubic inches.

$$\text{Rkw. In.} = (417 \times D) - 17.5$$

Where D is hardened depth.

$$P \times \text{Rkw. In.} = \frac{V + 0.12}{0.0024} \times [(417 \times D) - 17.5]$$

Multiplying these equations by each other,

$$P = \frac{V + 0.12}{0.0024 \times \text{Rkw. In.}} \times [(417 \times D) - 17.5]$$

The use of this equation is illustrated by the following: Assume that a 1-inch round bar is to be hardened to 0.150 inch depth for a length of 1.4 inches and that the hardenability of the material to be used is 44 Rockwell Inches. Substituting these values in the formula gives an energy requirement of 290 kilowatt-seconds. A bar of this material was actually hardened for this specified depth and length by using 280 kilowatt-seconds input. The hardened depth selected for this illustration was one that gives a desirable microstructure.

Summary

Data have been presented which indicate that the superhardness of parts surface hardened by induction heating is due to quenching stresses rather than a difference in microstructure.

There exists a direct relation between hardenability, as ex-

pressed in Rockwell Inches, and hardened depth for a given bar size and power input.

The effect of changes in power input on surface hardness, hardened depth, and microstructure have been indicated. The tests on different bar sizes indicate a direct relation between power input and hardened volume for material of a given hardenability.

A hardened depth of 0.125-0.150 inch is indicated as the optimum for the most desirable microstructure and surface hardness, regardless of bar size, when using a current of 3000 cycles frequency.

The effect on notch toughness of increasing the hardening temperature from 1500 to 1950 degrees Fahr. (815 to 1065 degrees Cent.) is indicated as a drop in Charpy value of 30 to 35 per cent.

The variables, power input, Rockwell Inches and hardened volume are combined into a formula based upon test results.

DISCUSSION

Written Discussion: By H. B. Osborn, Jr., research and development engineer, TOCCO Division, The Ohio Crankshaft Co., Cleveland.

The authors have done a splendid piece of work on a complex subject in presenting in a factual manner some of the relationships existing between depth and magnitude of hardness, power input, and microstructure produced in surface hardening by induction. Due to the equipment they had available for test, they necessarily limited their investigation to results obtainable with 3000-cycle current and mention that the frequency of the current used plays an important role on the results obtainable, especially on depth of hardness.

The authors use kilowatt-seconds as an energy factor varying the time of heating, with power input varied only in the ratio of two to one, in determining optimum hardened depth, and reached the conclusion that any attempt to exceed this depth results in overheating of the surface and a drop in hardness. This is true only under the conditions of the tests made by the authors.

If, however, they had used a factor of kilowatts per square inch instead of kilowatt-seconds (with practically constant power input) and increased the heating time for greater depth with much lower power input than used in the tests, a much greater depth of hardness than indicated could be obtained.

If, as the authors imply, 0.150 inch is the optimum hardened depth obtainable, this would preclude the use of induction heating for deep or through hardening of sections over 0.300 inch in diameter. There are many thousands of parts being induction hardened hourly for war use by the Government which we are not at liberty to discuss, but which require through hardening very much in excess of the 0.150-inch depth mentioned by the authors.

Fig. A illustrates the greater depth of hardness than that obtained by the authors, which is being obtained on bar diameters as indicated. This greater depth is obtained in spite of the higher frequency of the current used, that

is, 9600 cycles, which is more conducive to shallow surface hardening by nature of the inherent higher skin effect than the 3000-cycle current used by the authors. The kilowatts per square inch used for hardening the specimens in Fig. A was but a fraction of that used by the authors in their tests.

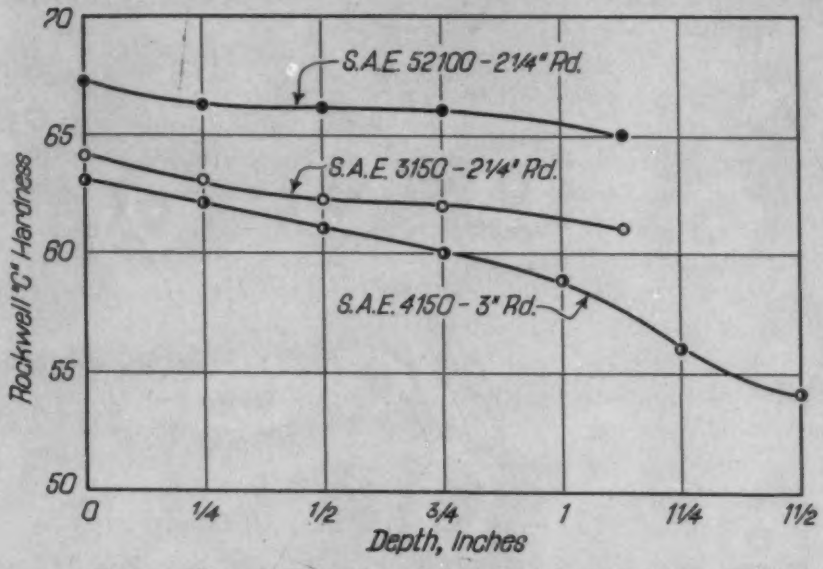

Fig. A—Through Hardening of Bar Stock with Induction Heating Using 9600-Cycle Current and Power Input as Low as 0.5 Kilowatts per Square Inch.

Within reasonable limits, it is possible to obtain any desired depth of hardness without obtaining grain growth or coarsening or incomplete solution by merely using the correct amount of power and time. Other things being equal, high power input per square inch and short heating time result in shallow depth, whereas low power input per square inch and long heating time produce greater depth. Further, as pointed out in a previous paper by M. A. Tran and the writer, a depth of hardness can be obtained on a bar which is in excess of the critical radius of the material hardened.

Recent developments and investigations with induction hardened specimens of certain types of steel have shown the drop in hardness noted by the authors and we concur with their explanation based on quenching stresses and have so stated in some of the trade magazines. Further, careful examination of hardened specimens seems to indicate this stressed condition to be at least partially responsible for the "superhardness".

We join the authors in expressing our hope that additional work will be undertaken on this subject and venture to predict further development and use of the hardenability relationships which they have compiled.

Authors' Reply

We acknowledge with appreciation Dr. Osborn's comments. As pointed out in the paper, our problem was to evaluate the metallurgical factors involved in *surface hardening* plain carbon steel, using the single impulse induction

method for heating. In this type application, the prime requirement is to produce a highly hardened surface and a hardened depth within a specified range while retaining original core properties. To accomplish this, power input and time (kilowatt-seconds) must be such that the zone heated above the critical temperature is confined to that depth specified to be hardened. Obviously, this means heating and quenching in the shortest possible time consistent with producing the best metallographical qualities.

Data were presented showing the minimum and maximum power input and time limitations, expressed as kilowatt-seconds, consistent with sound metallurgical results; that is, complete solution without overheating. This method should not be confused with the practice required for through hardening parts made of highly alloyed steels with relatively low critical cooling rates.

Since the latter type of heat treatment is not comparable to surface hardening practice, the thousands of parts referred to by Dr. Osborn as being hardened for war use are not a basis for comparison. Similarly, the curves illustrated in Fig. A, since they represent results obtained with highly alloyed steels, afford no comparison with the shallow hardening plain carbon steels of relatively high critical cooling rate used in our investigation. In fact, it would be impossible, with any combination of power input and time, to harden the plain carbon steels to depths illustrated by the curves in Fig. A.

We are gratified to note that Dr. Osborn qualifies his statement, "It is possible to obtain any desired depth of hardness without obtaining grain growth or coarsening, or incomplete solution, by merely using the correct amount of power and time", with the phrase "within reasonable limits".

One of the prime objectives of our investigation was to definitely establish these "reasonable limits", consistent with proper metallographic structure, for *surface hardened* parts. Data were presented to substantiate our conclusions regarding these limitations for the type of heat treatment under consideration and the materials normally used for the applications.